THE INSTALLATION OF SUCTION CAISSON FOUNDATIONS FOR OFFSHORE RENEWABLE ENERGY STRUCTURES

By

Oliver Cotter

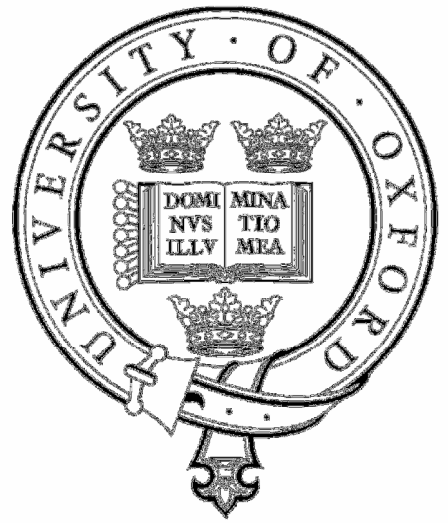

A thesis submitted for the degree of

Doctor of Philosophy

at the University of Oxford

Magdalen College,

Michaelmas Term (2009)

Abstract

Installation of Suction Caisson Foundations for Offshore Renewable Energy Structures

A thesis submitted for the degree of Doctor of Philosophy

Oliver Cotter

Magdalen College, Oxford

Hillary Term 2010

Renewable energy structures, constructed offshore, may use suction caisson foundations. Standards for calculating installation suction do not yet exist, and for the technology to be widely employed, robust installation behaviour must be demonstrated. The soil conditions for these installations will vary significantly. This work describes a programme of physical model tests involving the installation of caissons into soil selected to be representative of conditions present around the coast of the UK. An investigation was undertaken to identify experiments which are non-dimensionally similar to field installations. The soil samples comprised clay over sand, sand over inclined clay and sand with a hydraulic barrier. The tests investigated the conditions for which installation is possible, and provide guidance for calculating the required suction pressure. The onset of plug lift and caisson refusal was demonstrated in soil profiles comprising clay over sand. A framework quantifying the onset of plug lift is presented and confirmed by the test series. The results of a series of installations are described, during which selective skirt tip injection was undertaken. The objective of these tests was to steer the caisson and investigate the effect of this process on maximum penetration depth. The effect of injection on pore pressure adjacent to the skirt tip is modelled and tested against measured data. A framework for calculating the effect of injection on suction is presented. Experience has shown that suction installation has a detrimental effect on caisson moment resistance. Experiments investigating the effect of pressure grouting caissons after installation are described. Foundation settlement and stiffness during combined V, H, M, loading were measured and compared to jacked footings.

Acknowledgements

I would like to thank my supervisors Professor Guy Houlsby and Dr Byron Byrne for their guidance and valuable help throughout this project.

The Civil Engineering technicians, Clive Baker, Bob Sawala and Chris Waddup, assisted with the manufacture of apparatus.

I wish to acknowledge the support provided by EPSRC, Fugro Ltd, The Department of Engineering Science and Magdalen College. I would like to thank Professor Guy Houlsby and Dr Byron Byrne for organising the project, and Professor Mark Cassidy, from The University of Western Australia, for generous assistance to undertake centrifuge experiments at UWA.

List of Symbols

$2R\theta$	Rotational displacement
N_c	Specific
A	Area
A_i	Inside skirt area
A_o	Outside skirt area
A_p, A_{tip}	Area of skirt tip
A_{plug}	Area of plug
A_s	Area of skirt
B	Strip footing width
C_D	Drag coefficient
C_I	Inertia coefficient
C_u	Coefficient of uniformity
D	Diameter of caisson
D_{10}	Maximum grain size of 10% of material
DOF	Degree of freedom
E	Young's Modulus
F	Dimensionless flow factor
F	Force
G_s	Specific gravity of soil
H	Horizontal force
K	Coefficient of lateral earth pressure
M	Moment load (Nm)
M/DH	Moment load ratio
N_c	Bearing capacity factor for cohesion
N_q	Bearing capacity factor for surcharge
N_γ	Bearing capacity factor for soil weight
$N_{nozzles}$	Number of nozzles
OCR	Over-consolidation ratio
$P_{caisson}$	Installation pressure
P_{plug}	Pressure to lift clay plug
Q	Total flow rate
R	Caisson radius
R_d	Relative density
T	Torque
V'	Buoyant force
W	Submerged weight of caisson
Z	Stress enhancement group
a	Pore pressure factor
a_1, etc	Coefficients for pore pressure factor calculation
c	Cohesion
d	Penetration depth
d_{ca}	Foundation depth factor
f_o, f_i	Load spread factors (outside and inside caisson)
g	Acceleration due to gravity
h	Height of skirt
h_c	Height of clay layer
h_s	Height of sand layer
i	Hydraulic gradient
i_c	Critical hydraulic gradient
k	Soil permeability
k_f	Permeability ratio
k_f	Side resistance factor
k_p	Skirt tip pressure factor
p_a	Atmospheric pressure
p_{inj}	Injection pressure
$p_{manifold}$	Manifold pressure
$p_{hydrostatic}$	Hydrostatic pressure
p'_o	Effective overburden at base
p_{tip}	Skirt tip pressure
q	Unit flow rate
q_c	Cone resistance
q_p	End resistance of skirt
r	Distance from water source
s	Suction pressure
s_{ca}	Foundation shape factor
s_u	Undrained shear strength
t	Time
u	Pore pressure
u	Horizontal displacement
v	Velocity
w	Water content
w	Vertical displacement
z	Depth below soil surface
$\dot{z}$	Penetration rate
α	Adhesion factor
α_f	Vertical normal stress increase to skirt wall friction ratio
β_1, β_2	Yield surface curvature parameters
δ	Interface angle of friction
γ_c	Unit weight of clay
γ_s	Unit weight of sand
γ_w	Unit weight of water
γ'	Buoyant unit weight
θ	Rotation
θ_x	Rotation about x axis
θ_y	Rotation about y axis
κ	Unload/reload slope
λ	Normal compression line
σ'	Effective stress
τ	Shear stress
φ'	Angle of friction
φ_{cs}'	Critical state angle of friction

Table of Contents

1 Introduction

1.1 Alternative energy supply in the UK and caisson foundations

1.1.1 Description of a suction caisson

Suction caissons are sometimes referred to as bucket foundations, suction piles, or suction anchors. These terms refer to a foundation which has been constructed by attaching a skirt to a flat footing, creating a caisson. The footing is installed with the assistance of suction, as outlined in the next section. Often the caisson is constructed from steel, such as those used on the Draupner jacket (Bye *et al.* (1995)), see Figure 1.1.1, but reinforced concrete can also be used such as for the Gullfaks C foundations (Tjelta *et al.* (1990)).

Caisson sizes can vary considerably. Small diameter caissons are often used for anchorages (Andersen *et al.* (2008)), as they can withstand tension and be removed rapidly with a minimum of expense. Large diameter caissons have been used for permanent structures such as the Gullfaks C Oil Platform, where the foundations were 28 m diameter (Tjelta *et al.* (1990)).

The reported skirt thickness to diameter ratios (t/D) for steel caissons take values of approximately 0.003 to 0.005 (Draupner, Tjelta), and values for concrete skirts are approximately 0.014 (Gullfaks, Tjelta *et al.* (1990)). Commonly, stiffeners are attached to the skirt to support the relatively thin steel structure when suction is applied.

1.1.2 Methods of caisson installation

The benefit of using a suction caisson foundation is that it offers the possibility for installation using the self weight of the structure and hydraulic pressure provided by a pump. The caisson would typically be constructed onshore and taken to site on a barge. The valves in the lid would be open, and a crane would lift the caisson off the barge into the water. While the caisson is in water, the valves would allow any trapped air to escape. The crane would then slowly lower the foundation onto the seabed. The skirt would penetrate into the soil under the weight of the foundation.

The structure's weight will generally not be sufficient to bury the full skirt length. A pumping system would then be connected to the vents, to remove water from within the skirt and lower the pressure within the caisson below ambient. A net downward force arises, causing the caisson to install further into the soil. When the desired skirt penetration has been achieved, the pumps are stopped, and all vents are closed off to stop water flow into the interior.

The pumping operation can be carried out using substantially less equipment than is necessary for offshore pile driving, allowing the possibility of lower overall foundation costs, particularly for deep water, where pile driving becomes difficult. Pumping can also be undertaken during weather which would stop offshore pile driving operations.

For a jacked installation, the initial phases would be similar to those for suction installation. The vents in the lid would need to be left open to allow water to escape from inside the skirt. If the weight of the structure was insufficient, additional force would be provided mechanically to drive the skirt further into the ground. This force may be applied by pumping water into a tank mounted on the structure, or by a jack using a heavy weight as a reaction.

1.1.3 History of suction caisson usage

The first reported use of a suction caisson was in 1958 (Mackereth (1958)), where the concept was used to support the apparatus for an underwater site investigation. One of the first large scale uses of suction caissons is described by Senpere and Auvergne (1982). The paper describes the successful installation of suction caissons which were then used as anchorages for mooring buoys at the Gorm Oil Field. The paper outlined the first commercial application of suction installation, and for this reason it merits closer examination.

In the paper, the authors described that the first pile to be installed encountered installation refusal at 6.6m depth. Divers were sent down to inspect the condition of the foundation, and reported that

significant plug movement had occurred. The piles were subsequently installed after a system of plug liquefaction had been developed. The success of the installations is remarkable considering the scale of plug lift created by the suction process. The paper lists sufficient data to enable an estimate of the suction pressure required. Using the installation theory of Houlsby and Byrne (2005b), it was estimated that the maximum penetration depth would be only 3.06 m before the onset of piping. It is noteworthy that plug heave occurred inside the caisson, as this is consistent with the expectation that critical hydraulic gradients would cause piping failure.

Tjelta *et al*. (1990) describe the installation of a large concrete gravity platform (Gullfaks C) in the North Sea at a water depth of 220 m. The platform was, at that time, the largest and heaviest concrete structure ever built, and was to be located in a region of challenging soil conditions. The designers opted to use 16 skirted concrete piles with a thickness of 0.4 m extending to a depth of 22 m. The skirts were to be installed by using a combination of the large platform weight and a system of suction. The paper describes that installation was completed successfully without any problems being encountered.

The success of the Gullfaks C installation led to other projects adopting the foundation, such as the Europipe 16/11E jacket structure. Bye *et al.* (1995) describe the design analysis undertaken. Particular attention was paid to installation, as the 6 m long skirts would need to penetrate through very dense sand and previous large scale installations had not tested whether this would be possible. A series of field tests were undertaken along with cone penetration tests (CPTs) to gather data to allow correlation of penetration resistance with cone tip resistance. These tests proved at a large scale that suction reduced the skirt tip resistance to a value close to zero.

Suction caissons have been used extensively as both foundations and particularly as anchor systems. Andersen *et al.* (2005) reported that by 2004, more than 485 suction caissons had been installed for use as anchors at over 50 separate locations. The industrial experience with the concept as an anchor scheme was reported as positive as there were no cases of anchor failure.

1.1.4 Aims of present work

Offshore renewable energy structures will require a large quantity of relatively cheap foundations. The conditions for these installations will vary significantly. As outlined in Chapter 1.3, standard methods of calculating the installation suction required do not yet exist. To permit the technology to be widely employed, robust installation behaviour must be demonstrated.

This work will describe the installation of model caissons into soil samples selected to be representative of conditions present around the coast of the UK. The key conditions outlined are clay over sand, sand over inclined clay and sand with a hydraulic barrier. The aims of the tests were to indicate whether the installations are feasible, and provide guidance for calculating the suction pressures required.

Experiments will be described, undertaken with the aim of exploring whether caissons can be steered and the skirt penetration depth extended. A method of selective injection at the skirt tip will be outlined, developed with the aim of meeting the objectives above. The effect of skirt tip injection should be quantified and a method of accounting for injection pressure will be presented.

Offshore caissons are suction installed, whereas those tested in laboratories were often jacked in place. The effect of pressure grouting caissons post installation has not been studied before. Experiments were undertaken to study this effect, and the foundation response to combined V, H, M, loading was measured. The aim of the tests was to measure the difference between suction caissons which had been pressure grouted and those left ungrouted. The settlement response and foundation stiffness were of primary concern in these tests.

1.1.5 Current UK electricity consumption and forecast.

In 2007, the UK consumed approximately 400 TWh of electricity (see Figure 1.1.2). Statistics show that the consumption of electricity in the UK has steadily risen since 1998 levels reaching a peak in 2006. In 2006, approximately 75 % of the UK's electricity supply was generated from coal, oil and gas, while only 4 % was generated renewably (BERR (2008)).

Many coal fired power stations are set to be decommissioned, as many are currently thirty to forty years old. These power stations do not comply with the Large Combustion Plant Directive (LCPD) and would require substantial modification to meet the minimum standard. Consequently, many operators have concluded, that it will not be economically viable to continue their operation after 2016. The predicted loss of coal generational capacity is shown in Figure (1.1.3) (Sharman and Constable (2008)). To avoid supply shortages arising from these closures, more generating capacity must be constructed soon.

With the need for more generating capacity, and with other options being unattractive, producers are likely to invest in more Combined Cycle Gas Turbine plant by default. The result will be that UK gas consumption will increase dramatically, placing greater demand on its suppliers. Historically, much UK gas was supplied from the North Sea. However, these supplies are now declining. The consumption of gas in the UK has become so large that, in 2008, the UK was the fifth largest consumer in the world (Sharman and Constable (2008)). It is estimated that by 2016 the UK will be the world's largest gas importer (Sharman and Constable (2008)).

For the UK, the most relevant gas suppliers will be Norway and Russia. There is already a supply pipeline network in place to supply gas from Norway. However, this gas alone will not be sufficient to supply the UK's 2015 consumption, as it will exceed total Norwegian 2015 production. This implies that Russian gas will be relied upon to meet the shortfall. Russian gas reserves, such as the offshore Schtokman Field, are large, and are capable of supplying the Russian domestic market with sufficient capacity left over for export. However, the necessary investment to increase production has not been made, and in 2006 Russian demand exceeded local production.

It is clear that the cost of gas is likely to increase in the future as demand is likely to exceed supply. As the cost of electricity is substantially governed by the cost of fuel, this cost will increase accordingly. Gas prices may become volatile, if supply cannot keep up with demand, and some markets may not be supplied, as has been experienced in Europe.

1.1.6 Security of electricity supply

Energy plays an essential part in every aspect of modern life. As other large countries are now developing rapidly (China, India), their energy consumption is set to increase, providing greater competition for available resources. The EU relies very heavily upon Russian gas, with approximately 25 % of its total supply being supplied by Russia, 80% of which flows through the Ukraine. Disputes have resulted in supply interruptions to European countries, leaving some countries, such as Germany, particularly badly affected, as Russian gas supplies 42 % of its needs.

The UK finds itself in a similar situation to the rest of Europe. It is therefore seeking to develop renewable energy sources under domestic control. Overall, there is an abundance of renewable energy available to meet the long term energy requirements of the UK. The Energy White Paper (BERR (2007)) states that available wind resources for exploitation stand at 150 TWh/annum, so wind energy could make a substantial contribution to generating capacity.

1.1.7 Current renewable energy position

It is planned that wind turbines be used to meet a substantial portion of new generating capacity. Many are to be installed offshore where there is unused space and reliable wind availability. Offshore installations will cause less noise and visual disturbance, because they can be placed away from areas of population. However, they suffer from more challenging foundation construction issues than those onshore. Figure 1.1.4 and Figure 1.1.5 show the location of Round 1 and Round 2 wind farm development sites respectively. Some of the Round 1 sites have been constructed, and Table 1.1.1 (BWEA (2009)) presents the status of those wind farms.

The UK Government has outlined a strategy to stimulate renewable energy generation in the Renewables Obligation. To reduce the environmental impact of electricity use, the UK Government has set a target to produce 15 % of UK electricity from renewable sources by 2015. It is planned that a substantial contribution to this target will be provided by wind power.

Wind power has often been criticised for being potentially intermittent, and therefore not a reliable source of energy. Any generating equipment cannot work 100 % of the time, but it is often assumed that wind power output fluctuations are problematical, as wind shortages are not controllable. During periods of excessive wind speeds, which can harm equipment, the turbines are stopped and no power is produced. Research has shown that the likelihood of no-wind, or excessive wind days, affecting the whole country simultaneously are small. (Only 1 hour/year where over 90 % of the UK experiences wind speeds less than 4 m/s (BERR (2007)).) Therefore by ensuring wind farms are distributed at widely varying locations, the reliability of power production can be ensured.

1.2 Forces exerted on a wind turbine foundation

1.2.1 Wind forces on a wind turbine

Figure 1.2.1 presents a photograph of wind turbines constructed offshore (BWEA (2010c)). The tower, rotor and nacelle are visible and have been labelled. Current rotor diameters are of the order of 90 m constructed on towers approximately 105 m high. The trend for future design is toward larger machinery, which will require larger rotors and towers. Figure 1.2.2 presents a diagram of the component arrangement in a typical nacelle (Vestas (2004)). Transformers are often placed at the base of the tower. The systems are designed to be capable of running with long service intervals due to the expense of access.

Figure 1.2.3 presents the power curve for a Vestas 3 MW wind turbine, which demonstrates the typical operating characteristic of such a device. Power generation can commence at wind speeds of 4 m/s with maximum power generated at wind speeds of between 14 and 25 m/s. At wind speeds higher than 25m/s, the turbine must be stopped. When the wind speed exceeds 14 m/s, the turbine blades are feathered, to avoid overloading the equipment, which limits the maximum generating capacity of the unit. In the region of wind speeds between 4 and 14 m/s, the power generated increases as the cube of

the wind speed. This machine characteristic implies that power output in this region varies drastically with small changes in wind speed.

The forces, and power output, of a wind turbine can be estimated using the Actuator Disc concept (Burton *et al.* (2001)). Figure 1.2.4 shows a diagram of a wind turbine with air travelling from an upstream source, through the turbine, and continuing downstream. The upstream speed is v_1 and the downstream speed is v_2. Using conservation of energy and momentum, the average air speed through the turbine (v_t) can be calculated from Equation 1.2.1:

$$v_t = v_1(1-a) = \frac{(v_1+v_2)}{2} \qquad \text{Eqn. 1.2.1}$$

The power output is given by Equation 1.2.2:

$$P = 0.5\rho A v_1^3 4a(1-a)^2 \qquad \text{Eqn. 1.2.2}$$

The power is often expressed by the power coefficient (C_p) which is defined in Equation 1.2.3:

$$C_P = \frac{P}{(0.5\rho A v_1^3)} = 4a(1-a)^2 \qquad \text{Eqn. 1.2.3}$$

The maximum power that can be obtained from the wind was calculated by Betz in his book Wind-Energie (1926). Betz calculated the optimal change in speed which allowed the air to slow down, but still move away from the turbine. The maximum power available for extraction is calculated by finding the maximum of Equation 1.2.2 above. The variation of C_p with a is plotted in Figure 1.2.5 which shows that the maximum power output occurs when a = 1/3, where the power extracted is 16/27 of the total power available.

The electrical power output from the machine will be lower than the power extracted from the wind, and the power generated can be calculated by the product of the wind power and the power coefficient of the turbine. Figure 1.2.6 displays the power coefficient curve for the Vestas 1.6 MW turbine (Vestas (2008a)). The power coefficient changes considerably with wind speed, and for this case has a maximum value of 0.44 which is positioned in the cubic section of the power curve before the blades are feathered.

The maximum horizontal force (F) exerted on the nacelle of a wind turbine can be estimated by the momentum change of air flowing through the blades as.

$$F = 0.5\rho A v_1^2 4a(1-a) \qquad \text{Eqn. 1.2.4}$$

The force is often expressed as a thrust coefficient, which is the ratio of force to that produced by the free stream stagnation pressure acting over the turbine area:

$$C_T = \frac{T}{(0.5\rho A v_1^2)} = 4a(1-a) \qquad \text{Eqn. 1.2.5}$$

The maximum force occurs when maximum power is generated, which is at the point were a = 1/3. At this point, the force coefficient is equal to 8/9.

Taking a Vestas 3 MW turbine, with a rotor radius of 45 m, upstream wind speed of 15 m/s, and air density of 1.2 kg/m^3, the nacelle force can be estimated, assuming that the exit wind speed is 1/3 of the entry speed in accordance with Betz, to be 0.76 MN. A plot of force variation with wind speed is presented in Figure 1.2.7. Future wind turbines will be much larger, and currently one of the largest is the Repower 5 MW prototype. This turbine has a rotor radius of 63 m, which assuming similar wind conditions above, would result in a horizontal force of approximately 1.5 MN.

1.2.2 Wave and current forces

Foundations for offshore wind turbines must withstand both wind forces and forces imparted by the sea. The most significant hydraulic forces arise from the presence of waves and water currents. Ship impact loading is also possible, so should be considered at the design stage.

Figure 1.2.8 shows the bathymetry of the sea around the UK. It can be observed that the locations set aside for wind farms generally encounter water depths of up to 30 m, with 10 m being common. Figure 1.2.9 shows a chart of the peak mean flows for a spring tide in the waters around the UK. From the chart, it can be observed that tidal velocities of up to 1.5 m/s can be encountered.

The relevant British Standard for the construction of offshore structures is BS 6349 – Maritime Structures. In BS 6349 (1986), the stated method to estimate the current load on a shaft is outlined in Equation 1.2.6.

$$F = 0.5 C_D \rho A u^2 \qquad \text{Eqn. 1.2.6}$$

For a 6 m diameter pile constructed in 10 m deep water, and with uniform current velocity of 1.5 m/s, as taken from Figure 1.2.9, the force on the pile would be 47 kN. (C_D = 0.7 BS6349 (1986))

To estimate the force on a pile from wave action, BS 6349 (1986) specifies that Morison's equation should be used. This equation expresses the total force on a pile as the sum of a drag and an inertia term. For the 6 m diameter shaft installed in 10 m water depth, if there were waves of height 4 m and no current, the total force on the pile would be approximately 630 kN. If the pile were subjected to both wave and current forces, the total force would be calculated by adding the current velocity vectorially to the particle velocity term. This implies that the force from otherwise moderate wave loading can increase significantly when combined with currents.

To obtain the loads acting on the shaft foundation, the forces from the water and wind loads are combined and expressed as a vertical load, horizontal load and moment about a reference point at the base of the foundation. These loads are shown in Figure 1.2.10.

It is now possible to estimate the forces applied by a wind turbine on its foundations when installed offshore at locations available around the UK. For this example a 3 MW Vestas wind turbine shall be used installed into water of 10 m depth. The hub height is 105 m above mean sea level, and the wave height is 4 m with a 10 s period. There is no current.

The horizontal force from the rotor exerts a force of 760 kN as calculated above acting over a lever arm of 115 m. The horizontal force from the water is estimated to be 631 kN, acting to invoke a moment load of 3.27 MNm. The weight of the tower, nacelle and rotor are reported to be 396 tonnes (Vestas

(2008b)) and the underwater supporting structure is estimated to impart an additional 100 tonnes on the foundation. These estimated loads are presented in Table 1.2.2 (case 1).

As can be observed in Figure 1.2.8, water depths of 20 m are also available around the UK. Installing the 3.0 MW turbine into this deeper water with waves of height 10 m, would increase the loads on the foundation. The horizontal load doubles while the moment increases by almost 30 %. The prototype Vestas 4.5 MW turbine will exert much larger loads on a foundation, see Table (1.2.2). It is noted from these calculations that the moment loading is large compared to the restoring moment available from the relatively low vertical force. This presents a challenging foundation design condition for a stable system.

1.3 Previous research into suction caissons installation

1.3.1 Introduction

Good foundation design would ensure that the chosen method of installation was feasible and did not have a detrimental effect on caisson behaviour. Many large scale caissons are suction installed, whereas most laboratory caissons were installed by jacking (Byrne (2000)). It has been shown that the moment resistance of a suction installed caisson is lower than a jacked caisson (Villalobos *et al.* (2005)), and therefore this must be considered during design.

The calculations for installing a caisson vary depending upon the soil conditions. When suction installation is undertaken in sand, the pore pressure changes within the soil cause significantly different behaviour than would be observed in clay. When both sand and clay are expected to be present in layers, it is currently not clear what method of calculation would be appropriate.

The data available for installation at a site would also influence the calculations that can be undertaken, as some methods use the data from a CPT test. When these are unavailable, a method of proceeding may be to use a representative CPT log composed from data taken at nearby sites. However, there are no published methods available to make this possible.

Standard methods for predicting the likely installation resistance of a caisson have, until relatively recently, been sparse (Raines *et al.* (2005)). There have been a number of installation calculation methods proposed, which are reviewed below.

1.3.2 Det Norske Veritas (DNV) Method

A method of calculating caisson installation resistance was suggested by Det Norske Veritas (DNV (1992)). Two approaches are described depending on whether steel or concrete skirts are to be used.

For the steel skirt case, the method is based upon the results of cone penetration tests (CPTs) to be undertaken at the location of caisson installation. The resistance, at a particular depth, is calculated as the sum of the skirt end bearing and side friction forces.

End bearing is calculated by relating the cone tip resistance to the caisson skirt tip pressure using a parameter k_p. The force on the end of the skirt is then calculated by taking the product of the skirt tip pressure and the tip area of the skirt.

The side resistance is related to the average CPT cone pressure by the factor k_f. The total force on the side of the skirt is calculated as the product of the installed skirt side area and the unit side resistance. The method states that where CPT testing reveals that layered soils are present, an average cone resistance should be calculated for each layer along with the area of skirt in contact with that layer. Side resistance then becomes the sum of the forces arising from each layer. Equation 1.3.1 below summarises the method.

$$Penetration\ Resistance = k_p(d)A_p\overline{q_c}(d) + A_s\int_0^d k_f(z)q_c(z)dz \quad \text{Eqn. 1.3.1}$$

Great care needs to exercised when choosing the k_f or k_p values, as these will directly influence the magnitude of resistance calculated. No laboratory tests are suggested to directly measure these parameters, so penetration tests are often undertaken to support design assumptions. When steel skirts are used, the DNV method suggests using the range of values for k_f and k_p listed in Table 1.3.1. The lower value is called the "most probable" and the higher one is called the "highest expected" value. The likely installation resistance is then expected to fall somewhere between the two extremes.

Where concrete skirts are incorporated into the design, the method states that skirt tip pressure should be estimated using bearing capacity formulas. For clay, the method is outlined in Equation 1.3.2:

$$q_p = N_c s_u(1 + s_{ca} + d_{ca}) + p'_o \quad \text{Eqn. 1.3.2}$$

For sand, Equation 1.3.3 is to be used:

$$q_p = \frac{1}{2}\gamma' B N_\gamma + p'_o N_q \quad \text{Eqn. 1.3.3}$$

For oil platforms with shallow skirts (≤0.5m), the skin friction component is neglected. For deeper skirts, the method suggests using the second part of Equation 1.3.1.

These calculations do not capture the mechanisms mobilised as the skirt penetrates the soil. It is therefore difficult to form a basis upon which to choose the k_f and k_p parameters if non-homogeneous soils are present. A key assumption is that the caisson would be installed using mechanical force alone, so beneficial seepage effects are ignored.

1.3.3. Adaptation of the CPT method to suction installation in sand

CPT testing is a popular site investigation tool for offshore construction. A large number of CPTs have been undertaken to date, allowing companies to build up large databases which can be used to generate a broad characterisation of the soil at offshore sites. Consequently, there is interest in incorporating the

sand resistance reduction to a CPT profile. A method is proposed by Senders and Randolph (2009). In this method the authors describe three phases of suction caisson installation.

1. The first phase corresponds to self weight penetration.
2. The second phase is suction installation with water pressure exit gradients below critical values.
3. The third phase corresponds to installation while a critical hydraulic gradient is maintained in the soil plug.

For the self weight penetration phase, the installation prediction method is exactly the same as that used in the DNV method. The DNV method would be applied to the problem, and an estimation of the self weight penetration depth would be made.

For phase two, the following assumptions about the forces on the skirt are made. The outside friction force is assumed to remain unmodified by the changes in pore pressure created by the application of suction. The internal skirt friction and skirt tip resistance are assumed to reduce from their self weight penetration values to zero as a linear function of the ratio of applied pressure to that required to create critical plug exit gradients.

The authors state that for the third phase of installation, the installation would proceed while critical hydraulic gradients were present in the sand. The authors proposed that the suction pressure required to install the caisson is equal to the pressure required to just bring the hydraulic gradient in the soil plug up to a critical value. The variation of suction pressure then follows as a linear function of depth as was suggested by Tran (2005).

The authors state that the CPT directly measures the sand resistance, and propose that it is therefore most appropriate to use the value of cone resistance for calculations rather than relate the data to other geotechnical parameters. The installation of a caisson skirt into soil causes an enhancement of stress at the skirt tip. The enhancement arises from the skirt friction acting to push the adjacent soil downwards

as the skirt installs into the soil. The roughness of a CPT rod is different to that for a caisson skirt (Andersen *et al.* (2008)), so the stress enhancement at the cone tip will not be the same as that caused by a skirt. The differences in stress enhancement at shallow and deep skirt penetration would need to be incorporated into the conversion factor k_p to be able to accurately predict the installation resistance from a CPT log. However, a method is not suggested to characterise how k_p should change with depth or sand density, so at this stage the designer must apply engineering judgment in the calculation of skirt end resistance.

A CPT does not have the same plan geometry as a caisson skirt. The soil strains for a CPT will therefore not be the same as for the caisson, and the conversion factor for estimating the skirt tip resistance must reflect the difference in the soil deformation mechanisms. The paper suggests that estimation for the parameter k_f could follow the method for piles suggested by Lehane *et al.* (2005). However, substantial modification had to be made to one of the constants to obtain good agreement with the data. The CPT used in the validation tests presented in the paper had a diameter of 7 mm, implying that steady state cone resistance would occur below the depth of interest for the experiments. This necessitated adjustment to the cone resistance for use in the installation calculations undertaken to validate the hypothesis.

The method disregards changes in friction on the outside of the skirt caused by seepage. Other research has noted that the outside skirt friction increases slightly (Houlsby and Byrne (2005b) and Andersen *et al.* (2008)). Disregarding this effect introduces an unconservative element into the method, as the measured suction will tend to be higher than calculated. The estimation of lower than required suction pressures is unconservative for caisson installation calculations.

Another method for predicting the installation resistance of a caisson in sand was proposed by Andersen *et al.* (2008). For the self weight penetration phase, the paper compares the results of a CPT based method with an effective stress based method. The paper then presents a suction installation model

based upon data gathered from a database of laboratory and prototype installations. The work resulted from a joint industry sponsored project which allowed the authors access to a proprietary database.

For the purely empirical model, CPT data was related to side friction and tip resistance by two factors, k_{tip} and k_{side}. These factors can be compared to k_p and k_f respectively as they serve the same function in analysis. Values of k_{tip} and k_{side} were back calculated using the measured penetration resistance by setting k_{tip} to a constant value and then calculating k_{side}. A table of the findings is presented in Table 1.3.2. The calculation model was also applied to laboratory installations to back calculate appropriate k_{tip} parameters. The laboratory tests used a caisson which could directly measure skirt tip resistance. By measuring the installation force and using the skirt tip resistance data, the skirt wall friction could be accurately estimated. The parameters calculated are listed in Table 1.3.3. The values of k_{tip} obtained from the model tests were much higher than those calculated for the prototype installations. The authors proposed that the differences are attributable to the CPT cone used.

The caisson used for the reported laboratory experiments had a significantly larger ratio of skirt thickness to caisson diameter (*t/D*) than the prototypes. Figure 1.3.1 presents a plot of the average back calculated k_{tip} factors and the reported (*t/D*) ratios. The Figure demonstrates how the ratio for the laboratory caisson was much larger than the prototype caissons by a factor of over two. Figure 1.3.1 includes the values applicable for the caisson reported by Senders and Randolph (2009). The data appears to demonstrate that there is a trend of increase in k_{tip} with *t/D* ratio, and therefore experiments should approximate this ratio accurately. A list of the k_{side} and k_{tip} factors is presented in Table 1.3.4 for comparison between the values found and those recommended. The spread of values for k_{tip} covers a wide range, which makes estimation of installation suction difficult as the expected pressures can only be bracketed within broad limits.

1.3.4. Installation in sand

During suction installation in permeable soils, seepage will occur modifying the soil stresses as discussed by Hogervorst (1980). Water will flow upwards inside the caisson plug, reducing the vertical

effective stresses, and therefore the lateral earth pressure on the caisson skirt. Flow around the tip of the caisson will reduce the skirt tip resistance. In dense sand, seepage enables installation to occur where it would otherwise not be possible due to the high resistances encountered. There is much literature which has focused on seepage during installation in sand (Erbrich *et al.* (1999), Hogervorst (1980)).

Modelling a caisson as an open ended pipe pile with a tip area corresponding to the thickness of the skirt would yield the installation resistance relationship in Equation 1.3.4:

$$V' = \frac{\gamma' h^2}{2}(K \tan\delta)_o(\pi D_o) + \frac{\gamma' h^2}{2}(K \tan\delta)_i(\pi D_i) + \left(\gamma' h N_q + \gamma' \frac{t}{2} N_\gamma\right)(\pi D t) \qquad \text{Eqn. 1.3.4}$$

Using this theory alone would underestimate the installation forces required, which can be acceptable for pile design but not for caisson installation as larger suction levels would be necessary.

The method of estimating caisson jacking force, proposed by Houlsby and Byrne (2005b), is displayed in Equation 1.3.5:

$$V' = \int_0^{h_c} \sigma'_{vo} dz (K \tan\delta)_o(\pi D_o) + \int_0^{h_c} \sigma'_{vi} dz (K \tan\delta)_i(\pi D_i) + \sigma'_{end}(\pi D t) \qquad \text{Eqn. 1.3.5}$$

The calculation of soil stress adjacent to the skirt should account for the enhancement of σ'_v by the action of the skirt penetrating the sand. As the skirt penetrates the soil, shear forces arise due to the action of friction between the metal and the soil in contact with the skirt. The consequence of friction on an element of soil is that it acts in addition to the soil weight and increases σ'_v at the base of the element. The result of this action is increased significantly with skirt penetration, as the area over which the friction acts is larger, and the vertical stresses are higher at deeper penetrations.

Houlsby and Byrne (2005b) examined the cases where the contribution of enhanced stress acted over the entire area of the plug and over a constant area outside of the caisson, which lead to solutions for σ'_v of an exponential form. The paper suggested that a more realistic approach would be to assume that the area of material which is subjected to enhanced stresses should be allowed to increase with depth. A reasonable assumption would be to allow the stresses to increase at a linear rate with depth. A further

refinement may be to assume that the increased vertical stresses close to the caisson are larger than those radially further away.

Figure 1.3.2 presents a diagram of the assumptions made regarding the variation of the area over which the enhanced stresses act. The rates of change of area are taken to be f_o and f_i on the outside and inside of the caisson respectively. Inside the caisson, the maximum area of sand which can undergo stress enhancement is limited by the plug area. At this point, it is assumed that the entire plug area undergoes uniform stress enhancement.

Taking the equilibrium of a soil element outside the caisson, (Figure 1.3.3) allows Equation 1.3.6 to be constructed, which enables the variation of vertical stress adjacent to the caisson skirt to be determined.

$$\frac{d\sigma'_{vo}}{dz} = \gamma' + \frac{\sigma'_{vo}}{Z_o} \qquad \text{Eqn. 1.3.6}$$

A similar analysis of an annulus of soil inside the caisson allows Equation 1.3.7 to be formed.

$$\frac{d\sigma'_{vi}}{dz} = \gamma' + \frac{\sigma'_{vi}}{Z_i} \qquad \text{Eqn. 1.3.7}$$

where

$$Z_o = \frac{D_o\left(\left(1 + (2f_o z/D_o)\right)^2 - 1\right)}{(4(K\tan\delta)_o)} \qquad \text{Eqn. 1.3.8}$$

and

$$Z_i = \frac{D_i\left(1 - \left(1 - (2f_i z/D_i)\right)^2\right)}{(4(K\tan\delta)_i)} \qquad \text{Eqn. 1.3.9}$$

The end bearing stress can be calculated when the stress distribution is known. The skirt tip is modelled as being equivalent to an embedded strip footing. However, the soil stresses adjacent to the tip on the inside and outside the caisson are not of equal magnitude, so the average end bearing stress cannot be calculated using simple strip bearing capacity equations. The relative magnitudes of the internal and external relative stresses will govern whether soil flows into or around the caisson. Due to the effects of stress enhancement, σ'_{vo} will be smaller than σ'_{vi} as the annulus area is smaller within the caisson. The following method was proposed to calculate σ'_{end}.

If

$$\sigma'_{vi} - \sigma'_{vo} \geq \frac{2tN_\gamma\gamma'}{N_q} \quad \text{Eqn. 1.3.10}$$

then the flow of soil is around the caisson and

$$\sigma'_{end} = \sigma'_{vo}N_q + \gamma' tN_\gamma \quad \text{Eqn. 1.3.11}$$

Else, if

$$\sigma'_{vi} - \sigma'_{vo} < \frac{2tN_\gamma\gamma'}{N_q} \quad \text{Eqn. 1.3.12}$$

Then the flow of soil is partly inside and around the caisson and the following is used to estimate σ'_{end}.

$$\sigma'_{end} = \sigma'_{vo}N_q + \gamma'\left(t - \frac{2x^2}{t}\right)N_\gamma \quad \text{Eqn. 1.3.13}$$

where

$$x = \frac{t}{2} + \frac{(\sigma'_{vo} - \sigma'_{vi})N_q}{4\gamma' N_\gamma} \quad \text{Eqn. 1.3.14}$$

For calculation of the installation suction required after self weight penetration has been completed, Houlsby and Byrne (2005b) proposed that Equation 1.3.15 be used.

$$V' + s\frac{\pi D_i^2}{4} = \int_0^h \sigma'_{vi} dz (K \tan\delta)_i (\pi D_i) + \int_0^h \sigma'_{vo} dz (K \tan\delta)_o (\pi D_o) + \sigma'_{end}(\pi D t) \quad \text{Eqn. 1.3.15}$$

The effect of suction is accounted for by assuming that a uniform downward hydraulic gradient exists outside the caisson while an upward gradient is applied to the soil within.

Erbrich *et al.* (1999) undertook a numerical investigation to examine the effect of suction on seepage flows in sand, and compared their findings to model test data. Calculations were undertaken to examine seepage flows and critical suction gradients developed in the soil during an installation using (ABAQUS). Erbrich *et al.* (1999) assumed that seepage flows cause sand loosening leading to higher permeability values. Initially, the effect of soil permeability was examined, so an annulus of soil adjacent to the skirt, equivalent to 0.07*D* wide was given an increased permeability followed by increase of permeability of the entire plug. From this analysis, it was discovered that the highest seepage gradient occurs at the caisson tip. When the quantity of disturbed soil was increased, the seepage

gradient within the caisson reduced, and increased in the soil outside the footing. During installation, the main parameter measured is applied suction. Erbrich *et al.*(1999) defined a "Suction Number" to assess suction required to induce critical hydraulic gradients which is defined in Equation 1.3.16:

$$S_N = \left(\frac{H}{d}\right)\left(\frac{\gamma_w}{\gamma'}\right) \qquad \text{Eqn. 1.3.16}$$

Where the soil permeability had increased, the suction required to induce the critical hydraulic gradients was higher than for cases where the soil permeability was unchanged.

ABAQUS was used to analyse the effect of seepage upon skirt friction. It was found that the load to overcome skirt friction was higher than that expected using an in-situ stress field. The reason outlined was that skirt friction increased the vertical effective stresses adjacent to the skirt. This analysis revealed that very high seepage gradients are required to reduce substantially skirt friction. Erbrich *et al.*(1999) suggested using the value of K_o and OCR defined by Mayne *et al.* (1982) to analyse the effect of seepage on skin friction:

$$K_o = K_{o(nc)} OCR^{sin\varphi'} \qquad \text{Eqn. 1.3.17}$$

In this case, OCR for sand is defined as the ratio of stress before suction began to the stress level with seepage present. A reasonably good correlation was found between this assumption and the finite element analysis.

Degradation of tip resistance by seepage was also studied using ABAQUS, though it was pointed out that the flow regime modelled was more applicable to a skirt stiffener. The results indicated that the end resistance degraded linearly with seepage gradient and that increasing the angle of friction increased the bearing resistance of the soil. Soil friction angles are not constant in real tests due to dilatant behavior caused by stress changes. This work demonstrated that installation suction varies with changes to permeability ratio (k_f). However, the change of k_f during installation was not evaluated, so this effect should be measured to enable more accurate installation pressures to be estimated.

Andersen *et al.* (2008) applied a bearing capacity approach to field and test data, where the jacked installation resistance was calculated using formulas for tip resistance and skirt friction. The formulas used are presented below:

$$P_f = q_{tip}A_{tip} + f_{s,av}A_{wall} \quad \text{Eqn. 1.3.18}$$

where

$$q_{tip} = 0.5\gamma' tN_\gamma + qN_q \quad \text{Eqn. 1.3.19}$$

and

$$f_{s,av} = 0.5K\gamma' z \tan\delta \quad \text{Eqn. 1.3.20}$$

The enhancement of stress adjacent to the skirt tip was included by allowing the overburden parameter (q) to increase with skirt shear stress as well as overburden in the manner presented in Equation 1.3.21.

$$q = \gamma' z + \alpha_f f_{s,tip} = \gamma' z\left(1 + \alpha_f K \tan\delta\right) \quad \text{Eqn. 1.3.21}$$

In this case, α_f is the ratio between vertical normal stress increase and skirt wall friction. The model was applied using a drained triaxial friction angle and a plane strain friction angle. It was found that the best agreement between the installation resistance and the predictions could be obtained when the drained triaxial friction angle was used. The overall conclusion was that the bearing capacity method produced better results when applied to the dataset than an empirical model using k_{tip}. The reason stated was that the bearing capacity method included the interaction between side and tip resistance.

Where suction is used to install a foundation, Andersen *et al.* (2008) proposed a method to calculate the installation suction necessary, from previous experience with suction caisson installation. The method is based upon the maximum installation depth being governed by the friction force on the outside of the skirt. When the friction force has been estimated, account is made of the downwards hydraulic gradient, and increase in soil stress, present in the soil outside the caisson. The suction required to reach penetration depths after the application of suction, but before full penetration is achieved, is estimated from curves created from installation data obtained from field tests and prototypes.

In this method, the critical suction number (Equation 1.3.16) needs to be determined. To estimate this value, the change of soil permeability ratio caused by installation has to be estimated. The permeability ratio is the ratio of permeability of sand inside the caisson to that outside the caisson. The method relates permeability to the change of relative density caused by strains arising from skirt installation. It is not clear how robust this model is when applied to different soils.

When the critical suction number has been found, a chart is presented for use to estimate the penetration caused by the application of suction. The curves on the chart are plotted as *z/t* (penetration depth/ skirt thickness) ratios, which were created from previous installation experience. As the penetration depth becomes large, the curves plot closely together making it difficult to estimate the sensitivity of installation depth to suction.

Where an installation is to be undertaken in homogeneous sand, the method may be successfully applied, however, where non-homogeneous conditions are encountered, it is unclear how the method could be modified to account for variations of soil conditions.

1.3.5. Installation in Clay

Skirt penetration in clay commences by self weight penetration. When self weight penetration has finished, further installation can be induced by either jacking or by suction. During suction installation, no modification of the soil stresses by seepage occurs and the installation force is provided by a net downwards pressure acting on the caisson in combination with the weight of the caisson.

Tests undertaken by Chen and Randolph (2003) demonstrated that the installation force required for a jacked installation was similar to that manifested by suction acting on the caisson lid. When the same value of adhesion factor (α) was used both inside and outside the caisson during back-analysis of the installation tests, the average α values were 0.36 for suction and 0.39 for jacking.

The installation and maximum penetration of a caisson in kaolin clay was studied by House *et al.* (1999). The stability of the soil plug was monitored by measuring the quantity of water discharged from the interior of the caisson. An assumption of no flow through the soil or around the skirt was made. House *et al.* (1999) stated that the required installation suction ($\Delta P_{caisson}$) can be calculated as the sum of the end bearing and friction on the skirt, taking into account caisson weight, as follows:

$$\Delta P_{caisson} = \frac{(N_c s_u + \gamma' l)A_{tip} + \alpha_i \bar{s_u} A_i + \alpha_o \bar{s_u} A_o - W}{A_{plug}} \quad \text{Eqn. 1.3.22}$$

where W is the caisson weight, and l is the skirt tip depth. The variables A_{tip}, A_{plug} and A correspond to skirt tip area, plug area and skirt area respectively. The subscripts i and o refer to inside or outside the caisson and α is the adhesion factor. House *et al.* (1999) demonstrated that the suction force driving plug lift, was resisted by shaft friction, plug weight and reverse end bearing in the manner outlined in Equation 1.3.23:

$$\Delta P_{plug} = \frac{(N_c s_u - \gamma' l)A_{plug} + \alpha_i \bar{s_u} A_i + \gamma' l A_{plug}}{A_{plug}} \quad \text{Eqn. 1.3.23}$$

where A_{plug} is the area of the plug. By equating these equations, the depth at which plug will failure occurs can be calculated.

Houlsby and Byrne (2005a) stated that when suction is applied, this should be accounted for during calculation of the end bearing term. This would reduce the end bearing term thereby reducing suction requirements shown in Equation 1.3.24:

$$V' + s(\pi D_i^2/4) = \alpha_o s_{u1} h(\pi D_o) + \alpha_i s_{u1} h(\pi D_i) + (\gamma' h - s + s_{u2} N_c)(\pi D t) \quad \text{Eqn. 1.3.24}$$

The installation balance was re-arranged to enable the plot of installation suction to be generated (shown in Equation 1.3.25 for convenience).

$$s_{caisson} = \frac{4}{\pi D_o^2}(\alpha s_u(\pi D_o z) + \alpha s_u(\pi D_i z) + (\gamma' z + s_u N_c)(\pi D t) - V') \quad \text{Eqn. 1.3.25}$$

Houlsby and Byrne (2005a) proposed that the force required for caisson installation into clay by jacking can be calculated by the equation given below:

$$V' = \alpha s_u(\pi D_o z) + \alpha s_u(\pi D_i z) + (\gamma' z + s_u N_c)(\pi D t) \quad \text{Eqn. 1.3.26}$$

The motivating force for installation, on the left hand side of the equation, is the sum of any mechanical force applied including the buoyant self weight of the structure.

Houlsby and Byrne (2005a) examined the stresses in clay due to the installation of a skirt. It was proposed that the vertical stresses would increase in the vicinity of the skirt due to adhesion effects as the skirt penetrated the soil. The outside soil stress was expressed as the sum of the overburden and the adhesion force on the skirt, spread over an area defined by a load spread parameter. A load-spread value was not specified, however, if the load is assumed to be uniformly spread over a constant size annulus outside the caisson, the vertical soil stress is described by Equation 1.3.27:

$$\sigma_{v,outside} = \gamma' h + \frac{\pi D_o h \alpha_o s_{u1}}{\pi (D_m^2 - D_o^2)/4} \qquad \text{Eqn. 1.3.27}$$

A similar analysis can be carried out for the inside of the caisson except the maximum load-spread area is limited by the inside caisson diameter.

Andersen *et al.* (1999) discussed the installation of caissons installed in the field. The penetration resistance (Q_{total}) suggested is set out in Equation 1.3.28:

$$Q_{total} = Q_{side} + Q_{tip} = A_{wall} \alpha s_u^{\overline{DSS}} + \left(N_c s_{u,tip}^{av} + \gamma' z\right) A_{tip} \qquad \text{Eqn. 1.3.28}$$

The area of the wall is composed of the total of the inside and outside skirt areas. Though this equation resembles closely that proposed by House *et al.* (1999), Andersen proposes that the undrained shear strength of the clay (s_u) be selected differently, and applies the same adhesion factor (α) to the skirt wall inside and outside the caisson. The adhesion factor is assumed to be the inverse of the clay sensitivity, and clay strength parameters are chosen from tests resembling the mechanism of clay movement at that point on the pile. Solhjell *et al.* (1998) used a similar expression to Andersen *et al.* (1999). for the Visund mooring suction anchors, but decided that an empirical value for α should be used rather than the inverse of clay sensitivity to account for clay remoulding.

Andersen *et al.* (1999) noted that the installation mechanism for a suction installed caisson would not mobilise the same skirt resistance as jacking. This was attributed to the suction causing inwards soil

flow rather than to the outside, as with jacked installations. As a result, the effective stresses outside the skirt would be lower, causing less adhesion resistance. Chen *et al.* (2003) concluded that the assumption of complete soil flow into the caisson was not valid for the suction tests. However, the caisson used for these tests featured internal stiffeners which may have resisted soil flow into the caisson.

1.3.6. Installation in layered soil

Many sites being made available for wind farms consist of non-homogeneous materials, where both sand and clay are present in layers. Concerns have been raised by Masui *et al.* (2001) and Raines *et al.* (2005) that where a layer of impermeable material overlies sand, a hydraulic blockage may be induced. This blockage may stop seepage occurring in sand, which in turn inhibits changes in effective stress. Installation resistances will then be very high and suction may no longer be a viable installation method.

Raines *et al.* (2005) conducted experiments at 100g, in which model piles were installed into normally consolidated kaolin using self weight and suction. Raines *et al.* (2005) described a test where a pile was to be installed through a layer of medium dense sand placed 30mm above full skirt penetration. The report stated that the pile could not be installed using suction, and skirt penetration into sand was only 2mm. This result suggests that the sand resistances increased dramatically due to the presence of the overlying clay layer.

Masui *et al.* (2001) described the installation of a caisson by suction and ballasting. Soil geology consisted of a 3 m thick layer of soft clay over medium dense sand. Installation through the clay was undertaken by self weight with very low penetration resistance measured. Skirt resistance increased dramatically from 5 MN in clay to over 30 MN after only 0.6 m penetration into the sand. The skirt was divided into five compartments, each of which could be either evacuated or filled with water to cause further penetration and reduce inclination. The report stated that suction was unable to reduce the vertical effective stresses in the sand due to the presence of the impermeable clay, causing high sand resistances to be encountered.

Tran *et al.* (2005) undertook a 100g centrifuge investigation to examine the effect of installing a caisson into sand with silt layers present. Suctions required to install the caisson were higher than those needed for installation in homogeneous sand, but not as high as when a jacked installation was undertaken in sand. Tran *et al.* (2005) suggested that the lower permeability of the silt required more suction to set up a seepage flow to lower tip resistance. The possibility that silt scouring occurred was also suggested, as the suction was not as high as expected for an intact layer of low permeability soil. Variation of the silt thickness from 10 to 5 mm did not decrease the suction required.

Senpere *et al.* (1982) described the first use of suction piles used as anchors in the Gorm Oil Fields. The soil conditions were loose, becoming dense, sand overlying soft, becoming stiff clay. Installation requirements were calculated using an empirical method which accounted for the reduction in resistance due to seepage. During installation of each pile, problems were encountered due to excessive plug movement causing refusal.

Tjelta *et al.* (1986) describe a large scale test carried out in the North Sea to assess the possibility of installing 22 m long concrete skirts for the Gullfaks C platform. In this test, two 6.5 m diameter steel cylinders were attached to an instrumented 2.4 m long, 0.4 m wide concrete panel. The soil profile was clay over clay and sand with sand at the base of the proposed installation.

In this test, suction was found to have little effect on tip resistance. However, the paper states that there is a need for a general method which takes into account the effect of suction at the level of the skirt tip. Instrumentation was capable of measuring skin friction. This was found to vary with penetration rate and, in the sand layers, with suction.

1.3.7. Grouted suction caisson installation

Villalobos *et al.* (2005) undertook moment loading tests on model caissons to investigate the effect of installation method on foundation response. It was found that the failure load depended on the method of installation, and that suction installed caissons withstood lower loads, during moment loading, than

jacked caissons. In order to maximise foundation efficiency, it would be useful to restore the full moment capacity of a suction caisson back to the jacked levels.

Field installed caissons are sometimes pressure grouted after penetration has been completed (Broughton *et al.* (2002)). Grout is forced into the void between the lid and the soil, and sets to match the caisson lid to the shape of the seabed. Though literature makes reference of this process, Carlsen *et al.* (1977), Gerwick (1974), no experimental work has been found which examines the effect this operation has on foundation response. A test series would enable the change of foundation response to be analysed after pressure grouting.

2 Relevant soil conditions and installation calculations

2.1 The theoretical framework for analysis

2.1.1 General approach

There are several approaches, outlined in Chapter 1.3, which could be chosen to study caisson installation. As experiments were to be undertaken in the laboratory, the framework needed to be relevant over a range of scales spanning approximately two orders of magnitude. For this reason, methods developed from previous experience with full size caissons could not be used, as the parameters derived from back analysis may not transfer appropriately to model scale. The chosen method of analysis required formulation of calculations reflecting the assumed mechanisms present during installation.

2.1.2 The approaches chosen for installation analysis

In sand, methods for estimating the forces arising during suction installation are sparse. The approach chosen for this series of tests should be capable of accurately predicting resistances when seepage was present, or when water flow was constricted. The empirical method proposed by Andersen *et al.* (2008), was based upon data taken from full size installations. This lends credibility, however, the method cannot be readily adapted to installations in soils other than homogeneous sand.

The method of Senders and Randolph (2009) applied a factor to theoretical skirt resistances to account for seepage. The assumptions for this method may not be rational for cases where layered soils containing hydraulic barriers are encountered. The method also relies upon empirical factors for relating CPT resistance profiles to installation forces. The method cannot be used at locations where CPTs are yet to be undertaken.

The method of analysis adopted was that proposed by Houlsby and Byrne (2005a). The method estimates the soil resistance acting on the caisson, and can be modified to encapsulate alternative assumptions arising from installation in different soil conditions. The method requires the variation of

skirt tip pore pressure to be estimated. To achieve this, the installation is split into a series of quazi-static steps, where steady state conditions are assumed. At each point of consideration, a calculation is undertaken to estimate the excess pore pressure at the skirt tip to obtain the variation with depth. Different installation conditions can be considered, by calculating the appropriate excess pore pressure variation.

In clay, approaches to estimate installation resistance were outlined in Chapter 1.3. Calculations generally incorporated relationships between s_u and skirt forces. For calculations where layered soils are encountered, particularly clay over sand, a strategy for estimating the clay vertical stress is required. The reason is that the stress boundary condition, at the soil interface, is required to correctly estimate the sand effective stresses. A method for estimating stresses in clay during skirt penetration was outlined by Houlsby and Byrne (2005a).

2.2 Dimensional analysis

2.2.1 Introduction

Dimensional analysis provides a means to generalise from experience and apply the knowledge to a new situation. When planning a series of experiments, this technique can be used to select experimental conditions which are relevant to the situation under examination. If the conditions are similar both in the experiment and the examined situation, then it is more likely that the model and prototype will behave in the same way.

2.2.2 Application of dimensional analysis to installation in clay

Figure 2.2.1 presents a diagram of a caisson partly installed in clay. The physical quantities relevant to this problem are shown on the diagram.

The variables relevant to this problem are: s, ρ'_c, g, D, V', t, k, s_u, α, N_c, h, $\dot{z}$, z.

The appropriate physical dimensions are mass, length and time. The formation of dimensionless groups can be undertaken using Buckingham's "Pi" theorem (Buckingham (1914)). An enhanced approach to dimensional analysis was presented by Butterfield (1999), who highlighted conditions where indiscriminate application of dimensional analysis can fail to provide satisfactory groups. A method of dimensionless analysis was presented which built on the work of Van Diest (1946), Langhaar (1951) and Palacios (1964). The method introduced further conditions to be satisfied, and leads to the correct amount of dimensionless groups being formed, and unambiguous specification of their content. This method was applied to the work below.

If ρ'_c, g, and D are chosen to be repeating variables, the following groups can be formed. The product of density and gravity is written as unit weight ($g\rho'_c = \gamma'_c$).

$$\frac{s}{\gamma'_c D}; \frac{V'}{\gamma'_c D^3}; \frac{z}{D}; \frac{t}{D}; \frac{h}{D}; \alpha; \frac{s_u}{\gamma'_c D}; \frac{\dot{z}}{\sqrt{gD}}; \frac{k}{\sqrt{gD}}; N_c$$

These dimensionless groups are examined to determine their significance to the problem. The groups $\frac{z}{D}$ and $\frac{t}{D}$ are geometrical ratios, which should be kept the same between model and prototype. This implies that the skirt thickness should be small and should be a scale model of the prototype. This ratio would take a value of approximately 0.002 as this value is commonly encountered for field caissons (Andersen *et al.* (2008)). The group containing z can be used for non-dimensionalising the skirt tip depth to compare results of non-dimensionalised suction variation. $\frac{h}{D}$ is a geometrical ratio, for which model caissons should exceed a minimum value. Skirt lengths over the minimum value will not affect correct modelling.

The groups α and N_c are influenced by material properties. The adhesion factor, α, is dimensionless, and will be similar if a metal caisson is used with similar surface finish to a prototype. N_c is the bearing capacity factor for a deep strip footing in clay, for which the value 9 is often adopted in the field and for experiments (Houlsby and Byrne (2005a), Randolph and House (2002)).

The groups $\frac{\dot{z}}{\sqrt{gD}}$ and $\frac{k}{\sqrt{gD}}$ can be combined to make $\frac{\dot{z}}{k}$. This group defines the installation rate for the experiments. The permeability of clay is very low compared to installation rates used for prototypes, so this ratio will become large. This group indicates that laboratory installations should be undertaken at similar rates to those observed for prototypes.

The groups $\frac{s_u}{\gamma'_c D}$ and $\frac{s}{\gamma'_c D}$ represent the ratios of clay shear strength and suction, to vertical stress at a depth equivalent to one caisson diameter. The first group can be combined with $(z/D)^{-1}$ to make $\frac{s_u}{\gamma'_c z}$ which can be used to define the clay shear strength profile. The second group can be used to scale installation suction.

The $\frac{V'}{\gamma'_c D^3}$ group defines the force applied to a caisson during an experiment. It is the ratio of vertical force to the weight of a clay cube of size D. This group may be multiplied by $4/\pi$ to make $\frac{V'}{\gamma'_c \pi D^3 / 4}$ which represents the ratio of applied force to the weight of a clay plug of height equivalent to the caisson diameter.

2.2.3 Application of dimensional analysis to installation in sand

Figure 2.2.2 presents a diagram of a caisson partly installed in sand. The quantities relevant to this problem are shown on the diagram.

The relevant variables are: s, ρ'_s, g, D, V', t, N_q, N_γ, $K\tan\delta$, k, $\dot{z}$, Q, h, z.

The appropriate physical quantities are mass, length and time. ρ'_s, g, and D are chosen to be the repeating variables, and the groups below are formed. Again, groups containing the product of density and gravity are written as unit weight ($g\rho'_s = \gamma'_s$).

$$\frac{s}{\gamma'_s D};\ \frac{V'}{\gamma'_s D^3};\ \frac{z}{D};\frac{t}{D};\ \frac{h}{D};\ N_q;\ N_\gamma;\ K\tan\delta;\ \frac{k}{\sqrt{gD}};\ \frac{Q^2}{gD^5};\ \frac{\dot{z}}{\sqrt{gD}}$$

The significance of these dimensionless groups is now examined. The groups $\frac{z}{D}$ and $\frac{t}{D}$ are geometrical ratios as described above, and should be kept similar between the model and prototype. The minimum skirt length for the model caisson is governed by $\frac{h}{D}$.

The groups N_q, N_γ and $K\tan\delta$ concern material properties. In a frictional material where no dilation occurs, these terms will scale correctly if the same sand is used. However, dilation results in deviations from perfect scaling. It is, therefore, necessary to consider the sand state before undertaking relevant experiments. By arranging the sand into a loose sample, dilation can be reduced. The sand particle size is also important to ensure that the same mechanisms are invoked at small scale as for a larger caisson.

The group $\frac{s}{\gamma'_s D}$ represents the ratio of suction to the vertical effective stress at a depth equivalent to one caisson diameter, and can be used to scale the installation pressure. The $\frac{V'}{\gamma'_s D^3}$ term defines the quantity of force applied to a caisson during an experiment, and represents a similar ratio as the clay group. This is the ratio of the vertical force to the weight of a cube of sand of size D. Multiplication by $4/\pi$ creates $\frac{V'}{\gamma'_s \pi D^3/4}$ which represents the ratio of applied force to a sand plug of height equal to the caisson diameter.

The terms $\frac{k}{\sqrt{gD}}$, $\frac{Q}{D^2\sqrt{gD}}$ and $\frac{\dot{z}}{\sqrt{gD}}$ are relevant to sand permeability, installation flow and installation rate. The first and last terms can be combined to make $\frac{\dot{z}}{k}$. This term defines the ratio of installation rate to sand permeability. Laboratory installations should, therefore, be undertaken at a speed governed by the permeability of the sand sample. This ratio determines that the installation speed ought to be similar to field installations if sand of similar permeability is used.

The first two terms can be combined to make the following parameter: $\frac{Q}{kD^2}$. If this group were multiplied by 4/π (dimensionless), it would represent the ratio of pump-flow to unit seepage flow distributed over the plug area. $\left(\frac{4Q}{\pi kD^2}\right)$

2.3 Application of non-dimensionalisation to suction installation

2.3.1 Calculations for caisson installation in sand using non-dimensionalised conditions

The non-dimensional relationships explored in Chapter 2.2 enable installations to be characterised and then compared if the relevant conditions are similar. This should apply even when the magnitude of physical parameters varies substantially between tests, provided the specified ratios remain the same.

The calculation framework described in Chapter 2.1 will be used for modelling installation experiments undertaken for this work. The framework has been successfully applied to caissons installed in the laboratory and to large scale prototypes such as the Draupner E foundations (Villalobos (2008), Houlsby and Byrne (2005a), Houlsby *et al.* (2006)). When the calculations were applied, good agreement was observed between recorded data and the estimates. The particular model chosen for these calculations considered stress enhancement over an area of sand which increased with depth (Equation 1.3.8). The rate of radius increase adopted was 0.75 m for each metre of installation depth.

If appropriate non-dimensional relationships are chosen, then installations undertaken at similar non-dimensional conditions should produce the same results when examined in non-dimensional form. Installation calculations will now be applied to four caissons of diameter: 0.182 m, 1 m, 5 m and 15 m. The input parameter values are presented in Table 2.3.1.

The results of the calculations are presented in non-dimensional form in Figure 2.3.1. Applying non-dimensionalisation to the results has allowed installations to be directly compared. It can be observed that despite the vast differences between each case, every test represents the same installation on a non-dimensional plot. This result is consistent with successful application of non-dimensionalisation to installation in sand, because the non-dimensional conditions were the same for each case. The values of the non-dimensional groups are presented in Table 2.3.1.

2.3.2 Installation in clay using non-dimensionalised conditions

The non-dimensionalisation for clay outlined in Chapter 2.2 is now applied to installation calculations. The framework of Houlsby and Byrne (2005a) is adopted, and the same caisson sizes will be assumed as were considered for the sand investigation. The values of the calculation inputs are presented in Table 2.3.2.

The results are presented in Figure 2.3.2. Examining the results on a non-dimensional plot, demonstrates that each case was the same despite different diameter scales. Again, the results of these tests are consistent with those expected when appropriate non-dimensional scaling groups are chosen to define the problem. These scaling groups will be adopted for use when choosing appropriate variables for modelling installation conditions in this work.

2.4 The application of non-dimensionalisation to pumped water volume

2.4.1 Using non-dimensional conditions to estimate water flow during installation in sand

In sand, seepage causes pumping flow to exceed those arising from installation of the caisson volume. The pumping system must be capable of extracting water sufficiently quickly to maintain suction. A method of estimating water flow from a caisson would be useful for planning an installation to ensure that suitable equipment was made available. This section will only focus on pumped flow in sand as the action of suction installation in clay does not cause significant seepage. The pumping flow rate in clay is assumed to be proportional to the caisson diameter and installation speed.

In Section 2.2, the following non-dimensional relationships were presented for use with flow calculations during installation: $\frac{\dot{z}}{k}$ and $\frac{Q}{kD^2}$. The $\frac{\dot{z}}{k}$ group defines the installation rate relative to the permeability of the sand into which installation is made. To maintain the similarity of this group between models and prototypes, the speed of penetration should be chosen to achieve the appropriate ratio. The speed of installation can be varied by changing the pumping rate. Using laboratory equipment, the rate of installation can be controlled over a wide range of speeds up to over 20 mm/s. This wide range of penetration rates enables the rate group to be accurately modelled when soils of different permeability are used. If an installation is to be undertaken in the laboratory using sand collected from the site of installation, the permeability of the model and prototype would be similar, so the same installation rate should be applied in both tests. Choosing the correct installation rate, allows the pumped water volume to be correctly modelled, as seepage volume will depend on both permeability and installation time. The rate of installation for field tests is recorded to be in the range of 0.1 to 2 mm/s, and the sand permeability is recorded to be 4×10^{-5} to 1.4×10^{-4} m/s. The sand in the laboratory has a permeability of 1.5×10^{-4} m/s (Kelly *et al.* (2004)) which results in appropriate laboratory installation rates of 0.1 to 0.5 mm/s. Therefore, installations undertaken at rates outside this range are not relevant for scaling to prototype dimensions.

The $\frac{Q}{kD^2}$ group is a non-dimensional flow rate, which can be used with the non-dimensional installation depth to plot the variation of flow rate. This group is the dependant variable which can be compared when all other groups are maintained similar.

2.4.2 Preliminary estimate of the pumping discharge during installation in sand

In sand, the installation suction estimate, outlined in Chapter 1, assumed that the hydraulic gradient within the caisson varied linearly with depth. A relationship was proposed for the variation of excess pore pressure at the skirt tip with penetration. These assumptions can be used as the basis for a flow discharge calculation. Assuming that no plug heave occurs, the flow out of the caisson (Q_{total}) is the sum of seepage flow ($Q_{seepage}$) and the volume of caisson installed per unit time ($Q_{caisson}$).

$$Q_{total} = Q_{seepage} + Q_{caisson} \qquad \text{Eqn. 2.4.1}$$

The discharge flow can be related to installation rate ($\dot{z}$) and the area of the caisson ($A_{caisson}$) in the following manner:

$$Q_{caisson} = A_{caisson}\dot{z} \qquad \text{Eqn. 2.4.2}$$

Applying Darcy's law to the plug inside the caisson, where it is assumed that the sand permeability (k) is uniform and the tip pressure can be calculated by the suction factor a, the seepage discharge is estimated to be:

$$Q_{seepage} = \frac{A_{caisson}k(s - as)}{gz} \qquad \text{Eqn. 2.4.3}$$

The estimated discharges for the caissons described in the previous Section are displayed in Figure 2.4.1. The seepage flow has been non-dimensionalised. It can be observed that the discharge from caissons installed at similar installation rates may be non-dimensionally similar if the discharge can be accurately modelled using the assumptions set out above. This calculation assumes a 1-Dimensional flow field, appropriate for deep installations but less accurate at shallow depths. The maximum pumping rate is reached at the end of installation, and governs the choice of suitable equipment. As the pumping rate at the end of installation is of most interest, where the assumptions best match the flow field, the calculation may enable pumping requirements to be estimated.

2.5 Known soil profiles present around the UK

2.5.1 Soil profiles present at locations of future offshore wind farm development

The sites made available for Round 1 and Round 2 wind farm development are shown in Figure 1.1.4 and Figure 1.1.5. A report commissioned by the DTI, (Sea and Land Power (2005)) examined the soil conditions present at the locations of Round 1 development. From Figures 1.1.4 and 1.1.5, it can be observed that there are generally three main areas of interest. The report refers to these areas as The Irish Sea Area, The Thames Estuary and East Anglia/ Skegness area. The study estimated the likely subsurface soil conditions for each site, based upon data held at the Fugro Geotechnical Database. The study then grouped geologically similar soil conditions within the top 20 m of soil for each site. As caissons are relatively shallow foundations, filtering results over the top 20 m of soil should produce a relevant classification.

From this exercise, three main soil profile types were identified which the report called "soil provinces". They are listed below:

- Soil Province 1. Sand to a depth exceeding 15 m.

- Soil Province 2. Sand over clay. The sand depth at these locations was estimated to be less than 15 m. This soil province was split into three sub-provinces according to the strength of clay beneath the sand.
    - Sub-province 2a consisted of clay material up to a strength of 100 kPa.
    - Sub-province 2b contained profiles where the clay strength was in the range 100 to 250 kPa.
    - Sub-province 2c consisted of any clay stronger than 250 kPa.

- Soil Province 3. This category contained any site where bedrock was encountered at less than 15 m depth. The soil above the bedrock was classified as being either mostly sand or clay as follows.

- Sub-province 3a contained sites with less than 15 m of sand over bedrock.
- Sub-province 3b contained sites with less than 15 m of clay over bedrock.

Table 2.5.1. shows an extract from the DTI report, where the soil conditions for each Round 1 wind farm development are listed. From this study it was concluded that the seabed around the UK, at the locations and within the depths of interest, consisted most usually of sand overlying clay. In the conclusions, the report stated that at some areas the clay may be up to 15 m thick while at others the sand may be negligible. If a site was encountered where there was clay present with a negligible sand layer, then for a shallow foundation installation, the site may be appropriately characterised as consisting of clay.

The report contains useful information specific to Round 1 locations. For Round 2 sites, the soil conditions are likely to vary, and although the Round 1 data provides a good indication of soils present, a further assessment would need to be carried out wherever development is planned on a case by case basis.

For this project, new data were obtained from the Fugro Geotechnical Database of the likely soil conditions available at the three main areas set aside for development in Round 2 developments. The data are shown in Appendix A, issued by Fugro through personal communication. In the site descriptions, the area referred to as “Spurn” corresponds to the area by East Anglia/ Skegness, and the Liverpool Bay region corresponds to the relevant area in the Irish Sea. Soil profiles were made which were characteristic of soils present in areas relevant to Round 2, but no attempt was made to characterise the soils at individual sites.

As expected, both soil descriptions are broadly similar, as they both originate from the same database. The second dataset was obtained because it included more detailed soil descriptions. For instance, the first East Anglia/ Skegness profile, adds detail regarding the presence of cobbles and boulders. The

presence of boulders may disrupt attempts to install a small caisson if the resistance they impose cannot be overcome.

The data were used to characterise relevant conditions for study, in an investigation of suction caisson installation. The Sea and Land Power (2005) findings were that relevant caisson sizes lay in the range of 5 to 25 m diameter, and the range of skirt sizes lay in the range 0.6 to 12.5 m length depending on whether quadruped or monopod foundations were to be used. In practice, scour considerations may limit the minimum skirt size, however, it is noted that skirt lengths have a large range of variation.

In the detailed soil description, the first East Anglia/ Skegness profile states that gravel over clay, or only clay may be encountered over the first 5 to 10 m depth. The description states that the clay is likely to contain layers of sand amongst occasional layers of gravel and cobbles. The thickness of the sand layers is not mentioned, however, over a large area this thickness is likely to vary, and may become large enough to be considered of significance when planning a caisson installation.

The third East Anglia/ Skegness soil profile, states that soil may comprise sand over clay reached at a depth of approximately 1.5 to 2 m below the surface. However, the sand description states that pockets of clay may be encountered, and the clay description indicates that occasional gravel and sand may be present. For small diameter caissons, this installation may then be appropriately modelled by a sand installation containing a clay layer encountered at 1.5 to 2 m depth.

The third Liverpool Bay area soil profile, states that the top soil layer may be sand or clay overlying clay with sand (which is in turn interbedded with clay) to a depth of between 5 to 30 m.

From the descriptions outlined in the detailed soil data, it is noted that due to the range of variation of caisson skirt sizes, the soil conditions local to a caisson may appear to comprise either homogeneous clay, homogeneous sand or layered materials. Where layering is encountered, the soils may be clay over sand or sand over clay. Therefore experiments investigating installations in homogeneous sand or clay

are relevant, as are experiments which investigate installations into sand over clay or clay over sand. The relevant thickness of the layering depends on the size of caisson to be installed at the site.

2.5.2 Strength of soils present around the UK

In Table 2.5.1., the most frequently encountered soil profiles belong to the 2b and 2c soil provinces, which are present at all three main areas of wind farm development. These correspond to clay profiles which are greater than 100kPa. Wherever 2c is expected, 2b is expected as well, with the exception of Kentish Flats. However this site lists the expectation of encountering 2a, so variable ground conditions are likely. Soft clay soils are present in Round 1 development areas at both developments in the Thames Estuary and at Shell Flats where soil province 2a is expected. Soil province 2a corresponds to s_u of up to 100 kPa.

The detailed Fugro soil data can be used to classify more closely the strength of clay present at Round 2 sites. The strengths are defined according British Standard 5930 – Code of Practice for Site Investigations. A data summary with applicable clay strengths are presented in Table 2.5.2. At the East Anglia/ Skegness area, the first soil profile describes that up to 10 m thick clay may be present over sand. The third East Anglia/ Skegness profile describes the presence of clay to a depth of up to 15 m containing areas of sand. This soil profile describes that sand may be present over clay for depth of up to 2 m.

In the third Liverpool Bay description, the top 5 m of soil may comprise Estuarine deposits composing clay described as being soft to very stiff. As the description states that deposits may contain sand and gravel, there is a potential for caisson installation to encounter a clay over sand soil profile. This profile describes that s_u will be variable. For clay over sand profiles, the clay strengths likely to be encountered lie in the wide range of 20 to 300 kPa.

In the Thames Estuary, the second soil profile describes that very soft to soft clay may be encountered at depths of 10 m. This clay description states that sand may be encountered in the clay. The clay is

overlain by sand, so a large caisson installation with a skirt length of 12.5 m (the upper end of the DTI range) may encounter sand with a clay lense. If no sand were encountered within the clay, then the installation would be into sand over clay with strength less than 40 kPa.

There are many descriptions outlining the possibility of encountering sand over clay. For example, the first Thames Estuary soil profile, states that there is likely to be up to 3 m of sand covering firm to stiff clay. The second East Anglia/ Skegness site describes up to 2 m of sand over clay. All sand descriptions state that the relative density corresponds to medium dense or greater, with the exception of the second East Anglia soil profile, where the sand is loose to very loose.

2.6 Plug lift potential in clay over sand

2.6.1 Introduction

The installation of a caisson into homogeneous soil, particularly clay, has been the subject of a number of investigations. However, there has been little attention paid to how the effects of two different soil conditions may affect installation behaviour. The reason for this is perhaps that caisson technology has been used offshore, often in the oil and gas sector, for foundations or anchorages where the soil conditions are uniform over extensive areas.

The subsurface soil around the UK is expected to be significantly variable, particularly in estuaries. The installation of a suction caisson may be in clay in which there are significant pockets of sand (see Section 2.5), and therefore installation will comprise of penetration through clay into sand.

Andersen *et al.* (2008) briefly mention the effect that a clay layer has on installation in an otherwise sand only soil. The suction requirement was found to be much larger, and sand seepage was substantially reduced, compared with installation in homogeneous sand. No calculations or results were presented in support of the claim.

While installation in layered soils has not been studied in the same level of detail as installations in either clay or sand, some research has been directed towards the problem. Tran (2005) studied the effect of layered silt and cemented materials on caisson installation. It was found that low permeability silt hindered the set up of seepage gradients in sand, and the consequence was that larger suction pressures were required. Cemented layers were found to increase the pressure required for installation, but installation was still possible. The work did not provide specific guidance on how to quantify the installation of a prototype so more work is necessary to enable the findings to be of practical use.

Senders *et al.* (2007) examined installation into clay over sand with the objective of testing whether the skirt could be installed to a target depth in dense sand. The purpose of the study was to support the design of an offshore foundation. The paper published the result of a caisson installation undertaken in a centrifuge at 150 g. The caisson was jacked to penetrate the skirt tip into the sand layer at which point suction was applied to test whether further penetration was possible. A small degree of further installation was achieved before the test ended. High suction pressures at the end of the test led the authors to state that lifting of the clay plug may have occurred. Flow calculations using pumped water volume data were presented to support this hypothesis.

While the installation of a skirt through clay may be possible in very low shear strength soils or where the self weight of the structure is particularly high, problems may be experienced in soils of moderate to high shear strength or where the structure has a low self weight. The problem encountered may be that a high shear strength soil needs more suction to install the caisson, and the magnitude of this suction may be sufficient to cause the clay plug to lift. It is therefore necessary to separately investigate the phase of installation in clay, before sand has been reached. The work of Senders *et al.* (2007) did not cover this aspect of installation.

2.6.2 Relevant caisson sizes and soil conditions

To plan a series of experiments, field data should be consulted to obtain clay strength data. In Chapter 2.6.1, caisson sizes were identified to lie in the range of 4 to 30 m diameter. Caissons are generally

constructed from steel, and the wall and lid thicknesses may be approximately 40 mm for monopods. For tripods, where the diameters will be smaller, wall and lid thicknesses of approximately 25 to 30mm may be encountered. The properties of these caissons are listed in Table 2.6.1, along with the dimensions of laboratory caissons including those for the model used in the centrifuge.

Field caissons for wind turbines would be installed with attachments to enable connection to a super-structure. This structure adds to the self weight of the caisson and should be taken into account when calculating the installation load. For preliminary calculations, it was assumed that a 1 m diameter, 25mm thick, steel shaft was attached to the caisson of length equivalent 1.5 times the caisson diameter.

Data for the field conditions at the three proposed wind farm sites has been described in Chapter 2.5 where it was noted that the range of s_u values of interest is wide. Table 2.6.1 lists the properties assumed for the soil used in the lab and on site.

Using the field data, it is possible to calculate the $\frac{V'}{\gamma'_c D^3}$ and $\frac{s_u}{\gamma'_c D}$ ratios for the tests to be undertaken. The results are listed in Table 2.6.1. It can be observed that the calculated s_u values of interest are achievable in the laboratory using standard consolidation equipment. If a slightly larger caisson is used, then the clay strength may be increased accordingly.

The self weight values of the caisson are low, of the order of a few Newtons. The caisson should be provided with a counterbalance system to closely control the applied force. Again, where a larger caisson is to be used, the force applied will increase. This will happen rapidly, as the relationship is proportional to the cube of the diameter.

The values appropriate for use in a centrifuge have been provided for an actual caisson size of 0.08 m diameter installed at 100g. Using standard centrifuge scaling convention, this would be equivalent to a prototype size of 8 m diameter. The soil unit weight in flight would be 620 kN/m^3. The force and

undrained shear strength relationships were calculated using the non-dimensional relationships defined above. The result was that the clay strength should be the same as in the field, and the applied force should be 41 N. This is entirely consistent with centrifuge scaling where s_u scales in the centrifuge to the same value as at 1g and the applied vertical load scales with N^2.

The installation conditions of interest can be plotted in non-dimensional space. This is presented in Figure 2.6.1. The grey area corresponds to the area within which a field installation is likely to fall. The calculations undertaken to define this area assumed that the range of caisson sizes lies within the range of 4 to 30 m.

The large diameter caissons lie to the left of the grey area, whilst the small diameter caissons plot to the right hand side as they are estimated to be installed with a larger self weight proportional to their size. The magnitude of the grey area is limited on the vertical scale by the maximum clay shear strength encountered before the clay becomes weak mudstone.

2.6.3 Calculations to estimate plug lift in clay over sand

During installation in clay over sand, suction will be applied to the interior of the caisson to provide additional hydraulic force to install the foundation. The suction pressure acts not only over the underside of the caisson, but also on the interior of the skirt and the top of the soil. The large areas over which suction acts allows the pressure to develop significant forces, and therefore skirt stiffeners are sometimes needed to avoid the relatively thin component buckling during installation.

While suction is applied, the pressure above the plug decreases, whilst the water pressure on the underside remains unaffected because the clay provides a hydraulic barrier. The pressure difference results in a net upward force on the plug. Plug lift will occur when the forces disturbing the plug exceed those available to keep the plug in position. Where the clay layer is not intact, the hydraulic barrier is broken and the application of suction will decrease the pressure beneath the base of the clay plug.

To estimate whether plug lift will occur, the suction required for installation and the suction required for plug lift will be calculated as a function of depth. These two equations will have two unknowns, the suction (s) and the depth (z) at which plug lift will occur. By substitution of one into the other for the unknown s, it is possible to estimate the depth at which plug lift will occur for a given clay strength (if it happens at all).

Figure 2.6.2. shows a diagram of a caisson being installed into soil consisting of clay over sand. The pressures marked on the diagram refer to deviations of water pressure from the hydrostatic case at the labelled location. The pressures are $p_{ambient}$, $p_{suction}$, and p_{base}, which correspond to pressures just above the caisson lid, inside the caisson and in the sand just below the clay layer respectively. To simplify calculations, two pressure differences will be defined, s_{plug} and s. The definitions of these pressures are as follows:

$$s_{plug} = p_{suction} - p_{base} \quad \text{Eqn. 2.6.1}$$

$$s = p_{ambient} - p_{suction} \quad \text{Eqn. 2.6.2}$$

The parameter s corresponds to caisson installation suction. As the pressure inside the caisson reduces, the installation suction increases. A limit for the magnitude of s is imposed by $p_{ambient}$ as the absolute pressure inside the caisson cannot be reduced to below 0 kPa.

The suction causing the plug to move (s_{plug}) is governed by water pressure changes from hydrostatic above and below the plug. If installation suction affects only the water inside the caisson, the magnitude of the parameter s_{plug} increases since p_{base} remains the same, and an upward force will act on the plug. If suction causes the pressure at the base of the clay to decrease, then this will decrease the pressure difference at the top and base of the clay and reduce the uplift force.

The suction estimate for a caisson in clay is made by calculating the equilibrium of the forces acting on the caisson (see Figure 2.6.3.). The equation below shows the equilibrium of these forces (Houlsby and Byrne (2005a)).

$$V' + s_{caisson}\frac{\pi D_o^2}{4} = \alpha s_u(\pi D_o z) + \alpha s_u(\pi D_i z) + \left(\gamma' z + s_u N_c\right)(\pi D t) \quad \text{Eqn. 2.6.3}$$

The forces acting on the plug are outlined in Figure 2.6.4, and the calculation for equilibrium is shown below.

$$F_s = W' + F_\tau + F_{shear} \quad \text{Eqn. 2.6.4}$$

Force to lift plug = force to overcome skirt adhesion + force to shear intact clay + Force to support plug weight

$$s_{plug}\pi\frac{D_i^2}{4} = \gamma_c' h_c \pi\frac{D_i^2}{4} + \alpha s_u \pi D_i z + s_u \pi D_i (h_c - z) \quad \text{Eqn. 2.6.5}$$

$$s_{plug}\pi\frac{D_i^2}{4} = s_u \pi D_i (z(\alpha - 1) + h_c) + \gamma_c' h_c \pi\frac{D_i^2}{4} \quad \text{Eqn. 2.6.6}$$

Re-arranging the plug lift and installation equations for suction yields the following equations:

$$s_{caisson} = \frac{4}{\pi D_o^2}\left(\alpha s_u(\pi D_o z) + \alpha s_u(\pi D_i z) + \left(\gamma' z + s_u N_c\right)(\pi D t) - V'\right) \quad \text{Eqn. 2.6.7}$$

and

$$s_{plug} = \frac{4}{D_i^2}\left(s_u D_i (z(\alpha - 1) + h_c) + \gamma_c' h_c \frac{D_i^2}{4}\right) \quad \text{Eqn. 2.6.8}$$

Both of these equations are functions of z. Taking a model caisson installed in the laboratory, it is possible to estimate, using the theory above, the suction required for installation and plug lift. In this example, the caisson is 200 mm diameter with a skirt thickness of 2 mm and a submerged weight of 15 N. The clay layer undrained shear strength is assumed to be 6 kPa, with a thickness of 100 mm (half the diameter of the caisson). It is also assumed that the adhesion factor is 0.4 and the submerged unit weight of the clay is 10 kPa/m.

Figure 2.6.5. presents the variation of suction required for plug lift and installation plotted on the same axis. It can be seen that, the suction required for plug lift is lower than that required for installation when the skirt has reached the base of the clay layer. It is expected that when the suction required for installation exceeds the plug lift value, further installation into the clay would result in plug lift if suction did not affect the water pressure at the base of the clay.

Substituting for the clay suction into the installation balance equation above yields the following expression which determines the depth at which plug lift may occur, assuming all forces act over an area proportional to *D*:

$$z = \frac{4V' + \pi D^2 \gamma'_c h_c + 4\pi D s_u h_c - 4\pi D t s_u N_c}{\pi D \left(8\alpha s_u + 4t\gamma'_c - 4s_u(\alpha - 1)\right)} \quad \text{Eqn. 2.6.9}$$

It is noted both in the expression, and Figure 2.6.5, that the lowest suction for clay lift occurs when the skirt tip reaches the base of the clay layer ($z = h_c$). Substitution of h_c for z into the above equation yields the following:

$$V' = \alpha s_u \pi D h_c + \left(\gamma' h_c + s_u N_c\right)(\pi D t) - \gamma'_c h_c \pi \frac{D^2}{4} \quad \text{Eqn. 2.6.10}$$

which can be rearranged to calculate the strongest clay material into which installation can be undertaken without encountering plug lift before the skirt tip reaches the base of the clay layer.

$$s_u = \frac{V' + \left(\frac{\gamma' h_c \pi D^2}{4}\right) - \gamma' h_c \pi D t}{(\alpha h_c \pi D + N_c \pi D t)} \quad \text{Eqn. 2.6.11}$$

If s_u is greater than the value calculated above, plug lift would be expected before the skirt reaches the base of the clay layer. The equation for s_u can be rearranged by multiplying both sides by $\frac{1}{\gamma'_c D^3}$ yielding the following non-dimensionalised equation:

$$\frac{V'}{\gamma'_c D^3} = \frac{s_u}{\gamma'_c D}\left(\alpha\pi \frac{h_c}{D} + \pi N_c \frac{t}{D}\right) + \frac{h_c}{D}\left(\pi \frac{t}{D} - \frac{\pi}{4}\right) \quad \text{Eqn. 2.6.12}$$

Using this equation, it is possible to plot on Figure 2.6.6. the zones where plug-lift occurs in non-dimensional space. The clay layer is assumed to be half the thickness of the caisson diameter. The line on the plot shows the conditions where plug lift is expected when the skirt tip reaches the base of the clay layer. Installations made in the zone below the line (Safe zone) will not experience plug lift during installation in clay, while those above will (Unsafe zone). (Where installation is to continue into the sand below the clay, plug lift may occur if the sand resistances subsequently become large enough.)

In Figure 2.6.7, the ranges of clay strength have been added to illustrate the relationship between clay strength and plug lift for a 4 m diameter caisson. The areas have been chosen to correspond with the clay strength definitions given in BS5930 (1999) shown in Table 2.5.2. In Figure 2.6.8., the ranges of clay strength have been plotted which correspond to a 20 m diameter caisson. The same scale vertical axis has been used as Figure 2.6.7. It is clear that the non-dimensional clay strength reduces for a given clay strength when the caisson diameter increases.

The weight of the caisson and structure attached to the footing needed to be estimated for calculation of where field conditions lie in relation to the uplift line. For this estimation, the assumption was made that the caisson would comprise the skirt and lid without stiffeners, with a simple structure attached at the top to provide connection to the rest of the structure. The entire footing was assumed to be submerged below the water and comprise entirely of steel.

The thickness of the caisson skirt was assumed to be 0.002 the diameter of the foundation which is similar to the ratios recorded for installed structures (Andersen *et al.* (2008)). The minimum skirt thickness was set as 25 mm, as the skirt needs to maintain sufficient rigidity when encountering obstacles in the ground. The caisson lid was assumed to be the same thickness as the skirt and the skirt length was assumed to be 0.75D. The structure attached to the caisson was assumed to comprise of a steel cylinder of height equal to the caisson diameter. The diameter of the tube was assumed to be 1.5 m and the thickness of the steel was assumed to be the same as the thickness of the caisson skirt.

In Figure 2.6.9, two example installation conditions taken from the field data have been plotted. From the plot, it can be seen that field installation conditions lie on either side of the boundary of plug lift. Taking two example installations of a 20 m and 10 m diameter caisson into two locations outlined below, the 20 m diameter caisson can be successfully installed into clay with an average strength of up to 83 kPa. Therefore, installations using a 20 m diameter caisson through stiff or hard clays may experience plug lift. The data shows that installation may be possible in clays which are firm or

weaker. The 10 m diameter caisson can be installed into clay of average shear strength up to approximately 90 kPa.

In the area of Liverpool Bay, where the data shows soft to stiff clay present in layers of up to 5 m thickness, installation of a 10 m diameter caisson may therefore be possible using suction as a principle installation force. Good familiarity of the site would be necessary, however, to ensure that installation does not encounter clay which is stiff.

At the East Anglia development area, the clay overlying sand is anticipated to be stiff to hard and therefore the shear strength is likely to be a minimum of 75 kPa. The calculations outlined above suggest that plug lifting may occur if a 20 m diameter caisson is installed using suction at the East Anglia site.

In Figure 2.6.10, the sensitivity of the uplift boundary with respect to variation of adhesion factor is presented. As the adhesion factor increases, the uplift boundary is lifted allowing caissons to be installed into stronger clay before the onset of plug lift presents itself. For installations where the adhesion factor within the caisson is the same as that outside, larger adhesion factors allow deeper penetration depths to be achieved. A lower adhesion factor outside the caisson would be beneficial for lowering the resisting forces acting on the caisson without lowering the suction necessary for plug lift.

2.7 Conclusions

The framework of Houlsby and Byrne (2005a and 2005b) was chosen to study the installation of caissons in clay and sand. This framework was chosen because the calculation of forces acting on the caisson offered a robust method which could be adapted to consider installation in layered soils.

Key parameters were identified for the installation of caissons in clay or sand. These parameters were then used as the quantities for a dimensional analysis investigation. The method recommended by

Butterfield (1999) was used to create dimensionless groups. These groups can be used to characterise field installations, and create laboratory installations which have similar conditions but different (smaller) dimensions. To enable the characterisation of field installations, the dimensions appropriate to these installations were presented and the corresponding dimensionless groups were calculated. Calculations were undertaken to test the non-dimensional groups on different size caissons to demonstrate that the installations were the same.

Data was obtained outlining the known soil conditions present around the coast of the UK at the locations set aside for Round 2 wind farm developments. It was discovered that the expected clay strength varied widely and that sand was expected at many locations. The sites of development are also expected to encounter areas where both sand and clay are present in layers.

Calculations were presented to estimate the possibility of encountering clay plug lift during an installation into clay over sand. The calculations enabled comparison of installation suction and plug lift suction. It was concluded that plug lift can occur before the skirt tip reaches the base of the clay layer.

The non-dimensional conditions for plug lift were identified and presented on a non-dimensional plot. The areas where plug lift was possible, the Unsafe zone, were separated by a linear boundary from those where installation was calculated to be achievable, the Safe Zone. It was determined that some field installations can plot in the Unsafe Zone, and therefore may encounter plug lift. The relevant range of laboratory parameter values were identified, based upon non-dimensional installation conditions, to enable similar model experiments to be undertaken.

3 Generic equipment

3.1 Introduction

The apparatus and software needed to be constructed before any experiments could be undertaken. At the design stage, it was chosen to create a robust system so that modifications could be easily undertaken when necessary to study unforeseen installation behaviour.

3.2 Description of soil properties

The sand used for the tests undertaken at the University of Oxford was Redhill 110. The properties for this sand are listed in Table 3.2.1 (taken from Kelly *et al.*(2004), and Villalobos *et al.* (2005)) . Redhill 110 is a sieved silica sand with a d_{50} of approximately 150 μm. A particle size distribution curve is shown in Figure 3.2.1 (WBB Minerals (2001)).

3.3 Sample preparation and tank sizes

The dimensions of the aluminium tank used for homogeneous sand installations are listed in Table 3.3.1 (small tank). The sand was weighed when dry so that the relative density could be calculated. The sample was prepared by liquefaction with an upward hydraulic gradient and settlement after the gradient had been removed. The bottom of the tank was fitted with four jets which were connected to a single source of water pressure. The water pressure was distributed over the bottom of the sand by attaching a layer of geotextile over the jets. When pressure was supplied, the geotextile lifted partly away from the base of the tank creating a void which filled with water. The geotextile permitted water to pass from the void into the sand supplying the upward hydraulic gradient for liquefaction.

After the sand had settled, the relative density of the sample was very loose. The sides of the tank were then tapped with a soft-face mallet to vibrate the sand, compacting it to the required density for the experiments. The volume of the sample was measured to calculate the relative density of the sand. The caisson was installed in the centre of the tank with one installation undertaken in each sample.

3.4 Model caissons

Seven caissons were used for the experiments described in this report. The dimensions of the caissons are listed in Table 3.4.1. All caissons had two pressure transducers attached which allowed measurement of water pressure inside and outside the caisson. An opening in the lid of each caisson allowed water to be removed from the interior during installation.

3.5 Test apparatus

The apparatus for the homogeneous soil installations was designed to restrict lateral displacements and rotations. The caisson was to be counterbalanced to enable the appropriate self weight force to be applied during the installation, irrespective of the weight of attached instruments. Figure 3.5.1 presents a diagram of the installation apparatus, and Figure 3.5.2 shows a photograph of the equipment with a caisson fitted.

One of the main test objectives was to measure the installation forces. This was to be accomplished by measurement of suction pressure, and the submerged caisson weight. The system needed to restrain the caisson with a minimum of friction between the slider and the frame, as this force would introduce an error into the resistance calculations.

A linear guidance system was constructed by making a slider, which comprised of a 510 mm long, 12.5 mm diameter, stainless-steel bar, inserted through two 13 mm diameter holes spaced 76.2 mm apart. The holes were bored into aluminium box section, which comprised part of the guidance frame, and reamed to ensure that they were smooth. The design did not need lubrication, so any sand which entered the bearing simply fell back out again. The clearance between the rod and the hole was sufficiently large to be greater than the size of the particles of sand. A clamp was incorporated into the system to suspend the caisson above the installation site for convenience.

A pulley counterbalance system was added to the frame to control the penetration weight of the caisson. The counterbalance system was connected to the caisson at the top of the stainless-steel rod. The counterbalance wire was chosen to be small diameter, to minimise the forces required to run over the pulleys. The pulleys ran on ball bearing races to lower the friction of the system.

An LVDT transducer mounted on the guide frame was used to measure the installation depth of the caisson. The LVDT piston could not be submerged in water, so the top of the stainless steel rod was used as the displacement reference point.

A gear pump, manufactured by Ismatec, was chosen for pumping which could be controlled with an RS232 link from a PC. The gear pump head incorporated components which were made from (PTFE) plastic and would have been harmed if sand became entrained in the pumped water. To protect the pump from damage, a sand trap and in-line paper filter were used to remove any material from the flow of water before it entered the pump. A diagram of the pumping scheme is shown in Figure 3.5.3.

The water pressures inside and outside the caisson were measured by two Druck transducers. Transducer signals were conditioned by RDP 611 instrument amplifiers and pressure calibration was undertaken by applying a series of known pressures using a water column. The purpose of the transducer above the caisson was to record the ambient pressure as the caisson was installed which acted as a reference point to calculate the installation suction pressure.

The water pumped out of the caisson was collected in a tank which was suspended from a load cell. The load cell was calibrated by application of a series of known forces and measurement of the voltage signal with each force application. By recording the weight of the water pumped out of the caisson, the volume of water pumped could be measured throughout installation. The water was pumped through 8 mm diameter transparent plastic tube. The pipe was sufficiently flexible to allow the caisson to move relative to the installation pump, positioned on the laboratory bench, without causing significant changes of applied force on the suction caisson.

The signals from the transducers were logged by a 16 bit analogue to digital Texas Instruments PCI-6221 card. The card enabled data acquisition and was supplied with LabView software. The data was sampled and average values were taken at a frequency of approximately 3 Hz. Both the raw voltages and calibrated values were written to disc.

A pumping control and data logging system was designed and written specifically for these experiments by the author to control caisson installation. The controller worked by sampling the installation depth from the calibrated LVDT output. By using the time difference between the values, the rate of installation was determined. An input for the target rate of installation was available, and the controller compared the current rate of installation with the target rate, and varied the pumping speed, based upon the error between the two values. The control loop feed-back factor could be changed by the user as the experiment was undertaken to allow complete control of the system.

The controller allowed the user to start and stop the pumps from the PC, and for convenience, incorporated an over-ride mode to manually control the pumping speed. As installation was undertaken, provision was made to allow monitoring of transducer readings. A graph was displayed of suction applied against installation depth.

For jacking, the caisson was mechanically pushed using the 3 DOF rig described by Martin (1994) with the control programme installed by Byrne (2000). The caisson was attached to a “Cambridge” load cell capable of measuring vertical, horizontal and moment loads. The control programme allows the caisson to be installed at a constant rate which can be specified by the user. The loads are displayed to the user throughout the test so that performance can be monitored. The load data was used to evaluate when the caisson had been installed fully, as the load increased at a significantly higher rate when the lid was in full contact with the soil plug.

4 Installation into layered soils

4.1 Introduction to caisson installation in homogeneous sand, clay and layered materials

4.1.1 Introduction

Suction caisson installation in homogeneous soils has been studied (Hogervorst (1980), Tjelta *et al.* (1986), Tjelta (1995), El-Gharbawy (1998) and Feld (2001)). These tests have generally focussed on installation into either homogeneous clay or sand soil profiles. Villalobos (2006) undertook model suction caisson installations in homogeneous sand. The theory of Houlsby and Byrne (2005b) was described and applied to installations. The calculations assumed the variation of pore pressure parameter, *a*, calculated by Junaideen (2004). Caisson installation disturbs the soil plug causing the permeability to increase (Erbrich and Tjelta (1999)). As the pore pressure parameter varies with changes of permeability ratio (k_f), it would be useful to measure the pore pressure at skirt tip during installation.

Andersen *et al.* (2008) published the results of calculations performed on a variety of caisson sizes from 0.557 m to 14 m diameter. The authors proposed an installation suction calculation for caissons installed into homogeneous sand, based upon data supplied by the industrial project partners. This approach is useful for sand installations, but it is not clear how this approach is to be modified when the prototype is to be installed in conditions which are fundamentally different to the cases present in the data.

The pumped water volume during installation varies when the permeability of the soil within the caisson changes. An estimate of the pumping requirement would be of practical use before an installation to provide assurance that sufficiently high flow rate pumps are available. Erbrich and Tjelta (1999) undertook Abaqus calculations and concluded that soil permeability influenced seepage gradients during installation. Therefore changes in permeability will influence the maximum installation depth of a caisson. The variation of permeability during installation has not been measured. Therefore tests

measuring the permeability variations arising due to installation would be valuable to determine the expected behaviour of a caisson.

As has been discussed in Chapter 2, the sites available for wind farm development in the UK contain both sand and clay soils present in layers. Where thick layers are present, installation may be modelled as undertaken in a homogeneous material. Where thin layers are present, the assumptions regarding homogeneous installation may not be adequate. The effect of caisson installation in layered materials needs to be investigated.

The program of tests from which the results in this Chapter are presented, is outlined in Table 4.1.1 and Table 4.1.2. The tests undertaken with the Caisson 2, as part of the skirt tip injection series, are listed in Table 5.3.1.

4.1.2 Clay preparation

Speswhite kaolin was obtained in powdered form and prepared in a similar manner to that used by Gue (1984). Moisture contents were measured for the kaolin powder (1 to 1.2 % typical) to determine the quantity of water required to make slurry with a moisture content of 120 %. To mix the slurry, the required water was weighed and poured into a 110 litre ribbon blade mixer. The kaolin was then added and allowed to sink before mixing commenced. The mixing trough was then pressure sealed, and a vacuum supply was attached to the mixer which lowered the pressure in the mixer by 75 kPa. The minimum mixing time with vacuum, for each batch, was 2 hours. At the end of mixing, the mixing vessel was brought back up to atmospheric pressure and the slurry was then pumped into the consolidation tank and placed under water onto the sand to avoid trapping air in the slurry mixture.

The initial height of the slurry required to ensure sufficient sample height was calculated, based on voids ratio, as follows:

$$H_f = H_i \frac{1 + e_f}{1 + e_i} \qquad \text{Eqn. 4.1.1}$$

where H_f is the final sample height and H_i is the initial slurry height. e_f and e_i are the final and initial voids ratios respectively. To be valid, it was important to ensure that the slurry was completely saturated (S=1) with no trapped air, hence the requirement for vacuum during mixing. Void ratio can also be expressed as Equation 4.1.2:

$$e = \frac{G_s w}{S} \qquad \text{Eqn. 4.1.2}$$

so the height of the solids can be calculated using:

$$H_s = \frac{H_i}{(1 + w_i G_s)} \qquad \text{Eqn. 4.1.3}$$

as the initial water content of the slurry (w_i) is known. The initial height of the solids (H_s) can be calculated as follows:

$$H_s = \frac{H_i}{1 + e_i} \qquad \text{Eqn. 4.1.4}$$

The effect of swelling can be accounted for using consolidation theory and the following parameters taken from Gue (1984). e on the Normally Consolidated Line was taken to be 2.58 at 1 kPa pressure, λ = 0.25 and κ = 0.04. A plot of the consolidation path followed is shown in Figure 4.1.1.

4.1.3 Sample tank and soil sample preparation for layered soil installations

The large diameter consolidometer was designed by Hazell (2004). The consolidometer has an internal diameter of 1000 mm and can be used to make kaolin samples from slurry heights of up to 800 mm.

The consolidation pressure is applied to the piston using hydraulic pressure available from a water supply. The water pressure was supplied over the whole area of the piston, so consolidation could be achieved with water pressures of up to 2.5 bar. The piston is located by a central shaft which is exposed to air at atmospheric pressure at the top. An estimate of the consolidation pressure (p_{sample}) from the supplied water pressure (p_{water}) needs the following correction:

$$p_{sample} = p_{water} \frac{A_{piston}}{A_{sample}} \qquad \text{Eqn. 4.1.5}$$

Where A_{piston} is the wetted area of the piston and A_{sample} is the area of the sample. The consolidation pressure was found to be consistently lower than the corrected pressure applied to the sample as friction between the piston and the bore created a significant restraining force. The method of consolidation adopted was to consolidate the sample incrementally, taking undrained shear strength measurements until the required strength had been achieved. The sand used for the layered soil installation tests was Redhill 110 which has the properties described in Chapter 3.2. The clay over sand samples were prepared using the method described below and the large consolidometer.

The sand was rained under water onto a Vyon sheet at the base of the consolidometer. The sand was rained slowly up to the required level, taking care not to allow air to become trapped in the soil. The surface was levelled by draining the water out of the bottom of the consolidometer to the level of the highest point of the surface. The low areas were then filled with sand up the water level. After the sand had been prepared, the required volume of slurry was then placed onto the sand, the consolidometer lid was attached to the tank and consolidation was begun.

Consolidation pressures were initially increased slowly to avoid generating excessive slurry leakage past the Vyon filter. When sufficient filter cake had built up, consolidation pressure was increased by larger amounts. When consolidation pressure was reached, the pressure was maintained until piston movement stopped. The pressure was subsequently reduced in steps of up to 80 kPa to guard against water cavitation, allowing the sample to swell. Displacements during consolidation were measured using an LVDT transducer and the water pressure was measured with a calibrated pressure transducer, both of which were logged by PC. A plot of typical sample height is presented in Figure 4.1.2. Hand shear vane tests were conducted on the clay after testing using a calibrated 33 mm diameter vane.

For the experiments investigating caisson installation into a soil sample consisting of sand with a clay lens, the sample was made by first consolidating clay over sand, and then placing the required thickness of sand on the clay.

Provision was made to allow the sand beneath the clay layer to drain if pressure changes arising from installation caused seepage in this layer. This enabled experiments to model boundary conditions corresponding to a large expanse of sand. To drain the sand, eight drains were cut through the clay layer and maintained open with tubes to support the clay. While the experiment was being undertaken, the sand at the bottom of the tubes was disturbed to ensure that fine material was not forming a layer creating a barrier to the flow of water into the sand.

The inclined clay layer tests required that a soil sample of sand over clay be produced where the clay/sand interface was inclined at an angle to the axis of installation. To achieve this, a four sided pyramid structure was manufactured from marine plywood which fitted closely into the bore of the consolidometer (see Figure 4.1.3). The clay surface produced can be observed in the photograph in Figure 4.1.4, and Figure 4.1.5 displays the installation layout used for the experiments.

The method used to make the inclined clay layer was to place the required quantity of slurry into the consolidometer. The pyramid was liberally coated with grease on all four sides. A plastic membrane was then cut as required and placed over the pyramid sides. The purpose of the membrane was to assist the removal of the pyramid after consolidation, as there was a significant surface area of pyramid onto which the clay could adhere causing a large force to be required for removal. After the pyramid was positioned into the consolidometer, a Vyon sheet was placed on top to provide a filter so that the fine material would not enter the drain, and consolidation was undertaken in the usual fashion.

4.1.4 Description of Caisson 3 used for layered soil installations

The small diameter caisson used for layered soil installations was constructed from brass tube (see Figure 4.1.6). A flange was trepanned out of brass plate and soldered to the end of the tube creating a water tight joint. The caisson lid was bolted to the flange and was sealed with a rubber gasket. The lid was constructed out of 25.4 mm thick transparent Perspex which allowed the plug inside the caisson to

be visually monitored throughout installation. A bracket was attached to the centre of the lid to facilitate connection to the vertical guidance and counter-balance system.

4.1.5 Description of Caisson 5 used for layered soil installations

The large diameter caisson, used for the layered soil experiments, was constructed entirely from sheet steel. The lid and skirt were rigidly crimped together producing a water tight seal. The lid needed to be stiffened to ensure no deformations occurred after the application of suction, so stiffeners, constructed out of 25 mm angle, were welded to the top. The plug could be monitored by the removal of two bungs inserted into the lid of the caisson. A picture of the caisson is shown in Figure 4.1.7.

4.1.6 Description of Caisson 2 used for homogeneous soil installations

The caisson used for the homogeneous soil installations was constructed by attaching a stainless steel tube to the base of a Dural flat footing. To support the skirt, a step was cut into the outside of the lid to maintain a circular plan aspect. The skirt was sealed to the lid with an epoxy resin adhesive. A rigid bracket was attached to the centre of the caisson which connected the footing to the guide system which stopped caisson rotation as the footing was installed.

4.1.7 Installation apparatus for layered soil tests

The tests undertaken in the large consolidometer used the same apparatus as that used for the homogeneous sand installations described in Chapter 3.5. The guide frame was designed to be sufficiently wide to span the large consolidometer and so could be used for both test series without modification. A photograph of the installation apparatus can be viewed in Figure 4.1.8.

4.1.8 Method of jacking installation

Jacked caissons were installed with the 3 DOF rig. The test began with the caisson fully submerged with all vents open and the skirt just touching the soil. The rig was then operated to begin installation while the pressure inside the caisson was monitored. Water was allowed to flow freely from the interior of the caisson to avoid pressure build-up and piping. The applied loads were continually monitored. As

the lid came into contact with the soil, the load increased rapidly as the footing became significantly stiffer due to the increased area of the foundation. To avoid causing footing failure, a vertical load limit was set which, if reached, caused the actuator to automatically stop installation.

4.1.9 Method of suction caisson installation

Caissons installed by suction used the apparatus described in Section 3.5. The test began with the caisson submerged and clamped while the system was de-aired. The clamp acted to stop the caisson from moving downwards, but allowed upward movement. The counterbalance system was then attached. Weights were added until the caisson was just on the point of moving downwards when lifted slightly from the clamped position to compensate for friction. To apply the required self weight force, weights were removed from the counterweight. The weight removed corresponded to the self weight force acting on the caisson.

Penetration began by slowly lowering the caisson, by hand, into the soil with the pumping hose disconnected. The pressure inside the caisson was monitored. When the weight of the caisson was just supported by the soil resistance, the clamp was applied and the pumping hose was attached. Subsequently, the clamp was released and the installation pump was operated at the lowest speed. The pumping speed was manually increased until the correct installation rate had been reached. The pump controller was then introduced to maintain the installation rate automatically. Installation was undertaken until penetration stopped, or sand was drawn into the system. For the plug lift experiments, pumping was stopped, when either the caisson lid contacted the soil, or the plug had obviously started to lift.

4.2 Caisson installation experiments in homogeneous clay

4.2.1 Introduction

Suction installation and jacking were undertaken in clay to assess the performance of the caisson in the laboratory. Caisson 2 was used for this investigation using the apparatus described in Chapter 3. The

sample used for suction installation was consolidated under a vertical stress of 200 kPa. The sample was relatively strong in comparison to the size of the caisson, when compared using the method outlined in Chapter 2, and would not be used for scaling purposes. The clay strength was approximately 10 kPa.

4.2.2 Measurement of clay shear strength

The undrained shear strength was measured using a hand shear vane in accordance with the method outlined in BS5930: Code of Practice for Site Investigations (1999). The measurements were made after the installation had been completed, to enable installation into a sample that was essentially undisturbed. The location diagram of the shear vane tests is shown in Figure 4.2.1. Five tests were undertaken at a depth of 70 mm, and two were undertaken at 170 mm.

The undrained shear strength profile for the clay was assumed to follow the form:

$$s_u = A\sigma'_{vi}(OCR)^B \qquad \text{Eqn. 4.2.1}$$

The average measured undrained shear strengths allowed the parameters A and B to be calculated. The values were 0.259 and 0.715 respectively. The assumed clay strength profile is shown in Figure 4.2.2.

4.2.3 Suction required for caisson installation in clay

The installation pressures were compared to those resulting from the suction calculation outlined in Equation 1.3.25. To undertake the calculation, the self weight of the system was measured and the adhesion factor needed to be determined. Chen and Randolph (2003) published the results of back-calculated adhesion factors for a series of caisson installations in kaolin clay. Based upon this work, the adhesion factor was assumed to take a value of 0.3. The submerged caisson weight was 15 N, and the soil unit weight was 16.6 kN/m^3.

As the self weight penetration was very small, the caisson was manually jacked a short distance beyond equilibrium to ensure that the application of pumping would lower the pressure within the caisson and begin installation. The rate of installation was chosen to be 0.1 mm/s, which corresponded well with those encountered in the field. The installation rate is shown in Figure 4.2.3. It can be seen that the rate

was maintained at low levels for the early stages of installation up to an installation depth of z/h_c = 0.23 (33 mm) and then increased up to the required installation rate for the experiment.

For this experiment, the suction estimate shown in Figure 4.2.4 was generated. The suction values have not been non-dimensionalised to provide indication of the pressures measured during these experiments. The calculation estimated that the caisson would install to a depth of less than 1 mm before suction was required, and that suction pressures up to 23.5 kPa would be necessary for full installation.

Figure 4.2.4 presents the suction pressures recorded during installation. It can be observed that reasonably good agreement was obtained between the estimated suction and that recorded for installation. Where direct agreement was not reached, the estimate conservatively over-predicted the expected pressures. At the end of installation, the suction pressures rose rapidly, coinciding with the lid contacting the clay. The measured suction at the end of installation, just before the pressure rose rapidly, was 21 kPa, which is 89 % of the estimated value.

Some methods of suction estimation recommend using the residual shear strength for the estimation of the side resistance on the skirt (Andersen and Jostad (1999), Chen and Randolph (2003), Villalobos (2006)). During the mini site investigation, the residual undrained shear strength was recorded along with the peak values. The average residual undrained shear strengths were 2.4 and 3.6 kPa. These values were used to determine a profile of residual undrained shear strength, shown in Figure 4.2.2 (A = 0.259, B = 0.715). Figure 4.2.5 shows a plot of the suction required to install the caisson and the suction estimates using the peak and residual undrained shear strength methods. The suction data lies between these two approaches.

As expected, no plug lift occurred as, using Equation 1.3.23, it was estimated that 113 kPa would be required. The lid contacted soil at a depth of 139.9 mm indicating that the plug heaved by 3.1 mm. The total volume of the installed skirt was equivalent to a plug movement of 5.8 mm. As the plug heaved by approximately half of the height expected for purely inward flow, half the clay displaced by the skirt is

assumed to have flowed into the caisson. The other half is assumed to have flowed toward the exterior of the skirt.

4.2.4 Pumped water volume

During the self weight penetration phase, the pumping hose was not attached to let the water escape from the interior. During suction installation, the volume of water pumped (v_{pumped}) was measured as described in Chapter 3. The volume pumped out of the caisson is assumed to be equal to the sum of the volume of water displaced by the reduction of volume of the interior of the caisson ($v_{caisson}$), and the volume of water seeping through the soil, and around the skirt into the caisson ($v_{seepage}$). This is summarised in the equation below:

$$v_{pumped} = v_{caisson} + v_{seepage} \qquad \text{Eqn. 4.2.2}$$

The volume of the pumping system has been assumed to remain constant for these tests, as the pressures used were sufficiently low to avoid causing volume changes in the system. The water volume removed from the caisson as a result of installation is related to depth by Equation 4.2.3.

$$v_{caisson} = \frac{\pi D_i^2}{4} z \qquad \text{Eqn. 4.2.3}$$

Therefore the flow rate contribution due to volume change can be calculated using Equation 4.2.4:

$$Q_{caisson} = \frac{\pi D_i^2}{4} \dot{z} \qquad \text{Eqn. 4.2.4}$$

where $\dot{z}$ is the installation rate of the caisson. For kaolin clay, the permeability is very low, so seepage flow will have been negligible.

Figure 4.2.6 shows a plot of the total water volume pumped out of the caisson after pumping had begun. The volume is shown in litres to show the order of magnitude of this variable. The plot also shows the variation of $v_{caisson}$ described above. $v_{caisson}$ increases linearly with installation, as expected, and v_{pumped} increases at the same rate offset by the quantity not pumped during the self weight penetration phase.

To enable better understanding of v_{pumped} and $v_{caisson}$, the difference between the pumped volume and the installed volume is plotted in Figure 4.2.7, expressed as a percentage of the volume of caisson installed. The large noise during the phase of slow installation appears by nature of a slower logging rate being used over this period. It can be seen that over the course of installation, the excess water pumped corresponded to no more than 2 % of the installed caisson volume. The measured plug heave of 3.1 mm corresponds to a volume change equivalent to 2.2 % of the total installed caisson volume, and therefore this accounts for all the excess water pumped. It can be concluded that there was negligible seepage flow during this experiment. It can also be observed that the close correlation of water pumped with caisson volume installed indicates that the skirt made a good seal against the surrounding clay and no water 'leaked' down the outside of the skirt into the interior of the caisson.

This experiment illustrates an appropriate modification to the pumping continuity equation, which will be used later for evaluating the plug lift experiments. The continuity of flow should take into account the volume of water displaced by plug movement (v_{plug}) in the total discharge flow equation. This can be included as follows:

$$v_{pumped} = v_{caisson} + v_{seepage} + v_{plug} \qquad \text{Eqn. 4.2.5}$$

4.2.5 Jacking installation in clay

Caisson 3 was installed by suction into a sample of clay, and then some days later by jacking in the same sample. The strength of the clay was measured to be 5.5 kPa directly after suction installation, and the self weight of the caisson was 4.9 N. A calculation was performed to estimate the suction required to install the caisson, using Equation 1.3.26. The estimate is plotted in Figure 4.2.8 along with the measured values during installation. It can be observed that there is reasonably good agreement between the calculated and measured suction values.

The caisson was jacked into position with the 3 DOF rig. The estimated forces are plotted along with the measured values in Figure 4.2.9. It can be observed that the calculated curve does not fit the data as

accurately as the suction calculation. In the time between the clay strength measurements and the jacking test being undertaken, the sample was allowed to swell and the clay undrained shear strength will have decreased. If the clay strength decreased by only 1 kPa, the jacking force estimate shown in Figure 4.2.10 arises. It can be seen that the jacking force estimate agrees more closely with the data, particularly for installation at deep skirt penetrations. As shear strength data at the surface could not be obtained, the calculation assumed s_u was uniform throughout the sample. The accounts for the over-estimate of jacking force at shallow penetration depths.

4.3 Caisson installation in homogeneous sand

4.3.1 Caisson resistance during jacking in sand

A series of jacked installations were carried out in loose sand using Caissons 6 and 7. The relative density of these sand samples lay in the range of between 55 to 79 %. The sample was arranged to be loosely compacted to reduce dilation. Excessive dilation was unwanted, as the angle of shearing would become unrealistically large compared with values experienced in the field where the vertical effective stresses are much higher (Bolton (1986)).

The results of the installations are shown in Figure 4.3.1. The overall trend is that the installation force rose smoothly with penetration depth until the lid made contact with the plug. When this happened, the stiffness of the foundation increased significantly, which can be seen at the end of some of the curves where the load increases at far higher rates. The Figure shows data for two skirts lengths (100 and 150 mm). An installation calculation has been performed for this series of tests which is plotted on Figure 4.3.1 as the thick black line.

Equation 1.3.5 was used to estimate the installation force. The estimate shown in Figure 4.3.1 made allowance for the enhancement of σ'_v by the action of skirt penetration. The jacking calculations were solved using a spreadsheet to estimate the jacking load required. As the jacking and self weight

penetration load calculations are the same, similar calculations were undertaken in a Matlab programme to estimate the caisson penetration by self weight before the application of suction.

The equations defining the stress distribution (Equations 1.3.6 and 1.3.7) needed to be integrated to obtain the variation effective stress as a function of depth. The relationships are ordinary first order differential equations, which can be solved using a fourth order Runge-Kutta method (RK4). The boundary condition chosen to solve the problem was to set the stress at the surface of the soil equal to zero.

$$\sigma'_{vo}(z_o) = 0 \qquad \text{Eqn. 4.3.1}$$

The RK4 method, when applied to Equation 1.3.6, is set out below:

$$\sigma'_{ov\,(n+1)} = \sigma'_{ov\,(n)} + \frac{1}{6}\Delta z(k_1 + 2k_2 + 2k_3 + k_4) \qquad \text{Eqn. 4.3.2}$$

$$z_{n+1} = z_n + \Delta z \qquad \text{Eqn. 4.3.3}$$

where

$$k_1 = f(z_n, y_n) \qquad \text{Eqn. 4.3.4}$$

$$k_2 = f(z_n + 0.5\Delta z, y_n + 0.5\Delta z k_1) \qquad \text{Eqn. 4.3.5}$$

$$k_3 = f(z_n + 0.5\Delta z, y_n + 0.5\Delta z k_2) \qquad \text{Eqn. 4.3.6}$$

$$k_4 = f(z_n + \Delta z, y_n + \Delta z k_3) \qquad \text{Eqn. 4.3.7}$$

The installation force was obtained by first calculating the soil stresses adjacent to the skirt and then numerically integrating the forces using small displacement steps along the skirt. The sum of the forces was obtained, using Equation 1.3.5, which enabled the self weight penetration distance to be obtained.

For calculation of installation suction after self weight penetration had been completed, the soil stresses were obtained by integration of the stress variation with the hydraulic gradients applied. For these calculations, an iterative strategy was chosen. The method chose a suction value, calculated the soil stresses and forces, then compared them to the installation forces. The new value of suction for the next iteration was chosen based upon the error present in the installation force balance (Equation 1.3.15). An

iterative strategy was adopted as it was readily modified for estimation of the skirt resistances when STI was applied in later experiments.

In the calculation presented in Figure 4.3.2, the same load spread parameter was assumed on the inside and outside of the skirt. The parameter was estimated to allow stresses to spread at a rate of 1 m/m depth. K was assumed to take a value of 0.9, $\varnothing'$ was assumed to be 38º which is appropriate for silica sand, and δ was assumed to be 2/3 $\varnothing'$. It can be seen that the calculation closely resembles the data.

4.3.2 Caisson resistance during suction installation in homogeneous sand

The suction calculation, outlined by Houlsby and Byrne (2005b), will now be applied to model caisson tests to characterise the appropriate parameters for use in the analysis of experiments undertaken later. Work by Villalobos (2006) applied the theory of Houlsby and Byrne (2005b) to the installation of caissons, however these caissons were attached to the 3 DOF loading rig (described by Martin (1994)). The 3 DOF rig is tuned to hold accurately a combination of loads on a footing, but cannot respond quickly to a change of load due to speed limitations imposed by the actuator and control system. When the forces acting on a caisson change rapidly, the system must be permitted to respond freely to those changes in order to enable accurate modelling of the installation conditions. It is therefore important to install caissons in homogeneous sand to determine the relevant inputs for the soil resistance calculation.

Andersen *et al*. (2008) listed a set of parameters used to study the installation of caissons in the field and laboratory tests. The installations were undertaken in a variety of different conditions and the parameters vary over a range of values. This work provides a useful reference for information regarding relevant soil data. The variables required for the installation estimate are listed in Table 4.3.1. By making further assumptions about the installations, some variables can be derived from others. For example the bearing capacity factors adopted (N_q and N_γ), were those applicable for a strip footing and can be derived from $\varnothing'$.

$\varnothing'$ was used as a basis for estimating the interface friction angle (δ) between the sand and the skirt. Andersen *et al.* (2008) adopted the value of approximately 0.9 $\varnothing'$ for the installations presented. In the British Standard for Pile Design (BS8009: 1986), the recommended value of δ between a metal shaft and sand is 2/3$\varnothing'$. Another source for this value was proposed by Wetzel *et al.* (1989) who partook in a pile capacity prediction event. A discussion of appropriate values of δ is presented and the value proposed for pipe piles is 0.7$\varnothing'$.

The δ term appears in combination with the K factor as $K\tan\delta$. One approach may be to consider these parameters in combination, to define a set of appropriate values the function should take. In practice, this is not performed, and work undertaken by Andersen *et al.* (2008), for example, varies K between different sands. The values of K published in the examples vary over a wide range from 0.8 to 1.85. The API Guidelines (1993) recommend that the value of K adopted for drained shaft friction for open ended unplugged piles should be equal to 0.8, and this value is adopted by industry for calculations of large diameter field installations.

A discussion of the appropriate values for K was presented by Villalobos (2006). Villalobos stated that depending upon the roughness of the skirt, the appropriate relationships for K would be defined by the Krynine and Rankine calculations. The Krynine value would be suitable for cases where full friction mobilisation was obtained, and the Rankine value should be used for completely smooth skirts. The Krynine and Rankine passive K values are higher than those outlined above when typical $\varnothing'$ values are used. For example, for soil with a friction angle of 42°, the Krynine K value would be 2.62 and the Rankine value is 5.04. The author needed to adopt low values of δ to obtain suitable $K\tan\delta$ values for accurate estimates of suction. A method of calculating such low values of δ was not presented, and instead reference was made to sand/Duraluminium shear tests undertaken by Lings and Dietz (2005) to support the values.

For this work, the value of K was fixed at 0.9 and the value of δ was assumed to take the value obtained by 0.66$\varnothing'$. The shaft interface friction angle relationship was adopted as most literature suggested

values of this order were appropriate. The K value was adopted based upon the widely used API Guidelines where a value of 0.8 is recommended. The value was increased slightly (to 0.9) to account for the radial constriction of sand by the sides of the installation tank. The constriction would limit the radial sand movement which would cause higher lateral reaction stresses to act on the skirt wall.

Kelly *et al.* (2004) undertook a consolidated-undrained triaxial test on Redhill 110 sand. In this test, the peak friction angle was measured as 43.9°. The calculations for installation are based upon the drained triaxial friction angle so this ought to be used as the input. However, the drained friction angle should be measured at stress conditions similar to those that will be encountered during installation. When the skirt penetrates the soil, the radial movement caused by sand displacement for penetration will increase the soil stresses relative to those assumed to be present in-situ. The action of seepage causes soil loosening in the vicinity of the skirt which will serve to lower the stresses in that area. As the extent to which loosening is unknown, it is therefore not possible to specify the stresses at which the test should be undertaken to measure the appropriate undrained friction angle of the sand.

The purpose of the tests described in this work was to measure the behaviour of the caisson when installed in conditions likely to be encountered offshore. One method of estimating the friction angle would be to install the caisson in homogeneous sand and then back calculate the friction angle. The friction angle could subsequently be used for calculations where the caisson was installed into layered soils. The value derived for use was 42° as this gave good approximation for the experiments undertaken.

The slope of the stress influence factor (f_i) used by Houlsby and Byrne (2005b) in the example calculations was equal to a rate of 1. Andersen *et al.* (2008) proposed that the stress influence of the skirt friction on the end bearing could be accounted for by using a factor (α_f) to relate the side shear stress to the end bearing. The factor used for the calculations presented was 1 which was maintained constant throughout the penetration calculations. The method of Houlsby and Byrne (2005b) enables account to be made for a variation of vertical stress caused by skirt friction. This becomes important at

an interface between clay overlying sand where the adhesion force causes the vertical stress in the sand to be enlarged due to the action of installation. As a variable area of stress enhancement was assumed, the values of f_i and f_o adopted lay in the range of 0.75 to 1. The same values were used inside the caisson as were assumed for the outside.

The values of γ' can be easily determined for the sand used. For this series of tests, γ' had a value of 10.2 kN/m^3. The γ' values published by Andersen *et al.* (2008) ranged between 9.8 to 11.2 kN/m^3. This value will vary between different soil types, but most calculations use values of similar magnitude.

The installation estimate was applied to a caisson installed into Redhill 110 sand. The parameters used for the estimate are listed in Table 4.3.1. The suction recorded for the test is plotted on Figure 4.3.3 as a function of depth. The estimated suction for installation is displayed on the plot alongside the recorded values. Using the parameters outlined above, an accurate estimate of the suction required can be achieved.

The estimated penetration suction is sensitive to input parameters, particularly the angle of friction. For example, changing $\varnothing'$ by ±2° significantly changes the estimate, as shown in Figure 4.3.4. Varying the rate of stress enhancement also changes the suction estimate, as this parameter affects the calculated stress magnitude adjacent to the caisson. The effect of varying the stress enhancement rate is presented in Figure 4.3.5.

In practice, the installation calculation is over-defined as there are more unknown parameters than equations. Undertaking an installation to back-calculate the input parameters will not yield a single solution which can be applied to subsequent tests. An estimate of installation suction should therefore incorporate a sensitivity analysis to plot the variation of suction with small input parameter changes.

The method for estimating the pumped water volume was outlined in Chapter 2. The estimate was reliant on an accurate value of suction pressure. The estimated flow rate for installation has been plotted

against the measured flow rate for an installation in sand in Figure 4.3.6. For this estimate, the recorded suction during installation was used in the calculation as this enables the performance of the flow model to be evaluated.

It can be observed that the estimated flow rate is under-predicted by the model. The amount by which the model under-predicts the flow increased with installation. Despite the inability of the estimate to closely follow the recorded pumped water flow, the estimate may still be sufficiently accurate for use to select pumping equipment for a field installation, as pumps can generally operate over a range of pumping flow rates. Equipment brought to site would need to be capable of a minimum rather than a maximum pumping requirement, so the method could be used as a starting point for elimination of unsuitable equipment.

The recorded flow rate increases with penetration depth more rapidly than the estimate. The reason for this is attributed to the permeability of the soil increasing as a consequence of suction installation. In the calculation, a constant sand permeability was assumed at all penetration depths. If the assumed soil permeability were to be increased as installation progressed, the calculated seepage flows would be larger. The effect of installation on sand permeability is examined further below.

The model used for the flow calculations assumed that the suction across the base of the caisson is uniform and equivalent to a magnitude *as*. Flow calculations undertaken for caissons installed into sand show that the equipotential pressure contours at the base of the skirt do not span horizontally across the base as assumed, but bulge beneath the skirt. This is shown schematically in Figure 4.3.7. The effect of the assumption is to over-estimate the average seepage gradient within the caisson, which over-estimates the seepage flows. An improved model of the seepage estimate would use an average suction gradient generated from an analysis of the variation of pressure over a plane of sand over the bottom of the caisson. The effect of the seepage gradient assumption serves to partly compensate for the change of sand permeability as installation is undertaken.

When the same parameters used for estimation of suction are applied to a jacked installation (see Table 4.3.1) the result obtained is presented in Figure 4.3.8. It can be observed in the Table that the parameters used for estimation of caisson resistance are similar irrespective of the method used to install the caisson. The properties are specific to the soil, and the different mechanisms invoked by the installation technique are captured by the assumptions encapsulated in the theory. By making small changes to the input parameters, the estimate could be varied and made to follow the measured resistance recorded during the test. Figure 4.3.9 illustrates the change of estimated jacking force when small variations are made to $\varnothing'$.

4.3.3 The variation of pore pressure parameter (a) during suction installation in homogeneous sand

For installations in homogeneous sand, the variation of water pressure at the skirt tip was measured using the STI caisson, shown in Figure 4.3.10. Houlsby and Byrne (2005b) defined the pressure reduction at the skirt tip as a fraction (a) of the installation suction (s) (see Equation 4.3.8).

$$a = \frac{\Delta u_{suction}}{s} \qquad \text{Eqn. 4.3.8}$$

The variation of a with penetration was calculated by Junaideen (2004). The calculation was undertaken for cases where the permeability of the soil plug was similar to the surroundings, and for cases where the permeability of the plug had increased. The ratio of inside to outside permeability is defined by $k_f = k_i/k_o$. Figure 4.3.11 schematically illustrates the variation of hydraulic gradient in the soil during suction installation in sand. The colours correspond to water pressure deviations from hydrostatic. The increase of hydraulic gradient within the skirt can be observed.

The pressure in the distribution manifold was measured using a pressure transducer. As water has a high bulk modulus (K_w = 2.3 GPa), the flow of water out of the manifold was insignificant. Equation 4.3.9 illustrates that small pressure variations (Δp) will cause negligible flow out of a small system volume (V_{system}):

$$\frac{K_w}{V_{system}} = \frac{\Delta p}{\Delta V_{system}} \qquad \text{Eqn. 4.3.9}$$

The changes in manifold pressure were assumed to be proportional to the change in pore pressure and the change of skirt tip penetration depth. As the change of hydrostatic water pressure next to the caisson was measured, it was therefore possible to use this data to obtain the pore pressure changes at the skirt tip as a result of installation suction in the following manner:

$$\Delta u_{suction} = \Delta u_{tip} - \Delta u_{hydrostatic} \qquad \text{Eqn. 4.3.10}$$

Figure 4.3.12 shows an example plot of the calculated variation of pore pressure parameter and the published estimates of Junaideen (2004). Generally, when installation began, calculated values of a were similar to the theoretical case for k_f = 1, but then did not decrease at the rate expected for no change in soil permeability. This result indicates that the soil permeability inside the caisson increased throughout installation.

It was found that a decreased less with depth as the installation rate increased. For the slowest penetration rate (0.02 mm/s), a began at a value close to the estimate where k_f = 1 and decreased approximately along the line associated with k_f = 1 (see Figure 4.3.13). Installations undertaken at rates in the range of between 0.1 to 0.4 mm/s produced calculated values of a starting close to the theoretical values appropriate for k_f = 1, but then decreased in such a way that, by the end of installation, a values were close to the prediction using k_f = 2. The fastest installation was undertaken at a rate of 1 mm/s. At a depth of z/D = 0.84, the calculated value of a corresponded to a permeability ratio of 2. This indicates that installations are affected by the penetration rate, and confirms the conclusion in Chapter 2 where it was noted that the group $\dot{z}/k$ should be similar for experiments and prototypes. Therefore tests undertaken at very high rates of penetration should not be used as a guide for understanding field behaviour (Tran (2005)).

The calculated variation of a could be used to identify the variation of permeability ratio by interpolating the measured values between the published estimates. This has been done for the cases shown in Figure 4.3.14. The plot shows that the variation of k_f appears to follow a linear relationship

with depth. A best fit line, calculated by a least squares linear regression, has been added to each of the cases and is also included in the Figure. It can be seen from the equations describing each line, that k_f increased more rapidly when higher rates of penetration were used.

The intercepts of the lines do not begin at 1. Each caisson was installed by self weight for the initial stages of penetration. During this period, the water pressure inside the caisson was slightly higher than ambient, creating downward water flow inside the caisson, and upward flow outside the skirt. Andersen *et al.* (2008) stated that upward water flow caused soil loosening, resulting in the soil outside the caisson becoming more permeable. Consequently k_f may decrease to a value below 1.

Knowledge of the variation of a is significant for the calculation of installation suction. Reducing the pore pressure at the tip of the caisson has the effect of increasing the downward hydraulic gradient which causes more downward flow of water outside the caisson. Increasing this flow causes larger effective stresses, which in turn increase the outside skirt resistance. Reducing the pore pressure at the skirt tip, while maintaining constant suction, causes the seepage gradient to decrease, reducing the upward seepage flow. This leads to less reduction of effective stress and larger resisting forces acting inside the skirt. Therefore if installation causes the sand permeability within the caisson to increase, the value of k_f will rise, resulting in larger suctions being required for penetration. The effect of permeability variation on skirt tip pressure is illustrated in Figure 4.3.15. In both diagrams, the skirt tip penetration and soil permeability outside the caisson are the same. In the second diagram, the soil permeability within the caisson has been increased to be three times that of the surrounding material. It can be observed that the hydraulic gradient within the second caisson is lower than that in the first diagram. The pressure loss occurring outside the skirt is much larger for the case where k_f is larger.

The installation calculations presented by Houlsby and Byrne (2005b) allow a to vary as a function of depth based upon the results of FE calculations undertaken at assumed permeability ratios (k_f). In these experiments, the variation of a has been directly measured and a linear variation of k_f with depth has been found. The installation calculations can be re-performed using the linear relationship of

permeability ratio to obtain a better estimate of the suction required for installation. The result of this calculation is shown in Figure 4.3.16 (Test: 8N Test 2), where the measured suction has been plotted against the installation estimate for uniform permeability ratio and the estimate resulting from the variable permeability ratio.

4.3.4 Pumping volume and plug permeability during suction installation in homogeneous sand

The experiments included measurements of the pumped water volume. By subtracting the volume of caisson installed, it was possible to evaluate the variation of seepage volume with caisson penetration using the relationship below.

$$v_{seepage} = v_{pumped} - v_{caisson} \qquad \text{Eqn. 4.3.11}$$

The measured data for suction (s) and measured tip pressure ($p_{tip} = as$) were then used to estimate the overall permeability ($k_{overall}$) of the plug within the caisson. This was achieved using Darcy's law ($v = ki$) assuming uniform pore pressure over the base of the soil plug at the depth of the skirt tip.

$$k_{overall} = \frac{s - p_{tip}}{\gamma_w z} \qquad \text{Eqn. 4.3.12}$$

Figure 4.3.17 shows a plot of the results. As the rate of installation was increased from 0.02 to 1 mm/s, the calculated permeability at the end of each installation had increased. This calculation also supports the finding that overall soil plug permeability increased with installation depth, as the increase in permeability can be clearly seen on each plot.

Calculations for the non-dimensional flow factor F (see Equation 4.3.13 below) were made, based upon the measured flow rate and installation suction assuming k_o remained uniform.

$$F = \frac{q\gamma_w}{k_o D s} \qquad \text{Eqn. 4.3.13}$$

Figure 4.3.18 presents some examples of the results for different installation speeds. It can be observed that for most results, the values of F closely follow the estimate relevant to $k_f = 1$, so this result does not support the findings that the permeability of the soil plug increases with depth. The only exception to this finding was the fastest installation shown on the plot. When estimating F, it was assumed that a uniform pressure existed across the bottom of the caisson. Finite element simulations, such as those

reported by Erbrich and Tjelta (1999), demonstrated that pore pressure is not constant across planes of soil within the footing. The negative pore pressure at the axis of the footing is smaller than the negative pore pressure at the skirt tip resulting in over-estimation of the pumped water volumes.

4.3.5 The influence of the rate of installation on the suction required for penetration

Figure 4.3.19 presents measured suction pressures for a series of tests undertaken at different rates. The rates were varied from 0.02 to 1 mm/s. It can be observed that there is no clear trend between the rate of installation and suction pressure, with the exception of the test where the slowest rate of installation was chosen (0.02 mm/s). For this test, the suction required for penetration was smaller than for the other experiments.

The suction required for installation is influenced by variations of *as*, as the skirt tip pressure works in conjunction with the suction at the top of the plug to set the seepage gradient. The installations measured the water pressure at the base of the skirt, and from this data it is possible to calculate the variation of pore pressure factor for the installation. The pore pressure factors for different installation rates can be compared to evaluate whether the installation suction would be expected to vary with installation rate. The pore pressure factors were presented in Figure 4.3.13, where it can be observed that, with the exception of the slowest installation rate, similar values were calculated for each installation rate. This result is consistent with the model, as similar suctions were recorded for each installation apart from the experiment undertaken at the slowest rate. This result indicates that the seepage gradients present in the plug, during installation, were similar for tests undertaken at rates in the range of 0.1 to 1 mm/s.

4.4 Installation of caissons into clay over sand

4.4.1 Introduction

The installation of suction caissons into soil profiles consisting of clay over sand will be examined in this Section. As discussed in Chapter 2, the soils around the coast of the UK may contain profiles which consist of clay over sand. First, the conditions for a prototype installation need to be identified, second,

the relationships proposed in Chapter 2 will be used to identify conditions which can be created in the laboratory to allow similar experiments to be undertaken.

4.4.2 Calculations for the appropriate installation conditions in clay over sand

For correct modelling of suction installation, the conditions should be the same in the laboratory as for the prototype. The variables outlined in Chapter 2.4 were used to maintain similarity between the model and a prototype to investigate the possibility of plug lift during installation in clay over sand.

The groups $\frac{t}{D}$, $\frac{h_c}{D}$ and $\frac{h_s}{D}$ are geometrical ratios and were maintained between the envisaged prototype and the model caissons by designing the caissons to be a scale model of a field structure. The clay layer thickness was chosen to be appropriate for the caisson diameter.

The groups $\frac{\gamma'_s}{\gamma'_c}$, α, and N_c, concern the scaling of materials. The unit weight ratio of sand to clay will be similar in experiments and prototypes. α is dimensionless and was appropriately scaled by using metal caissons with unpainted surfaces. No surface treatment was applied to the caisson, however, the skirt was cleaned prior to any installation tests being undertaken and any surface corrosion was carefully removed using a 'Scotchbrite' pad. The parameter N_c is dimensionless and the value of 9 is often used for both model tests and field installations.

The groups $\frac{s_u}{\gamma'_c D}$, and $\frac{V'}{\gamma'_c D^3}$ were used to characterise soil strength and self weight for each test.

The groups $\frac{s}{\gamma'_c D}$ and $\frac{z}{D}$ were to be measured during experiments, with the first group representing scaled suction, and the second group representing the skirt tip installation depth.

To plan a series of experiments, the relevant field data were consulted for clay strength parameters, and estimates were made of relevant caisson sizes for consideration. Monopod caissons are approximately 10 to 30 m diameter and are constructed from steel. The wall and lid thicknesses may be approximately 40 mm. Quadruped caissons are generally smaller than monopod foundations and are likely to comprise sizes in the range of 4 to 10 m diameter, with skirt thicknesses of 25 to 35 mm. The properties of these caissons are listed in Table 4.4.1.

Field caissons for wind turbines would be installed with supplementary attachments for connection to the main structure. This additional weight should be taken into account when calculating the caisson installation load. For preliminary calculations, it was assumed that a 1 m diameter, 25 mm thick, steel shaft would be attached to the caisson of length equivalent 1.5 times the caisson diameter.

The data for field conditions at the proposed wind farm development locations were used to determine the relevant soil strengths for laboratory work. In Chapter 2.5, it was concluded that the range of s_u values of interest lay in the wide range of 20 to 300 kPa. Table 4.4.1 lists the range of variables considered for this problem, and the range of the values of the resulting non-dimensional parameters used for experimental design.

Table 4.4.2 lists the range of values presented in Table 4.4.1 with laboratory apparatus dimensions and material parameters added. The parameters for centrifuge work are included, with actual dimensions and prototype dimensions listed in the usual manner for comparison.

Examining the 1g conditions, it can be seen that good scaling was achievable in the laboratory. s_u needed to be low, 2 to 8 kPa to maintain the soil strength group $\frac{s_u}{\gamma'_c D}$ parameter in the range 0.34 to 6.7. The caisson self weight was controlled by the counterbalance system. The range of non-dimensional force applied was 0.075 to 0.36 which necessitated the self weight of caissons to vary between 1 and 346 N. As the caisson did not weigh 346 N, this force was applied by placing the

appropriate amount of lead weights at the centre of the caisson. The weight of lead added was calculated taking buoyancy effects into consideration.

4.4.3 Installation experiments undertaken at The University of Oxford

All experiments in this Section were undertaken under conditions which may be encountered by a prototype installation and therefore plot in the grey shaded area in Figure 4.4.1. The aim of the test series was to undertake sufficient installations to confirm the location of the uplift boundary line.

The lid of Caisson 3 was constructed from transparent Perspex plastic, and it was therefore possible to monitor plug movement visually. It was not possible, however, to measure and record the movement of the plug directly as the experiment was being carried out. When suction had reached a level sufficient to cause plug lift, it was noted that installation stopped. This could be monitored on the installation control programme output.

Plug movement was inferred from measurements of water volume pumped out of the caisson in the following manner:

$$v_{plug} = v_{pumped} - v_{caisson} - v_{seepage} \qquad \text{Eqn. 4.4.1}$$

As the seepage/leakage flows were found to be consistently low for installation in clay, the seepage volume pumped was assumed to be negligible. The installed caisson volume was known, as was the pumped water volume, so the onset of plug lift could be calculated.

Figure 4.4.1 shows a plot, in non-dimensional space, of results for each of the experiments undertaken. It was found that there are cases where clay uplift can occur, and experiments which ended with plug lift are plotted on the chart with a triangular symbol. The experiments which ended without plug lift occurring are plotted on the chart with a green diamond symbol. The proposed boundary for plug lift is plotted on the chart with a solid black line. The data confirm that there is a boundary for plug lift, as installations which plot above the boundary resulted in plug lift and those that plot below did not. Figure 4.4.2 shows a photograph taken of Caisson 3 after plug lift had been recorded. The plug can be

seen through the lid at the top of the caisson. Figure 4.4.3 shows a photograph taken of Caisson 5 after plug lift happened. The lid of this caisson was not transparent, however, a large bung could be removed to inspect the plug.

On the plot in Figure 4.4.4, data recorded for the large diameter caisson has been presented in non-dimensional form with suction and installation depth normalised in the manner outlined in Chapter 2. The plot has the depth of the clay/sand interface and an estimate of installation suction added. The pressure for uplift reduces with depth and this estimate has been added to Figure 4.4.5. In this experiment, the conditions were chosen for uplift to occur while the skirt tip was in clay. It was observed that installation suction increased in the usual manner at the beginning of penetration into the clay. As the skirt tip approached the depth at which plug lift was expected, the suction magnitude increased and exceeded that estimated using the installation calculation. Eventually, as suction approached the pressure at which uplift was expected, plug lift occurred, and installation stopped whilst pumping pulled the plug up the skirt (see Figure 4.4.5).

Figure 4.4.6 presents an installation, using Caisson 3, which ended with plug lift. The installation conditions were varied to explore the uplift region, which accounts for the different values of non-dimensional suction recorded. It can be observed that the suction trend followed the estimate until the suction for uplift was approached, at which point suction began to exceed that estimated for installation. When suction reached a value at which uplift was predicted, plug lift occurred and installation stalled.

For experiments ending with plug lift, lower suction pressures were observed while the plug was drawn up the caisson as demonstrated in Figure 4.4.6. The reason for this response is that as the plug began to move, a maximum shear resistance was reached and then overcome due to the large displacements associated with plug lift. Figure 4.4.7 shows a plot of shear strength variation against rotation for stepper motor controlled shear vane tests undertaken in a clay sample. It can be observed that a peak undrained shear strength was reached, followed by lower residual values at large rotations. An additional reason for the reduction in measured suction is that as the plug moved up the skirt, more clay

made contact with metal and the sliding resistance was then governed by αs_u rather than the resistance of clay shearing. As the force to shear clay past metal is lower than that required to shear intact clay, the suction necessary to create this force reduced.

Calculations show that the estimate for plug lift is sensitive to the adhesion factor (α) and the ability of the sand layer underneath the clay to drain. The variation of uplift boundary due to changes of α is indicated on Figure 4.4.8. From the plot, it can be concluded that a lower value of α may allow a caisson to install into stronger clays before uplift is encountered. For the homogeneous clay installation reported in Section 4.2, it was concluded that the adhesion factor between the clay and the caisson should take a value of approximately 0.3. For these tests, which used kaolin powder from the same source, the data points lie either side of the boundary lines calculated using adhesion factors of 0.3 and 0.4. A line is plotted using an unrealistically low adhesion factor of 0.2 to illustrate the movement of the uplift boundary with variation of α.

Ding *et al.* (2001) described the installation of a 9 m diameter caisson into clay over sand. Sufficient information was provided to determine the non-dimensional installation conditions, which are included in Figure 4.4.8. It can be observed that the installation plots beneath the boundary for uplift. As the caisson was installed without any report of plug lift, the result agrees with the expected outcome from the uplift model.

Data for pumped water volume shows that the clay layer effectively cuts off seepage (see Figure 4.4.9). When no plug lift occurred, the pumped water volume closely matched the volume of the installed caisson. Plug lift can be observed, where it happens, by a sharp increase in pumped water volume when plotted with respect to caisson penetration (see Figure 4.4.10).

For two tests, the pumping rate was increased. The installation conditions for these tests were chosen so that they plotted in the uplift region. The purpose of these installations was to investigate the effect of sand drainage. As the pumping rate had been increased, the plug would lift more quickly, causing water

to flow into the void at a higher rate than previous installations. To achieve this, the pressure of water in the void would need to be lower than the previous installations, and could reach levels allowing installation to proceed.

The experiment was undertaken in a clay sample which was 112 mm thick. A plot of estimated installation suction, and the suction required to lift the plug is presented in Figure 4.4.11. The estimate concluded that plug lift was expected to occur when the tip of the skirt approached the base of the clay. The experiment was undertaken at an installation rate of 0.5 mm/s.

The result of one of the installations is presented in Figure 4.4.12. The installation was able to install the skirt completely through the clay layer into the sand beneath. It was noted that, installation suction increased marginally above the estimate as the skirt approached the base of the clay.

The stability of the plug can be monitored by comparing the pumped water volume with the volume of caisson installed. The plot is presented in Figure 4.4.13. On the plot it can be observed that the pumped water volume closely matched the installed caisson volume at shallow penetration depths in clay. As the skirt tip approached the base of the clay, the pumped water volume slightly exceeded the installed volume of the caisson indicating that plug movement had begun. After the skirt tip had entered the sand layer, the pumped water volume exceeded the volume displaced by the caisson by larger volumes.

The installation conditions were chosen to enable plug movement. The recorded displaced water volume demonstrated that plug movement began, however, the distance the plug moved was much smaller than observed for experiments undertaken at slow rates of installation.

4.5 Installation of caissons into sand with a clay layer

4.5.1 Introduction

For suction installation in sand, the seepage flows at the skirt tip and inside the caisson act in a way to lower the total force required for installation. Indeed were it not for the seepage flows, in some circumstances, it would not be possible to fully install the caisson without relying on much higher self weight or jacking forces, as the suction pressures necessary could not be generated.

As the creation of seepage flow is critical for installation, it is therefore important to study caisson behaviour in circumstances where the set-up of seepage flow may not be possible. One example is where a caisson is to be installed in a soil profile containing a relatively thin clay layer in an otherwise homogeneous sand material. The soil profiles reported in Chapter 2 state that sand with clay lenses may be encountered. The permeability of clay is much lower than that of sand. It is possible that as the skirt tip approaches the top of the clay layer, the seepage flows will become reduced, as the area through which the water can flow diminishes. If seepage within the caisson becomes sufficiently reduced, the resistances experienced during installation may be similar to those encountered during a jacked installation.

To investigate whether the presence of a clay layer in sand would have negative consequences installation, a series of tests reported below were conducted to understand the effect of a clay layer on installation suction.

4.5.2 The results of installation in sand with a thin clay layer

For these experiments, the sample was produced using the method outlined in Section 3. The depth of the top of the clay was located at 106 mm below the sand surface and the clay thickness was 64 mm. s_u was measured with a hand shear vane and found to be 6.4 kPa at a depth of 50 mm from the top of the clay. Caisson 3 was used for these tests, installed using the apparatus described in Chapter 3 with an

applied load of 5 N. For these tests, the pumped water volume was measured throughout the course of installation.

Figure 4.5.1 presents the results of the five tests undertaken. It can be observed that each test followed a similar pattern of behaviour. While the skirt tip was installed through the sand, the installation suction increased with depth up to a point where the skirt tip was about to penetrate the clay. At this point, the suction increased at a much higher gradient up to the depth where the tip penetrated the clay. After the tip had entered the clay, the gradient of the suction curve can be observed to decrease slightly.

For tip penetration in clay, the suction increased more rapidly than when in sand. Suction increased up to a peak value, then decreased rapidly while the skirt tip was still in clay. After the rapid loss of pressure, installation was still possible, however, the suction gradient was much reduced. For the period of installation after suction pressure reduced, it can be observed that installation suction did not follow a smooth trend characteristic of most other installations. Installation was subsequently achieved to the base of the clay layer, and then into the sand beneath. For the experiments undertaken, the maximum penetration depths recorded lay in the range of 210 to 245 mm.

The chart in Figure 4.5.2 presents the results of test SCS_3, and the results of a calculation estimating the suction required for installation into a homogeneous sand sample. Examining first the section of installation where the skirt tip was penetrating the top sand layer, it can be observed that the suction pressure required for installation at shallow depths was similar to that estimated to be necessary for installation in homogeneous sand. Suction deviated significantly away from the homogeneous sand installation estimate when the skirt tip approached the layer of impermeable clay. Figure 4.5.2 also shows a plot of the force estimated to be required for jacked installation expressed as pressure. On the chart, it can be seen that at the point where the skirt tip entered the clay, the suction required for installation did not reach the levels expected if the caisson were being jacked in place.

There are two possibilities for why suction did not reach jacked installation levels. The first possibility is that the presence of the clay layer did not impede the flow of water sufficiently to hinder the reduction of soil forces on the skirt. The second possibility may be that that the skirt end bearing resistance diminished as the caisson reached the clay. In a homogeneous sand installation, it can be calculated that the end bearing force on the skirt would be approximately 154 N. In clay, it was estimated that the end bearing force on the skirt may be approximately 49 N. Expressing these two forces as equivalent pressures, the sand end bearing corresponds to a pressure of 6.23 kPa and the clay end bearing corresponds to an equivalent pressure of 1.99 kPa. The suction pressure recorded when the skirt tip entered the clay was 3.8 kPa and the estimated equivalent suction for a jacked installation is estimated to be 8.6 kPa. The difference between the recorded installation suction and the estimated equivalent suction for jacked installation is 4.8 kPa which is similar to the difference between the sand and clay end bearing pressures, 4.24 kPa. During installation, when the skirt tip is about to enter the clay layer, it may be appropriate to assume that the bearing capacity force, generated by the skirt tip, is governed principally by clay rather than by the thin layer of sand directly underneath the skirt, and therefore the estimate for the resistance should reflect this effect.

The influence of soil type on skirt bearing capacity should not extend a large distance beneath the skirt, as the thickness of the skirt is small. If the skirt is to be modelled as a strip footing, then the depth of the bearing capacity failure mechanism will be proportional to the width of the footing. In the tests recorded here, suction deviated away from the homogeneous sand estimate approximately 15 mm before the tip reached the clay. As the skirt thickness was 1.7 mm, this would suggest that suction was influenced by the clay layer before the skirt had reached the point at which the clay bearing capacity effect would be expected to become significant.

Examining now the first reason for why suction pressures may not have reached levels estimated by the jacked installation model. The installation suction depends on the pore pressure ratio at the tip of the caisson. The pore pressure ratio calculations assumed that homogeneous sand was present, which was reflected in the resulting flow net. When a clay layer is present in close proximity to the tip of the skirt,

the flow net which was relevant for homogeneous installation becomes invalid and a new flow net should be calculated taking into account the impermeability of the clay. The new flow net can then be used to estimate the variation of pore pressure factor with depth. The calculation of pore pressure factor variation with depth, close to a clay interface, has been performed by Leblanc-Bakmar (personal communication) and the new parameters are applied to these experiments. Figure 4.5.3 shows the proposed variation of pore pressure parameter when the clay layer is present, and is plotted with the homogeneous sand variation for comparison. On the plot, the variation is shown for where the ratio of the height of the clay layer to caisson diameter (h_l/D) is equivalent to 0.6, which corresponds closely with the ratio 0.59 as used for this series of tests. On the plot, it can be observed that the estimates of pore pressure factor begin at the same value but then deviate progressively with depth. The calculation predicts that a minimum value of pore pressure factor will be reached before the factor increases again at deeper penetration depths.

The proposed relationship for how the pore pressure factor varies with depth, supplied by Leblanc-Bakmar, is shown in Equation 4.5.1.

$$a = a_o + 0.15\frac{z}{D}\left(\left(\frac{z}{h_c}\right)^2 + \frac{D}{h_c} - 1\right) \qquad \text{Eqn. 4.5.1}$$

where a_o is the pore pressure factor variation for homogeneous sand as presented by Junaideen (2004). The equation below can be used for a_0:

$$a_o = 0.45 - 0.36\left(1 - exp\left(\frac{-z}{0.48D}\right)\right) \qquad \text{Eqn. 4.5.2}$$

The effect of the impermeable clay layer is shown schematically in the series of diagrams in Figure 4.5.4. In this series, skirt depth was kept constant while the impermeable layer was moved towards the skirt tip. This allows the hydraulic gradient change due to installation to be rejected, leaving the observed changes made by the movement of the clay layer relative to the skirt. It can be observed that when the skirt approaches the clay, the hydraulic gradient between the skirt tip and the clay increases, causing the gradient within the caisson to become lower. This has a beneficial effect on installation as it

allows deeper installation depths to be available before the onset of piping. As expected, when the skirt is almost touching the clay, the gradient within the caisson becomes very low.

The suction estimate resulting from this variation is shown in Figure 4.5.5 plotted against the measured results for Test SCS_3. It can be observed that better agreement between the data and the estimate was produced for installation in sand.

The relationship for the variation of *a* (Equation 4.5.1) was compared with the results of the analysis, undertaken by Leblanc-Bakmar, to construct the relationship. The error between the proposed function and the results of the analysis increased over the final depths of installation. Figure 4.5.6 shows a plot of the variation of *a* predicted by the relationship displayed with the results of the analysis. Recalculating the suction estimate using the values obtained directly from the analysis and interpolating linearly between each data point produced the result in Figure 4.5.7. It can be observed that good agreement was obtained at shallow depths, but as the skirt tip approached the clay, the large increase in suction was not reproduced.

The suction factors were calculated for sand with uniform permeability. It was concluded above, that during installation, the permeability of soil within the caisson increases. For these installations, where similar permeability changes are expected to have occurred, the recorded suction pressures would therefore be larger than those calculated assuming no soil disturbance.

When the skirt tip is in the clay, the suction required for installation may be estimated by assuming that all water flow within the caisson ceases. When this happens, the friction on the side of the skirt for the portion that is contacting the sand may be estimated using the resistance model described for jacked installation. The forces on the skirt arising from the contact with clay may be estimated using a similar method outlined for installation in homogeneous clay with adjustments made to reflect the area of clay in contact with the skirt.

An important adjustment to the clay installation resistance estimate must be made to calculate the end bearing force on the skirt tip. The end bearing term for an installation in homogeneous clay may be calculated using the equation recommended below (N_q =1):

$$F_{end} = (\pi Dt)(\gamma' z + s_u N_c) \qquad \text{Eqn. 4.5.3}$$

In the second bracket, the $\gamma' z$ term accounts for the vertical stress adjacent to the base of the footing. For installation in homogeneous clay, the enhancement of stress adjacent to the base of the skirt by adhesion effects is conventionally not calculated in the end bearing force. For an installation in sand, the effect of stress enhancement by friction is accounted for, and is a necessary consideration to achieve accurate modelling of the installation resistance.

In the method of suction estimation outlined here, the frictional effects in sand are accounted for, but the effect of adhesion on the vertical stresses in the clay, adjacent to the tip of the caisson, are not. Thus, the stresses adjacent to the skirt tip, while the caisson is in clay, are calculated as the sum of the estimated vertical effective stress in sand at the interface with the clay, and the product of the unit weight of the clay and skirt tip depth within the clay. This relationship is expressed below:

$$\sigma'_{v,skirt\ tip} = \sigma'_{v,sand} + \gamma_c'(z - h_s) \qquad \text{Eqn. 4.5.4}$$

where h_s is the sand layer thickness. The resulting suction estimate is displayed in Figure 4.5.8. From Figure 4.5.8, it is possible to observe that a good estimate can be obtained up to the point where suction decreases rapidly.

At the point at which suction pressure rapidly decreased, it was calculated that plug lift may have occurred. The suction for plug lift is plotted on the chart in Figure 4.5.9 along with the estimated suction required for installation and the measured data. It can be observed that the estimated suction for plug lift decreased at deeper penetration depths. The rapid reduction of suction can be observed to occur close to the intersection of the installation and plug lift suction estimates. After plug lift occurred, the clay beneath the caisson would have become disturbed, lowering s_u, which accounts for why the installation suction decreased rapidly.

The plug lift estimate assumed the forces outlined in Figure 4.5.10. To estimate the friction force between the skirt and the sand, it was assumed that an enhancement of stress would occur by the action of sand moving relative to the skirt. The movement of the skirt relative to the sand is the same during caisson installation and plug lift, so the calculation was performed in a similar manner as for installation. The expression for plug lift is shown below:

$$F_{plug} = F_{sand\ weight} + F_{clay\ weight} + F_{clay\ shear} + F_{adhesion} + F_{sand\ friction} \quad \text{Eqn. 4.5.5}$$

The force required for plug lift was then expressed as a pressure by dividing through by the internal area of the plug. The terms above were calculated according to the relationships below:

$$F_{sand\ weight} + F_{clay\ weight} = \left(\pi D_i^2/4\right)(\gamma'_s h_s + \gamma'_c h_c) \quad \text{Eqn. 4.5.6}$$

$$F_{clay\ shear} + F_{adhesion} = (\pi D_i)\left(s_u(h_s + h_c - z) + \alpha s_u(z - h_s)\right) \quad \text{Eqn. 4.5.7}$$

$$F_{sand\ friction} = (\pi D_i)(K tan\delta) \int_0^{h_s} \sigma'_{v,sand}\, dz \quad \text{Eqn. 4.5.8}$$

Figure 4.5.11 shows installation suction along with two estimates of the suction required for installation beneath the clay layer. The estimates correspond to suction installation in homogeneous sand, and jacked installation in sand (accounting for the presence of clay). It may be observed that the suction was higher than that expected for suction installation in homogeneous sand but did not reach the values expected for installation by jacking.

The maximum penetration depth was 245 mm which corresponded to 75 mm below the base of the clay layer. It was noted that installation ended with a rapid loss of suction pressure, similar to the behaviour observed when piping failure occurred. The chart in Figure 4.5.12 shows a plot of the pumped water volume during installation for Test SCS_1. Inspection of the water volume pumped at the end of installation reveals that water flow had not ceased despite installation no longer recording skirt penetration. This behaviour is consistent with installation ending by the onset of piping in the lower sand layer.

In Figure 4.5.12, the installed caisson volume is plotted as a function of depth for comparison with the total water volume pumped. As expected, the pumped water volume in the top layer of sand exceeded

the volume of caisson installed. When the skirt tip entered the clay layer, it can be observed that the water pumped per unit installation depth decreased rapidly. The gradient of the pumped water line has been calculated and is shown for the early stages of installation into the clay. The gradient of the pumped volume to install the caisson is displayed for comparison. It can be observed that the gradient of the water pumped during early stages of penetration in clay is of similar value, but, in all cases lower than that for the required pumped water volume necessary for installation. As the pumped water volume exceeded the volume of caisson installed, this would indicate that either a small degree of seepage was experienced during installation, or perhaps that installation was causing a small quantity of plug lift even when the skirt tip had just entered the clay layer.

The pumped water volume can be observed to rapidly increase as the skirt tip approached the depth at which the suction had become large enough for plug lift to occur. The charts in Figure 4.5.13 through to 4.5.17 present suction and volume of water pumped. It can be observed that a rapid increase of pumped volume accompanied the sudden loss of installation suction.

For each experiment, further caisson installation was still possible despite plug lift having occurred. This contrasts with the clay over sand installations where plug lift was accompanied by caisson refusal. Analysis of the pumped volume charts reveals that after plug lift, the pumped water volume exceeded the volume of caisson installed. Since observed plug movement was small, the volume of water removed associated with plug lift will have been small. Therefore the excess water pumped is likely to have been supplied by seepage occurring in the lower sand layer. This outcome may indicate that the thin plug did not remain intact after plug lift had occurred.

Seepage, in the sand beneath the clay, would have lowered the installation resistances. As the installation suction was not as high as expected for the case where jacking resistances were encountered, seepage may have contributed to a reduction of installation resistance in the lower sand layer. A firm conclusion cannot be drawn on this aspect, as plug lift would also have lowered the surcharge acting on the sand reducing the effective stresses.

Using suction data and the estimated variation of flow factor with depth, the pumped seepage volume can be estimated using the strategy outlined in Section 2.4 for the top layer of sand. The suction across the plug at the depth of the skirt tip was assumed to be uniform, creating a uniform seepage flow within the volume of the plug. The flow factor variation assumed for this estimate used the data of Leblanc-Bakmar and therefore was appropriate for a caisson installed in sand approaching an impermeable layer.

The estimated variation of pumped water volume is presented in Figure 4.5.18, plotted along with the measured values for experiment SCS_3. The pumped volume is only displayed for the phase of installation where the skirt tip was in the top sand layer. The water volume arising from the reduction in caisson volume due to installation is plotted on the chart to enable comparison between the seepage volume and that arising from installation. It can be observed that the estimated seepage flow corresponds favourably with the measured volume over the period of installation when the skirt tip was in sand. The seepage volume in this series of tests was larger than the caisson volume. The seepage estimate was also applied to experiment SCS_1 and is presented in Figure 4.5.19. Again, the calculated volume to be pumped was similar to that recorded over all depths of installation in the top sand layer.

The estimated seepage volume was smaller than the volume pumped because the estimate did not take account of the variation of plug permeability as installation proceeds. The estimated volume pumped agreed closely with the recorded volume at shallow penetrations but progressively under-predicted the pumped volume at deeper penetrations.

4.6 Installation of caissons in sand overlying inclined clay

4.6.1 Introduction

In practice, it is unlikely that sand will be encountered overlying a perfectly flat clay horizon, such as those tested in the laboratory, as the influence of geological processes move the layers. The proximity of clay causes the pore pressure ratios to be higher than those encountered at similar depths in

homogeneous sand. When the suction factors at the skirt tip are increased, the suction required to install the caisson becomes correspondingly larger.

Installation into inclined clay presents an interesting problem for analysis, particularly where the inclination of the clay is steep. As the skirt tip approaches the highest point of the clay layer, the seepage will become reduced by the impermeable soil. For the side of the caisson down slope of the clay, there may still be significant distance between the skirt tip and the clay, which may leave seepage relatively unaffected. If seepage can be significantly cut off, the sand resistances are anticipated to become relatively high. On the other hand, if seepage flows can still be maintained throughout the plug, despite the entry of water being partly blocked by the clay, installation may still be possible.

For this series of tests, the strategy taken was to install a caisson under conditions chosen to be close to the theoretical limit for maximum penetration by suction without causing critical hydraulic gradients to form. If the caisson could be installed, the next experiment would be undertaken under more challenging conditions. If the caisson could not be installed, the conditions would be changed to make installation more favourable.

4.6.2 The suction and water volume pumped when installing in sand over inclined clay

The suction measured during installation is shown in Figures 4.6.1 to 4.6.4 and the depth of clay is plotted for each case. This depth corresponds to the point at which the skirt tip becomes completely installed into the clay (the maximum penetration distance of the skirt tip in sand). As the clay inclination was 33.2º, the transition depth was 119 mm.

At shallow depths, the suction was similar to that which would have been estimated for homogeneous sand installation. Deviations from the homogeneous sand estimate occurred, progressively, as the skirt tip approached the sand/clay boundary.

The undrained shear strength of the clay was measured with a hand shear vane and found to have an average value of 3 kPa. The end bearing force on the skirt imposed by clay would be larger than that imposed by sand when in the presence of seepage. As the skirt tip approached the clay, it was therefore expected that the installation resistance would have increased. This was reflected by an increase of pressure variation.

The suction equivalent to the force necessary for caisson installation without water flow has been included on Figures 4.6.1 to 4.6.4. Throughout installation in sand, resistances lower than those expected for jacking were encountered. This implies that as the area through which seepage could flow reduced, the seepage which was available reduced the sand resistances effectively. A positive outcome may be that for caissons which are to be installed mainly by jacking, for example in places where substantial seepage flows are not expected, the application of suction may still greatly assist an installation even if only small seepage flows can be produced.

Figures 4.6.5 to 4.6.8 show the volume of water pumped during each installation for this series of tests. From the plots, it can be observed that while the skirt tip penetrated the sand, the volume of water pumped exceeded the volume of caisson installed, confirming that seepage was present. During installation in clay, the extracted water volume closely matched that required for skirt volume installation, indicating negligible seepage flows. This outcome is consistent with the conclusions made after the installation in homogeneous clay.

In all tests, it was possible to install the caisson to the base of the sand layer and then into the clay beneath. The plug heave for the sand could be calculated for tests SIC_3 and SIC_4 as the full skirt length was installed up to the point where the lid touched down onto the sand. Plug movement was measured as 30 and 28 mm for tests SIC_3 and SIC_4 respectively. Installing the skirt fully required that a volume of sand equivalent to a uniform plug heave of 13.8 mm be displaced. As the volume of material displaced in the plug heave soil was greater than the volume of soil displaced by the skirt, the

installation caused additional soil movement. These movements may be partly attributed to plug loosening as observed by other research (Andersen *et al.* (2008)).

The installation conditions were chosen to test whether the presence of a clay layer hindered the penetration of caissons in the sand. The self weight for the first three tests was 30 N with test SIC_4 being undertaken at a self weight of 10 N. As SIC_4 was undertaken with the deepest penetration distance in sand and at the lowest self weight condition, this represents the most critical condition for installation. For the first three tests, the depth of sand was increased by 50 mm for SIC_2 and a further 50 mm for SIC_3. As the onset of piping becomes more likely with penetration due to higher hydraulic gradients caused by suction, test SIC_2 was thought to be more critical than test SIC_1 and test SIC_3 more critical than test SIC_2. Using the onset of critical gradients as the limit for caisson installation, it was estimated that the brass caisson could be installed by 140 mm in homogeneous sand. This condition set the installation depth for test SIC_1, and depending on the outcome of this experiment, the sand depth for the remaining tests could be increased or decreased accordingly until refusal was obtained. However, in all cases, the caisson could be installed into the clay.

In Figure 4.5.4, it was schematically shown that as the clay layer approached the skirt tip, the hydraulic gradient at that location increased as a result of the constriction of flow. The gradient inside the caisson decreased as a consequence. The presence of an inclined clay horizon would cause a similar effect which would enable deeper skirt penetration before piping failure was encountered. To enable this effect to be measured, a flow analysis should be undertaken using a 3D flow net.

A calculation of the suction required to create a reverse end bearing failure for a caisson installed 85 mm into clay of similar strength to the sample used in these experiments, estimated that a pressure of 28 kPa was necessary. The reverse end bearing factor for a flat clay horizon was used, whereas in these experiments the clay was inclined. The result is that the suction required to cause failure would be lower, as there would be less material to shear on the ‘down-slope’ side of the skirt, so it may be possible that for tests SIC_3 and SIC_4, where large plug heaves were recorded and the suction

pressures reached levels of over 20 kPa, the clay at the base of the sand failed, causing large plug heave levels to be recorded.

The onset of a reverse end-bearing failure would be consistent with the observed movement of the sand on the surface of the sample. Figure 4.6.9 shows a photograph taken of the sand directly adjacent to the caisson on the 'down-slope' side of the inclined clay layer. The photograph was taken during installation while the skirt was penetrating the soil. The photograph shows a large quantity of soil movement adjacent to the skirt, seen as a large depression opening up on the sample surface. The depression would be consistent with the clay flowing into the interior of the caisson, causing sand to drop into the void created by soil movement.

4.7 Conclusions

For suction installation in homogeneous sand, estimates of water flow were made using the assumed hydraulic gradients and found to be consistently lower than those recorded during experiments. The values of pore pressure parameter (a) were directly measured using the modified caisson developed for this work. It was noted that k_f increased linearly with depth, and increased by a greater amount with faster installation rates. For installations undertaken at rates of approximately 0.1 mm/s, it was recorded that k_f began at a value of approximately 1 and increased to 2 by the end of installation.

Measurements of discharged water volume supported the conclusion that, the overall plug permeability increased with depth. The overall permeability also increased with installation speed, and the suction required for installation was found to be broadly similar over the range of installation speeds used with the exception of the slowest installation undertaken.

Installations were undertaken in clay over sand soil. It was discovered that it was possible for the caisson to become stuck during the course of installation. The action of plugging was observed both visually and by comparison of the pumped water volume with the installed caisson volume.

When the plug lift results were plotted in non-dimensional space, a boundary was observed which defined the success of installation to the base of the clay layer. Experiments plotting in the region above the boundary ended with plug lift, while those plotting in the region below the line ended with the skirt being installed to the base of the clay. This was consistent with the calculations made based upon the proposed model of plug lift. Rapid installations undertaken at conditions which enabled plug lift were able to install the caissons further into the soil than those undertaken at a comparatively slower rate. For caissons installed through the clay into the sand beneath, the installation suction was found to be very much higher than that estimated to be necessary when considering installation in homogeneous sand.

Installations were undertaken into homogeneous sand containing a thin clay layer. All experiments were able to install the caisson through the clay layer. When the skirt tip entered the clay, it was found that suction increased substantially due to hydraulic blockage. Installation calculations, for the case of sand with a clay layer, were undertaken using a variation of pore pressure parameter which accounted for the proximity of the clay and the calculated suction variation agreed well with observed values. During these installations, plug lift was observed during penetration in clay. The onset of plug lift could be estimated using similar calculations outlined in Chapter 2.

Installations were undertaken through sand into an inclined clay layer. It was possible to install the skirt into the clay for all experiments. As the size of the seepage channel was reduced, the recorded seepage flow volume diminished. For inclined clay experiments, where piping failure was expected, the caisson did not become stuck. Installation continued until the skirt had been fully installed into the clay, after which piping would not occur as seepage was blocked. When the skirt had been fully installed, it was observed that reverse end bearing failure had developed.

5 Caisson installation in sand with skirt tip injection and steering

5.1 Introduction to skirt tip injection and caisson steering

5.1.1 Introduction

The foundations for offshore renewable energy structures may comprise either monopod or multi-footing configurations. For the Sleipner T and Draupner E platforms (Bye *et al.* (1995), Andersen and Jostad (1999)), four caissons were installed simultaneously. Levelling of the platform was achieved by penetrating the high corners of the structure further than the others. Such a method would not work for monopod designs where there are no other caissons to use for correcting levels.

The seabed is unlikely to be level at all locations of installation, and caissons placed onto an inclined seabed are likely to commence installation at undesirable angles as demonstrated at field scale (Colliat *et al.* (1996)). It is therefore critical that caisson inclination can be corrected early in the installation phase. Additionally structures attached to the caisson transfer the centre of gravity away from the axis, disrupting attempts to install the caisson level (Sparrevik (2002), Houlsby *et al.* (2005)).

A caisson levelling system would therefore be useful. The system should finely control the plane of inclination, and ideally should be capable of being remotely controlled from a floating vessel using relatively cheap and readily available equipment. The effect of the levelling system on maximum skirt penetration depth should be known to avoid unexpected caisson refusal.

5.1.2 Description of STI caisson

Figure 5.1.1 presents a photograph of the caisson capable of skirt tip injection. The caisson used for the steering tests was constructed by attachment of a transparent Perspex lid to a stainless-steel tube. The lid was machined to locate the top of injection supply pipes which were positioned on the outside of the caisson skirt, and attached with epoxy resin. The top of each injection supply tube was connected to a

manifold, to which was supplied pressurised water. The manifold had a Druck pressure transducer fitted to allow water pressure measurement. The injection pipes were constructed from 5 mm diameter stainless steel pipe with a wall thickness of 0.1 mm. Thin wall tube was chosen to minimise the skirt tip area. Initially, eight injection nozzles fitted for the first test series, after which the caisson was modified to accept 16 for the second series.

5.1.3 Installation apparatus for skirt tip injection experiments

All skirt tip injection experiments were undertaken in the small installation tank. The apparatus for the homogeneous soil installations was used with the STI caisson (described in Chapter 3.5) for this series of tests, with the addition of a pumping system to supply the skirt tip injection pressure.

The skirt tip injection pressure was provided by a second Ismatec pump which was identical to the one used to create the installation suction pressure. The pump could be controlled from the PC in the same manner as the installation pump. The pump fed pressurised water to the manifold which distributed water to the skirt tip injection pipes.

The skirt tip injection flow rate was measured during installation in a similar manner as for the pumped flow rate arising due to installation. The water for skirt tip injection was held in a reservoir which was weighed using a load cell. As the water was injected, the change of weight was recorded which allowed the flow rate to be calculated.

5.1.4 Installation apparatus for caisson steering tests

The caisson steering tests were undertaken in the small installation tank. The apparatus for the homogeneous soil installations was used for this series of tests with modifications. The changes made to the apparatus allowed the caisson to move in all six degrees of freedom to accomplish the objectives of the tests. The self weight of the caisson still had to be controlled with the counterbalance system however, as the caisson was too heavy to model a prototype caisson appropriately.

The force applied to the caisson for counterbalance purposes needed to be applied in such a way that the effect of counterbalancing was only to lower the self weight of the caisson and not to cause a moment or lateral load. The caisson was disconnected from the brass rod and a metal loop was attached at the centre of the caisson. The caisson was then attached to the counterbalance system via the loop with a 1 mm diameter stainless-steel cable. The caisson was then hung from the wire and the instruments on the top of the caisson were carefully positioned so that the caisson hung level. The purpose of this was to position the centre of gravity underneath the centre of the caisson lid so that when the counterbalance force was applied, the force would act through the centre of gravity and not impart a moment load on the caisson.

All sources of moment loading needed to be eliminated or minimised as much as possible for the steering tests, as the objective was to measure the changes of caisson angle to selective skirt tip injection. The water supply pipes were changed to 4 mm diameter pipework as the smaller diameter pipes could be bent using much less force than was necessary for the 8 mm diameter pipework. The reason for this being that the walls of the small diameter pipe were 0.75 mm thick while those for the large diameter pipe were 1.4 mm. As the force required for bending is proportional to the second moment of area (I) of the section, both materials being the same, the smaller diameter pipe would only need one fifteenth of the force required to make a unit radius bend when compared to the large diameter pipe.

The pressure transducers were connected to the instrument amplifiers by cables. The suspended weight of the cables was relatively high compared to the caisson weight, so the cables were counterbalanced using the counterbalance system as was the weight of the water supply tubes.

An inclinometer, manufactured by Level Developments (see Figure 5.1.2), was used to measure caisson inclination. The inclinometer was capable of measuring angles along the x and y axis up to ± 30º from the horizontal with a resolution of 0.01º. The output of the inclinometer was displayed as the

experiment was undertaken to allow monitoring of the steering inputs. The inclinometer could not be submerged under water, so was held above the caisson by a bracket.

5.1.5 Limits to suction assisted penetration

The maximum penetration depth of caissons installed in sand is limited by the onset of critical hydraulic gradients within the soil plug. After critical hydraulic gradients have been formed, there is a risk that the flow of water opens up large seepage channels through which water can pass without incurring significant head loss. With this pressure loss, the pressure in the interior of the caisson may not be sufficiently low to provide the assisting force to drive installation.

The upward hydraulic gradient at which the flow of water in the soil becomes critical occurs when the following condition is satisfied:

$$\gamma' z - (1 - a)s = 0 \qquad \text{Eqn. 5.1.1}$$

The effect is that the maximum suction that can be applied is limited to the following value which varies with depth:

$$s = \frac{\gamma' z}{(1 - a)} \qquad \text{Eqn. 5.1.2}$$

Houlsby and Byrne (2005b) proposed that an alternative limit for suction can be calculated by setting the condition for inflow into the caisson to be defined as follows:

$$\sigma'_{vo} = N_q \sigma'_{vi} \qquad \text{Eqn. 5.1.3}$$

The method using Equation 5.1.3 would be to calculate the stresses during installation, and check the depth at which the condition is satisfied. In practice, either method can be usefully employed as they both offer similar values. Equation 5.1.3 allows the maximum penetration depth to be determined when different boundary conditions are imposed. This may occur, for example, if a surcharge (or lack of it) is present on the top of the sand and is therefore a more robust approach.

For the parameters commonly encountered in sand, the limit of installation is approximately equivalent to the diameter of the caisson. While this may be acceptable for many applications, it would be

worthwhile investigating methods to increase this limit as skirt installation into deeper soil would increase bearing capacity and be beneficial to the overall stiffness of the structure. It would also enable greater protection against the effects of scour.

5.1.6 Development of skirt resistance control system

Inspecting the installation equation (Equation 1.3.15), it is possible to examine whether the driving forces can be enhanced, or the resisting forces can be decreased. Increasing suction is not possible, and increasing the caisson self weight is undesirable as this requires more equipment which tends to be expensive to employ offshore. Alternatively, a method of reducing the soil resistances would be preferable, particularly if it could incorporate the levelling requirements outlined above. The method outlined in the following Section is to use skirt tip injection to facilitate modification of the pore water pressure on the outside of the skirt directly adjacent to the skirt tip.

A field installation was conducted by Senepere and Auvergne (1982) who undertook installation of suction piles where the base of the skirt incorporated a modification to allow high pressure jetting. The piles were relatively long compared to their diameter, causing the onset of critical hydraulic gradients and significant plug heave, hindering full installation. The piles were modified to permit jetting into the top of the soil plug to create liquefaction enabling removal of the plug as it moved. No report was made regarding the behaviour of skirt jetting or whether it was at all used.

In this Chapter, the application of skirt tip injection will be studied. This process differs slightly from jetting, as lower pressures are planned. The aim is simply to modify the pressure of the pore water to change the effective stresses and therefore the soil resistance. For a jetting process, the aim is to physically move soil particles away from the path of the skirt by applying forces to the particles using very high pressures.

The use of skirt tip injection (STI) has been reported by Tjelta *et al.* (1986), where it was noted that tip resistance could be reduced when water pressure was applied. However, no description or analysis of

this method was reported. A caisson capable of skirt tip injection can be readily modified to allow selective injection to enable steering. A series of tests investigating the performance of these methods, may open the way for further confidence in the adoption of caissons as a foundation system in addition to their widespread use as anchors.

5.2 The operation of skirt tip injection

5.2.1 The effects of injection on skirt resistance

For skirt tip injection to be most effective, the injection of pressure should result in augmentation of the beneficial effects of suction installation and minimise or even reverse the negative effects of suction installation at deep penetration depths. During jacking, the flow of soil particles displaced by the action of the skirt is assumed to be partly into the caisson and partly to the outside of the skirt (Chen and Randolph (2003)). The reason can be attributed to the stress redistribution created by this method of installation. The action of installation augments the in-situ stresses within the soil on either side of the caisson skirt. For homogeneous sands, the stress augmentation within the caisson will be higher than for soil outside the caisson, and the soil has a larger component of flow to the outside of the skirt.

For suction installation, the effective stresses are substantially lower inside the caisson, causing the flow of soil displaced by the penetrating skirt to be mainly toward the interior of the foundation. This flow results in increased plug heave observed after suction installation, and also causes plug loosening which increases the permeability of the soil (Erbrich and Tjelta (1999)).

The skirt resistances can be split into components and examined to assess how the injection of water pressure might influence each force. Unfortunately, the individual components of resistance cannot be measured directly, as only self weight and installation suction are recorded, so the effect of STI will be assessed as an overall effect on suction and penetration depth. There have been attempts to measure the end bearing stress on the tip of model foundations, for example Andersen *et al.* (2008). However, the skirt thickness to diameter ratio did not model a field condition accurately, which would lead to

unrealistic soil strains during skirt penetration. For this reason, measurement of individual force components was not attempted.

5.2.2 Effect of water injection on the soil resistances outside the skirt

The water flow around the outside of the skirt is downwards which serves to increase the vertical effective stresses. These in turn increase the friction resisting installation. If the hydraulic gradient along the outside of the skirt were lowered, the flow of water would be reduced, which would reduce the friction acting on the outside of the skirt. The hydraulic gradient could be lowered by increasing the pressure of the water at the tip of the skirt.

5.2.3 Effect of water injection on the skirt tip resistance

During suction installation, water flows around the skirt tip from the outside toward the inside. The gradient of the hydraulic flow at this point has been widely reported to be particularly high and contributes to reducing the tip resistance of the skirt (Erbrich and Tjelta (1999), Iskander *et al.* (2002), Tran (2005)). Injection of water outside the skirt, adjacent to the skirt tip, could create larger hydraulic gradients, augmenting the reduction of skirt tip resistance.

5.2.4 Effect of water injection on the soil resistance inside the caisson

Water flow within the caisson is predominantly in the upward direction, particularly at high penetration depths. During suction installation, the hydraulic gradient will eventually become critical, leading to the risk of piping failure. Water injection should be undertaken in a way which minimises the enhancement of the hydraulic gradient within the caisson, as the result would be that critical gradients occur at shallower installation depths.

5.2.5 Method of water pressure delivery at the skirt tip

The method chosen to achieve the conditions outlined above was to pump water through narrow tubes attached to the outside of the skirt, and allow the water to emerge at the skirt tip outside the caisson. By pumping water using this method, the water pressure associated with this flow would be placed

strategically for interaction with the flow around the base of the skirt and with the downward flow along the outside of the skirt.

Water injection could be selectively applied to individual nozzles, or nozzle groups, allowing caisson steering to be attempted. The effect of injection on steering and the suction necessary for installation was trialled at various depths. This was because the rotational stiffness of the foundation may vary with penetration, and the deepest penetrations are of greatest interest if STI is to be used for extending the maximum installation depth.

5.2.6 Estimation of the effect of water injection at the base of the skirt

The effect of water injection should be quantified for application to prototypes. It was assumed by Houlsby and Byrne (2005b) that the gradients of water flow in the interior and exterior of the caisson vary linearly in the following manner:

$$Outside\ gradient = \frac{as}{\gamma_w h} \qquad \text{Eqn. 5.2.1}$$

$$Inside\ gradient = \frac{(1-a)s}{\gamma_w h} \qquad \text{Eqn. 5.2.2}$$

If the effect of water injection was to supply an average uniform pressure to the base of the caisson tip, the pressure distribution between the surface of the sand and the point of water injection could be estimated by the superposition of the hydraulic gradients imposed by suction installation and the hydraulic gradients created by water injection. With no STI present, but with seepage caused by suction installation, the effective stress outside the caisson can be calculated by substituting Equation 5.2.3 for γ' in Equation 1.3.6 and integrating with respect to depth.

$$\gamma' + \frac{as}{h} \qquad \text{Eqn. 5.2.3}$$

Inside the caisson, the hydraulic gradient lowers the effective stresses, which can be calculated by integrating Equation 1.3.7 if Equation 5.2.4 is substituted for γ'.

$$\gamma' - \frac{(1-a)s}{h} \qquad \text{Eqn. 5.2.4}$$

Where STI will be applied, if the hydraulic gradients can be modified using the assumptions outlined above, the stress at the base of the skirt may now be calculated by substituting Equation 5.2.5 into Equation 1.3.6 to obtain the effective stress variation outside the caisson:

$$\gamma' + \frac{as}{h} - \frac{p_{inj}}{h} \qquad \text{Eqn. 5.2.5}$$

and inside the caisson, Equation 5.2.6 may be substituted into Equation 1.3.7 to obtain the variation of effective stress:

$$\gamma' - \frac{(1-a)s}{h} - \frac{p_{inj}}{h} \qquad \text{Eqn. 5.2.6}$$

where p_{inj} is the pressure of the water injected at the base of the skirt. Therefore the gradient of the effective stress outside the caisson is expressed as follows:

$$\frac{d\sigma'_{vo}}{dz} = \gamma' + \frac{as}{h} - \frac{p_{inj}}{h} + \frac{\sigma'_{vo}}{Z_o} \qquad \text{Eqn. 5.2.7}$$

and the effective stress gradient inside the caisson can be estimated by the expression below:

$$\frac{d\sigma'_{vi}}{dz} = \gamma' - \frac{(1-a)s}{h} - \frac{p_{inj}}{h} + \frac{\sigma'_{vi}}{Z_i} \qquad \text{Eqn. 5.2.8}$$

The equations can be solved using a 4th order Runge-Kutta method. These calculations were incorporated into a spreadsheet which enabled the soil stresses to be estimated and then used to determine the skirt resistance.

The pressure distribution was assumed to be uniform around the skirt despite the water being delivered to individual locations. This was reflected in the stress gradient expressions, as the calculated stresses were then distributed around the caisson to estimate the resisting force mobilised by the soil.

5.3 Installation experiments using skirt tip injection

5.3.1 Method of suction caisson installation for skirt tip injection tests

The sample was arranged according to the method described in Chapter 3. The pumping systems were de-aired to ensure that only water was injected at the skirt tip. The caisson was allowed to suction

penetrate to a depth of 50 mm before the skirt tip injection was applied. It was found that application of skirt tip pressure at shallow depths caused piping failure to occur.

During initial suction penetration, the water supply to the injection manifold was shut off to ensure that water was not drawn through the injection system to the skirt tip. As a comparison was to be made between the non-injected case and skirt tip injection phases, the water needed to be channelled along the appropriate routes. When the caisson had reached the required depth, the valve supplying the injection manifold was opened and the skirt tip pressurisation pump was started. The speed of the pump was increased in small steps while the recorded manifold pressure was monitored. The pump speed was then controlled to maintain the skirt tip pressure at the level necessary for the experiment. Installation was stopped when the caisson had either been installed, or piping failure was encountered.

5.3.2 Experiments using eight points of injection at the base of the skirt

Table 5.3.1 shows the tests performed in Test series one, using the eight port caisson. Test series two performed using the 16 port caisson is listed in Table 5.3.2, and a table of the steering tests undertaken, also with the 16 port caisson, is presented in Table 5.3.3. The caissons are described in Section 5.1.2.

The first series of tests used an eight nozzle caisson. The pressure was applied at a depth of approximately 50 mm to avoid critical hydraulic gradients. Installations were undertaken with injection pressures ranging from no pressure up to those sufficient to cause plug failure. The purpose of installing the caisson without injection was to assess the installation resistance of the caisson with the injection system attached, as the modifications increased the skirt tip plan area and the surface area of the exterior of the skirt. The skirt tip area was minimised as much as possible by choosing the thinnest wall pipe available. All tests were undertaken at an installation rate of 0.1 to 0.15 mm/s.

5.3.3 The pressure applied for water injection

When injection was applied to the base of the skirt, the pressure was measured in the supply manifold from which the water was distributed to the nozzles. The supply manifold was positioned at the top of the caisson and moved with the skirt. To determine the injection pressure, it was necessary to account for the hydrostatic pressure which increased as the nozzles penetrated the sand. The injection pressure (Δp_{inj}) was calculated in the following manner:

$$\Delta p_{inj} = \Delta p_{manifold} - \Delta p_{hydrostatic} \qquad \text{Eqn. 5.3.1}$$

The injection pressure was manually stepped up from low pressures over a small distance of installation as can be observed on the injection pressure plots (for example Figure 5.3.1). Small variations in pumping rate could significantly affect the pressure applied and possibly lead to critical gradients within the soil.

5.3.4 Demonstration of STI

Figure 5.3.1 shows a plot of the variation of suction and injection pressures with depth for a typical experiment. In Figure 5.3.1, it can be observed that when STI was applied, the suction for installation decreased. For this experiment, STI pressure was applied in a series of six steps after the skirt had reached a depth of 54 mm.

For this experiment, the STI pressure was 10 kPa. It can be observed that when STI was stopped, greater suction pressures were immediately required to maintain installation. Installation was then undertaken up to a depth of 135 mm at which point installation stopped by the onset of piping. When piping occurred, it can be observed that the suction inside the caisson dropped almost instantaneously.

It is remarkable that the high injection pressure at the nozzles could be maintained over a relatively large distance of installation without encountering soil liquefaction. Installation ceased at a depth of 135 mm when the suction pressure in the interior of the caisson had reached almost 1.8 kPa. From the charts of the variation of pore pressure factor (a) with depth (Houlsby and Byrne (2005b)), the factor at 135 mm

or z/D = 0.893 is estimated to have been approximately 0.146. Using this value, the hydraulic gradient within the caisson is calculated as having been 1.169.

When injection was applied, 10 kPa could be maintained at much shallower installation depths. The injection pressure reached steady state at a depth of 60 mm and the suction pressure within the caisson was 0.625 kPa. Assuming the pore pressure at the tip was 10 kPa, the calculated hydraulic gradient inside the caisson is 18.05. This gradient is over 15 times higher than the one which caused the caisson to cease installation (1.169), so the effect of STI on pore pressure over the depth of the plug must be reconsidered (see Section 5.5). The highest injection pressures recorded during the tests was 16 kPa (in test 8N test 33), however, the onset of piping failure was observed shortly afterwards. Injection at this pressure was begun at a depth of 79 mm.

5.3.5 Water volume injected during STI installation

The injected water volume pumped during STI is shown in Figure 5.3.2. The total volume of water pumped was just over 500 ml. The chart indicates that the water was consumed linearly with depth, indicating a uniform flow rate. The water volume pumped out of the caisson is shown in Figure 5.3.3 where it is recorded that 3500 ml of water was removed. The recorded water pumped during installation without the use of STI is shown in Figure 5.3.4, which records that 3000 ml was pumped. The difference in water volume pumped between the tests which used STI and those which did not, is 500 ml, which is equivalent to the volume of water recorded pumped into the STI system. This result would appear to indicate that the use of STI at the base of the skirt mainly increased the flow of water within the plug and did not reduce the flow of water into the caisson by reducing the water flow down the outside of the skirt.

5.3.6 The effect of STI on the suction required for installation

The effect of STI on suction will now be examined. The installation suction is presented in Figure 5.3.5 for experiments using a series of injection pressures. For experiments undertaken in similar soil samples, the suction required for installation should be the same in each test if all conditions are the

same. For the tests described here, each installation was undertaken in a separate soil sample leaving no room to undertake a second for comparison. The variation between samples was minimised by using the same sand and method of preparation, but inevitably a series of identical samples could not be produced. Therefore, it is not sufficient to compare the suction pressure between tests, as this method does not account for sample variation.

This series of tests intended to measure the reduction of suction pressure resulting from the application of STI. As the injection pressure was increased in a series of stages up to the target, the depth of the caisson when the target injection pressure had been obtained was substantially different to the depth at which injection had begun. Therefore, the difference between the suction at the start of injection and the suction when target pressure was obtained are not comparable as the datum for measurement had changed.

The method of comparison for the effectiveness of STI proposed here uses the initial stage of the installation as a reference against which the change of suction caused by STI can be compared. For most tests, injection was applied after the caisson had been installed by approximately 50 mm, and target pressure was reached by the time the caisson had been installed by 60 mm. To quantify the effects of STI, the installation suction pressures at a depth of 100 mm, 60 mm and 40 mm were recorded for each successful test. For tests where the injection pressure had not stabilised by 60 mm depth, the pressure data was recorded for 50 mm, 70 mm and 110 mm. These points maintain the same distance between samples.

The change of suction per unit depth could then be calculated between the two sampling points. The two depths provide an indication of the effect of STI shortly after application, and at relatively deep installation depths. The results of the calculations are tabularised in Table 5.3.4 for the 8 nozzle caisson. A comparison could be made by examining the pressure difference. However, the numbers are small, so the difference is converted into a gradient to assist comparison. The gradient is expressed as the ratio of the difference in depth between the two samples and the difference in suction. As the most effective STI

application would cause the suction difference to be smallest, larger numbers represent a greater pressure reduction due to STI.

A direct comparison between the injection pressures is now made by considering the average pressure difference for each series of injection pressures, Table 5.3.5. From the Table, it can be observed that both series of comparisons follow the same trend. The data demonstrates that the application of STI lowered the suction for installation both at shallow and deep penetration depths as the gradient for each injection pressure is higher than for the no injection case over that depth. The only exception to this trend is the shallow comparison made at 5 kPa for which the average gradient (66.2 mm/kPa) has been lowered by a particularly large pressure difference recorded in one of the tests. Inspection of the suction plot (shown in Figure 5.3.6) reveals that the installation phase before injection was begun follows a particularly curved trend out of character with that observed in other experiments. If this data point is removed, the average gradient for the shallow comparison at 5 kPa becomes 74.4 which matches the observed trend.

Both comparisons conclude that higher injection pressures were more effective at lowering the installation suction than low pressures. The differences between the average gradients for injection tests and the no-injection gradients are shown in Table 5.3.5 and Figure 5.3.7, where it can be observed that, as expected, the lowest injection pressure made little difference to suction.

5.3.7 Installation with no injection pressure but with water 'short-circuiting' enabled

One method of supplying pressure to the base of the skirt without the use of injection may be to simply attach pipes to the outside of the skirt leaving the tops open. Water could then flow through the pipes to the skirt tip without incurring head loss through the soil. Provided that sufficient water could be supplied, the downward flow outside the caisson would be smaller reducing the soil resistance increases outside the skirt.

Figure 5.3.8 presents the results of an installation undertaken with the STI caisson where the top of the injection tubes were open to ambient pressures. The caisson was subsequently re-installed with STI flow blocked for comparison of the installation suction. It can be observed that the suction required for installation of the open port caisson was lower for all installation depths above 60 mm penetration. The reduction in suction for this test at 100 mm penetration was 150 Pa.

This modification has a limited effect on the suction levels recorded. However, for installations in shallow water, a useful reduction of installation suction can be achieved with a relatively simple modification to the caisson. No further equipment is required other than what is necessary to install the caisson by suction.

5.3.8 Experiments using sixteen points of injection at the base of the skirt

The second series of tests used a caisson capable of injecting water at sixteen points on the skirt. The purpose of doubling the nozzle quantity was to investigate the effect of approximating the injection at the base of the skirt as a strip of pressure more closely. A further modification was to exchange the aluminium lid for Perspex to enable the onset of piping to be observed. When piping occurred, it could be observed inside the caisson as a small jet of water containing large volumes of sand adjacent to the skirt.

The tests with the 16 nozzle caisson were similar to those undertaken using 8 nozzles. Figure 5.3.9 shows a plot of selected results. Increasing the injection pressure reduced the suction required for installation in a similar manner observed for the eight nozzle experiments. The data for the 16 nozzle test series were evaluated using the method outlined above. Table 5.3.6 summarises the results and the gradients obtained from the data. Table 5.3.7 contains the average gradients obtained for each injection pressure, and the average gradients obtained for the 8 nozzle caisson for comparison. The observed trend is similar to the 8 nozzle caisson where the pressure for installation could be lowered by increasing the injection pressure available at the nozzles. It appears that by doubling the nozzles on the caisson, the process of skirt tip injection was improved as the gradients associated with the 16 nozzle caisson are

greater than those for the 8 nozzle caisson at each injection pressure. For the 16 nozzle caisson, the effect of injection pressure varied the average recorded gradients in an almost linear variation.

If a point of injection only affects the local pore pressure, most of the skirt could be unaffected by the action of injection. Using 16 nozzles doubled the length of skirt exposed to high pressure water, which caused a greater effect on the suction required to drive installation. The injection pressures used were still very high, of the order of 12.5 kPa, which was expected to create piping failure, but none occurred.

The use of a greater number of nozzles can reduce sensitivity to the effects of nozzle failure. During installation, sand could be forced up the supply tube as there was no filter placed over the ends. The injected water would have had to flow through the sand before it emerged at the tip of the caisson. As the water passed through the sand within the tube, a hydraulic gradient would have been present, and the pressure of water emerging at the skirt would have been lower than for other nozzles which had no sand blockage.

The pressure loss of water flowing through sand trapped in the injection nozzles is estimated to be high. The measured STI flow rates for the 16 nozzle caisson were of the order of 1.75×10^{-6} m^3/s. Assuming this flow was evenly distributed amongst the nozzles, results in an average flow of 1.09×10^{-7} m^3/s per nozzle. Assuming the sand permeability was 8×10^{-5} m/s (Kelly *et al.* (2004)), the hydraulic gradient within a tube of 5 mm diameter would be 69.6 m/m, which results in an estimated pressure loss of 683 Pa/mm. Therefore, if a nozzle became filled, the effect would be that the water emerged at the tip at significantly lower pressure, exposing the affected area of skirt to substantially less pore pressure change. Increasing the nozzle quantity on a given size caisson reduces the skirt distance between nozzles, enabling the pressure for each portion of skirt to be more greatly influenced by the surrounding nozzles.

5.3.9 The effect of STI on the maximum installation depth

For tests undertaken using STI, the onset of piping failure was encountered at shallower penetration depths than for experiments where no injection was undertaken. This may result from the hydraulic gradient within the soil plug becoming influenced by the action of skirt tip injection. Where no STI was used, the average gradient within the soil is governed by the suction applied to the interior of the caisson and the pore pressure at the base of the skirt estimated by the suction factor a. The application of injection at the base of the skirt increased the water pressure above the levels present when suction alone was used, which in turn increased the hydraulic gradient within the soil plug. As piping failure occurs when a threshold value of hydraulic gradient is reached, the onset of piping happened sooner for STI experiments. The suction at which piping failure occurs for a fixed penetration depth decreased linearly as injection pressure was increased. The failure of STI to extend skirt penetration may be the reason why Senepere and Auvergne (1982) had to modify their anchors to enable plug jetting rather than skirt tip jetting.

Examining the depths at which piping failure occurred for the non-STI installations, the average depth reached when the onset of piping was encountered was 124 mm, with many experiments recording values between 127 to 130 mm depths (see Table 5.3.8). The average suction pressure reached before piping occurred was 1.87 kPa. A similar comparison for experiments with injection pressure of 10 kPa, concludes that the average suction reached was 1.27 kPa and the average installation depth was 96 mm.

Two methods for estimating the maximum caisson penetration depth were outlined in Chapter 5.1. These were applied to an installation undertaken without STI. To calculate Equation 5.1.2, it was necessary to determine the variation of a with depth. Equation 5.1.2 was initially calculated using the variation corresponding to constant soil permeability ratio (k_f) and subsequently using values of a corresponding to larger k_f values. A back-calculation of installation suction was used to estimate the k_f variation for the experiment, for which the results are presented in Figure 5.3.10. Equation 5.1.3 was calculated using stress values obtained assuming k_f varied with depth. The assumed variation of k_f was the same as that assumed in the second calculation series using Equation 5.1.2.

It can be observed that good agreement was obtained between the suction estimate and the pressures recorded during the test. The maximum suction estimate using Equation 5.1.2 and the variable permeability ratio predicted the onset of piping better than where the fixed permeability was assumed. The estimate of maximum suction made based upon Equation 5.1.3 also accurately predicted the pressure at which piping failure occurred.

The concluded effect of STI is shown in Figure 5.3.11, which shows a diagram of the pressure contours associated with STI. Comparing Figure 5.3.11 when STI is applied with Figure 4.3.7, the pressure gradient within the soil inside the caisson is higher than that which would be present if suction installation were undertaken, which limits the maximum suction. Outside the caisson, it can be observed that the hydraulic gradient has reversed allowing the soil resistances to become lower.

Figure 5.3.12 presents the suction variation with depth for a caisson installed using an injection pressure of 7.5 kPa. The caisson could be installed to a depth of 121 mm at which point piping failure occurred and penetration stopped. Both suction and injection were quickly turned off and the pore pressures were allowed to stabilise. Suction was then reapplied in the absence of injection, and a further phase of penetration was achieved up to a depth of 128 mm where piping re-occurred. The depth at which piping occurred for the second time was similar to the depths recorded for caissons installed without the use of any injection. When piping failure appears during the course of an installation, it does not appear to hinder the final penetration depth, provided that it is not allowed to continue to an extent where large volumes of soil are disturbed.

5.4 Installation experiments using selective skirt tip injection for caisson steering

5.4.1 Outline of the steering strategy

The STI tests concluded that for fixed values of installation suction, the depth of penetration could be extended by increasing the injection pressure supplied to the nozzles, but that maximum penetration was

reduced. The tests revealed that the effect of nozzle pressure was localised, so that the distribution of pressure could be controlled by selecting individual points to apply STI. Therefore, it was hypothesised that if the pressure was supplied to only half the caisson, the installation resistance around that half would be lowered leaving the resistances around the other half largely unaffected, and the side of caisson exposed to lower resistances would penetrate further into the sand. A full scale caisson, capable of skirt tip injection and possibly steering, has been installed in Denmark, but the results of this installation have not been published.

The expected effect of steering was estimated from results of the STI experiments. Examining a test using an injection pressure of 12.5 kPa, shown in Figure 5.4.1, it can be observed that after the application of injection at a depth of 51.7 mm, the installation pressure was lowered from a suction of 0.4 kPa to 0.3 kPa. Installation was subsequently continued at the same rate and the depth at which suction reached 0.4 kPa was 62.8 mm. Therefore, the application of injection allowed the skirt to penetrate approximately 11 mm further into the sand. If selective injection could lower one side of the caisson by this distance, the change of angle for the caisson would be 4.2º.

The steering effect was expected to be smaller than the value calculated above as the rotation of the caisson would also be accompanied by lateral movement of the skirt. To enable the skirt to move laterally, soil would need to be displaced activating passive and active zones which require substantial net forces to mobilise.

All steering tests were undertaken using a caisson with 16 injection nozzles, which enabled steering to be accomplished by supplying pressure to eight adjacent nozzles. Flow to the other eight nozzles was blocked to force water down the outside of the skirt.

5.4.2 Method of caisson installation for caisson steering tests

The installation of a steered caisson began with the caisson clamped to the installation frame while it was de-aired, counterbalanced, and the attachments were arranged to ensure that it was level. The

caisson was slowly lowered until the weight was supported by the soil. For these tests, the pumping hose could not be attached after self weight penetration had been completed. Therefore, the hose was attached to the caisson before the installation was begun, which necessitated that the self weight penetration phase be performed while the pump was running at low speed to enable the water to discharge from the interior. Great care needed to be exercised to precisely match the rate of installation with the water discharged from the pump to avoid pressure (or suction) developing.

When the caisson had reached the end of self weight penetration, the pumping rate was increased up to the controlled installation speed. Steering was applied by opening a valve to let water flow to the side of the caisson to be steered. The injection pressurisation pump was then operated to increase the pressure in the injection manifold. The pressure was then maintained by varying the pump speed.

5.4.3 Demonstration of the effect of caisson steering

A trial was undertaken to investigate the effect of steering. For this experiment, the caisson was free to rotate in any direction by the influence of the forces acting on the skirt. Logging was maintained continually throughout the test to monitor all caisson movements. The inclinometer recorded the change of x and y angles (θ_x and θ_y). For this test, steering was to be applied to nozzles either side of the y axis, resulting in θ_y being the steered quantity. The y axis was defined by the orientation of the inclinometer.

The caisson was carefully placed onto the surface of the sand and installed by self weight penetration and subsequently suction. After a depth of 46 mm had been reached, suction was shut off to stop installation, and the caisson was left for some time to ensure that it was in a steady state. During the final stages of this phase, the caisson angle was found to be reasonably constant while the skirt penetrated into the sand.

The installation was then recommenced while injection was applied at a pressure of approximately 6.5kPa to the nozzles below the y axis. No other adjustments were made other than to maintain the installation rate and the injection pressure. After the caisson had been installed to 62 mm, both steering

injection and suction were stopped. The caisson was left for a period of time to ensure that it was in a steady state. When installation was started for the third time, injection was this time applied to the second group of nozzles at pressures of between 5 and 6 kPa. The caisson was installed by suction up to a depth of 86 mm. At this depth, all pumping was stopped and the caisson was left for a further period.

When installation was restarted for the fourth time, injection was not applied. The caisson was installed up to 100 mm where the test ended. The chart in Figure 5.4.2 shows a plot of the pressures applied to the caisson against time. The three regions where pumping pressures were shut off, and the two phases where injection was applied can be observed.

5.4.4 Experiments investigating caisson steering

The chart in Figure 5.4.3 presents a plot of caisson inclination with depth. Over the first 46 mm of penetration, the caisson was not steered, and the inclinations recorded are the result of the variation of forces applied by the sand to the skirt. θ_y began at 1.9º and increased to 2º over the period of self weight penetration. When suction installation was begun θ_y reduced, initially rapidly and then more slowly by the end of the suction installation. At the end of suction installation θ_y was 1.1º. During self weight penetration, θ_x started at a value of -0.3º and decreased slightly. Then when suction installation was begun, θ_x decreased initially rapidly, stabilising at a value of -0.75º and then did not vary significantly with penetration.

Further suction installation between 46 and 62 mm was accomplished with the injection described above. It can be observed that θ_y initially changed rapidly but towards the end of this phase, the rate of change of θ_y decreased significantly. The total change of θ_y was -0.89º. At the same time, θ_x decreased slightly from -0.75 to -0.88º. The change of θ_y over this period, was consistent with deeper skirt penetration in the vicinity of applied pressure. This suggests that the resistances on the skirt were being reduced by the application of injection.

For installation between 62 and 86 mm, injection was applied to the nozzles on the opposite side. θ_y started at a value of 0.27º and increased, initially rapidly, to a value of 1.14º having passed through a rotation of 0.87º. θ_x increased from -0.85º to -0.55º. The change of θ_y can be attributed to the action of injection being applied to the opposite side of the caisson as the caisson orientated itself so that the side with injection penetrated further into the soil.

As the caisson was steered to bring about a negative change of θ_y, θ_x also decreased. Similarly, when the caisson was steered to bring about a positive change of θ_y, θ_x increased. Table 5.4.1 summarises the changes of θ_x and θ_y for each phase of installation. The ratios of the total change of θ_y to the change of θ_x are presented for each phase. Each phase of steering caused a change of θ_y which was larger than the change of θ_x by a factor of at least 2.7. This is vital if selective injection is to be used to influence the orientation of a caisson. The ratio of angle change for each steering phase was larger than when no steering was applied.

For the final phase, where no injection was applied, θ_x increased by 0.08º, and θ_y decreased by 0.15º. This period of installation was undertaken to provide an indication of whether the caisson orientation changed when installation was undertaken with no injection applied. Both rotations over the final phase of installation were much smaller than the ones recorded when steering was applied.

The purpose of stopping installation between phases was to allow a clear transition between steering inputs to be observed. Figure 5.4.4 shows θ_y and suction plotted on a common time axis. The periods where no suction was applied correspond to the phases where the caisson was left. It can be observed that during those times θ_y remained constant. Therefore, as the caisson was stable before the start of a steering phase, the angle change did not result from instability present before the application of steering. Figure 5.4.5 shows a plot of installation depth (z) and θ_y plotted on a common time axis which demonstrates that steering only occurred during installation.

The caisson was steered in two directions to demonstrate that the movement was a consequence of steering. Also, steering was only applied after the caisson had apparently begun a stable course of installation after self weight penetration had finished. This test confirms that a caisson can be steered by the use of selective injection at the skirt tip. The steering was controllable, and rotations of up to 0.9º were observed. For both steering phases, the application of injection caused an initially rapid response followed by a slow rate of change.

5.4.5 The angle variations caused by selective steering

A test series was undertaken to investigate the effect of caisson steering. In each test, the caisson was installed according to the method outlined above. For most tests, the caisson was steered in both directions, but in two tests presented, the caisson was steered one way followed by a period of installation without steering followed by further steering in the same direction. The purpose of these tests was to compare the effect of steering at deep penetrations with shallow penetrations. For these tests, the injection pressures applied were in the range of 6 to 8 kPa.

An example of the results is shown in Figure 5.4.6 which plots suction along with the changes of θ_y. From the chart it can be observed that the application of steering made a small influence to the suction required for installation. Figure 5.4.7 shows the variation of θ_y, θ_x and injection pressure. In test Steered_23, the caisson was steered both ways, which resulted in the oscillation of θ_y. The first phase of steering was begun at a depth of 47 mm and maintained up to 62.5 mm. After this, the pressure was diverted to the other nozzles, and installation was completed.

In the second steering phase, it can be observed both angles changed simultaneously. In this test, steering the caisson in a positive y sense did not significantly affect θ_x, whereas steering the caisson in a negative y sense did. For this behaviour to occur, the action of steering must have caused a force which had a component about both axes. This could occur if a nozzle, or group of nozzles, performed significantly different to the others.

The effect of steering can be analysed by comparing the angle through which the caisson was steered. Table 5.5.1 contains a list of the angles through which the caisson was steered for each phase of steering (steering out, and steering back in). The change of angle for both axes is recorded in the table for each experiment. To assess the sensitivity of steering with depth, the distance covered to achieve the steered angle is recorded from which the average change of steered angle per unit depth was calculated.

The ratio of θ_y to θ_x is shown in the table. Ratios larger than unity correspond to larger angle changes of θ_y than θ_x. During the first phase of steering, the change of θ_y was up to ten times greater than θ_x and for all tests θ_y was over twice as large as θ_x. The trend for the second stage of steering was that the change of θ_y did not exceed the change of θ_x by the same factor. In the majority of tests, θ_y exceeded θ_x by a factor of between two and three.

For all tests, the steering gradient for the first phase of steering was larger than the gradient for the second steering phase. As the second stage of steering was undertaken at a deeper penetration depth, this demonstrates that the effect of steering decreased with penetration.

5.4.6 The reduction of steering effect with penetration depth

Figure 5.4.8 shows a plot of θ_y with depth for Test Steered_28, where the caisson was installed with two phases of steering, both in the same direction. The second steering phase was not applied directly after the first, as the caisson was allowed to install for 8 mm between steering inputs. During the first steering application, θ_y changed by -0.89º and during the second phase, θ_y changed by -0.27º. When no injection was applied between steering inputs, θ_y increased by 0.40º. This test demonstrated that the steering effect at shallow penetration depths was greater than when the same pressure was applied at deep penetrations as the initial θ_y angle could not be recovered.

For both phases of steering, it can be observed that, despite no further change in θ_y being observed after an initially large response, the application of injection was still necessary to maintain the angle. When injection was halted and installation proceeded, the angle changed rapidly back (see Figure 5.4.8).

5.4.7 The sensitivity of caisson inclination to steering inputs for level control

The controllability of steering was investigated by installation with the application of steering to install the caisson at an indicated angle of 0º. The final stage of installation was to be undertaken without steering to demonstrate that the caisson would not have been installed level without the application of steering. The results of this test (Steered_27) are presented in Figure 5.4.9. At the end of self weight penetration θ_y had a value of 0.7º, which was rapidly reduced over a depth of 11 mm, using an injection pressure of 6 kPa. θ_y could then be maintained within a tolerance of 0.03º. After the caisson had penetrated to 86.5 mm, injection was stopped and the caisson finished installation at an angle of 0.2º.

The pressure required for stabilisation gradually reduced with penetration. Therefore when the caisson is set up for installation at the desired angle, the caisson is likely to keep installing at a similar orientation at deeper penetration depths. This behaviour is similar to that observed by Colliat *et al.* (1996) during the large scale installation of suction anchors. As steering only used half the nozzles available, inputs using low pressures, such as 4 kPa, did not result in large steering responses therefore a large number of nozzles are necessary.

5.4.8 The effect of steering on the suction required for installation

Steering the caisson using selective injection reduced the suction required for installation. Figure 5.4.10 presents a plot of suction and steering pressure as a function of depth for comparison. It can be observed that when the steering pressure was applied, the suction reduced accordingly. For the example shown in Figure 5.4.10, the steering pressure (9 kPa) was stopped at a depth of 110 mm which resulted in the installation suction increasing by 65 Pa. Figure 5.4.11 presents a plot for an 8 nozzle STI test. The STI pressure of 10 kPa was turned off at a depth of 115 mm which resulted in a suction increase of 137 Pa. The suction change after injection was turned off during STI was over twice that for the steering test despite the number of nozzles being turned off being the same.

5.4.9 Deep self weight penetration depths caused by over-pressure

During these tests, it was observed that the caisson could install to unexpectedly large penetrations after the phase of self weight penetration had been completed. When self weight penetration had stopped, the weight of the caisson was just supported by the sand resistances. If a small disturbance was subsequently applied to the caisson in the absence of vertical restraint, final penetration depths up to twice those expected by self weight penetration could be achieved without any suction having been applied.

Figure 5.4.12 presents a plot of suction with respect to depth for an installation which captured this process. Self weight penetration was undertaken up to approximately 24 mm depth. The speed of self weight penetration was controlled to minimise the pressure build up within the caisson (see Figure 5.4.13). At a depth of 24 mm, the installation rate was no longer controlled and the caisson began to penetrate at much higher installation rates driven by the action of the weight of the caisson. After the installation rate had increased, the pressure inside the caisson became relatively large reaching a peak of approximately 2.5 kPa at a penetration rate of 12 mm/s. Penetration finally stopped at a depth of 61.4 mm at which point suction was applied to install the caisson further. The suction required for complete installation was not substantially different to other experiments where self weight penetration was undertaken at a slow rate.

The high pressures created inside the caisson would have affected the pore pressures in the soil. As the water attempted to flow from within the caisson through the soil to the outside, the water flow would have taken the opposite direction to that invoked by suction. The stresses inside the caisson would therefore have increased while those outside the caisson decreased. Any lateral flow around the skirt tip may have served to decrease the end bearing resistance at that point. If the flow of water decreased the net soil resistances sufficiently, the caisson would be able to penetrate further into the soil than the depths estimated without the presence of water flow.

This penetration method has similarities with suction installation, as an upward flow of water adjacent to the skirt serves to reduce the sand resistances. The suction installation method may cause deeper penetrations than those possible with over-pressure as the process reduces the soil stresses within the caisson rather than those on the outside. Previously, it was noted that the effect of skirt penetration causes larger vertical stresses to occur within the caisson than those on the outside. Therefore minimising these stresses will reduce the overall forces acting on the caisson more than opting to reduce the ones outside the caisson.

An advantage of using suction rather than over-pressure for installation, is that the direction of caisson movement serves to reduce the suction magnitude creating a negative feedback effect. Suction installation is controllable as suction can be removed to stop installation when necessary. For the over-pressure method, the direction of caisson movement causes a positive feedback effect, maintaining the water pressure and installation cannot be controlled without a means of mechanically restraining the caisson. The use of constant over-pressure may not be desirable for use with caisson installation, though a controlled installation strategy may increase installation as demonstrated by experiments undertaken by Allersma *et al.* (2001) in which a caisson was installed using an oscillating pressure inside the caisson.

Importantly, the presence of an unwanted and large pressure increase during caisson installation should be avoided to maintain caisson stability. When the pumping apparatus is connected, the water volume inside the caisson is contained by the skirt. The compressibility of water is very low, and a relatively small change of volume can create large pressures which could invoke the mechanism described above.

5.5 Pore water dissipation for STI

5.5.1 Skirt tip injection pore water pressure dissipation

The STI experiments were able to support much larger injection pressures than expected by the linear hydraulic gradient model and recorded lower installation suctions than when no STI was used. Suction

installations for the small caisson needed the application of approximately 2 kPa for full installation and experiments using approximately 10 kPa injection pressure delivered to 8 nozzles were able to reduce the installation suction by approximately 20 %. The application of larger injection pressures resulted in piping failure at shallower penetration depths.

The assumptions regarding water pressure dissipation with distance away from the point of injection need to be reconsidered. Treating an injection port in isolation, and neglecting the presence of the skirt and tube, the nozzle may be modelled as a point water source. By continuity of water flow, the flow of water from the source (Q_{total}) should be equal to the flow of water (Q_1) through the surface of a sphere of radius r_1 from the point source, which in turn should be equal to the flow of water (Q_2) through a sphere of radius r_2 (see Figure 5.5.1).

$$Q_{total} = Q_1 = Q_2 \qquad \text{Eqn. 5.5.1}$$

For uniform flow, the pore pressures at the surface of the spheres will be u_1 and u_2 and the water flux (q) will be uniform over the surface area of the sphere. The flow of water out of a sphere can be described by the water flux per unit area distributed over the area of the sphere.

$$Q = qA = q4\pi r^2 \qquad \text{Eqn. 5.5.2}$$

Combining Darcy's equation (Equation 5.5.3),

$$q = ki = -k\,\frac{1}{\gamma_w}\frac{du}{dr} \qquad \text{Eqn. 5.5.3}$$

with the flow continuity relationship (Equation 5.5.2), yields the following:

$$\frac{du}{dr} = \frac{-Q\gamma_w}{4\pi k r^2} \qquad \text{Eqn. 5.5.4}$$

which can be integrated to obtain the change in pore pressure at a distance r away from the source. The boundary condition assumed that injection does not cause a pore pressure change at an infinite distance from the source and hydrostatic pressures exist. The result is Equation 5.5.5 which estimates the change in pore pressure (Δu_{inj}) arising from an injection flow rate (Q) when the soil permeability (k) is known.

$$\Delta u_{inj} = \frac{Q\gamma_w}{4\pi k r} \qquad \text{Eqn. 5.5.5}$$

With typical sand parameters, the relationship estimates that the pore pressure change due to injection will reduce rapidly with distance from the source.

The injection of water around the caisson was performed by a group of individual points of injection. When individual points of injection are used simultaneously, the flows of water must be combined to estimate the distribution of pressure around the caisson. When two water sources are positioned adjacent to each other, the flow nets can be combined by superposition to estimate the pressures. Using this hypothesis, the pore pressure around the skirt will be estimated as the superposition of the pore pressures arising from the action of injection.

5.5.2 Skirt tip pore water dissipation test

To test this hypothesis, it was decided to install the 8 nozzle caisson with modifications to the injection system. The injection ports were alternately connected to one of two four-branch manifolds each incorporating a pressure transducer. One of the manifolds was supplied with water under pressure from the injection pump, and the other did not allow water to flow in or out. In this way it was possible to inject water at four points adjacent to the skirt tip, and measure the water pressure in between the injection points.

The geometry of the caisson used for the pore pressure dissipation test is shown in Figure 5.5.2. Each point of measurement was situated between two injection nozzles and affected by four points of injection. The distance to each injection nozzle from a measurement orifice is labelled on the diagram. The pressure change due to injection ($u_{measured}$) can therefore be estimated by the following relationship.

$$\Delta u_{measured} = \frac{\gamma_w}{4\pi k}\left(\frac{Q_1}{r_1} + \frac{Q_2}{r_2} + \frac{Q_3}{r_3} + \frac{Q_4}{r_4}\right) \qquad \text{Eqn. 5.5.6}$$

The pore pressure dissipation test was undertaken by installation of the caisson with the injection supply closed. Installation was stopped three times when the skirt tip had penetrated to depths of 60, 90 and 117 mm. When the caisson was stopped, the injection supply was opened and water was injected at a series of pressures while the flow rate was measured. The injection water flow was found to be very

much lower than the flows through the installation pump. In this test, the flow of water through all four nozzles was measured, but the flow through each nozzle could not be separated out. In the calculations, it was assumed that the flow through each nozzle was equal to one quarter of the total flow.

Figure 5.5.3 shows a graph of injection pressure and measured tip pressure. As the injection pressure was increased, the pressure at the measurement points increased proportionately. The measured pore pressure changes were approximately 200 times smaller than the injection pressures. For each depth, the injection test produced similar results. The magnitude of the injection pressure could be increased for each penetration depth as a larger distance existed between the skirt tip and the surface over which the pressure could dissipate. For this test, piping failure, and the consequential soil disturbance, was to be avoided as the change in permeability could not be measured.

The results of this test indicated that despite the application of skirt tip injection, relatively large distances of skirt were not significantly affected by the injection pressures applied. A possible modification to improve STI effectiveness could be to undertake injection at closer intervals around the skirt to allow a greater length of skirt to be influenced by higher water pressures.

The data for injected water volume were used to estimate the expected pore pressure change at the measurement points using the Equation 5.5.6. Figure 5.5.4 shows a plot of the injected water flow rate with respect to pressure at each penetration depth. The flow rate was computed by calculating the change in reservoir water volume between time steps from the data record. As a result of the small time steps used in the calculation, noise appeared in the flow rate plot.

Figures 5.5.5 to 5.5.7 display the estimated pressures using the flow rates recorded, and a sand permeability of 80×10^{-6} m/s, for each depth at which the pressure tests were undertaken. The measured pressures are plotted on the charts for comparison. It can be observed that there is good agreement with the measured and predicted values suggesting that the injection flow rate could be used as an indicator of water pressure adjacent to the skirt tip.

5.5.3 Application of pore water dissipation results to caisson installation calculations

For suction installation, where there is a uniform water flow down the outside of the caisson, the hydraulic gradient was assumed to follow Equation 5.2.1. For caissons installed with STI, the proposed water pressure gradient outside the skirt is described below:

$$\frac{du_{outside}}{dz} = -\frac{as}{\gamma_w h} + \frac{Q_{average}}{4\pi k r^2} \qquad \text{Eqn. 5.5.7}$$

Inside a suction installed caisson, the hydraulic gradient was assumed to follow Equation 5.2.2. Where installation is undertaken with suction and STI, the proposed hydraulic gradient within the caisson is described below:

$$\frac{du_{inside}}{dz} = \frac{s(1-a)}{\gamma_w h} + \frac{Q_{average}}{4\pi k r^2} \qquad \text{Eqn. 5.5.8}$$

In both cases, the direction of water flow acts to reduce the vertical stresses in the soil. The hydraulic gradient due to injection was incorporated into a spreadsheet calculation in a similar manner as for the incorporation of the gradient arising from suction and the spreadsheet was solved iteratively for a particular installation depth. The proposed gradient of vertical stress with depth outside the caisson is described below:

$$\frac{d\sigma'_{vo}}{dz} = \gamma' + \frac{as}{h} - \frac{Q_{average}\gamma_w}{4\pi k r^2} + \frac{\sigma'_{vo}}{Z_o} \qquad \text{Eqn. 5.5.9}$$

The proposed gradient of vertical stress inside the caisson is described below:

$$\frac{d\sigma'_{vi}}{dz} = \gamma' - \frac{(1-a)s}{h} - \frac{Q_{average}\gamma_w}{4\pi k r^2} + \frac{\sigma'_{vi}}{Z_i} \qquad \text{Eqn. 5.5.10}$$

The gradient of water flow adjacent to the skirt is proportional both to the flow of water through each nozzle and the number of nozzles positioned around the skirt compared to the caisson diameter. If the injection nozzles are modelled as water sources, then it may be possible to estimate the water pressure variation adjacent to the skirt tip with angular change around the caisson. This has been undertaken for the STI caisson for the cases with 8 nozzles and 16 nozzles. The geometry for the 8 nozzle caisson is presented in Figure 5.5.8 and for the 16 nozzle caisson in Figure 5.5.9. The calculated variation of water pressure is shown for the 8 nozzle caisson in Figure 5.5.10 and for the 16 nozzle caisson in Figure 5.5.11. As both problems are symmetrical, the Figures only display the pressure variation over a

fraction of the perimeter of the caisson spanning between the centreline of a nozzle to a point equidistant between two nozzles. The pressure at a point on the skirt tip was estimated to be the sum of the pressures arising from all the nozzles:

$$u_{total} = \sum_{1}^{n} u_n \qquad \text{Eqn. 5.5.11}$$

where the pressure (u_n) at the point of measurement arising from the action of a nozzle of distance r_n away was described by:

$$u_n = \frac{Q_{nozzle}\gamma_w}{4\pi k r_n} \qquad \text{Eqn. 5.5.12}$$

The flow rate through each nozzle was estimated from test data. For the 16 nozzle caisson, the total flow rate is displayed in Figure 5.5.12, which shows the flow rate for a test at which injection was supplied at 12.5 kPa. The permeability of the sand was assumed to be 8×10^{-5} m/s. The charts of pressure variation around the skirt demonstrate that despite the relatively high injection pressures used, the expected pressure change around most of the skirt is relatively small. For example, for the 16 nozzle case, the expected pressure change at a point next to the skirt between two nozzles is only 300 Pa. The calculation for the 8 nozzle caisson for which the injection pressure was 10 kPa estimates that the lowest pressure change next to the skirt would be 144 Pa. The STI flow for the second calculation is shown in Figure 5.5.13. The flow rate was equally distributed over the number of nozzles on the caisson which resulted in individual nozzle flow rates of 1.09×10^{-7} at 12.5 kPa and 1.25×10^{-7} m^3/s at 10 kPa. The average pressure over the skirt for the 8 nozzle calculation was estimated to be 265 Pa and 440 Pa for the 16 nozzle caisson and the ratio of these two average pressures is approximately 0.6.

The application of the proposed STI gradients to the installation calculations was attempted to estimate the suction required for installation of the caisson. The average skirt tip pressures were expected to be lower than the injection pressures as demonstrated by the calculations outlined above. The average hydraulic gradient over the side of the skirt was estimated to be related to the STI pumping rate (Q_{pumped}) in the following manner:

$$\frac{du}{dr} = \frac{Q_{pumped}\gamma_w}{4\pi k N_{nozzles}} F_{inj} \frac{1}{r^2}$$ Eqn. 5.5.13

where $N_{nozzles}$ are the number of nozzles on the caisson and F_{inj} is a factor relating the number of nozzles to the diameter of the caisson and the average flow of water up the side of the skirt to the nozzle discharge flow.

The soil parameters were first calibrated to the self weight penetration of the caisson and the suction required for installation. The calibrated soil parameters are shown in Table 5.6.1 and the calculation assumed stress enhancement occurred over an area which increased linearly with depth at a rate of 0.75m/m both inside and outside the caisson. Using the calibrated soil parameters, it was estimated that the self weight penetration of the caisson would be 31 mm, and that the suction for installation at a depth of 50 mm would be 0.4 kPa. The experiment for the 16 nozzle caisson recorded that self weight penetration stopped at 32 mm and the installation pressure at 50 mm was 0.38 kPa.

The calculation was performed for the 16 nozzle caisson where F_{inj} was estimated to take a value of 1. Figure 5.5.14 presents a chart of the results obtained from the calculation and the data from the experiment where injection was undertaken at 12.5 kPa. Figures 5.5.15, 5.5.16 present the data for the calculations where injection was undertaken at 7.5 and 5 kPa respectively along with the suctions recorded for the relevant tests. From the plots it can be observed that there is good agreement between the calculation and the recorded data for the suction required to penetrate the caisson with depth. For each of these calculations, the STI pumping rate used was the value recorded during the experiment.

Application of the same method of calculation for the 8 nozzle caisson was undertaken using exactly the same soil parameters. The estimation of pressure over the length of the skirt indicated that the average pressure arising from an 8 nozzle caisson may be smaller than that arising from a 16 nozzle caisson by a factor of 0.6. Therefore, for this calculation, the value of F_{inj} was changed to 0.6 from the value of 1 used for the 16 nozzle calculations.

The calculated pressure variation is shown in Figure 5.5.17 along with the recorded data for a test at which the injection pressure was 10 kPa. It can be observed that the trend and values of the estimated suction agree well with the values recorded to have been used in the experiment. Comparing the effect of using an inverse square pore pressure reduction with the linear profile assumed at the start of this Chapter, it can be concluded that the non-linear relationship leads to a more accurate estimation of the suction required to install the caisson.

5.5.4 The effect of hydraulic gradient on the maximum suction installation depth

The inverse square relationship between hydraulic gradient with distance from the source causes the assumed injection pressure to decrease rapidly. Even very close to the nozzles, the pressure is calculated to be only a few hundred Pascals when using an injection pressure of 10 kPa. The pressure variation of 350 Pa was calculated at the pipe wall of one of the nozzles from the recorded flow rate of an experiment where injection was undertaken at this pressure. This pressure change corresponds much more closely with the observation that piping at suction pressures 600 Pa lower than those observed in the absence of STI.

If an average pressure change at the base of the skirt, due to injection, can be calculated (p'_{inj}), a suitable modification to Equation 5.1.2 may be made (Equation 5.5.14) to estimate the maximum penetration depth of the caisson during injection:

$$z = \frac{s(1-a) + p'_{inj}}{\gamma'} \qquad \text{Eqn. 5.5.14}$$

5.6 Conclusions

A test series has been undertaken where caissons were installed in sand using suction and water injection at the skirt tip. The caisson used initially 8 injection nozzles for the first Test Series, and 16 nozzles for a second Test Series. A series of injection pressures were used during tests for each nozzle configuration. It was found that injection of water at the skirt tip reduced the installation suction. The amount by which the suction pressure was reduced was found to be proportional to the injection pressure. It was noted that high injection pressures could be sustained for large penetration depths

without encountering piping failure. Tests using injection at 16 points around the caisson lowered the suction required for installation by a greater margin than those using only 8 nozzles.

A proposed linear hydraulic gradient was initially assumed to be present during the injection process. However, the injection pressures sustained during installation did not support this assumption. A caisson was installed, capable of water injection at four nozzles, with water pressure measurements made in between these locations. The experiment concluded that the variation of water pressure reduced much more rapidly than was calculated when a linear hydraulic gradient was assumed.

On the basis of these tests, it was subsequently assumed that the injection nozzles may be treated as point water sources, and the hydraulic pressure may be estimated by the superposition of the point water source flows. A hydraulic gradient, assumed to follow an inverse relationship with distance, was applied to suitably modified calculations for estimating the suction required for caisson installation. The result of the application of this gradient was that lower suction pressure changes were achieved, which were consistent with the observations.

A series of tests were undertaken in which selective injection was applied to a 16 nozzle caisson to steer the axis of the caisson during installation. It was determined that caissons could be steered in one direction and then back again using this method. Caisson steering was found to be most effective at shallow penetration depths. The magnitude of the injection pressure applied determined the amount by which the caisson could be steered.

During the course of the tests reported above, it was found that deeper than predicted self weight penetration depths could be achieved by self weight alone when sufficient over-pressure was present inside the caisson. The over-pressure was caused by a slight disturbance of the caisson after self weight penetration had almost finished. Care should be taken when installing caissons in the field, that positioning is closely controlled, and that sufficient water flow can be achieved between the interior of the caisson and ambient without high pressures arising.

6 Moment load capacity of grouted caissons

6.1 Introduction to caisson grouting

6.1.1 Introduction

In the North Sea, the first concrete gravity platform to be installed was the Ekofisk Tank, placed into Norwegian waters in June 1973 (Hjelde *et al*. (2003)). Since then, in the OSPAR region, the total number of concrete gravity platforms installed numbers 27. Many gravity base structures incorporated skirts, such as those used for the foundation of the Maureen platform (Broughton *et al.* (2002)). The process of underbase grouting was necessary for all concrete gravity base foundations, and it is likely that it would be applied to caisson foundations. Underbase grouting was undertaken because voids were present between the underside of the foundation and the ground. These voids arose because the seabed was never absolutely the same shape as the underside of the gravity platform, and the skirts were often not fully installed at every location under the platform relative to the seabed. Additionally the seabed will often be inclined whereas the platform will be installed level, which creates a gap when installation is complete.

Underbase grouting enables the contact pressure to be equally distributed over the plan area of the platform (Hjelde *et al*. (2003), Gerwick (1974), Fjeld *et al.* (1977)) which allows locally high contact pressures to be avoided. By reducing the areas of soil supporting relatively high contact pressures, the settlements of the platform would be reduced. For structures with a requirement to maintain a high lateral load capacity, the base area of the foundation would be reduced by the presence of voids. The placement of grout increased the foundation area and restored the foundation shear capacity back to the maximum level possible for the plan area.

Eliminating the presence of voids reduces the trapped water present underneath the foundation. When the structure moves by the action of environmental forces, the pressure of the trapped water oscillates leading to the set up of hydraulic gradients and seepage. The continual movement of water can lead to soil erosion which in turn would lower the stiffness of the foundation. Gerwick (1974) suggested that

trimming the base of the foundation may be undertaken prior to caisson installation, however this requires expensive equipment, so grout injection is preferred. Gerwick (1974) stated that the uniform placement of grout is a difficult task, as the material is often confined to local areas of placement, or the material can be "lost" by flow into the soil. Another warning made by Gerwick (1974) was to avoid using grout mixtures which will later "bleed". Grout bleed conditions arise when excessive water is present in the composite mixture. When the mixture settles, the solid particles fall to the bottom of the mixture while the excess water rises to the top. This situation is to be avoided, as the purpose of undertaking grouting is to remove the voids and displace the water from underneath the foundation leaving the structure in good contact with the soil.

Though grout placement, or injection, is recommended, there is little in the way of research to support the requirement that the foundation be grouted to complete installation. Experiments undertaken by Villalobos *et al.* (2005) demonstrated that the performance of a suction caisson depended on the method of installation. It was concluded that the models installed by jacking were able to support greater moment loads than the models installed by a combination of suction and a low vertical load. The reasons for this performance disparity were not investigated. A program of tests should be undertaken to assess the impact of underbase grouting on caisson performance.

6.2 Method adopted for caisson grouting experiments

6.2.1 Introduction to caisson grouting

The grouting experiments needed to replicate the appropriate conditions present after a prototype caisson had been installed in the field. The comparison was to be made between a caisson which had been suction installed and then grouted, with a suction caisson which had been suction installed and not grouted. The reference was to be made with a jacked caisson which would represent the target response.

To achieve appropriate conditions after pressure grouting had been performed, the method chosen for pressure grouting was broadly similar to that used for the installation of field structures such as the

Maureen platform (Broughton and Davies (2002)). For the jacked in place caissons, the method of installation followed that adopted by Villalobos *et al.* (2005). The applied loads to the caisson were limited to low magnitudes after lid touch-down occurred as field installations would generally only supply sufficient force to embed the skirt. For the likely caisson sizes to be used for monopod foundations, a very large force would need to be applied to achieve a preload value equivalent to even 10 % of the ultimate caisson capacity. For example, a 20.5 m diameter caisson founded in clay of shear strength of 125 kPa would be able to support approximately 400 MN, while the load imposed by the turbine would be of the order of only 6 MN.

6.2.2 Sample tank and soil sample preparation

The sand used for the grouting tests was Redhill 110, the properties of which are listed in Table 3.2.1. The tank used for the grouting tests (large tank) was constructed from dural and had the dimensions listed in Table 3.3.1. For this tank, a maximum of 5 tests could be undertaken per sample. The position of the tests is shown in Figure 6.2.1.

The sample was prepared by liquefaction caused by application of an upward hydraulic gradient, which when removed allowed the sand to settle into a loose configuration. Liquefaction was assisted by stirring the sand. After the sample had been liquefied and allowed to settle, the sand was gently compacted. To achieve the required relative density, compaction was achieved by applying small durations of vibration from a rotating eccentric mass attached to the tank.

6.2.3 Description of caisson used for grouting experiments

The caisson used in the grouting experiments was constructed by attaching a 204 mm diameter stainless-steel tube to a 25.4 mm thick Perspex disc. The Perspex disc formed the lid of the caisson and was machined with a step so that part of the disc could be inserted into the steel tube to create a seal. A groove was machined into the side of the lid to allow an o-ring to be fitted which ensured that water could not leak into the caisson when suction was applied. The lid was securely attached to the skirt with machine screws to enable loading by a combination of vertical, horizontal, and moment loads.

Figure 6.2.2. presents a photograph of the grouting caisson. Eight vents were positioned around the circumference of the lid with an additional vent positioned in the centre of the footing. The vents were fitted with valves which could be separately shut off to control the flow of water through the vent. The purpose of these vents was to allow a grout mixture to be injected at various points under the caisson lid. By closing vents, it was possible to force the grout into different positions underneath the lid. The lid allowed the operator to see where grout had been placed and where it was necessary to inject more to ensure complete void filling.

6.2.4 Installation apparatus for caisson grouting tests

The caisson grouting installations were undertaken using the 3 DOF rig shown in Figure 6.2.3. The caisson needed to be attached to the loading arm before suction installation was undertaken as it was not possible to connect the rig to the caisson after installation without disturbing the footing.

For experiments where the caisson was to be installed by jacking, the caisson was jacked into position using the 3 DOF rig. Suction installations necessitated the use of both the 3 DOF rig to maintain the load required for modelling the self weight of the caisson, and the pumping control system to apply the suction installation force. The load control system was written in Visual Basic and the pump control system was LabView based, so the two systems could not be readily combined into an integrated controller. The experiments were therefore carried out using two PCs each running a control programme.

The 3 DOF control programme installed by Byrne (2000) was tuned to hold a load accurately when the footing was subject to small displacements at low displacement rates. The rate of caisson installation was fast compared to the speed of movements the control programme was optimised for. The control system could therefore not maintain the footing load within the acceptable error of approximately 2 N. To overcome the error between the imposed load on the foundation and the target load, the controller was modified so that the vertical load target could be manually changed while a load hold routine was

running. As installation was undertaken, the target load was changed to maintain the imposed load on the foundation within the acceptable limits. This method enabled the target load to be achieved without changing the control parameters from those known to be appropriate for the moment load cycling to be undertaken at the end of the experiment.

The caisson grouting mixture was made from casting plaster which could set when submerged in water. The grout mixture was made by adding 25 cm^3 of water to 100 g of casting plaster and mixing the two components thoroughly. The mixture was introduced into the caisson using a hand held syringe.

6.2.5 Outline of caisson grouting operations

The grout coverage could be visually monitored through the lid of the caisson. Good grout coverage was achieved between the lid and the soil, for all experiments where grouting was undertaken, without the grout mixture becoming "lost" into the sand as reported by Gerwick (1974). A photograph of a grout disc removed from the caisson after the end of an experiment is shown in Figure 6.2.4. The measured grout thickness varied over the area of coverage, from no grout, where the caisson had come to rest on the soil, to thicknesses of up to 5 to 6 mm. Most grout was observed in the vicinity of the suction connection, which was attributed to scour arising from pumping at the end of installation.

For the grouting tests, the grout was introduced into the caisson using a hand-held syringe. The grout was introduced at various points around the periphery of the caisson and allowed to flow over the soil plug to fill any available voids. The grout was introduced at one of the ports while all the remaining ports were left open to allow any water displaced by the grout to flow out of the caisson. The grout would flow to fill the gap between the lid and the plug until a point was reached where the path of least resistance was to flow through a port exiting the caisson. At this point, the leakage was shut off by closing the tap, and the introduction of grout was continued until the grout exited through the next point of least resistance. This procedure was repeated until all the outlet taps had been shut off.

The narrow bore syringe allowed high grout pressures to be produced when necessary with hand pressure applied to the piston. For caissons where the applied load was to be limited, the grouting was undertaken during a load hold routine, applied by the 3 DOF rig. For these tests, grout was introduced to the caisson and the pressure was slowly increased until movement was just recorded by the program. At this point, grout pumping was stopped and the caisson was sealed.

Where high pressure grouting was to be undertaken, the rig was set to hold the vertical displacement constant. The pressure could then be increased to high levels without caisson movement, and could be increased to a level which otherwise would have been sufficient to uninstall the footing. The load applied to the load cell was monitored to assess the magnitude of grouting pressure applied. During very high pressure grouting, it was observed that some ports would not allow any grout mixture to be pumped into the foundation after adjacent ports had grout introduced at high pressures. The caisson was then left for a period of at least one hour with the load held constant while the grout was allowed to set. If the caisson was grouted with the caisson displacements held constant, the displacements were maintained while the grout set.

Cyclic moment tests were then applied to the caisson using the 3 DOF rig. The control program was set to apply a target vertical load to the footing and then undertake cyclic displacement paths. Table 6.2.1. lists the experiments undertaken for this investigation. After the cycles had been applied to the caisson, the caisson was then slowly extracted using the actuator. Extraction was undertaken slowly to avoid causing excessive disturbance to the sand sites adjacent to the test site currently in use.

6.3 Comparison of laboratory tests on caissons installed in sand with grouted caissons

6.3.1 Moment loading tests

The caissons were installed by jacking, or by suction in combination with a small vertical load. The load applied to the foundation was minimised to the load necessary to ensure that lid contact had

occurred without excessive amounts of preload being subsequently applied. Large vertical forces would not be likely in a field installation.

A comparison of the loads required for installation is made in Figures 6.3.1 and 6.3.2 where the loads for jacking and those applied for suction installation are presented. For jacking, the loads necessary to install the caisson are much higher than those used for suction installation and the suction installation did not preload the foundation to a significant extent. For example, the suction installation applied a total force to the caisson of 45.5 N which was much smaller than the necessary jacking load of 163 N.

The lack of foundation preload after suction installation creates an important difference between the installations, as the caisson moment loading response is affected by the load history of the footing. Preloading the foundation expands the yield surface allowing the caisson to operate within the yield surface when moment loading is subsequently applied and the footing is in an overconsolidated state. When this happens, the behaviour of the footing is governed predominantly by a stiff elastic response.

For the suction installed caisson, the application of moment loading occurs when the foundation is in a normally consolidated state. After the foundation has been installed, the load state is at the apex of the yield surface. When moment loads are subsequently applied, the yield surface must expand and the corresponding displacements are governed by plastic deformation as well as the elastic response (see Figure 6.3.3). The initial response of the suction installed caisson may vary significantly to the jacked caisson which experienced preload, and therefore, the loads applied to the suction installed caisson were controlled to ensure that they did not exceed the values necessary to create the initial load state directly before the application of cyclic loading.

When the caisson had been installed, moment loading was undertaken. The loads applied to the caisson maintained the load ratio (*M/DH*) and vertical load constant, allowing the footing to rotate and translate. In this respect the loading tests were similar to the experiments described by Byrne *et al*. (2003). The tests were undertaken slowly to allow the system to behave in a drained manner. The ratio of (*M/DH*)

chosen for these tests was 1, and the vertical load applied was maintained at approximately 50 N as these conditions fall into the range applicable for wind turbines (Byrne *et al.* (2003)). As all tests were undertaken with the same diameter caisson and with the same loading conditions, the results can be directly compared. However, these tests are one of a series of moment loading tests which could be undertaken where conditions can be varied over a range of vertical load and horizontal loading ratios.

Figures 6.3.4 and 6.3.5 compare the horizontal load capacity and moment load capacity for the caisson for suction installation and jacked installation. The traces demonstrate that the method of installation has an effect on the subsequent behaviour of the caisson. The jacked in place caisson needed larger forces to displace the caisson than the caisson installed by suction. This is consistent with the findings of Villalobos *et al.* (2005). The applied vertical and moment loads for these tests are shown in Figure 6.3.6 as a function of time, and Figure 6.3.7 presents the horizontal load applied with respect to moment load.

Examining now the effect of grouting, the first trials injected grout into the caisson at a pressure sufficient to achieve full grout coverage of all voids. The loading rig was set into a hold routine, which targeted a compression load of 12 N on the load cell. This load was chosen because it corresponded to no load being applied to the caisson, and therefore if the grouting pressure rose to a level sufficient to overcome the sand resistance, the caisson would be able to move out of the soil. The experiments began with the caisson fully out of the water at which point the load cell was zeroed. The reason for why 12 N compression load corresponded to no load vertical load application on the caisson arose from the force of caisson buoyancy as the caisson was submerged under water. The change of caisson buoyancy was measured as a function of submerged depth by penetrating the caisson into a water filled tank.

Figure 6.3.8 presents a plot of the recorded loads for moment loading the caisson after grouting. It can be observed that the application of grouting did not significantly affect the loading behaviour of the caisson and did not bring the loads back up to those required to rotate the jacked caisson. Figure 6.3.9 presents the loads applied to the caisson for small rotations for the grouted and non grouted installations.

The behaviour of the caisson appears to be similar for both tests, and the amount of hysteresis is relatively small compared to that observed for larger rotations.

To enable better comparison of the tests, the normalised unloading stiffness for the tests was calculated and plotted against the normalised rotation in Figure 6.3.10. This was achieved using the methods outlined by Kelly *et al.* (2006). The unloading stiffness was used for the comparison rather than the loading stiffness as this did not incorporate the accumulation of displacement as cycling was undertaken. The normalised unloading stiffness was defined as the peak to peak normalised moments divided by the normalised rotation.

In Figure 6.3.10, it can be observed that the suction installed caisson was less stiff than the jacked caisson for all rotations. For both tests undertaken in this sand sample, the stiffness of the grouted caissons displayed a trend of stiffnesses which was similar to the suction installed caisson.

To determine the caisson response when pressure grouting was used, a series of caissons were installed where the grout mixture was introduced underneath the lid at the highest pressures that the apparatus would allow. The grouting was undertaken on caissons where the displacements were fixed, which enabled pressures to be used which would otherwise have caused uninstallation.

Figure 6.3.11 presents moment loading results of a grouted caisson allowing comparison to be made with a jacked and suction installed caisson. It can be observed that at large rotations the caisson became significantly stiffer than a suction installed caisson, and also stiffer than the caisson installed by jacking. Examining a plot of normalised unloading stiffness (Figure 6.3.12) allows comparison of the caisson performance after grouting to be made. For this sample, the unloading stiffness of the suction installed caisson was lower than the jacked in place caisson at all rotations. For the grouted caissons at large rotations, the caissons were stiffer than the jacked caissons, but at small rotations the stiffness was recorded to lie between the suction installed caisson and the jacked caisson. Therefore at very high

injection pressures, the grouting process did indeed improve the caisson stiffness of a suction installed caisson, and could even exceed the jacked caisson at large rotations.

The injection pressures used for these tests were very high. The pressures used for these tests caused the caisson to exert vertical loads on the load cell of between 329 and 684 N (see Figure 6.3.13). The method of grouting attempted to evenly distribute the mixture at high pressure under the lid. However, it was noted that when high pressures were used, some ports did not allow any grout to be injected. Examining the traces of moment load plotted against rotation, it can be observed that the loading stiffness was not symmetrical as was observed in the non-grouted experiments (see Figure 6.3.14). It is concluded that this method of grouting must be undertaken carefully to avoid the appearance of hard spots which may adversely effect the overall foundation performance.

The high pressure grouting experiments were useful for examining the maximum effect of grouting with the apparatus available, however, the loads required for restraining the caisson would have caused a significant foundation pre-load and were outside the bounds of relevant loads for wind turbine foundations. It was therefore decided to undertake a series of grouting tests where the maximum grouting pressures that were applied would not cause loads to exceed those that would be applicable for wind turbines. The grouting was undertaken using applied loads of 12 and 38 N. Examining the stiffness performance for these tests (Figure 6.3.15), it is clear that the performance of the low pressure grouted caisson could not be increased up to that of the jacked caisson. However, at small rotations the caisson stiffness was slightly greater than the suction installed case. The caisson grouted at the higher pressure was able to match the stiffness of the jacked caisson at all rotations apart from very small ones. It is noted that the load applied to the caisson was equivalent to a substantial part of the estimated scaled load applied by a wind turbine to the footing.

In these tests, it has been shown that pressure grouting caissons can increase the normalised secant stiffness of the caisson. However, large pressures must be applied to the grout for the stiffness to be

substantially increased. To enable the greatest pressures to be used, pressure grouting should be undertaken after the structure has been loaded to avoid causing skirt uninstallation.

6.3.2 Effect of grouting on caisson settlement during moment loading

The recorded vertical displacements during moment cyclic loading were compared for caissons installed by jacking and suction. The vertical settlement of caissons installed by jacking and by suction installation was similar, when cyclic moment loading was applied, as presented in Figure 6.3.16.

For installations where grouting had been undertaken, the vertical settlement of suction installed caissons was significantly reduced irrespective of the pressure used to grout the caisson. For example, where grout was introduced into a suction installed caisson while very low vertical loads were applied to the caisson during the grouting process, the caisson displacement was reduced from a total settlement of 1.4 mm to 0.83 mm (see Figure 6.3.17). For the tests where the caisson was grouted to very high pressures, the settlement could be further reduced, and for the highest pressures used, the recorded settlement was less than half the value for suction installation (Figure 6.3.18). For caissons grouted with an appropriately scaled vertical load, the maximum settlement was 42 % the amount recorded for suction installation.

The accumulation of settlement with respect to cyclic amplitude was calculated for the tests. As the amplitude of the cycles increased, the settlement of the footings increased correspondingly. Figure 6.3.19 presents a comparison of the settlements for low pressure grouted caissons with those recorded for a suction installed and jacked caisson. It can be observed that the settlements of the grouted caissons were smaller throughout the range of cyclical displacements applied than those recorded by the jacked or suction installed caissons. The effect of using higher grouting pressures on the settlement response, was to reduce the settlement caused by the application of cycling. It can be observed in Figure 6.3.20 that the amount of settlement for the high pressure grouted caissons was smaller throughout the experiments at all amplitudes applied. The load recorded after grouting for test HP Grouted 3 (GC6.5) was over twice the force recorded for test HP Grouted 1 (GC6.3), indicating that Test HP Grouted 3 had

been grouted to a much higher grouting pressure. The higher pressures did not significantly affect the settlement performance, however, as the settlements during cycling for both tests were broadly similar.

A comparison of the displacement profile of a footing installed without grouting and an installation which was high pressure grouted reveals that the insertion of grout underneath the lid of the caisson modified the behaviour of the footing when moment loading was applied. For caissons installed without grouting, the trend observed for small cycle behaviour was that the caisson penetrated into the sand for each application of load. When larger cycles were then applied, the caisson would then heave upwards over the quarter cycle where load was applied, however, the net accumulation of displacement was vertically downwards.

Where grouting had been used, the heave displacements over the quarter cycle where the load was applied were observed to be sometimes larger than those observed for the non-grouted caissons (see Figure 6.3.21). In some cases, the application of grouting affected the heave experienced over one loading direction significantly more than the other direction, indicating that the grouting process caused a "hard spot" to have been formed.

6.3.3 Effect of grouting on caisson horizontal displacement during moment loading

The horizontal displacements of the caisson were recorded for each test. A comparison of the horizontal displacement with respect to rotational displacement is made in Figure 6.3.22. It is observed that the method of caisson installation did not affect the magnitude of horizontal displacement as rotations were applied over the course of the tests. The suction installed caisson recorded similar horizontal displacements to those of the jacked caisson.

It can be observed that the application of high pressure grouting, shown in Figure 6.3.22, changed the horizontal displacement behaviour of the footing. The trend that can be observed for both high pressure grouted tests shown was that the variation of horizontal movement was no longer symmetrical with respect to rotational displacement. As rotational displacements were applied, the footing moved more

along one loading direction, resulting in accumulation of horizontal displacement. In the Figure, HP Grouted 3 moved the most which corresponded with the highest grouting pressure used. This behaviour, along with the observations of unsymmetric vertical heave, indicate that a "hard spot" was present caused by the insertion of grout at very high pressure which does not present itself after jacking or suction installation without subsequent grouting.

6.4 Conclusions

A series of experiments were undertaken which recorded the vertical, horizontal and moment loads necessary to displace a caisson about a predefined set of rotational displacements. The load conditions for these tests were chosen to be similar to those which are appropriate for monopod foundations installed offshore supporting wind turbines. Caissons were installed by jacking and suction installation. Of the suction installed foundations, some were then subsequently grouted or pressure grouted to investigate the effect this operation had on the foundation response. Comparison was then made between the grouted caissons, the suction installed caissons, and those installed by jacking.

The test series concluded that the normalised secant unloading stiffness of foundations installed by suction was lower than those installed by jacking, which agreed with previous research. The grouting operations where grout was inserted under the caisson lid at relatively low pressures did not significantly improve the normalised secant stiffness of the caisson beyond that of a suction installed caisson. However, pressure grouting using very high pressures, sufficient to cause a non-dimensional vertical load ($V'/\gamma' D^3$) exceeding 3.8, improved the normalised secant unloading stiffness of the caisson and could increase it to a level beyond that recorded by jacked caissons. The pressures used for these operations were much higher than those which would have caused skirt uninstallation, so transferring this method to a prototype would require a system of stabilisation to maintain the caisson location. Leaving this operation until the structure had been completed would enable higher pressure to be used as the caisson would have larger vertical loads acting on it.

The insertion of grout under the caisson lid was found to reduce the settlement of the footing over the course of cyclical moment loading. The use of high grout pressures were not necessary to significantly reduce the observed settlements. Grouting was not found to reduce the horizontal displacements of the footing over the course of moment loading.

The grouting tests revealed that control of the pressure grouting process is necessary to avoid the introduction of "hard spots" under the footing. These areas create a non-uniform response which causes the foundation to become stiffer at certain points which would cause differential settlements to arise. This behaviour only became significant for experiments where very high pressures were used.

7 Centrifuge installation experiments

7.1 Introduction to centrifuge tests

Chapter 4 describes experiments where caissons were installed through clay into sand and where high sand resistances were encountered. For these experiments, undertaken at small scale in the laboratory, the effective stresses were comparatively much lower than those encountered by prototypes and significant sand dilation could occur.

When a prototype caisson is installed by suction, the pressure causes the clay plug to be partially lifted, reducing the stress acting on the top of the sand layer. When this occurs, there will be substantially higher effective stresses present outside the skirt than in the interior. At small scale in the laboratory, the difference between these stresses will be of lower magnitude, and this may affect the skirt tip resistance magnitude.

To suppress dilation and to create conditions where high effective stresses are present outside the caisson, while those inside are much lower, the installation behaviour in sand when overlain by clay is best tested in a centrifuge. The purpose of the installation experiments described in this Chapter was to establish what the resistance of the skirt would be in the sand layer under high stress conditions and compared with 1g tests. The test series described in this Chapter is presented in Table 7.1.1.

7.2 Apparatus and method of installation

7.2.1 Description of soil sample used for UWA installation experiments

The 100g experiments were carried out at the University of Western Australia in the 1.8 m radius beam centrifuge. The sand used for the experiments undertaken at UWA comprised fine silica sand, the properties of which are listed in Table 7.2.1 taken from Tran *et al.* (2008). The dimensions for the strongbox used at UWA are listed in Table 3.3.1. All tests were undertaken in soil samples comprising clay over sand. The depth of the clay/sand interface was 30 mm below the surface, which corresponded to half the skirt length ($z/h_c = 0.5$). The locations of the tests are shown in Figure 7.2.1.

The sample was prepared by initially filling the strongbox with water to a depth of 150 mm. Dry sand was poured slowly into the water, taking care to distribute the sand evenly. Measurements were made of the sand height, and when the correct thickness had been placed, the sample was shaken on a vibrating table for 10 seconds. The sand depth was re-measured to assess the surface inclination and profile. More sand was placed on the areas which were low and the box was shaken again for 5 seconds. The properties of the kaolin clay used are listed in Table 7.2.1 (taken from Chen and Randolph (2003)).

Kaolin was made by mixing slurry, with a water content of 120 %, under a vacuum of 42 kPa for 3.25hrs. To achieve a clay layer thickness of 30 mm, 20 kg of kaolin slurry was required. The strongbox was placed on a pair of heavy duty weighing scales and kaolin was placed, using a scoop, under water on top of the sand in an even layer until the correct weight increase was achieved. The sample was then consolidated under a pressure of 80.6 kPa for 5 days. Samples tested in the centrifuge were allowed to consolidate for 3 hrs at 100g before any testing was undertaken. This method of sample preparation produced clay which was heavily overconsolidated.

Provision was made for the sand layer to drain by cutting a hole through the clay with a tube cutter at each of the corners of the strongbox. The void was filled with coarse sand to maintain the channel during testing. The water level was maintained by a water supply routed via a slip-ring at the axis of the centrifuge. CPT tests using a 7 mm diameter cone were carried out at the relevant acceleration to measure the sand density.

7.2.2 Description of UWA caisson

The caisson used for these experiments was constructed by attaching a stainless-steel skirt to the base of a dural flat footing. The connection between the skirt and the lid was mechanically pinned to allow forces to be transmitted between the two components without relative movements occurring. The connection between the skirt and lid was sealed with an epoxy resin. The caisson lid had a plug attached

which could be removed to allow inspection the soil within the interior. The caisson dimensions are listed in Table 3.4.1.

7.2.3 UWA centrifuge and associated loading apparatus

The centrifuge at UWA is a 1.8 m radius beam centrifuge, and is described by Randolph *et al.* (1991). A photograph of the centrifuge is shown in Figure 7.2.2. An actuator assembly was used (Randolph *et al.* (1991)) which enabled vertical and horizontal movements by two stepper-motor driven lead-screws (see Figure 7.2.3.). The stepper motors were controlled by a Labview based system, which moved the corresponding axis to a specified co-ordinate. Additionally, provision was made to maintain a target load on a load cell using a feedback routine.

An instrumented loading arm was used to measure moment loads, and a waterproof 3 kN load cell was fitted between the loading arm and the caisson to measure axial loads. Two miniature Druck pressure transducers were used to measure water pressures in the interior and exterior of the caisson. A diagram of the arrangement is shown in Figure 7.2.4. During centrifuge flight, suction was applied to the caisson by a syringe pump fitted below the test sample. For the 1g tests, a venturi suction pump was used to apply the suction for caisson installation.

7.3 Installation experiments undertaken at UWA

7.3.1 Results of 1g experiments

1g tests were undertaken for comparison with centrifuge tests. For 1g tests, two installations were undertaken using jacking as the principle installation method, and two installations were undertaken by a combination of jacking and suction. The jacked installations were undertaken for comparison with the 100g tests.

T-bar results at 1g, shown in Figure 7.3.1, show that the undrained shear strength of the kaolin layer increased with depth. Linear fits to this data were poor, so for analysis a nonlinear fit using Equation

4.2.1 was calculated. The results can be viewed in Figure 7.3.2. A MATLAB program was written by the author to undertake a least squares fit for this two degree of freedom problem. It was concluded from CPT tests 1 and 2 (Figure 7.3.3) that the sand in the region of CPT1 was more densely compacted than that in the region of CPT2 over the top 30 mm of the layer.

Examining Figure 7.3.4, which was derived in Chapter 2, it can be observed that the non-dimensional conditions for the Perth 1g tests correspond to those which are estimated to be relevant for a 4m diameter caisson, as may be used for a quadruped structure. The experiment reflected installation into 300 kPa (VERY STIFF) clay. Both these installations plot in the Unsafe Zone, so suction installation was expected to end with plug lift before the skirt reached the base of the clay layer.

Examining first the jacked installation results, the forces recorded are shown in Figure 7.3.5. Both tests required similar forces for penetration in clay. When the skirt tip encountered sand, the installation resistances increased rapidly and became much larger than those required for penetration in clay. Test 1 required a larger jacking force in sand than Test 4. However, this was expected as CPT tests show that the sand close to the location of Test 1 was more densely compacted causing higher tip resistances.

For Test 2, where installation was to be undertaken using suction, installation was initiated using the actuator to jack the caisson 6 mm into the clay to seal the interior. The forces recorded during this test are displayed in Figure 7.3.6. After the initial phase of jacking, a load of 8 N was applied to the caisson and suction was applied using the 'Venturi' pump. The suction pressures peaked at values of between 33 to 36 N without tip penetration. Clay was observed to appear in a transparent tube used to apply suction to the caisson.

A calculation was undertaken to determine the force necessary to shear the plug of clay into the caisson when the caisson was installed by 6mm using the nonlinear shear strength fit for t-bar1. The calculation performed is expressed below:

$$F_{plug\ lift} = \int_0^6 \alpha s_u \pi D_i dz + \int_6^{32} s_u \pi D_i dz + \gamma'_c \pi \frac{D^2}{4} h_c \qquad \text{Eqn. 7.3.1}$$

Force to lift plug = force to overcome adhesion on skirt + force to shear intact clay + plug weight

The force for uplift was calculated to be 24 N which is smaller than the recorded forces that were applied. Therefore it is concluded that plug lift occurred, which is consistent with the expected result from where the non-dimensional conditions plot.

The installation for Test 3 was undertaken using the same method as Test 2. The forces measured for installation are shown in Figure 7.3.7. The apparatus did not log the depth over the top 14 mm of installation which required that the outside pressure transducer be used to record the caisson position over this distance of movement. From the point at which depth data were available (z/h = 0.22) to a depth of z/h = 0.34, total installation force increased approximately linearly with depth. At z/h = 0.34, total load dropped slightly and installation was then undertaken at a virtually constant force until a depth of z/h = 0.46 when the force applied by suction abruptly reduced to zero, despite the pump still being operated. A calculation was undertaken to estimate the force required to shear the plug at a depth of z/h = 0.34 using the results of t-bar 2. It was calculated that 20.8 N would be required to lift the plug which compares well with the measured suction force of 17 N. It is concluded that the plug lifted at this point.

At the installation depth of z/h = 0.46, all suction pressure was lost and clay was observed in the suction tube. The actuator was used to complete the installation of the caisson by jacking. The total applied force recorded was 24 to 25N up to a depth of z/h = 0.7, after which the force increased rapidly. The friction on the skirts caused by the sand would have been relatively small as low vertical stress levels were present in this 1g test. The forces increased rapidly as the clay came into contact with sand.

7.3.2 Results of 100g experiments

All centrifuge experiments were undertaken at 100g. T-bar data for the 100g sample are presented in Figure 7.3.8. Cone penetration tests were undertaken which reached values of over 107 MPa in sand

(Figure 7.3.9). The sample was not uniform as CPT3 measured a 67 % higher peak resistance than CPT4. Measurements revealed that the clay was 30 mm thick overlying 5 mm of clayey sand with clean sand beneath. For this sample, one installation was undertaken by jacking and three installations were undertaken by a combination of jacking and suction.

Figure 7.3.10 presents a plot of jacking force for Test 5. While the skirt tip was in the clay layer, jacked installation was undertaken sharing similar loads as those recorded at 1g. The maximum load recorded for penetration through the clay was 36 N. Similar loads were recorded because s_u does not vary with acceleration, and T-bar data measured similar s_u profiles for both samples (see Figure 7.3.11). Examining the installation resistance relationship (Equation 1.3.24) it can be observed that the only term expected to be influenced by acceleration is the overburden term in the end bearing expression:

$$End\ Bearing\ Force = (\pi Dt)(\gamma' z + s_u N_c) \qquad \text{Eqn. 7.3.2}$$

As the skirt thickness was small (0.4 mm), the force caused by the tip increases comparatively very little due to stress level variation. For 100g tests, tip resistance was calculated to be 7.3 N at the bottom of the clay layer which is less than double that calculated at 1g at the same location. Account was made of acceleration by increasing the unit weight of soil and water by a factor of 100 in the following manner:

$$\gamma' z = \rho' g(Nz) \qquad \text{Eqn. 7.3.3}$$

where buoyant unit weight γ' is defined by the product of density and gravity ($\gamma' = \rho' g$). In the laboratory $N = 1$ and in the centrifuge $N = 100$.

In Test 5, when the skirt was jacked the skirt into the sand, resistance levels rose rapidly. As expected, the forces required for jacking through sand in the centrifuge were much larger than those measured for jacking in the laboratory. In sand, resistances are governed by effective stresses which were much larger in the 100g tests at the same penetration depth.

During suction installation, the actuator force applied was sufficient to push the caisson through the clay to the top of the sand. When suction was applied, installation could be progressed. Suction was applied until skirt refusal occurred. No suction tests were able to completely install the caisson.

Figure 7.3.12 displays the total installation force data for Tests 6 and 8. Resistances in clay increased approximately linearly up to a value of between 29 to 41 N, then increased rapidly as penetration began in sand. Similar resistances were measured for Tests 6 and 8. The deepest penetration was achieved in Test 8 for which Figure 7.3.13 displays the suction and actuator components of the total load applied.

An equilibrium balance of the soil plug at 100g concludes that a force of 119 N was required for plug lift. Data in Figure 7.3.13 shows that a suction induced load of 118 N was reached before suction briefly increased to 150 N so it can be concluded that the experiment ended with plug lift. The suction force reduced immediately after plug lift, as the movement of clay is likely to have blocked the hydraulic flow through the suction port.

During installation, the pumped water volume was measured. In Tests 7 and 8, it was found that the quantity of water pumped was higher than the caisson volume installed, which is attributed to small seepage flows (Figure 7.3.14). The excess water flow is defined as follows:

$$Excess\ Volume\ Pumped = \frac{Vol_{Water\ Pumped} - Vol_{Caisson\ Installed}}{Vol_{Caisson\ Installed}} \times 100 \qquad \text{Eqn. 7.3.4}$$

When suction was begun in Test 8, the excess volume pumped was equivalent to 43 % of the installed caisson volume, which increased to 120 % proportionally with installation depth. At a depth of z/h = 0.65, pumping rapidly exceeded the volume of caisson installed, supporting the hypothesis that plug lift occurred. Figure 7.3.15 presents the forces applied to the caisson in Test 5 and Test 8. It can be observed that in clay, the installation resistances were similar, but in sand, the jacked installation resistance was much higher. The suction installation required less overall force to install the caisson despite the presence of the clay layer substantially reducing the seepage volumes normally observed.

7.3.3 Comparison with calculations

Figure 7.3.16 compares the result of an installation calculation, using Equations 1.3.26 and 1.3.5, undertaken to predict the force required to jack in the caisson. Test 4 was used for this example. Figure

7.3.17 displays the installation fit for Test 1. A good approximation was achieved using similar calculation inputs as for Test 4. Table 7.3.1 presents the inputs used for these calculations.

To estimate accurately the installation resistance in the centrifuge, it is important to scale the stress boundary condition at the clay/sand interface correctly. The vertical stresses in clay, adjacent to the skirt, can be calculated by the superposition of in-situ stress and a term resulting from adhesion acting on the skirt which locally enhances the vertical stresses, as outlined in Equation 1.3.27. The in-situ stress component scales with acceleration. The term arising due to adhesion can vary as a function of load-spread in clay or adhesion. As neither adhesion or load-spread are expected to vary with acceleration, the enhanced stress term should remain the same in the centrifuge as at 1g. Consequently, the stress boundary condition at the clay/sand interface will not scale linearly with acceleration.

Figure 7.3.18 displays a plot of calculated installation force compared with results for Test 5. It may be observed that the resistance to installation at 100g can be calculated using parameters which accurately calculate the resistance at 1g conditions. The parameters used for the calculation are presented in Table 7.3.1. The soil and load-spread parameters, for both the clay and sand, used in the calculation were the same as those used for prediction of Test 1 results. This ensured that the stress term arising due to adhesion remained the same as it would have been at 1g for that clay strength.

For the 1g experiments, the non-dimensional installation conditions plotted above the uplift line in the area associated with uplift (the Unsafe Zone presented in Chapter 2). For both these tests, full skirt penetration by suction was not achieved and the plug lifted while the skirt tip was still in the clay layer. The installation conditions for these two tests were similar to those which may be experienced by a 4 m diameter caisson installed in very stiff clay, and therefore indicate that the outcome for a prototype being installed under similar conditions will be plug lift.

The jacked 1g test could be completely installed, as the jacking force supplied was sufficient to jack the caisson through the clay. While it is obvious that the plug will not move during this installation, it is

still possible to locate this installation in non-dimensional space. The maximum loads measured were 111 to 168 N which result in a relatively large non-dimensionalised vertical load $\frac{V'}{\gamma'_c D^3}$ of 35 to 53. In non-dimensional space (Figure 7.3.19), the jacked installation conditions plot in the Safe Zone, where no plug lift is expected to occur. Therefore these installations are consistent with the proposed mechanism outlined in Chapter 2. In the centrifuge, all suction installations ended in plug lift because the skirt tip was in sand. As no plug lift happened while the skirt tip was in clay, these results are also consistent with the uplift model.

The resistance in sand during suction installation was smaller than that recorded during jacking, indicating that the application of suction lowered the installation force. This could have been achieved by the application of suction to the top of the clay plug reducing the stress present at the clay/sand interface. This in turn would lower the resistances to installation. The seepage flows were much lower than those expected in homogeneous sand, however, any upward flow would contribute to smaller resistances being encountered.

7.4 Conclusions

Caisson installations were undertaken into clay over sand, both at 1g and 100g conditions. It was concluded that accurate estimation of installation resistance required the stress boundary conditions to be accurately defined at the top of the sand layer. To enable this to be accomplished, consideration must be given to the enhancement of stress due to the action of the skirt penetrating the clay layer above the sand.

The centrifuge experiments confirmed that plug lift can occur after the skirt had penetrated through the clay into sand. The outcome of the experiments supported the hypothesis presented in Chapter 2.

It was discovered that calculations undertaken to model caisson installation resistance in the laboratory could also model caisson installation resistance in the centrifuge by just making the appropriate change to the soil unit weight. The overall installation resistance in sand when overlain by clay was lowered by the presence of suction, but not to the extent observed during installation in homogeneous sand.

8 Conclusions

8.1 Concluding comments

This work has focussed on the determination of conditions under which suction caissons may be successfully installed. The primary focus of the thesis was on the conditions which are of relevance to installations likely to be undertaken for renewable energy structures. Experiments have been undertaken where model caissons were installed into soils representative of those which are found around the coast of the UK. The examples consisted of layered clay and sand profiles. Software and apparatus were developed to undertake these tests which enabled installations to be undertaken in a repeatable manner.

8.1.1 Potential for plug lift

A model for clay uplift during suction installation in clay over sand soil profiles was presented. The model focussed on the phase of penetration where the skirt tip was in the clay. A method of calculation was proposed to estimate the suction required for the onset of plug lift. This could then be compared with the expected installation suction variation to decide whether installation was feasible.

The conditions for uplift were plotted in non-dimensional space (Figure 2.6.6). On the same plot, the conditions were added within which it was calculated that installation could be achieved to the base of the clay layer. A boundary was observed, above which installations would end with plug lift. Conditions plotting below the boundary were calculated to achieve installation to the top of the sand.

A series of installations were undertaken into clay over sand soil profiles. The experiments were undertaken with non-dimensional conditions appropriate for modelling field installations outlined in Chapter 2. It was concluded that caissons can become stuck during penetration into the clay and the further application of pumping caused the plug to be pulled up the skirt. Plotting the results of each

installation in non-dimensional space (Figure 4.4.1) confirmed that the uplift boundary existed and supported the hypothesis presented in Chapter 2.

For experiments where skirt penetration was made into sand overlain by clay, it was noted that the resistances encountered were significantly higher than for when installation was made into homogeneous sand (Figure 7.3.15). It was also noted that to estimate the sand resistances correctly, the correct boundary conditions for the effective stress magnitude at the top of the sand layer were higher than those which would be calculated assuming in-situ stresses. Correct estimation of the effective stresses at the top of the sand should consider the action of skirt penetration in clay (Figure 7.3.18).

8.1.2 Homogeneous soil installations

Caisson installations were undertaken in homogeneous clay. The clay resistance could be accurately calculated and it was noted that negligible seepage occurred during suction installation (Figure 4.2.7). Installations were undertaken in sand using suction and jacking. For both methods, it was possible to estimate accurately the installation resistances (Figures 4.3.1 and 4.3.3). The pumping requirements were estimated, and it was found that the predicted pumped volumes were consistently smaller than those measured during installation (Figure 4.3.6).

Installations were undertaken in sand using a modified caisson which allowed the skirt tip pressure to be measured. The recorded data were compared with published estimates. The reduction of a was found to vary with installation rate. Higher penetration rates caused less reduction of a with depth than slow installation rates (Figure 4.3.13).

The discharged water volumes were measured during installation. From these data, and the recorded suction, it was concluded that the overall plug permeability increased with depth (Figure 4.3.14). The overall plug permeability was also greater during faster rates of penetration, which supported the

conclusions made from the measurements of a. Despite these variations, the influence of penetration rate on suction required was not significant.

8.1.3 Skirt tip injection

A test series was undertaken in sand, using a modified caisson capable of water injection at the skirt tip. Initially 8 injection nozzles were used, followed by 16 nozzles for a second test series. The tests showed that water injection reduced the suction required for installation as a function of the injected water pressure (Figure 5.3.5). Tests using the caisson with 16 nozzles needed less suction for installation than those with 8 nozzles when the same injection pressures were used. The application of injection pressure was found to cause piping at shallower penetration depths. Piping limited the maximum injection pressure that could be used.

The injection pressures used during installations did not support the assumption that injection caused a linear hydraulic gradient within the soil, which was confirmed by measurements of pore pressure changes arising from injection (Figures 5.5.5, 5.5.6 and 5.5.7). It was therefore assumed that the injection nozzles should be treated as point water sources. The resulting hydraulic gradient arising from this analysis was assumed to follow an inverse relationship with distance from the point of injection. A suitable modification to the installation resistance calculation was proposed to incorporate the hydraulic changes arising from injection. The calculations were then performed to estimate the suction required for installation, and found to estimate the installation pressures more accurately.

A series of tests were undertaken where selective injection was applied to a 16 nozzle caisson with the purpose of causing the caisson steering. The tests successfully steered the caisson in a controllable manner (Figure 5.4.3), and found that steering was most effective at shallow depths. The angle through which the caisson could be steered was found to be proportional to the injection pressure applied at the nozzles.

8.1.4 Sand with a clay layer

Installations were undertaken into a soil sample consisting of sand with a relatively thin layer of clay to test whether installation was possible. The conditions chosen for these tests were relevant to field installations and each installation was able to install the caisson into the clay layer. After the water flow had been blocked by the clay, installation suction increased substantially (Figure 4.5.1).

Installation resistance calculations were undertaken, for the sand sample with the clay layer, using a pore pressure variation which accounted for the proximity of the clay layer. The calculated suction variation obtained followed the test results closely (Figure 4.5.5). This test series demonstrated that plug lift may occur in soils consisting of mostly sand but with a thin layer of clay present. The onset of plug lift could be estimated using a suitably modified model of uplift as that presented in Chapter 2 (Figure 4.5.9).

8.1.5 Sand overlying inclined clay

A series of tests were undertaken in which installation was made through sand into an inclined clay layer to test whether this installation mode was possible. Again, dimensionally correct conditions were chosen, and each experiment was able to install the skirt into the clay fully. Full installation was possible even when conditions had been chosen to cause piping failure in the sand before the skirt tip had fully entered the clay (Figures 4.6.1, 4.6.2, 4.6.3 and 4.6.4).

8.1.6 Caisson grouting

Caissons were installed by suction into homogeneous sand and pressure grouted, using a variety of pressures, to investigate the effect of this operation on foundation response to moment loading. From the test series, it was concluded that the normalised secant unloading stiffness of foundations installed by suction was lower than those installed by jacking (Figure 6.3.12), which agreed with previous research. Pressure grouting, using very high injection pressures, increased the normalised secant unloading stiffness

of the caisson and could increase it to a level beyond that recorded by jacked caissons (Figure 6.3.12). Pressure grouting at moderate pressures did not significantly influence the stiffness (Figure 6.3.10).

It was concluded that the insertion of grout under the caisson lid reduced the foundation settlement over the course of the cyclic loading, and did not require high pressures to be used to achieve this improved response (Figure 6.3.17). The application of grouting was not found to influence the horizontal response of the caisson.

It was observed that the application of high-pressure grouting to foundations can introduce 'hard spots' under the footing. The result was a non-symmetric response to cyclic loading (Figure 6.3.22).

8.1.7 Implications for design and the applicability of caissons for use around the UK

Caissons can be suitable for use in soils present around the coast of the UK. Soils near to the shore are variable, however installation is still possible provided that certain conditions outlined in this work are avoided. Therefore the soil conditions must be accurately determined to ensure that successful installation occurs. This is particularly relevant where clay over sand is present, or sand with a clay layer, to avoid encountering instances of unexpected plug lift as the caisson can become stuck.

The action of grout injection serves to reduce in-service foundation settlements. The grout should be injected at high pressures underneath the lid to ensure good grout coverage over the soil plug. The grout should be injected at similar pressures over the foundation plan area to avoid the creation of "hard spots".

Over-pressure inside the caisson should be limited, particularly at the end of self weight penetration, as the resisting forces only just support the weight of the structure. This will avoid encountering uncontrollable installation due to loss of skirt resistance arising from water escaping from the interior.

8.2 Recommendations for further work

The installation suction calculations rely partly on appropriate values of the pore pressure parameter (a) to produce accurate estimates. For the case of installation into sand overlying an inclined clay layer, this relationship has not been calculated. The calculation may be undertaken by calculation of the appropriate flow net. However, as the problem is not axi-symmetric, a 3-Dimensional analysis would be needed. When this variation has been calculated, it may then be applied to the installation calculations to obtain the estimated suction requirement, and can be compared with the data obtained in this work. This analysis would be beneficial to allow conclusions to be drawn regarding the unexpectedly high installation depths achieved without piping failure occurring.

Further work should be undertaken to enable the application of skirt tip injection to be incorporated into the calculations for installation resistance. The work should investigate the relationship between the number of nozzles present around the perimeter of the caisson to the diameter of the footing.

For the foundations considered in this work, the current limit for suction caisson penetration in sand is approximately equal to the diameter of the footing. Further penetration using jacking or ballasting would be possible. However, these approaches involve the provision of expensive equipment. Investigation into methods of deep installation would be of use to enable the current limit to be extended, particularly for small caissons where scour effects may be significant. One method which may yield a useful improvement would be to try modification of the STI strategy, where the nozzles are strategically positioned on the outside of the skirt but at an elevation above the skirt tip. Injection of water at this point would influence the hydraulic gradient within the plug less, and may serve to reduce the skirt friction outside the caisson without causing the onset of piping at shallower depths.

The main further work now necessary should focus on field installations and the need to validate the results obtained in the laboratory at large scale. For example, the proposed mechanism for plug lift in clay over sand profiles should be proven at large scale to validate the mechanisms observed in the laboratory. Additionally, large scale installations would enable the effects of skirt tip injection to be evaluated.

Although many field size caisson installations have been undertaken, much of the data has not been released into the public domain. A report of large scale installations, would enable the assumptions of suction installation to be comprehensively evaluated. The reported installations would need to be accompanied by site investigation data to describe the soils present at the point of installation. This report would save the expense of undertaking a series of large scale tests.

The tests in this thesis have demonstrated that when soil conditions are known, calculations can be undertaken to reliably determine the feasibility of suction caisson installation. During this test program, installation was readily initiated at the beginning of each experiment purely by the application of pumping. During installation, no undesirable behaviour was observed which would lead to reservations about full scale use. These characteristics should permit designers to feel confident about choosing a caisson foundation system.

References

Allersma, H. G. B., Hogervorst, J. R. and Pimoulle, M. (2001). Centrifuge modelling of suction pile installation using a percussion technique. *Proceedings of the International Offshore and Polar Engineering Conference*, Stavanger, Norway, pp 620-625.

Andersen, K. H. and Jostad, H. P. (1999). Foundation design of skirted foundations and anchors in clay. *Proceedings of the Offshore Technology Conference*, Houston, Paper OTC 10824.

Andersen, K. and Jostad, H. P. and Dyvik, R. (2008). Penetration Resistance of Offshore Skirted Foundations and Anchors in Dense Sand. *Journal of Geotechnical and Geoenvironmental Engineering.* Vol. **134**, No. 1. pp106-116

Andersen, K. H., Murff, J. D., Randolph, M. F., Clukey, E. C., Erbrich, C. T., Jostad, H. P., Hansen, B., Aubeny, C., Sharma, P. and Supachawarote, C. (2005). Suction anchors for deepwater applications. *Proceedings of ISFOG: Frontiers in Offshore Geotechnics,* Perth, Australia, pp 3-30.

American Petroleum Institute API. (1993). "Recommended practice for planning, designing and constructing fixed offshore platforms." *API RP 2A*, American Petroleum Institute, Washington, D.C.

BERR (2008), http://www.decc.gov.uk/en/content/cms/statistics/source/electricity/electricity.aspx, Viewed 11 January 2010.

BERR (2008a), Atlas of UK Marine Renewable Energy Resources: Atlas Pages. *ABP Marine Environmental Research Ltd.*

BERR (2007), Energy white paper 2007: 'Meeting the energy challenge', Department for energy and climate change.

Betz, A. (1926). Wind Energie Wind-Energie und ihre Ausnutzung durch Windmühlen. Vandenhoek and Ruprecht, Goettingen, pp 64

Bolton M. D. (1986). The strength and dilatancy of sands. *Géotechnique*, **36**, No. 1, pp 65-78.

Bransby, M. F. and Randolph, M. F. (1998). Combined loading of skirted foundations. *Géotechnique*, **48**, No. 5, pp 637-655.

Broughton, P. and Davies, R. (2002). Refloating the Maureen Platform. *Civil Engineering*, **150**, pp 160-168.

Broughton, P., Davies, R. L., Aldridge, T. and Carrington, T. (2002). Foundation design for the refloat of the Maureen steel gravity platform. *Geotechnical Engineering*, **155**, No. 2, pp 111-118.

BS5930: 1999 Code of Practice for Site Investigations, British Standards Institute

BS6349: 2003 Code of Practice for Maritime Structures, British Standards Institute

BS8004: 1986 Code of Practice for Foundations, British Standards Institute

Buckingham, E. (1914). On Physically Similar Systems: Illustrating the use of Dimensional Analysis. *Phys. Rev.* **4**, pp 345-376.

Burton, T., Sharpe, D., Jenkins, N. and Bossanyi, E. *Wind Energy Handbook*. 2001, Chichester, New York: John Wiley and Sons Ltd. pp. 624. ISBN 0471489972. (page 42)

Butterfield, R. (1999). Dimensional analysis for geotechnical engineers. *Géotechnique*, **49**, No. 3, pp 357-366.

BWEA (2009a). http://www.bwea.com/offshore/round1.html, Viewed 11 January 2010.

BWEA (2009b). http://www.bwea.com/offshore/round-2.html, Viewed 11 January 2010.

BWEA (2009c). http://www.bwea.com/images/media/Blyth-Offshore-generating-c.jpg, Viewed 11 January 2010.

Bye, A., Erbrich, C., Rognlien, B. and Tjelta, T. I. (1995). Geotechnical design of bucket foundations. *Proceedings of the Offshore Technology Conference*, Houston, Paper OTC 7793.

Byrne, B.W. (2000). Investigations of Suction Caissons in Dense Sand. *DPhil thesis*, University of Oxford.

Byrne, B. W. and Houlsby, G. T. (2003). Foundations for offshore wind turbines. *Phil Trans of the Royal Society London*, **361**, pp 2909-2930.

Byrne, B. W., Villalobos, F., Houlsby, G. T. and Martin, C. M. (2003). Laboratory testing of shallow skirted foundations in sand. *Proceedings of the International Conference on Foundations*, Dundee, Scotland, pp 161-173.

Byrne, B. W. (2000). Investigations of suction caissons in dense sand. *DPhil Thesis*. University of Oxford.

Cassidy, M. J., Houlsby, G. T., Hoyle, M. and Marcom, M. R. (2002). Determining appropriate stiffness levels for spudcan foundations using jack-up case records. *Proceedings of the International Conference on Offshore Mechanics and Artic Engineering*, Oslo, pp 1-12.

Chen, W. and Randolph, M.F. (2003). Radial Stress Changes Around Caissons Installed in Clay by Jacking and by Suction. *Research Report No. C: 1871*, Department of Civil and Resource Engineering, The University of Western Australia, Perth.

Colliat, J-L., Boisard, P., Gramet, J-C. and Sparrevik, P. (1996). Design and installation of suction anchor piles at a soft clay site in the Gulf of Guinea. *Proceedings of the Offshore Technology Conference*, Houston, Paper OTC 8150.

Colliat, J-L., Dendani, H. and Schroeder, K. (2007). Installation of suction piles at deepwater sites in Angola. *Proceedings of the International Offshore Site Investigation and Geotechnics Conference: Confronting New Challenges and Sharing Knowledge,* London, pp 413-420.

Ding, H., Qi, L. and Xu, J. (2001). Bucket foundation platforms installed in shallow and ice-drifting area. *Journal of Cold Regions Engineering*, **15**, No. 4, pp 211-218.

DNV. (1992). Classification Notes. *No. 30.4, Foundations*, Det Norske Veritas.

El-Gharbawy, S.L. (1998). The pullout capacity of suction caisson foundations for tension leg platforms. *PhD thesis*, University of Texas, Austin.

Erbrich, C. T. and Tjelta, T. I. (1999). Installation of bucket foundations and suction caissons in sand – geotechnical performance. *Proceedings of the Offshore Technology Conference*, Houston, Paper OTC 10990.

Feld, T. (2001). Suction buckets, a new innovative foundation concept, applied to offshore wind turbines. PhD thesis, Aalborg University.

Fjeld, S., Braathen, N. F. and Hansvold, C. (1977). Installation of offshore platforms: reflections from a certification viewpoint. *Proceedings of the Offshore Technology Conference*, Houston, Paper OTC 2862.

Gerwick, B. C. Jr (1974). Preparation of foundations for concrete caisson sea structures. *Proceedings of the Rocky Mountain Regional Meeting of the Society of Petroleum Engineers of AIME*, Paper OTC 1946.

Greig E. (2004). Projected Operation and Maintenance Costs of UK Offshore Wind Farms Based on the Experience at Blyth. *Department of Trade and Industry.*

Gue, S. S. (1984). Ground heave around driven piles in clay. *DPhil Thesis*. University of Oxford.

Hazell, E (2004). Interaction of closely spaced strip footings. 4th Year Project Report

Hjelde, E., Hemmings, B., Olsen, E., Gudmestad, O.T., Sørensen, K.T. and Hall, M. (2003). Disposal of Disused Offshore Concrete Gravity Platforms in the OSPAR Maritime Area. Report No. 338. *International Association of Oil and Gas Producers.*

Hogervorst, J. R. (1980). Field trials with large diameter suction piles. *Proceedings of the Offshore Technology Conference*, Houston, Paper OTC 3817.

Houlsby, G. T. and Byrne, B. W. (2005a). Design procedures for suction caissons in clay and other materials. *Geotechnical Engineering*, **158**, No. GE 2, pp 75-82.

Houlsby, G. T. and Byrne, B. W. (2005b). Design procedures for installation of suction caissons in sand. *Geotechnical Engineering*, **158**, No. GE 3, pp 135-144.

Houlsby, G. T., Kelly, R. B., Huxtable, J. and Byrne, B. W. (2005). Field trials of suction caissons in clay for offshore wind turbine foundations. *Géotechnique*, **55**, No. 4, pp 287-296.

House, A. R., Randolph, M. F. and Borbas, M. E. (1999). Limiting aspect ratio for suction caisson installation in clay. *Research Report No. G: 1399, Dept. of Civil and Resource Engineering,* University of Western Australia, Perth.

Iskander, M., El-Gharbawy, S. and Olson, R. (2002). Performance of suction caissons in sand and clay. *Canadian Geotechnical Journal*, **39**, pp 576-584.

Junaideen (2004) Personal communication to Houlsby and Byrne (2005b).

Kelly, R. B., Byrne, B. W., Houlsby, G. T. and Martin, C. M. (2004). Tensile loading of model caisson foundations for structures on sand. *Proceedings of the International Offshore and Polar Engineering Conference*, Toulon, pp 638-641.

Kelly, R. B., Houlsby, G. T. and Byrne, B. W. (2006). A comparison of field and laboratory tests of caisson foundations in sand and clay. *Géotechnique*, **56**, No. 9, pp 617-626.

Langhaar, H. (1951). *Dimensional Analysis and Theory of Models*. New York: John Wiley

Lehane, B. A., Schneider, J. A., and Xu, X. (2005). The UWA-05 method for prediction of axial capacity of driven piles in sand. *Frontiers in offshore geotechnics: ISFOG 2005*, Taylor and Francis Group, London.

Lings, M.L. and Dietz, M.S. (2005). The peak strength of sand-steel interfaces and the role of dilation. *Soils and Foundations* **45**, No. 6, pp1-14

Mackereth, F.J.H. (1958). A portable core sampler for lake deposits. *Limnology and Oceanography*, **3** (2), pp181-191.

Martin, C. M. (1994). Physical and numerical modeling of offshore foundations under combined loads. *DPhil Thesis*. University of Oxford.

Masui, N., Yoneda, H., Zenda, Y., Ito, M., Iida, Y. and Hermstad, J. (2001). Installation of offshore concrete structure with skirt foundation. *Proceedings of the International Offshore and Polar Engineering Conference*, Stavanger, Norway, pp 626-630.

Mayne P.W. and Kulhaway F.H. (1982). K_o – OCR Relationships in Soil. *Journal of Geotechnical Engineering*. Proceedings of ASCE, Vol. **108**, No. GT6

Palacios, J. (1964). *Dimensional Analysis*. London: MacMillan.

Rademakers L.W.M.M., Braam, H., Zaaijer, M.B. and van Bussel, G.J.W. (2003). Assessment and Optimisation of Operation and Maintenance of Offshore Wind Turbines. European Wind Energy Conference 2003, Madrid, Spain, 16-19 June, 2003

Raines, R. D., Ugaz, O. and Garnier, J. (2005). Centrifuge modeling of suction piles in clay. *Proceedings of ISFOG: Frontiers in Offshore Geotechnics,* Perth, Australia, pp 303-308.

Randolph, M.F., and House, A.R. (2002). Analysis of Suction Caisson Capacity in Clay. *Proceedings of the Offshore Technology Conference*, Houston, Paper OTC 14236.

Randolph, M. F., Jewell, R. J., Stone, K. J. L. and Brown, T. A. (1991). Establishing a new centrifuge facility. *Research Report No. G: 1024, Dept. of Civil and Resource Engineering,* University of Western Australia, Perth.

Sea and Land Power (2005). Future Energy Solutions. The Application of Suction Caisson Foundations to Offshore Wind Turbines. Doc. No. 0216-G-RP-S-11078. Sea and Land Power and Energy Ltd.

Senders, M. R. and Randolph, M. F. (2009). CPT-based method for the installation of suction caissons in sand. *Journal of Geotechnical and Geoenvironmental Engineering*, **135**, No. 1, pp 14-25.

Senders, M., Randolph, M. and Gaudin, C. (2007). Theory for the installation of suction caissons in sand overlaid by clay. *Proceedings of the International Offshore Site Investigation and Geotechnics Conference: Confronting New Challenges and Sharing Knowledge,* London, pp 429-438.

Senpere, D. and Auvergne, G. A. (1982). Suction anchor piles – a proven alternative to driving or drilling. *Proceedings of the Offshore Technology Conference*, Houston, Paper OTC 4206.

Sharman, H. and Constable, J. (2008). Electricity Prices in the United Kingdom. Fundamental Drivers and Probable Trends. *Renewable Energy Foundation*. http://www.ref.org.uk/Publications

Solhjell, E., Sparrevik, P., Haldorsen, K. and Karlsen, V. (1998). Comparison and back calculation of penetration resistance from suction anchor installation in soft to stiff clay at The Njord and Visund Fields in the North Sea. *Offshore Site Investigation and Foundation Behaviour 198, SUT.*

Sparrevik, P. (2002). Suction pile technology and installation in deep waters. *Offshore Technology Conference*, Houston, paper 14241

Taiebat, H. A. and Carter, J. P. (2000). Numerical studies of the bearing capacity of shallow foundations on cohesive soil subjected to combined loading. *Géotechnique*, **50**, No. 4, pp 409-418.

Tjelta, T. I. (1995). Geotechnical experience from the installation of the Europipe Jacket with bucket foundations. *Proceedings of the Offshore Technology Conference*, Houston, Paper OTC 7795.

Tjelta, T. I., Aas, P. M., Hermstad, J. and Andenaes, E. (1990). The skirt piled Gullfaks C platform installation. *Proceedings of the Offshore Technology Conference*, Houston, Paper OTC 6473.

Tjelta, T. I., Guttormsen, T. R. and Hermstad, J. (1986). Large-scale penetration test at a deepwater site. *Proceedings of the Offshore Technology Conference*, Houston, Paper OTC 5103.

Tran, M. N. (2005). Installation of suction caissons in dense sand and the influence of silt and cemented layers. *Ph.D. thesis*, Department of Civil Engineering, University of Sydney.

Tran, M. N., and Randolph, M. F. (2008). Variation of suction pressure during caisson installation in sand. *Geotechnique*, **58** (No.1), pp1–11.

Tran, M. N., Randolph, M. F. and Airey, D.W. (2008). Installation of Suction Caissons in Sand with Silt Layers. *Research Report No. C: 2055*, Department of Civil and Resource Engineering, The University of Western Australia, Perth.

Van Diest, E. (1946). *Dimensional Analysis for Engineers*. Oxford: Clarendon Press.

Vestas (2004) V120-4.5 MW. Leadership in Offshore Presentation. Vestas Wind Systems, Denmark.

Vestas (2008a) V82-1.65 MW. Product Brochure. Vestas Wind Systems, Denmark.

Vestas (2008b) V90-3.0MW. Product Brochure. Vestas Wind Systems, Denmark.

Villalobos, F. A. (2007). Model Testing of Foundations for Offshore Wind Turbines, *DPhil thesis*, Department of Engineering Science, University of Oxford.

Villalobos, F. A., Byrne, B. W. and Houlsby, G. T. (2005). Moment loading of caissons installed in saturated sand. *Proceedings of ISFOG: Frontiers in Offshore Geotechnics,* Perth, Australia, pp 411-416.

WBB Minerals (2001). Redhill 110 PSD, http://www.wbbminerals.net/products/index.html

Wetzel, R. A. and McCullough, E. A. (1989). Pile capacity prediction. *Proceedings Predicted and Observed Axial Behaviour of Piles*, Northwestern University, Illinois, pp 129-140.

Tables

Chapter 1 Tables

Location	Status	Capacity	Developer/Turbines
North Hoyle	Operating (Dec 2003)	60 MW	NPower (Vestas 2 MW)
Scroby Sands	Operating (Dec 2004)	60 MW	E.ON UK (Vestas 2 MW)
Kentish Flats	Operating (Sep 2005)	90 MW	Vattenfall
Barrow	Operating (Sep 2006)	90 MW	Centrica/DONG (Vestas 3 MW)
Gunfleet Sands	Approved	30 turbines	DONG
Lynn/Inner Dowsing	Approved	57 turbines	Centrica
Cromer	Withdrawn	30 turbines	Edf
Scarweather Sands	Approved	30 turbines	E.ON /DONG
Rhyl Flats	Approved	25 turbines	NPower
Burbo Bank	Operational	25 turbines	DONG (Siemens)
Solway Firth	Approved	60 turbines	E.ON
Shell Flat	Submitted	90 turbines	ScottishPower/Eurus/ Shell/DONG
Teesside	Approved	30 turbines	Edf
Tunes Plateau *	Submitted	30 turbines	RES/B9 Energy
Ormonde *	Submitted	30 turbines	Eclipse Energy

* These two projects were outside the original Round 1 process, but conform to its terms. Ormonde is an innovative wind-gas hybrid project.

Table 1.1.1. A table showing Round 1 wind farms. The installed capacity is shown for the operating wind farms. The number of turbines is shown for the other schemes.

	Case 1	Case 2	Case 3
Wind turbine size, MW	3	3	4.5
Wave height, m	4	10	10
Water depth (*h*), m	10	20	20
Horizontal load (*H*), MN	1.4	2.8	3.6
Vertical load (*V*), MN	4.9	5.8	6.2
Moment load (*M*), MNm	91.0	117.6	187.6

Table 1.2.2 Loads on a wind turbine foundation as a function of water depth calculated for three example combinations.

	Most Probable		Highest Expected	
	k_p	k_f	k_p	k_f
Sand	0.3	0.001	0.6	0.003
Clay	0.4	0.03	0.6	0.05

Table 1.3.1. List of parameters recommended for use by DNV for estimation of the installation resistance of a caisson.

k_{side}	k_{tip} (min)	k_{tip} (max)
0.001	0.01	0.6

Table 1.3.2. Parameters taken from Andersen *et al.* (2008) for large scale installations.

k_{side}	k_{tip} (min)	k_{tip} (max)
0.0053	0.93	1.24

Table 1.3.3. Parameters taken from Andersen *et al.* (2008) derived from laboratory scale installations.

Source	End bearing factor (k_p or k_{tip})	Side friction factor (k_f or k_{side})
DNV	0.3 - 0.6	0.001 - 0.003
Senders and Randolph (2009)	0.2	0.0018 – 0.0026
Andersen (2008) field tests	0.01 – 0.6	0.001 – 0.0015
Andersen (2008) laboratory tests	0.93 – 1.24	0.0053

Table 1.3.4. Table of parameters suggested for use with CPT data to estimate the installation resistance of a caisson. The measured parameters show significant variability.

Chapter 2 Tables

Quantity	Non-dimensional group	Value of non-dimensional group	Physical dimension			
Caisson diameter, D	-	-	0.182 m	1 m	5 m	15 m
Vertical load, V'	$\frac{V'}{\gamma'_c D^3}$	0.5	0.031 kN	5.1 kN	636 kN	17179 kN
Skirt thickness, t	$\frac{t}{D}$	200	0.00091 m	0.005 m	0.025 m	0.075 m
Skirt length, h_c	$\frac{h_c}{D}$	0.5	0.091 m	0.5 m	2.5 m	7.5 m
Installation rate, $\dot{z}$	$\frac{\dot{z}}{k}$	1	0.00001 m/s	0.00001 m/s	0.00001 m/s	0.00001 m/s
Friction angle, φ'	φ'	42°	42°	42°	42°	42°

Table 2.3.1. Table of non-dimensional conditions used for comparison of installations in sand.

Quantity	Non-dimensional group	Value of non-dimensional group	Physical dimension			
Caisson diameter, D	-	-	0.182 m	1 m	5 m	15 m
Vertical load, V'	$\frac{V'}{\gamma'_c D^3}$	0.5	0.018 kN	3 kN	375 kN	10125 kN
Skirt thickness, t	$\frac{t}{D}$	200	0.00091 m	0.005 m	0.025 m	0.075 m
Adhesion factor	α	0.3	0.3	0.3	0.3	0.3
End-bearing factor	N_c	9	9	9	9	9
Skirt length, h_c	$\frac{h_c}{D}$	0.5	0.091 m	0.5 m	2.5 m	7.5 m
Clay undrained shear strength, s_u	$\frac{s_u}{\gamma'_c D}$	1.5	1.638 kPa	9 kPa	45 kPa	135 kPa

Table 2.3.2. Table of non-dimensional conditions used for comparison of installations.

Area	Wind Farm	Soil Province
Irish Sea Area	Solway Firth	2b/2c (some 1)
	Robin Rigg	2b/2c
	Barrow / Isle of Walney	2b/2c
	Shell Flats (3 sites)	2a
	Southport	2b/2c
	Burbo Bank	1/2b/2c
	North Hoyle	1/3a/3b
	Rhyl Flats / Constable Bank	1/2b/2c
Swansea Bay	Scarweather Sands	3b (some 3a & 2c)
Thames Estuary	Kentish Flats	2a/2c (some 3a)
	Gunfleet Sands	2a/2b/2c (some 3a)
East Anglia / Skegness	Scroby Sands	1
	Cromer	2b/3a
	Inner Dowsing	2b (some 3a)
	Lynn	2b (some 3a)
Northern England	Teesside	3a/3b

Table 2.5.1. Table of soil province classifications for Round 1 wind farm developments (Sea and Land Power (2005)). See text for soil province classification description.

Area of development	East Anglia/ Skegness	Liverpool Bay	Thames Estuary
Clay over sand (Applicable range of s_u)	Yes Greater than 75 kPa	Yes Greater than 20 kPa	
Sand with clay lense (Applicable range of s_u)			Yes Less than 40 kPa
Sand over clay (Applicable range of s_u)	Yes Greater than 75 kPa		Yes $40<s_u<150$ kPa

Table 2.5.2. List of expected soil profiles at sites of Round 2 wind farm development.

Property	Field Monopod	Field Tripod	Lab Caisson (1g)	Lab Caisson (1g)	Centrifuge (prototype)	Centrifuge (actual size)
Diameter (m)	10 - 30	4 – 8	0.18	0.572	8	0.08
Wall Thickness (mm)	25 - 60	25	1.7	1	40	0.4
Skirt Length (m)	7.5 - 25	3 – 6	0.355	0.263	6.35	0.0635
Applied Force (kN)	619 - 12220	118 - 409	-	-	409	-
Buoyant unit soil weight, (kN/m^3)	6.2	6.2	6.2	6.2	6.2	620
Range of s_u, (kPa)	0 - 300	0 - 300	-	-	0 - 300	-
Range of $\frac{V'}{\gamma'_c D^3}$	0.100 – 0.073	0.298 – 0.129	-	-	0.129	-
Range of $\frac{s_u}{\gamma'_c D}$	0 – 4.839	0 – 6.05	-	-	0 – 6.05	-
Target Range of s_u (kPa) for experiments	-	-	0 – 6.75	0-18.75	-	0 – 300
Target Range of V' (kN) for experiments	-	-	0.003 – 0.011	0.057-0.231	-	0.041

Table 2.6.1. Values of field and laboratory ratios.

Chapter 3 Tables

Property	Value
D_{10}, D_{30}, D_{50}, D_{60}, (mm)	0.08, 0.10, 0.12, 0.13
Coefficient of uniformity, C_u and curvature C_c	1.63, 0.96
Specific gravity, G_s	2.65
Minimum and maximum dry density, γ_{min}, γ_{max} (kN/m^3)	12.76 – 16.80
Critical state friction angle, φ_{cs}	

Table 3.2.1. Properties of Redhill 110 taken from Kelly *et al.* (2004) with critical state friction angle taken from Villalobos *et al.* (2005).

Tank detail	Perth Strongbox	Small sand tank	Large sand tank	Consolidometer
Plan shape	Rectangular	Circular	Circular	Circular
Diameter (mm)	390	450	1100	1000
Length (mm)	650	N/A	N/A	N/A
Depth (mm)	425	425	400	4 × 200

Table 3.3.1. Table of sample tank dimensions.

Caisson number	1	2	3	4	5	6	7
Caisson name	UWA caisson	Small caisson	Brass caisson	Steering caisson	Large caisson	Grouting caisson (short)	Grouting caisson (long)
Experiments	Centrifuge tests	Homogeneous soil installation	Plug lift tests	Steering tests	Plug lift tests	Grouting tests	Grouting tests
Diameter, D_o (mm)	80	150	181	150	572	204	204
Skirt length, h (mm)	63.5	142	355	142	263	100	150
Skirt thickness, t (mm)	0.4	1.5	1.7	1.5	1.0	2.0	2.0
Skirt material	Stainless steel	Stainless steel	Brass	Stainless steel	Steel (unpainted)	Stainless steel	Stainless steel
Lid material	Dural	Dural	Transparent Perspex	Dural	Steel	Transparent Perspex	Transparent Perspex
Comments			Transparent lid to enable inspection of soil plug.	Stainless steel pipes attached to caisson skirt to enable water injection at the skirt tip.	All surface corrosion was removed from the caisson skirt prior to installation.	Nine ports in the lid enabled pressure grouting over the top of the soil plug. Transparent lid to enable inspection of grout coverage over the top of the soil plug.	Nine ports in the lid enabled pressure grouting over the top of the soil plug. Transparent lid to enable inspection of grout coverage over the top of the soil plug.

Table 3.4.1. Table of dimensions for model caissons used in experiments

Chapter 4 Tables

Test ID	Test material	Installation method	Caisson	Test g
C1	Homogeneous clay	Suction	Caisson 2	1
C2	Homogeneous clay	Jacking	Caisson 3	1
SCS_1	Sand with a clay layer	Suction	Caisson 3	1
SCS_2	Sand with a clay layer	Suction	Caisson 3	1
SCS_3	Sand with a clay layer	Suction	Caisson 3	1
SCS_4	Sand with a clay layer	Suction	Caisson 3	1
SCS_5	Sand with a clay layer	Suction	Caisson 3	1
SIC_1	Sand over inclined clay	Suction	Caisson 3	1
SIC_2	Sand over inclined clay	Suction	Caisson 3	1
SIC_3	Sand over inclined clay	Suction	Caisson 3	1
SIC_4	Sand over inclined clay	Suction	Caisson 3	1

Table 4.1.1. List of experiments undertaken to investigate installation in layered soil profiles.

Test ID	Test material	Installation method	Caisson	Test g
CS_1.1	Clay over sand	Suction	Caisson 5	1
CS_1.2	Clay over sand	Suction	Caisson 3	1
CS_1.3	Clay over sand	Suction	Caisson 3	1
CS_2.1	Clay over sand	Suction	Caisson 5	1
CS_2.2	Clay over sand	Suction	Caisson 3	1
CS_2.3	Clay over sand	Suction	Caisson 3	1
CS_3.1	Clay over sand	Suction	Caisson 5	1
CS_3.2	Clay over sand	Suction	Caisson 3	1
CS_3.3	Clay over sand	Suction	Caisson 3	1
CS_3.4	Clay over sand	Suction	Caisson 3	1
CS_3.5	Clay over sand	Suction	Caisson 3	1
CS_4.1	Clay over sand	Suction	Caisson 5	1
CS_4.2	Clay over sand	Suction	Caisson 3	1
CS_4.3	Clay over sand	Suction	Caisson 3	1
CS_4.4	Clay over sand	Suction	Caisson 3	1
CS_5.1	Clay over sand	Suction	Caisson 5	1
CS_5.2	Clay over sand	Suction	Caisson 3	1
CS_5.3	Clay over sand	Suction	Caisson 3	1
CS_5.4	Clay over sand	Suction	Caisson 3	1
G1	Homogeneous sand	Suction	Caisson 6	1
G2	Homogeneous sand	Jacking	Caisson 6	1
G3	Homogeneous sand	Jacking	Caisson 6	1
G4	Homogeneous sand	Suction	Caisson 6	1
G5	Homogeneous sand	Suction	Caisson 6	1
G6	Homogeneous sand	Suction	Caisson 6	1
G7	Homogeneous sand	Suction	Caisson 6	1
G8	Homogeneous sand	Suction	Caisson 6	1

Table 4.1.2. List of experiments undertaken to investigate suction installation in clay over sand soil profiles and installation in homogeneous sand by suction and jacking.

Depth of measurement (mm)	Reading on scale	Measured undrained shear strength, s_u (kPa)	Average undrained shear strength (kPa)
70	6.6	9.7	9.3
70	6.5	9.6	
70	6.4	9.5	
70	6.4	9.5	
70	5.5	8.2	
170	8.3	12.2	12.0
170	8.0	11.7	

Table 4.2.1. Table of shear strength results recorded by hand shear vane in the homogeneous clay sample.

Soil property	Jacking estimate	Suction estimate
Angle of friction, (φ')	39°	39°
Buoyant unit weight (γ')	10.2 kN/m^3	10.2 kN/m^3
Bearing capacity factor, N_q	56	56
Bearing capacity factor, N_γ	92.2	92.2
Horizontal stress factor, K	0.9	0.9
Angle of friction between skirt and soil, δ	26°	26°
Stress influence gradient, f_i, f_o	0.75 – 1 m/m	0.75 – 1 m/m

Table 4.3.1. Table of parameters used as inputs for calculations of jacking and suction installation resistance in Redhill 110 sand.

Property	Field Monopod	Field Quadruped
Diameter, D (m)	10 - 30	4 – 10
Wall thickness, t (mm)	25 - 60	25 - 35
Skirt length, h (m)	7.5 - 25	3 – 7.5
Applied force, V' (kN)	619 - 12220	118 - 619
Range of soil strength, s_u (kPa)	20 - 300	20 - 300
Clay buoyant unit weight, γ' (kPa)	6.2	6.2
Adhesion factor, α	0.3 - 0.4	0.3 - 0.4
N_c	9	9
t/D	0.0008 – 0.006	0.0025 - 0.009
h_c/D	0 - 0.5	0 - 0.5
Range of $\frac{V'}{\gamma'_c D^3}$	0.073 - 0.100	0.100 - 0.298
Range of $\frac{s_u}{\gamma'_c D}$	0.1 – 4.839	0.3 – 12.10

Table 4.4.1. Values of non-dimensional ratios relevant for prototype installations.

Property	Field Monopod	Field Quadruped	Lab Value (1g)	Centrifuge (prototype)	Centrifuge (actual size)
Range of $\frac{V'}{\gamma'_c D^3}$	0.073 - 0.1	0.1 - 0.298	0.075 – 0.36	0.63	0.63
Range of $\frac{s_u}{\gamma'_c D}$	0.1 – 4.839	0.3 – 12.10	0.34 – 6.7	0.04 – 0.16	0.04 – 0.16
Range of s_u, (kPa)	20 - 300	20 - 300	2 - 8	2 - 8	2 - 8
Applied Force V' (kN)	619 - 12220	118 - 619	0.001 – 0.346	2000	0.2
Diameter, D (m)	10 - 30	4 – 10	0.18 – 0.572	8	0.08
Wall Thickness, t (mm)	25 - 60	25 - 35	1 - 1.7	40	0.4
Skirt Length h_c (m)	7.5 - 25	3 – 7.5	0.263 – 0.355	6.35	0.0635
Buoyant unit soil weight, γ' (kN/m^3)	6.2	6.2	6.2	6.2	620
Adhesion factor, α	0.3 - 0.4	0.3 - 0.4	0.3 - 0.4	0.3 - 0.4	0.3 - 0.4
N_c	9	9	9	9	9
t/D	0.0008 – 0.006	0.0025 - 0.009	0.004 – 0.009	0.005	0.005
h_c/D	0 - 0.5	0 - 0.5	0 - 0.5	0 - 0.5	0 - 0.5

Table 4.4.2. Values of non-dimensional ratios relevant for prototype installations.

Chapter 5 Tables

Test id (8N = 8 Nozzle)	Caisson size D, (m)	Installation method	Caisson load V', (N)	Number of nozzles	Installation rate, $\dot{z}$ (mm/s)	Sand density (%)	STI pressure (kPa)	Notes
8N test 1	0.15	Suction	15	8	0.10	Loose	0	
8N test 2	0.15	Suction	15	8	0.17	Loose	0	Effect of rate
8N test 3	0.15	Suction	15	8	0.11	59	0	Measurements of a and F
8N test 4	0.15	Suction	15	8	0.11	72	0	Measurements of a and F
8N test 5	0.15	Suction	15	8	0.08	-	0	
8N test 6	0.15	Suction	15	8	0.06	66	0	Measurements of a and F
8N test 7	0.15	Suction	15	8	0.07	53	0	
8N test 8	0.15	Suction	15	8	0.10	81	1	
8N test 9	0.15	Suction	15	8	0.09	57	5	
8N test 10	0.15	Suction	15	8	0.09	68	5	
8N test 11	0.15	Suction	15	8	0.11	79	5 max	
8N test 12	0.15	Suction	15	8	0.10	Loose	5	Effect of STI pressure
8N test 13	0.15	Suction	15	8	0.10	Loose	5	Effect of STI pressure
8N test 14	0.15	Suction	15	8	0.11	Loose	5	Effect of STI pressure
8N test 15	0.15	Suction	15	8	0.10	Loose	7.5	Effect of STI pressure
8N test 16	0.15	Suction	15	8	0.10	70	7.5	Effect of STI pressure
8N test 17	0.15	Suction	15	8	0.12	72	7	
8N test 18	0.15	Suction	15	8	0.09	66	7.5	
8N test 19	0.15	Suction	15	8	0.08	72	7.5	
8N test 20	0.15	Suction	15	8	0.11	66	7.5	Early piping failure encountered
8N test 21	0.15	Suction	15	8	0.10	72	10	
8N test 22	0.15	Suction	15	8	0.10	Loose	10	
8N test 23	0.15	Suction	15	8	0.12	Loose	10	
8N test 24	0.15	Suction	15	8	0.13	Loose	10	
8N test 25	0.15	Suction	15	8	0.09	Loose	10	
8N test 26	0.15	Suction	15	8	0.10	Loose	10	STI trial, with piping failure
8N test 27	0.15	Suction	15	8	0.09	66	10	
8N test 28	0.15	Suction	15	8	0.11	Loose	12	
8N test 29	0.15	Suction	15	8	variable	Loose	13	
8N test 30	0.15	Suction	15	4	variable	Loose	0 to 15	
8N test 31	0.15	Suction	15	8	0.11	Loose	14	
8N test 32	0.15	Suction	15	8	0.10	Loose	15	
8N test 33	0.15	Suction	15	8	0.15	Loose	16	
8N test 34	0.15	Suction	15	8	0.02	Loose	0	Effect of rate
8N test 35	0.15	Suction	15	8	1	Loose	0	Effect of rate
8N test 36	0.15	Suction	15	8	0.37	Loose	0	Effect of rate
8N test 37	0.15	Suction	15	8	0.23	Loose	0	Effect of rate
8N test 38	0.15	Suction	15	8	0.23	Loose	0	Effect of rate
8N test 39	0.15	Suction	15	8	0.12	Loose	0	Effect of rate

Table 5.3.1. List of installations undertaken using the eight port caisson.

Test ID (16N = 16 Nozzle)	Caisson size D, (m)	Installation method	Caisson load V', (N)	Number of nozzles	STI pressure (kPa)
16N test 1	0.15	Suction	17	16	0
16N test 2	0.15	Suction	17	16	0
16N test 3	0.15	Suction	17	16	0
16N test 4	0.15	Suction	17	16	5
16N test 5	0.15	Suction	17	16	5
16N test 6	0.15	Suction	17	16	8
16N test 7	0.15	Suction	17	16	7.5
16N test 8	0.15	Suction	17	16	12.5
16N test 9	0.15	Suction	17	16	12.5

Table 5.3.2. List of installations undertaken using the 16 port caisson.

Test Identity	Injection Pressure (kPa)	Initial conditions	Steering mode	Installation method	Notes
Steered 1	5	Free	1 sided steering	Suction	
Steered 2	7 to 8	Free	1 sided steering	Suction	
Steered 3	10 to 11	Free	1 sided steering	Suction	Knocked and piping
Steered 4		Free	1 sided steering	Suction	
Steered 5		Free	1 sided steering	Suction	Early piping failure encountered
Steered 6	0	Fixed	1 sided steering	Suction	
Steered 7	5	Fixed	1 sided steering	Suction	
Steered 8	7.5	Fixed	1 sided steering	Suction	
Steered 9	8	Fixed	1 sided steering	Suction	8kPa injection, early piping failure encoutered
Steered 10	1.5	Fixed	1 sided steering	Suction	
Steered 11	10	Fixed	1 sided steering	Suction	10 kPa injection, early piping failure encountered
Steered 12	6	Fixed	1 sided steering	Suction	
Steered 13	8	Fixed	1 sided steering	Suction	
Steered 14	5 to 7	Fixed	1 sided steering	Suction	Knocked and piping
Steered 15	4	Fixed	1 sided steering	Suction	
Steered 16	5	Fixed	1 sided steering	Suction	
Steered 17	4 and 5 and 6	Fixed	1 sided steering	Suction	
Steered 18	4 and 5 and 6	Fixed	1 sided steering	Suction	
Steered 19	3 and 4 and 5	Fixed	1 sided steering	Suction	
Steered 20		Fixed	1 sided steering	Suction	
Steered 21	3	Fixed	2 way steering	Suction	
Steered 22		Fixed	2 way steering	Suction	
Steered 23	6 to 7	Free	2 way steering	Suction	
Steered 24	6	Free	2 way steering	Suction	
Steered 25		Free	2 way steering	Suction	
Steered 26	7 to 8	Free	2 way steering	Suction	
Steered 27	variable	Free	2 way steering	Suction	Installation undertaken with indicated level caisson
Steered 28	6 to 7	Free	1 sided steering	Suction	
Steered 29	5.5	Free	1 sided steering	Suction	
Steered 30	variable	Free	2 way steering	Suction	Installation held at inidcated level rotation at end of test
Steered 31	6 to 7	Free	2 way steering	Suction	Installation undertaken with breaks between modes

Table 5.3.3. Table of steering tests undertaken using the 16 port caisson.

nozzles	Test ID (8N = 8 Nozzle)	Injection pressure (kPa)	Suction at 100 mm (kPa)	Suction at 60 mm (kPa)	Suction at 40 mm (kPa)	Suction difference between 40 and 60 mm (kPa)	Suction difference between 40 and 100 mm (kPa)	40/60 gradient (mm/kPa)	40/100 gradient (mm/kPa)
8	8N test 1	0	1.63	1.013	0.644	0.369	0.986	54.2	60.9
8	8N test 2	0	1.373	0.798	0.471	0.327	0.902	61.2	66.5
8	8N test 3	0	1.388	0.844	0.563	0.281	0.825	71.2	72.7
8	8N test 4	0	1.733	0.927	0.598	0.329	1.135	60.8	52.9
8	8N test 5	0	1.438	0.75	0.456	0.294	0.982	68.0	61.1
8	8N test 6	0	1.388	0.7	0.48	0.220	0.908	90.9	66.1
8	8N test 7	0	1.334	0.661	0.363	0.298	0.971	67.1	61.8
8	8N test 10	5	1.294	0.728	0.406	0.322	0.888	62.1	67.6
8	8N test 12	5	1.451	0.94	0.46	0.480	0.991	41.7	60.5
8	8N test 13	5	1.516	0.812	0.544	0.268	0.972	74.6	61.7
8	8N test 14	5	1.638	1.038	0.807	0.231	0.831	86.6	72.2
8	8N test 15	7.5	1.356	0.8	0.602	0.198	0.754	101.0	79.6
8	8N test 16	7.5	1.5	0.814	0.64	0.174	0.860	114.9	69.8
8	8N test 18	7.5	1.6	0.9	0.638	0.262	0.962	76.3	62.4
8	8N test 19	7.5	1.753	1.046	0.778	0.268	0.975	74.6	61.5
8	8N test 20	7.5	1.7	0.999	0.736	0.263	0.964	76.0	62.2
8	8N test 23	10	1.494	0.816	0.654	0.162	0.840	123.5	71.4
8	8N test 25	10	1.177		0.469		0.708		84.7
8	8N test 27	10	1.484	0.75	0.491	0.259	0.993	77.2	60.4

Table 5.3.4. Table of suction required to install the 8 nozzle caisson to the depths specified in the table. The inverse gradients of the suction change over the target depths are listed.

Injection pressure (kPa)	Average pressure gradient 40/60 (mm/kPa)	Difference between average gradient for stated injection pressure and gradient with no injection (mm/kPa)	Average pressure gradient 40/100 (mm/kPa)	Difference between average gradient for stated injection pressure and gradient with no injection (mm/kPa)
0	67.6	0.0	63.1	0
5	66.2	-1.4	65.5	2.4
7.5	88.6	21.0	67.1	4.0
10	100.3	32.7	72.2	9.1

Table 5.3.5. Comparison between average pressure differences calculated for a series of tests using an 8 nozzle skirt tip injection caisson. The difference in suction pressure was calculated between suction installation with no injection and the suction needed after injection was applied. The suction difference was calculated over two depths, the first depth being at 40 mm penetration at which injection had not been applied. The second depth was either 60 mm or 100 mm allowing shallow and deep comparison.

	Test ID (16N = 16 Nozzle)	Injection pressure (kPa)	Suction at 100 mm (kPa)	Suction at 60 mm (kPa)	Suction at 40 mm (kPa)	Suction difference between 40 and 60 mm (kPa)	Suction difference between 40 and 100 mm (kPa)	40/60 gradient (mm/kPa)	40/100 gradient (mm/kPa)
16	16N test 1	0	1.37	0.707	0.424	0.283	0.946	70.7	63.4
16	16N test 2	0	1.062	0.468	0.141	0.327	0.921	61.2	65.1
16	16N test 4	5	1.266	0.598	0.382	0.216	0.884	92.6	67.9
16	16N test 5	5	1.113	0.503	0.306	0.197	0.807	101.5	74.3
16	16N test 6	8	0.979	0.399	0.23	0.169	0.749	118.3	80.1
16	16N test 7	7.5	1.198	0.6	0.407	0.193	0.791	103.6	75.9
16	16N test 8	12.5	0.986	0.356	0.24	0.116	0.746	172.4	80.4
16	16N test 9	12.5	0.899	-	0.258		0.641		93.6

Table 5.3.6. Table of suction required to install the 16 nozzle caisson to the depths specified in the table. The inverse gradients of the suction change over the target depths are listed.

		Gradient between 40 and 60 mm installation depth (mm/kPa)		Gradient between 40 and 100 mm installation depth (mm/kPa)	
	Number of STI nozzles	8 nozzles	16 nozzles	8 nozzles	16 nozzles
Injection pressure (kPa)	0	67.6	65.9	63.1	64.3
	5	66.2	97.1	65.5	71.1
	7.5	88.6	111.0	67.1	78.0
	10	100.3	172.4	72.2	87.0

Table 5.3.7. Table of the results of calculations for the effectiveness of STI. The table shows a comparison of STI pressures and STI injection configuration. The larger the number, the greater the effect of STI for that experiment.

Test ID (8N = 8 Nozzle)	Number of nozzles	Caisson size D, (m)	Installation method	Caisson load V', (N)	Installation rate, $\dot{z}$ (mm/s)	Sand density (%)	STI pressure (kPa)	Piping depth, z (mm)	Suction just before piping, s (kPa)
8N test 1	8	0.15	Suction	15	0.10	Loose	0	127	2.009
8N test 2	8	0.15	Suction	15	0.17	Loose	0	130	1.951
8N test 3	8	0.15	Suction	15	0.11	59	0	128	1.794
8N test 4	8	0.15	Suction	15	0.11	72	0	129	2.057
8N test 5	8	0.15	Suction	15	0.08	-	0	104	1.500
8N test 6	8	0.15	Suction	15	0.06	66	0	127	2.000
8N test 7	8	0.15	Suction	15	0.07	53	0	129	1.780
8N test 21	8	0.15	Suction	15	0.10	72	10	81	1.255
8N test 22	8	0.15	Suction	15	0.10	Loose	10	96	1.150
8N test 25	8	0.15	Suction	15	0.09	Loose	10	109	1.300
8N test 26	8	0.15	Suction	15	0.10	Loose	10	90	1.050
8N test 27	8	0.15	Suction	15	0.09	66	10	106	1.600

Table 5.3.8. Table of final installation depths for caissons installed with injection and without injection.

Installation Phase	$\Delta\theta_x$ (degrees)	$\Delta\theta_y$ (degrees)	$\frac{\Delta\theta_y}{\Delta\theta_x}$
Suction installation without steering	-0.24	0.1	-0.4
Steering applied to reduce θ_y	-0.1	-0.9	9.0
Steering applied to increase θ_y	0.33	0.88	2.7
Suction installation without steering	0.1	0.14	1.4

Table 5.4.1. Table of caisson inclination change with depth for steering demonstration test.

Sand density, γ	20 kN/m^3
Sand friction angle, φ'	41°
Sand permeability, k	0.00008 m/s
$K\tan\delta$	0.465

Table 5.6.1. Table of soil parameters used to estimate the suction required to install a caisson with STI.

Test name	Injection pressure, p_{inj} (kPa)		Steering out θ at start (°)	Steering out θ at end (°)	Steering out change of angle, $\Delta\theta$ °	Steering back in θ at start (°)	Steering back in θ at end (°)	Steering back in change of angle, $\Delta\theta$ °	Steering out Installation depth at start, z (mm)	Steering out Installation depth at end, z (mm)	Steering back in Installation depth at start, z (mm)	Steering back in Installation depth at end, z (mm)	Steering out angle ratio $\left(\frac{\Delta\theta_y}{\Delta\theta_x}\right)$	Steering in angle ratio $\left(\frac{\Delta\theta_y}{\Delta\theta_x}\right)$	Steering out steering gradient $\left(\frac{\Delta\theta_{y,out}}{\Delta z_{out}}\right)$ (°/mm)	Steering back in steering gradient $\left(\frac{\Delta\theta_{y,in}}{\Delta z_{in}}\right)$ (°/mm)
1	6.5	θ_y	-1.180	0.020	1.200	0.020	-1.180	-1.200	47.000	62.500						
		θ_x	1.820	1.690	-0.130	1.690	1.150	-0.540			62.500	127.200	-9.231	2.222	0.077	-0.019
2	6.0	θ_y	1.510	0.690	-0.820	0.990	1.380	0.390	49.400	65.000						
		θ_x	1.020	0.660	-0.360	0.920	1.280	0.360			80.000	119.300	2.278	1.083	-0.053	0.010
3	8.0	θ_y	1.110	-0.010	-1.120	0.340	1.000	0.660	42.500	63.000						
		θ_x	0.190	0.300	0.110	0.270	0.410	0.140			76.000	108.000	-10.182	4.714	-0.055	0.021
4	7	θ_y	1.100	0.200	-0.900	0.270	1.150	0.880	46.000	62.000						
		θ_x	-0.760	-0.860	-0.100	-0.860	-0.530	0.330			62.000	86.000	9.000	2.667	-0.056	0.037
5 Single sided steering	5.5	θ_y	0.380	-0.660	-1.040	-0.230	-0.410	-0.180	45.000	65.000						
		θ_x	-0.580	-0.440	0.140	-0.240	-0.160	0.080			77.500	94.000	-7.429	-2.250	-0.052	-0.011
6 Single sided steering	7.0	θ_y	0.415	-0.470	-0.885	-0.070	-0.340	-0.270	47.500	71.900						
		θ_x	-0.500	-0.210	0.290	-0.140	-0.110	0.030			80.550	97.300	-3.052	-9.000	-0.036	-0.016

Figure 5.5.1. List of angles through which the caisson was steered in two way steering (steer out, steer in), and the depths covered during the steering phase. The ratios of the change in θ_y to change in θ_x are displayed for each test. It can be observed that steering at shallow penetrations has a greater effect.

Chapter 6 Tables

Test ID	Installation method	Cyclic test vertical load (N)	Grouting load
GC1.1	Jacked	56-65	No grout
GC1.2	Suction	55-66	12 N
GC1.3	Suction	57-66	No grout
GC1.4	Jacked	60-65	No grout
GC1.5	Suction	60-65	302 N
GC1.6	Suction	55-65	No grout
GC2.1	Jacked	60-70	No grout
GC2.2	Suction	55-60	14 N
GC2.3	Suction	56-65	No grout
GC2.4	Jacked	58-65	No grout
GC2.5	Suction	55-62	No grout
GC2.6	Suction	55-61	60 N
GC2.7	Suction	55-61	No grout
GC3.1	Jacked	40-45	No grout
GC3.2	Jacked	37-45	No grout
GC3.3	Jacked	40-50	No grout
GC3.4	Suction	38-43	40 N
GC3.5	Suction	36-43	No grout
GC4.1	Suction	40-45	No grout
GC4.2	Suction	38-42	No grout
GC4.3	Suction	40-42	No grout
GC4.4	Suction	40-45	40 N
GC4.5	Jacked	40-50	No grout
GC5.1	Jacked	47-56	No grout
GC5.2	Suction	31-42	No grout
GC5.3	Suction	40-46	0 N
GC5.4	Suction	43-50	0 N
GC5.5	Jacked	52-55	No grout
GC6.1	Jacked	57-68	No grout
GC6.2	Suction	26-40	No grout
GC6.3	Suction	40-50	329 N
GC6.4	Suction	50-62	412 N
GC6.5	Suction	66-73	684 N
GC7.1	Jacked	45-60	No grout
GC7.2	Suction	30-50	No grout
GC7.3	Suction	30-36	12 N
GC7.4	Suction	33-37	24 N
GC7.5	Suction	50-56	50 N
GC7.6	Jacked	50-51	No grout

Table 6.2.1. Table of experiments undertaken for investigating the effect of grouting on caisson moment response.

Chapter 7 Tables

Test Identification	Method of installation	Acceleration
Test 1	Jacking	1g
Test 2	Suction installation	1g
Test 3	Suction installation	1g
Test 4	Jacking	1g
Test 5	Jacking	100g
Test 6	Suction installation	100g
Test 7	Suction installation	100g
Test 8	Suction installation	100g

Table 7.1.1. Table of tests undertaken at the University of Western Australia.

Soil Property	Silica sand	Kaolin clay
Specific gravity, G_s	2.67	2.60
Saturated weight, γ_{sat}	19.4 – 21.2 kN/m^3	6.7 kN/m^3
Average grain size. D_{50}	0.18 mm	-
Range of void ratio, e	0.49 – 0.78	-
Consolidation coefficient, c_v	-	2.6 m^2/year

Table 7.2.1. Properties of silica sand and kaolin used for the experiments undertaken at the University of Western Australia.

Soil property	Test 1	Test 4	Test 5
Angle of friction, φ'	42º	42º	42º
Unit weight of sand, γ'_s	10.2 kN/m^3	10.2 kN/m^3	1020 kN/m^3
f_{clay}	0.3	0.3	0.3
f_{sand}	0.6	0.6	0.6
Metal interface angle of friction, δ	28º	28º	28º
Lateral stress coefficient, K	0.75	0.95	0.95

Table 7.3.1. Table of inputs used to back-calculate the results of installation tests undertaken in the laboratory centrifuge. The centrifuge parameter accounted for the enhancement of acceleration at 100g.

Figures

Chapter 1 Figures

Figure 1.1.1. The Draupner jacket showing the 12 m diameter caisson foundations at the base of each leg. (Statoil)

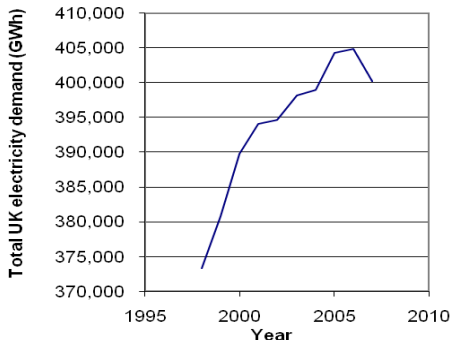

Figure 1.1.2. Total UK electricity demand in the period from 1998 to 2007. (BERR (2008))

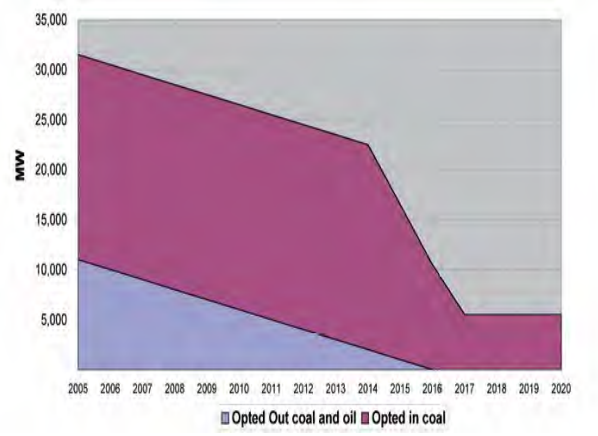

Figure 1.1.3. The projected decline of coal and oil fired condensing steam generating capacity in the UK. (Sharman and Constable (2008))

Figure 1.1.4. Round 1 locations. (BWEA (2010a))

Figure 1.1.5. Round 2 locations. (BWEA (2010b))

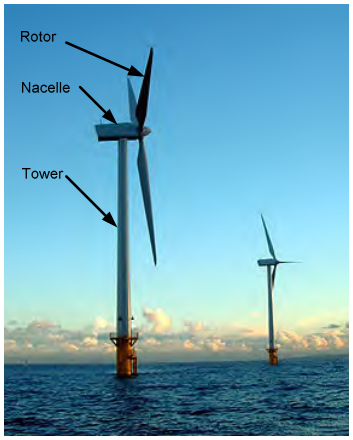

Figure 1.2.1. Picture of offshore wind turbines. (BWEA (2010c))

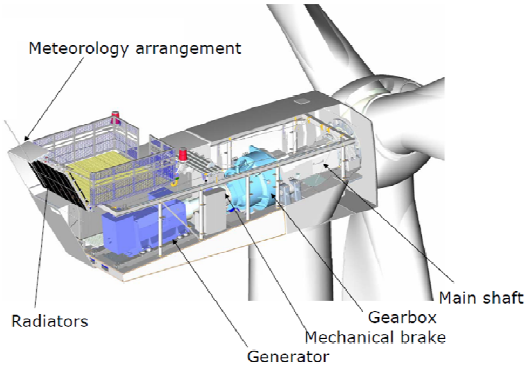

Figure 1.2.2. Ghost view of wind turbine nacelle, showing typical arrangement of turbine machinery including generator and gearbox. (Vestas (2004))

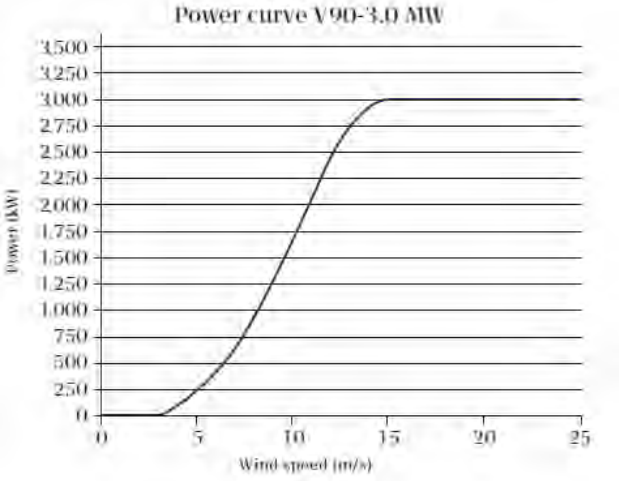

Figure 1.2.3. Power curve for a Vestas 3.0 MW wind turbine. The turbine must be shut down when the wind speed exceeds 25 m/s. (Vestas (2008b))

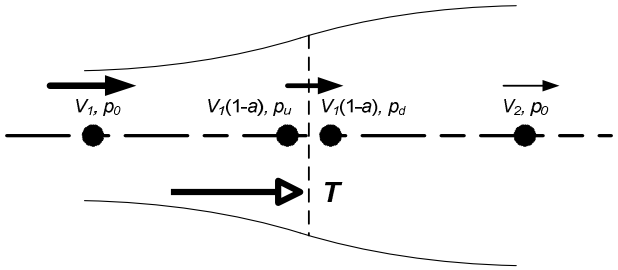

Figure 1.2.4. Diagram of a wind turbine showing the assumed path taken by the air as it passes through the blades. The vertical dashed line corresponds to the rotor axis. The circles correspond to points at which the air velocity (V) and pressure (p) are used in the calculations.

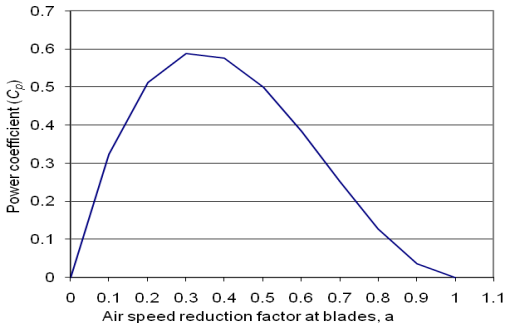

Figure 1.2.5. The variation of theoretical power coefficient (C_p) of a wind turbine with air speed reduction factor a. The maximum value of power coefficient (16/27) occurs when a = 1/3.

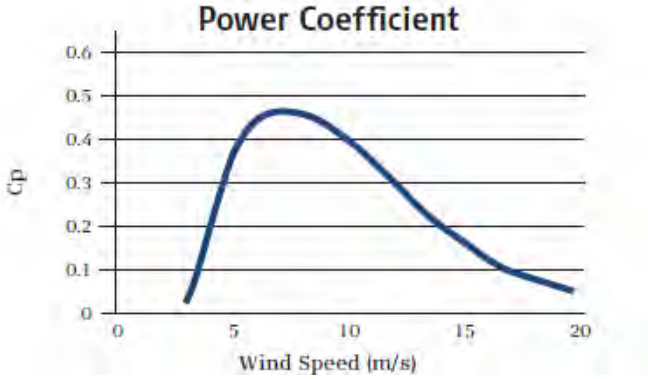

Figure 1.2.6. The variation of wind turbine power coefficient with wind speed for a Vestas 1.65 MW wind turbine. The trend of the curve is typical for commercially available wind turbines. (Vestas (2008a))

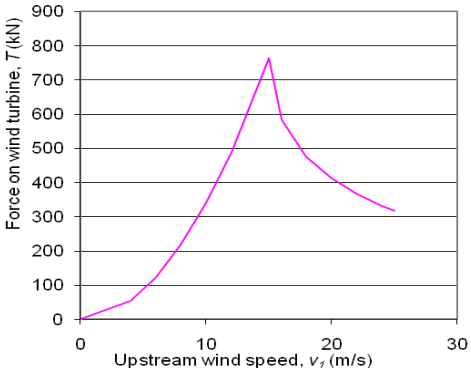

Figure 1.2.7. The force exerted by the rotor on the nacelle of a 3 MW wind turbine. The force reduces after the control system feathers the blades to limit the power output at high wind speeds.

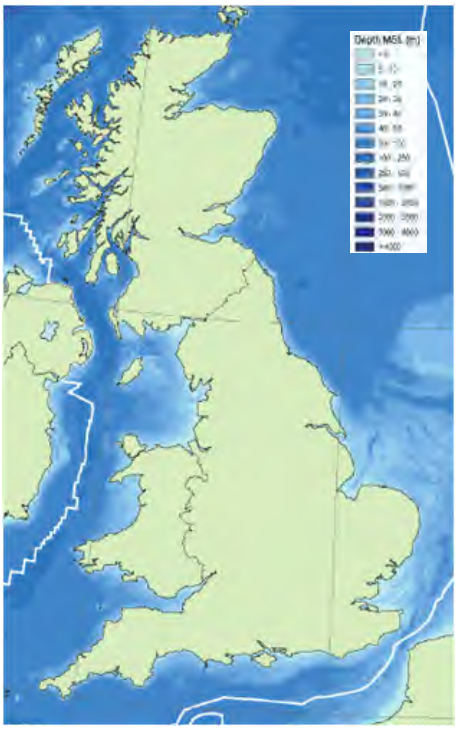

Figure 1.2.8. Diagram showing the bathymetry of the sea around the UK. (BERR (2008a))

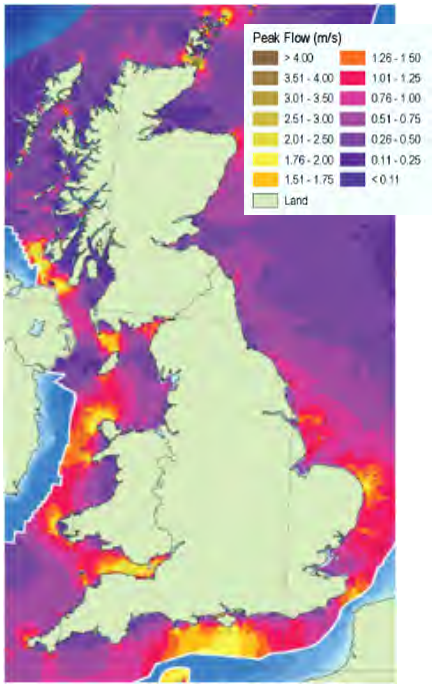

Figure 1.2.9. Map of the peak mean spring tide flows around the coast of the UK. (BERR (2008a))

Figure 1.2.10. Photograph of wind turbine with assumed loads shown acting at the base of the tower. (Vestas (2004))

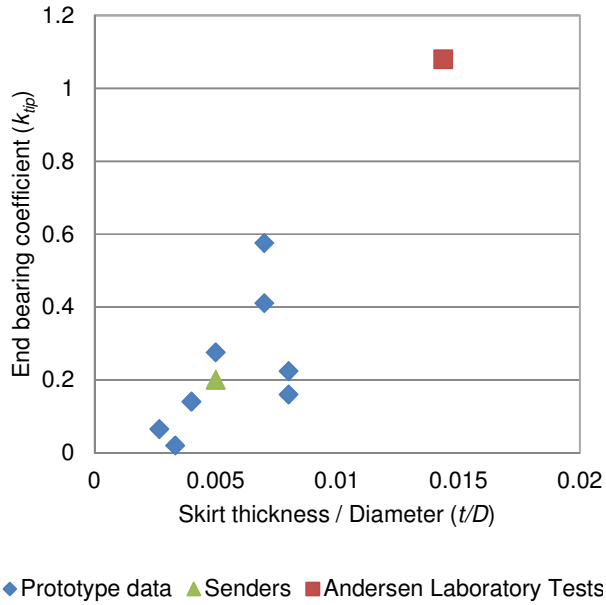

Figure 1.3.1. A plot of skirt tip thickness to diameter ratio and end bearing coefficient for the data presented in Andersen *et al.* (2008) with the data of Senders and Randolph (2009) included.

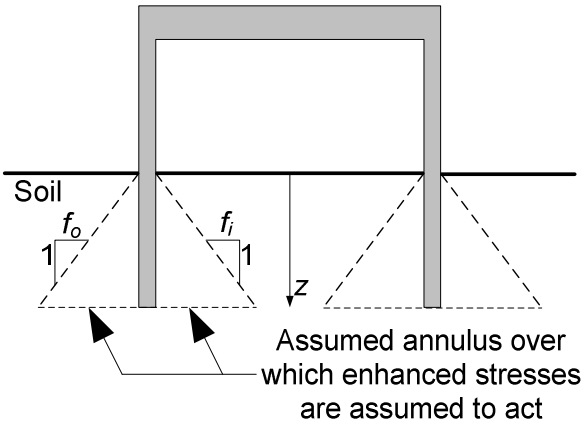

Figure 1.3.2. Diagram of the assumed area over which enhanced stresses act due to the installation of a skirt into sand. The variation of the area is assumed to vary proportionally to the factors f_i and f_o.

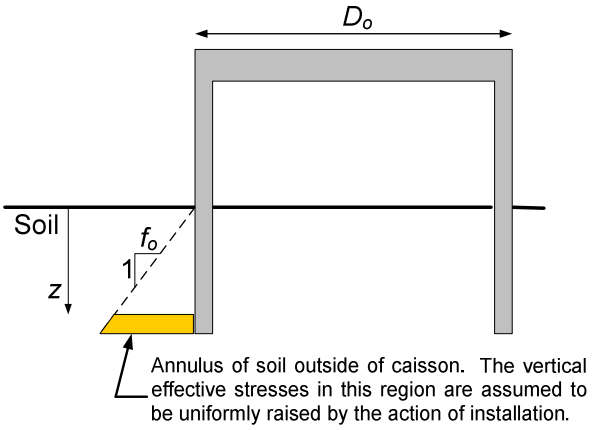

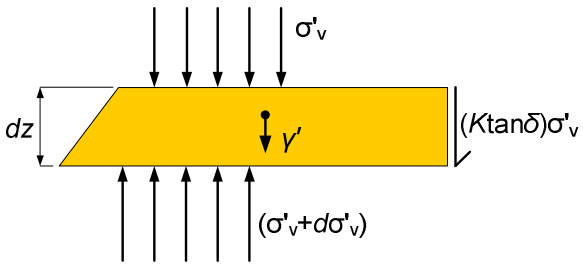

Figure 1.3.3. Soil element from the exterior of the caisson with stresses labeled. Balancing the resultant forces and solving the equation allows the vertical stresses in the soil to be determined.

Chapter 2 Figures

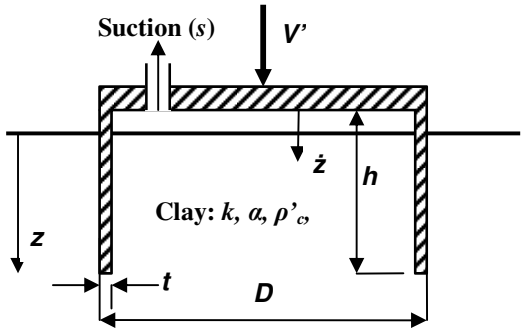

Figure 2.2.1. Diagram of caisson partially installed into clay. The variables associated with installation are shown on the diagram.

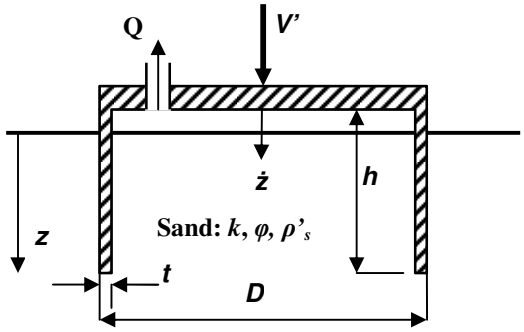

Figure 2.2.2. Diagram of caisson partially installed into sand. The variables considered for non-dimensional analysis are labelled on the diagram.

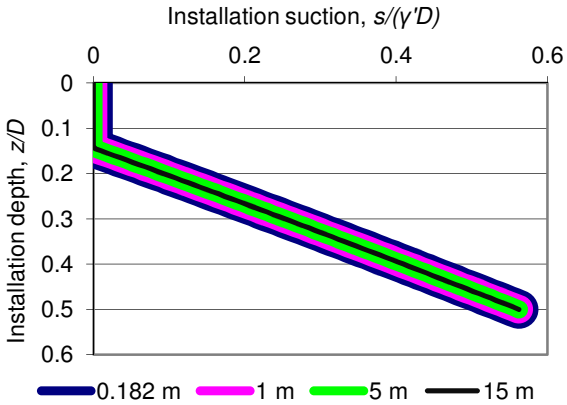

Figure 2.3.1. Figure of estimated installation suction requirement for caissons installed into sand. Estimates are presented in non-dimensional form. All installation conditions identified in non-dimensional analysis have the same value.

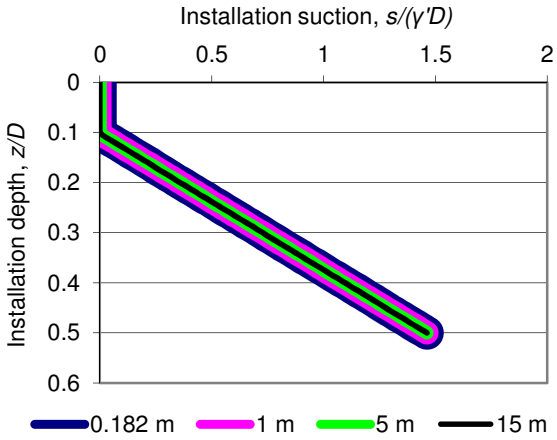

Figure 2.3.2. Figure of suction required for installation of a range of caissons in clay presented in non-dimensional form. All non-dimensional ratios identified were maintained similar.

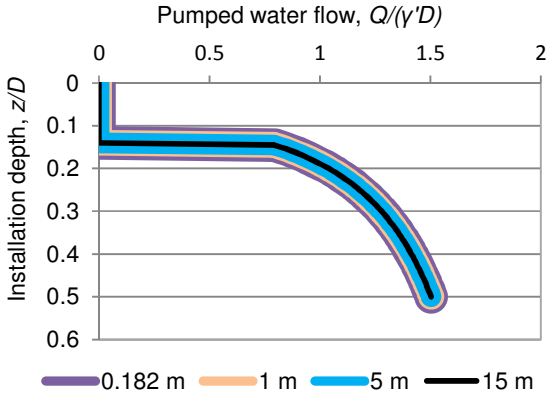

Figure 2.4.1. Plot of pumped water volume estimates plotted non-dimensionally.

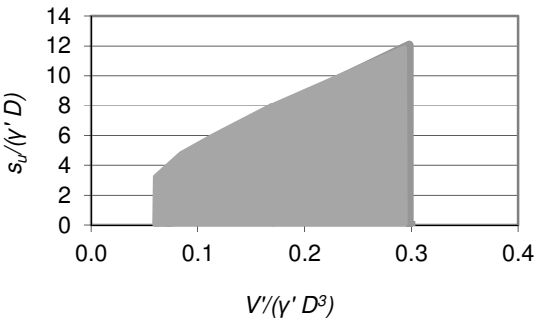

Figure 2.6.1. Range of ratios for field installations which need to be observed in the laboratory tests. The non-dimensional installation conditions are estimated to lie within the grey area.

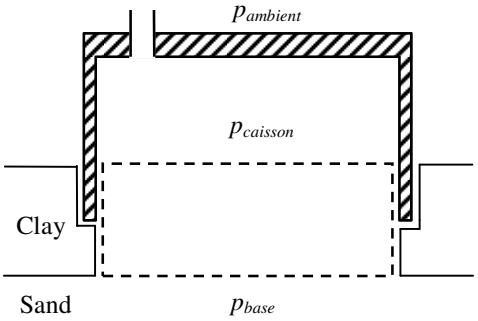

Figure 2.6.2. Diagram of water pressures present during caisson installation into clay over sand.

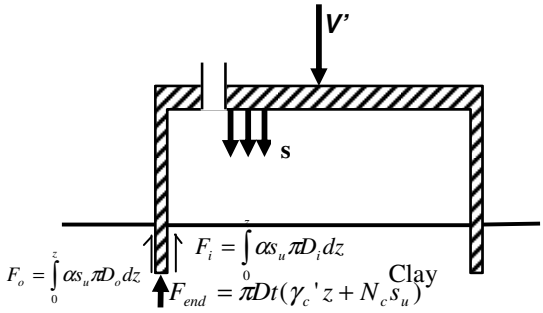

Figure 2.6.3. Forces acting on a caisson during installation in clay.

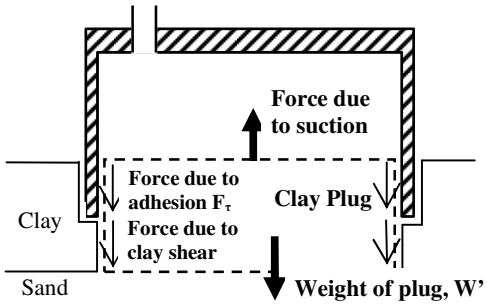

Figure 2.6.4. Diagram of the forces acting on the clay plug while the skirt is in the clay layer.

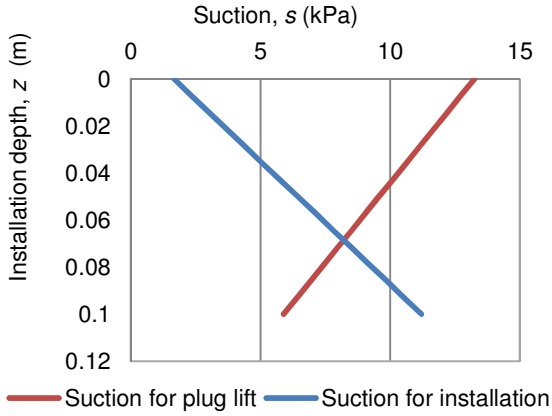

Figure 2.6.5. The variation of suction required for caisson installation and plug lift as a function of skirt depth when installing into clay over sand.

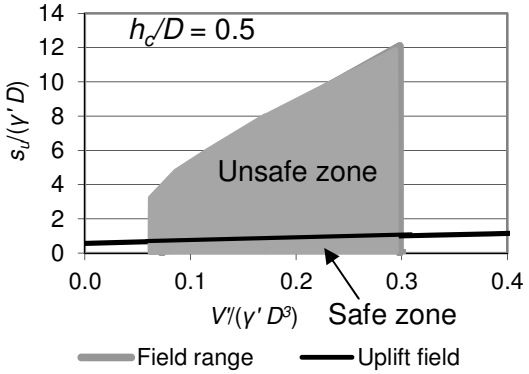

Figure 2.6.6. A non-dimensional plot showing the regions where installation into clay over sand is expected to end in plug lift (Unsafe zone) and the region where skirt penetration is expected to be achieved to the base of the clay layer (Safe zone). This plot was calculated for cases where the clay thickness is equal to half the caisson diameter (h_c/D = 0.5). Similar field installations for offshore foundations are expected to fall within the shaded grey area.

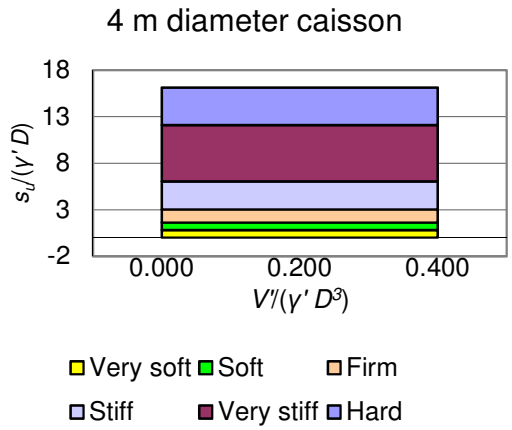

Figure 2.6.7. Plot of non-dimensional clay strengths according to BS5930 for installation of a 4 m diameter caisson.

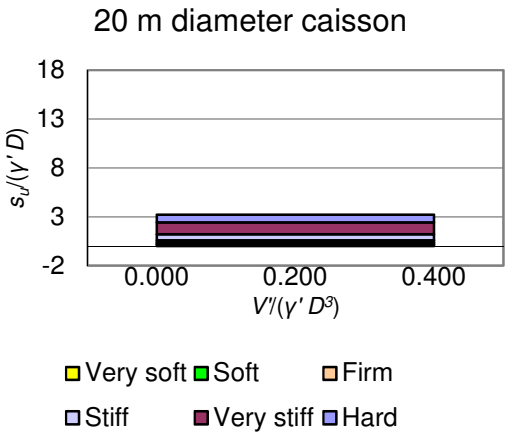

Figure 2.6.8. Plot of non-dimensional clay strengths for a 20 m diameter caisson. A similar axis scale is used as for the 4 m diameter plot for comparison.

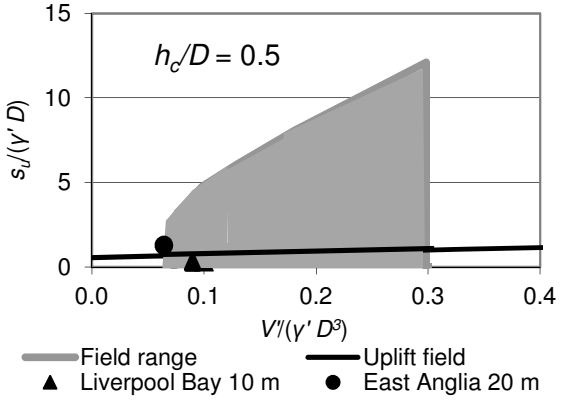

Figure 2.6.9. Diagram of the installation conditions expected at Liverpool Bay and at East Anglia/ Skegness for cases where the clay thickness is equal to half the caisson diameter.

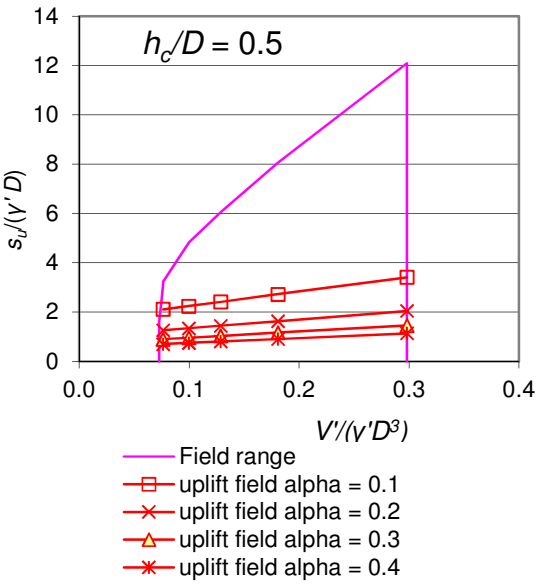

Figure 2.6.10. Plot showing the sensitivity of the uplift boundary to the variation of adhesion factor (α). This plot was calculated with the non-dimensional group h_c/D maintained at a value of 0.5.

Chapter 3 Figures

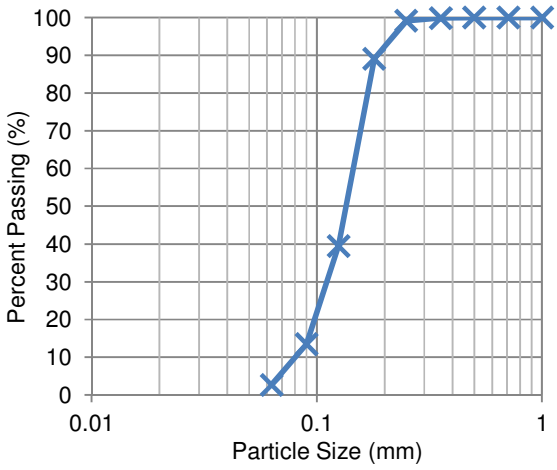

Figure 3.2.1. Redhill 110 particle size distribution curve (Kelly *et al*. (2004).

Figure 3.5.2. Photograph of the installation apparatus with Caisson 2 attached.

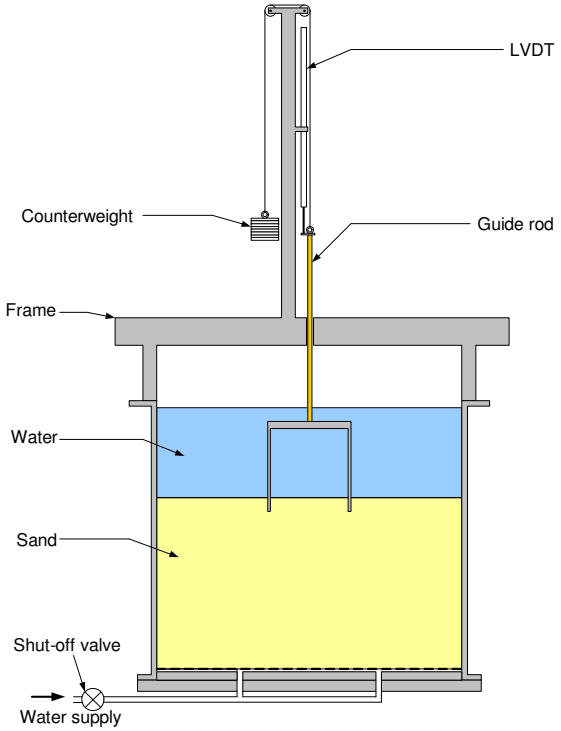

Figure 3.5.1. Diagram of the installation apparatus.

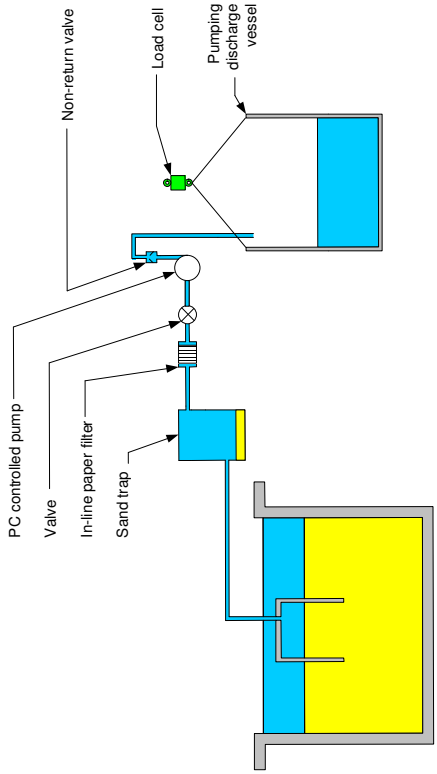

Figure 3.5.3. Diagram of the pumping scheme for installation of caissons.

Chapter 4 Figures

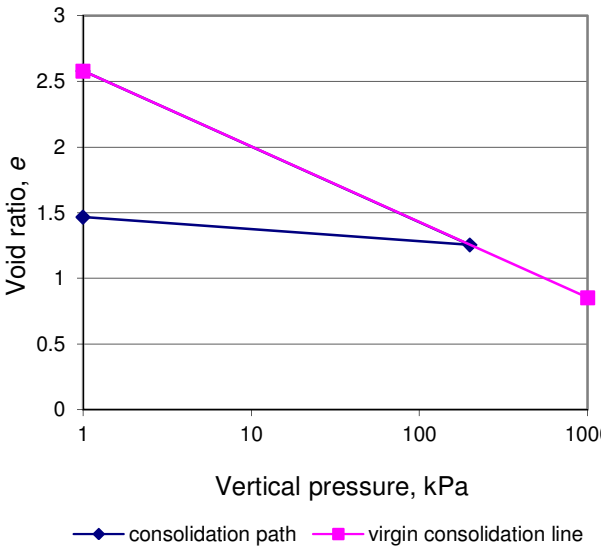

Figure 4.1.1. Consolidation path for kaolin used for clay experiments (Gue (1984)).

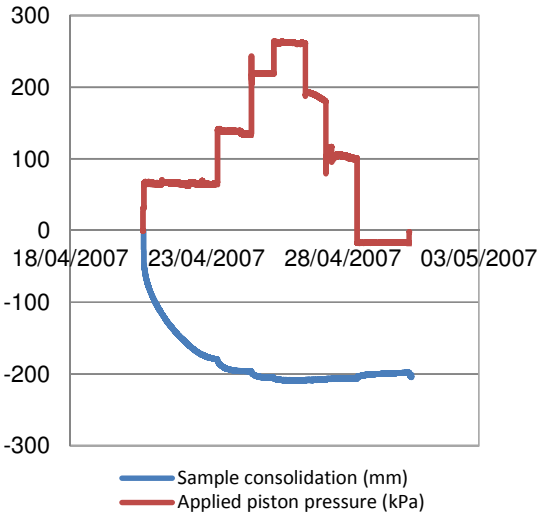

Figure 4.1.2. Log of sample height with respect to applied consolidation pressure for a sample used in the large consolidometer at Oxford University.

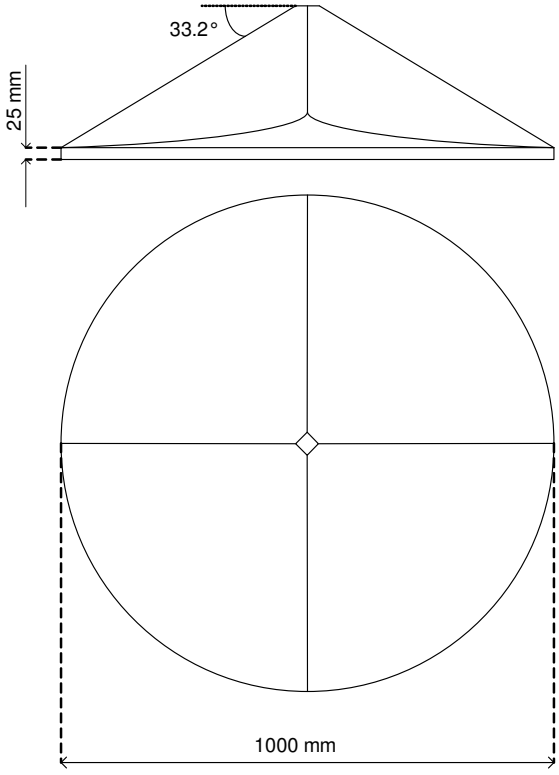

Figure 4.1.3. Diagram of the pyramid used to adapt the consolidometer piston for inclined layer installation tests.

Figure 4.1.4. Photograph showing the inclined clay surface before the placement of sand.

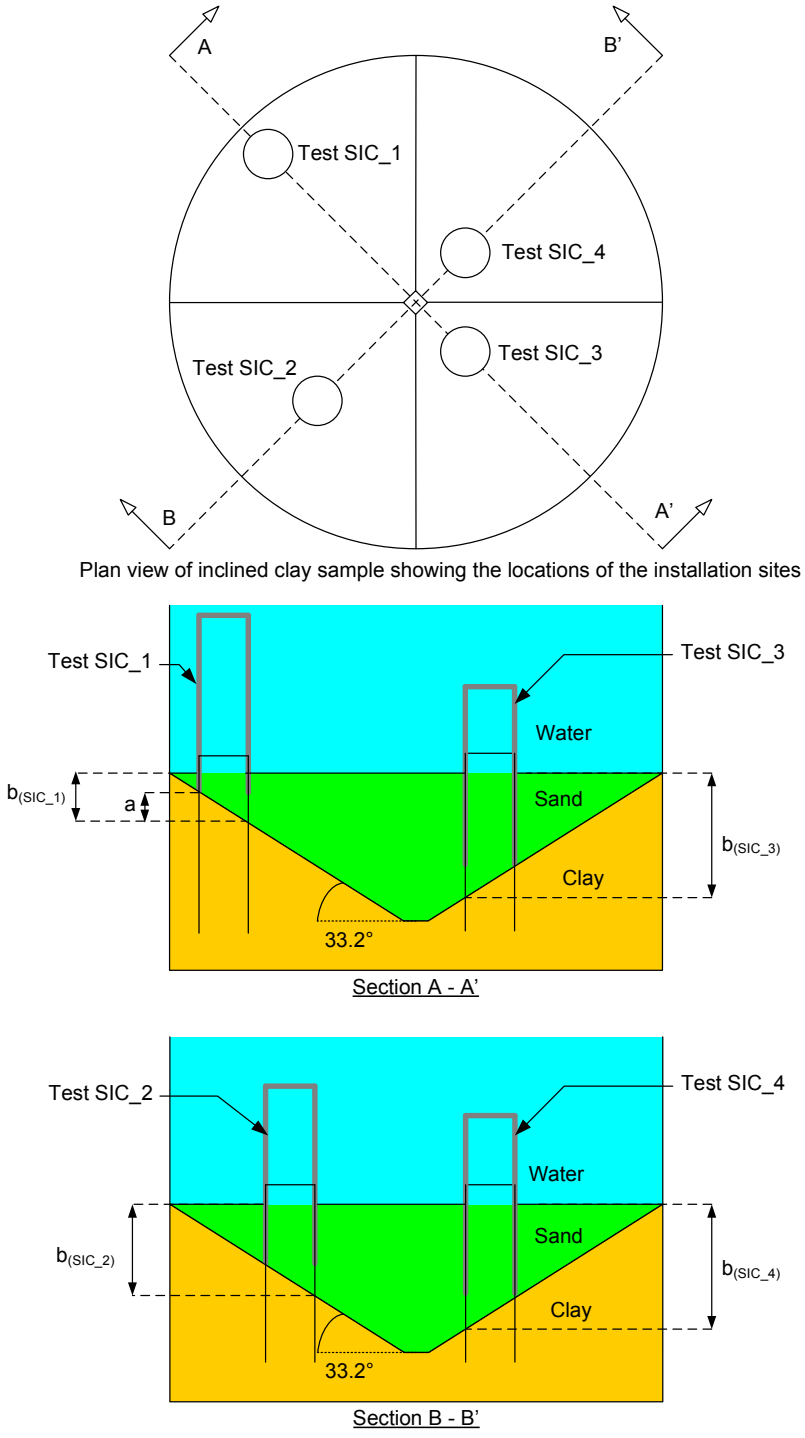

Figure 4.1.5. Diagram outlining the apparatus geometry used during inclined clay installations. The transition depth, labeled '*a*' on Section A – A', was the same in each experiment as the clay inclination and caisson diameter were the same in each test. The distance the skirt travelled in sand during installation, labeled '*b*' on the Sections, was increased for experiments SIC_1 to SIC_3. The depth of sand for test SIC_4 was the same as test SIC_3. All tests were undertaken between the corners of the profile on a uniform section of slope.

Figure 4.1.6. Photograph of Caisson 3 used for the layered soil installation tests.

Figure 4.1.8. Installation apparatus used for layered soil tests.

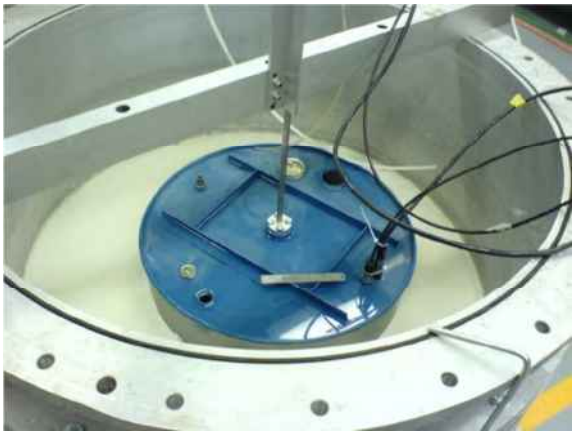

Figure 4.1.7. Photograph of Caisson 5 used for layered soil installation tests, shown installed into sample.

Figure 4.2.1. Diagram of the shear vane test locations undertaken to characterise the soil strength used for homogeneous clay installation.

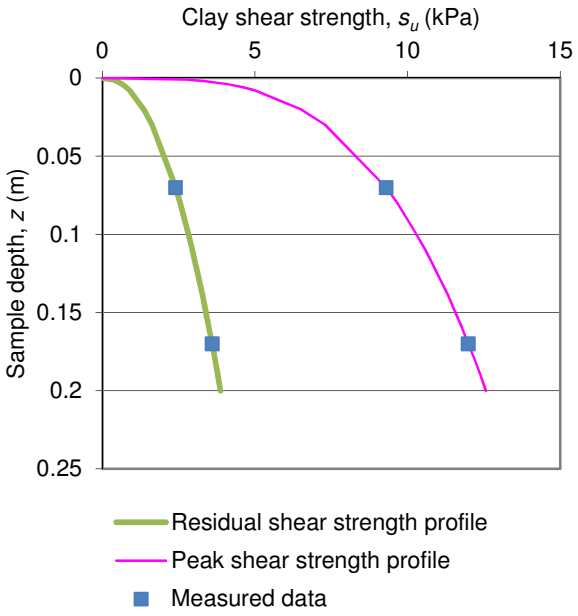

Figure 4.2.2. The assumed clay shear strength profile with depth for suction installation shown against the profile of assumed residual shear strengths determined using the residual shear strength data from the mini site investigation.

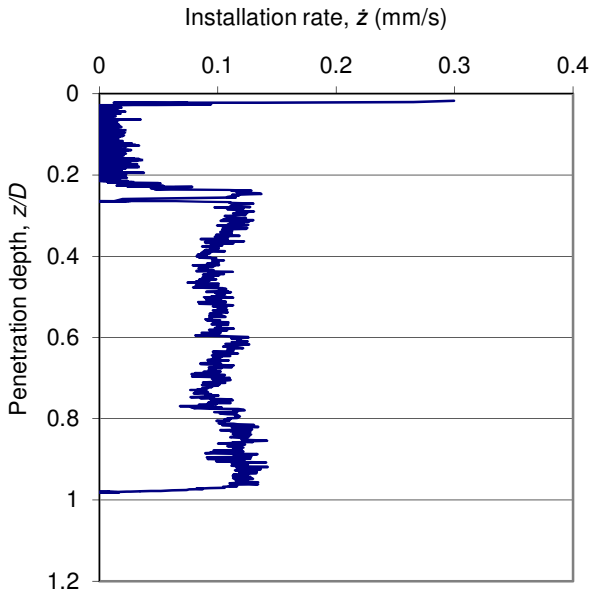

Figure 4.2.3. Installation rate of caisson installed using suction in homogeneous clay (Test C1).

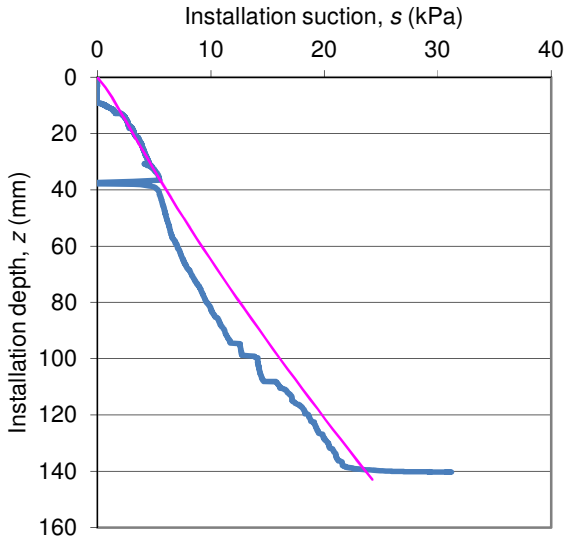

Figure 4.2.4. Figure showing the suction required to install Caisson 2 into homogeneous clay in the laboratory (Test C1). Estimated values are also shown on the plot.

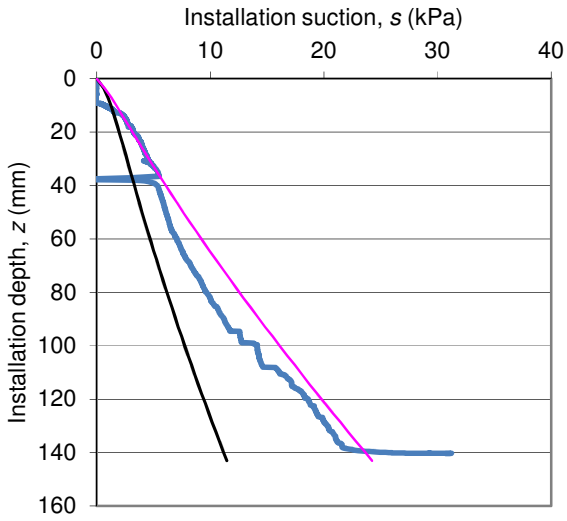

Figure 4.2.5. Plot showing the suction required to install a caisson in homogeneous clay (Test C1) and estimates made using the peak and residual shear strength methods.

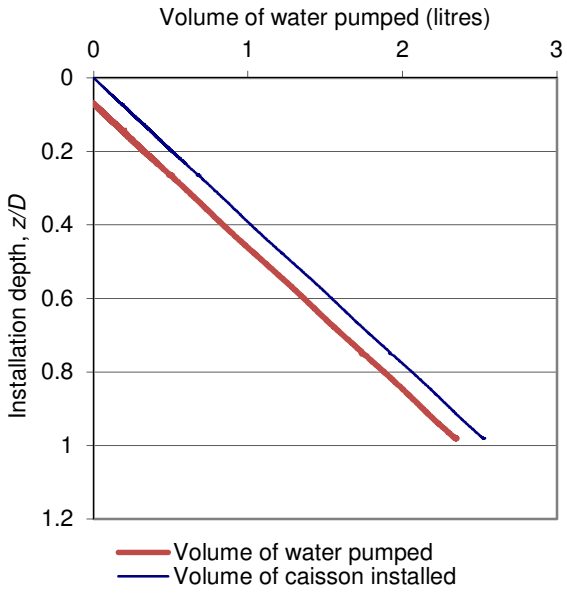

Figure 4.2.6. Plot of the total volume of water pumped during installation shown alongside the volume of caisson installed into the soil (Test C1).

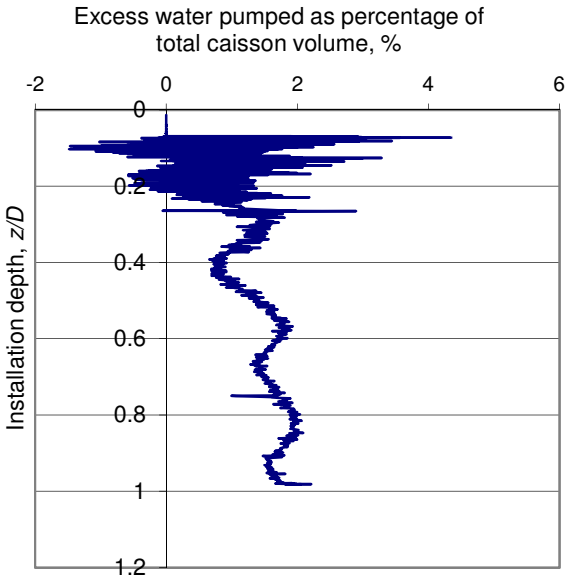

Figure 4.2.7. Plot of the water pumped in excess of that displaced by the caisson for installation (Test C1).

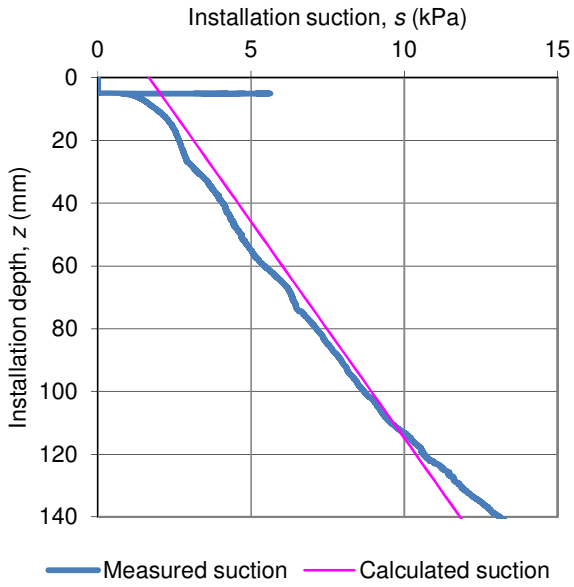

Figure 4.2.8. Figure showing the installation suction necessary to install Caisson 3 plotted against a calculated estimate (Test: CS_5.4).

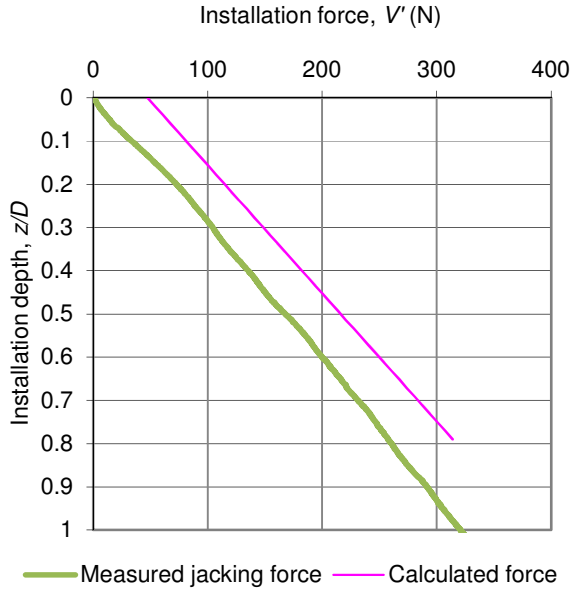

Figure 4.2.9. The force required to jack Caisson 3 into clay (Test C2).

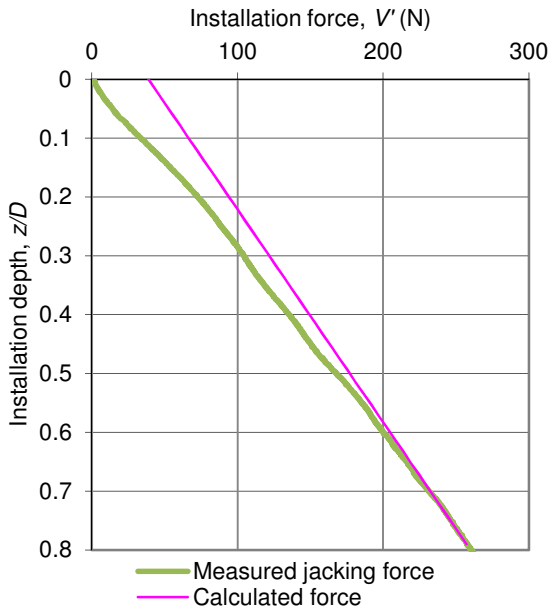

Figure 4.2.10. The force required to jack Caisson 3 into clay with revised soil strength assumptions (Test C2).

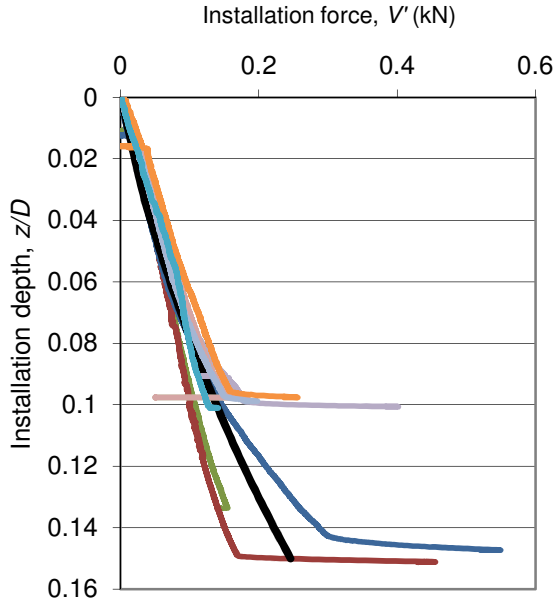

Figure 4.3.1. Plot of the load required to install Caissons 6 and 7 by jacking. The black line is the result of an installation calculation.

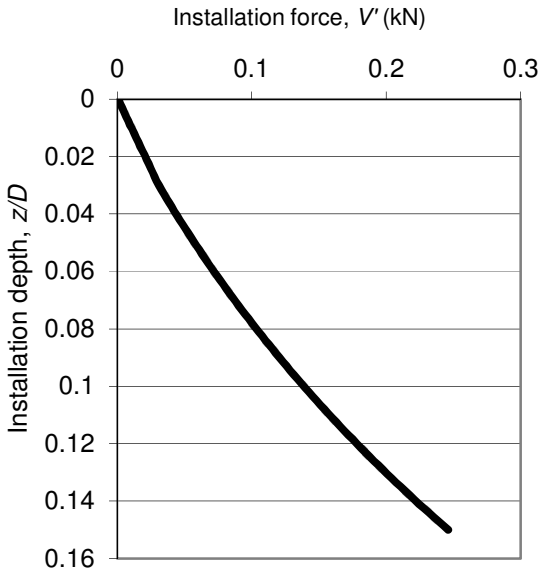

Figure 4.3.2. Plot of estimated load required to jack Caisson 6 into sand (The same estimate as presented in Figure 4.3.1 with experimental data removed for clarity.)

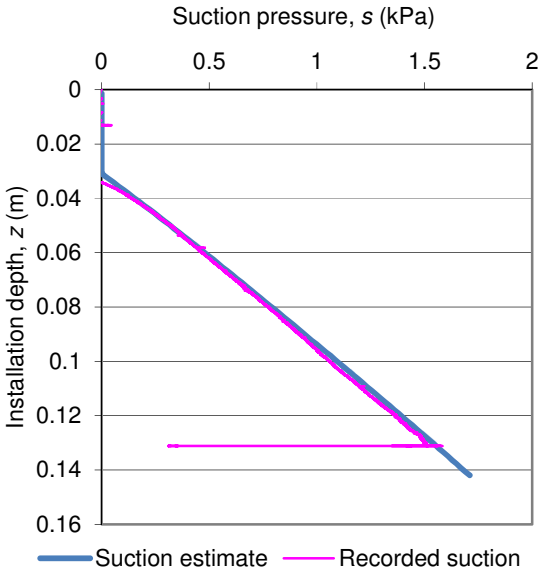

Figure 4.3.3. Plot of suction required for installation of a caisson presented along with the suction estimate produced from installation calculations (16N test 2).

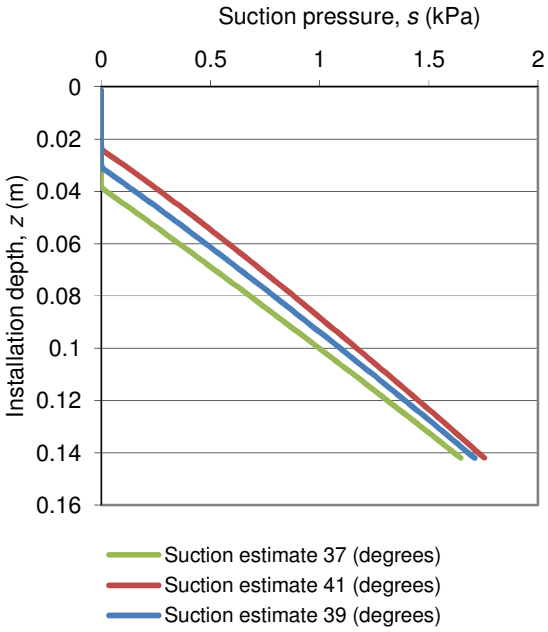

Figure 4.3.4. Plot demonstrating the degree of sensitivity of the suction estimate with variations of sand friction angle of 2 degrees.

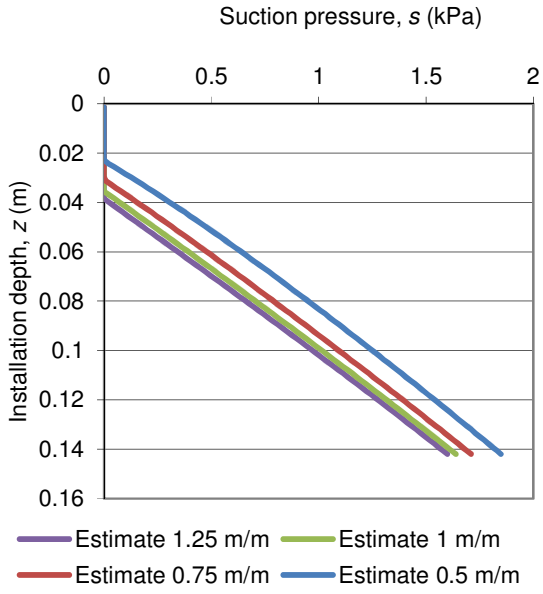

Figure 4.3.5. Demonstration of the sensitivity of suction estimate to variation of the rate of stress enhancement.

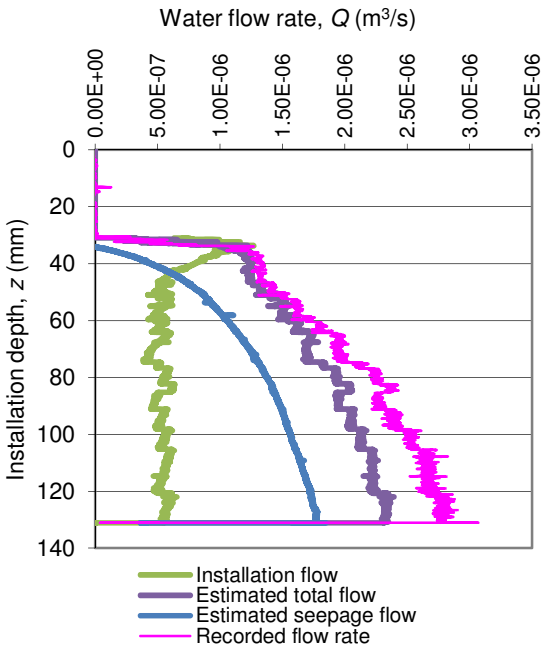

Figure 4.3.6. Plot of pumping flow recorded for installation in sand. The estimated pumping flows can be compared for the installation (16N test 2).

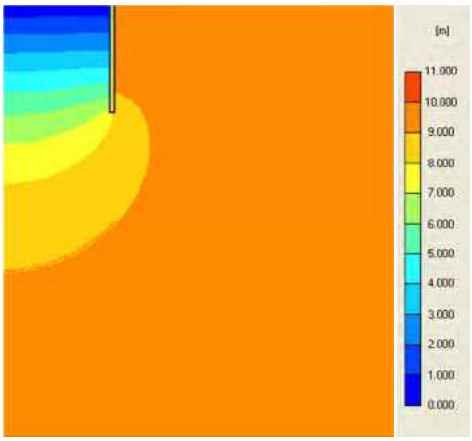

Figure 4.3.7. Diagram of the pressure gradients present during caisson installation in sand. The diagram illustrates that the pressure over a plane of sand at the bottom of the caisson is not uniform.

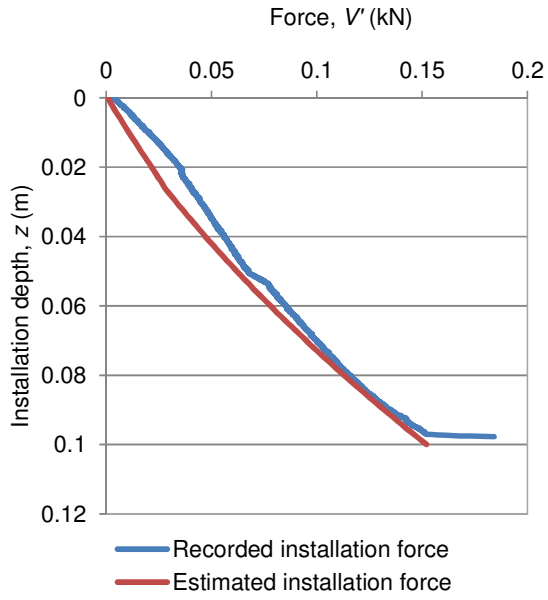

Figure 4.3.8. Force for jacking installation with estimate (Test: GC7.1).

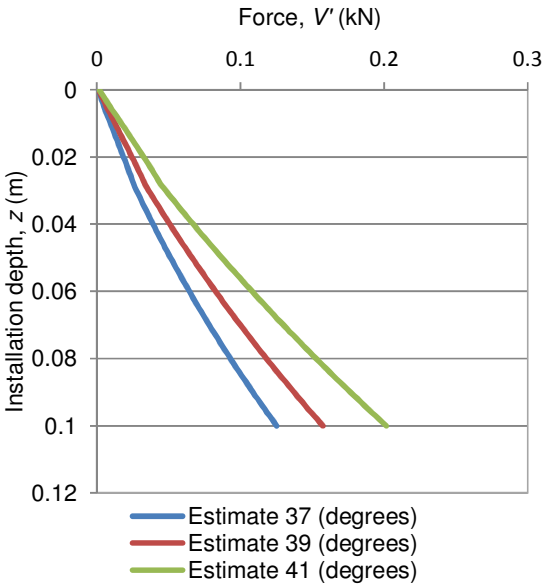

Figure 4.3.9. Sensitivity of jacking force estimate to variations of sand friction angle.

Figure 4.3.10. Photograph of Caisson 4 with the injection apparatus attached. The system could be configured to allow alternate injection and pressure measurement.

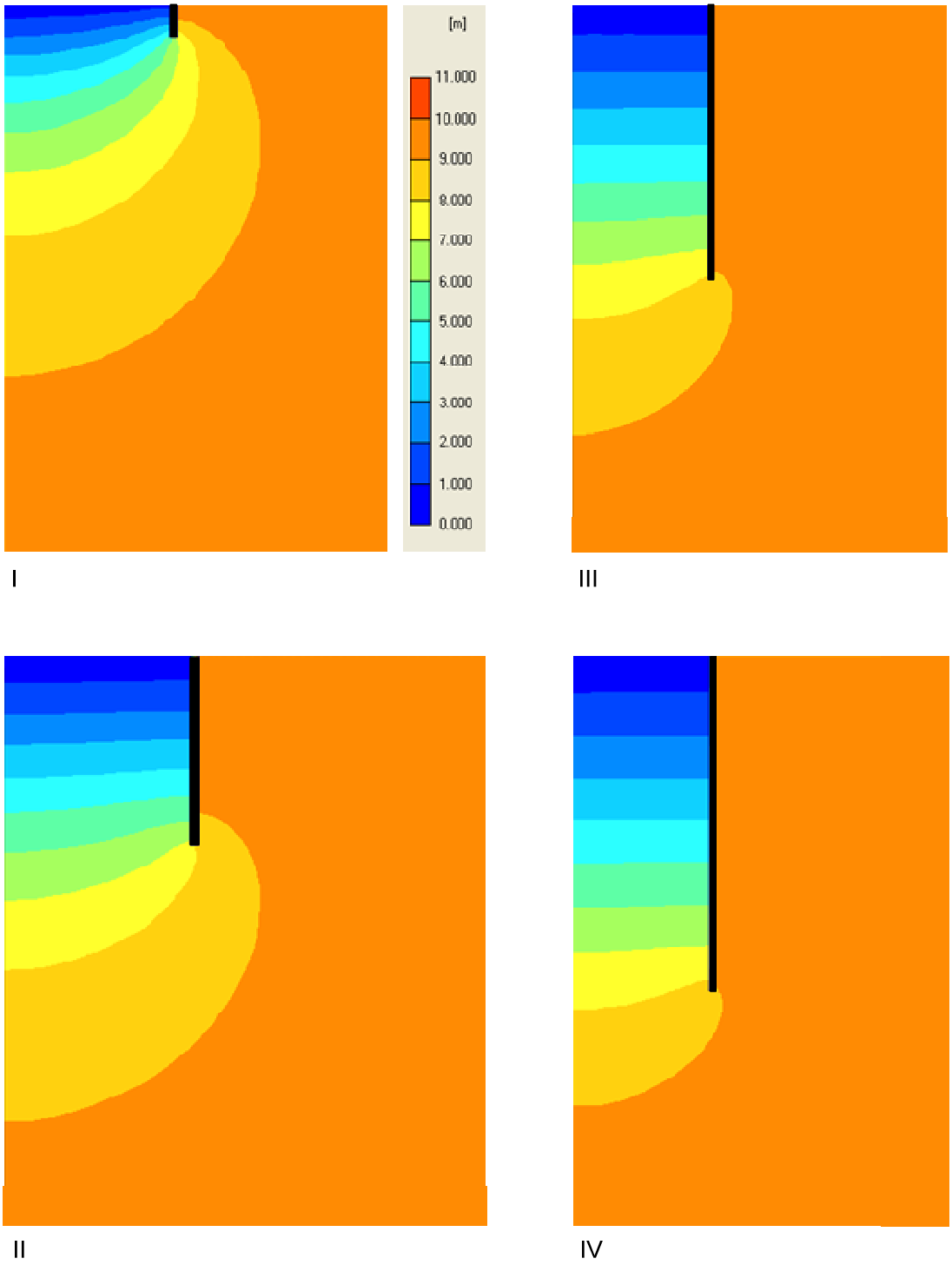

Sequence of diagrams schematically illustrating the hydraulic gradient changes during caisson installation in homogenous sand.

Figure 4.3.11.

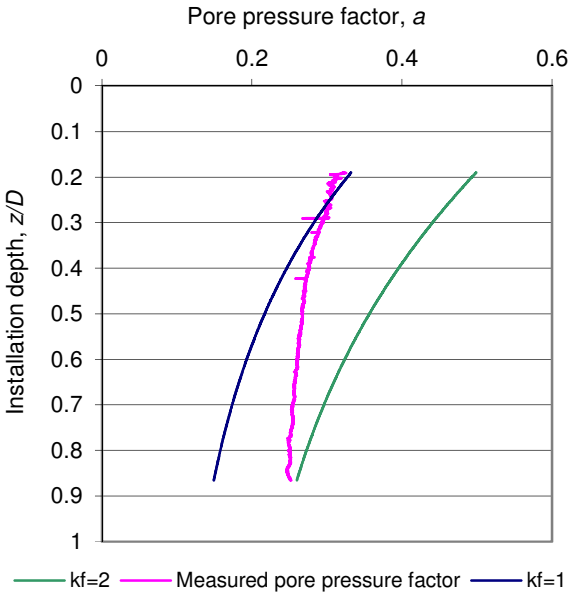

Figure 4.3.12. The variation of pore pressure parameter (*a*) with depth (8N test 2).

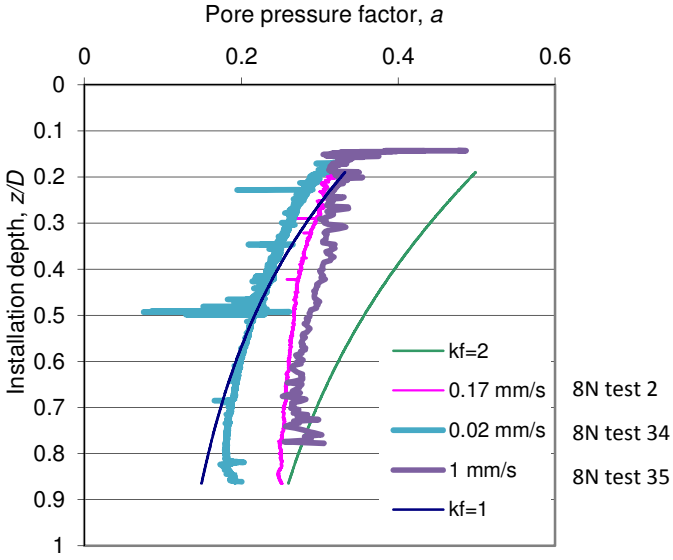

Figure 4.3.13. The variation of pore pressure parameter (*a*) with depth for experiments undertaken at different rates of installation.

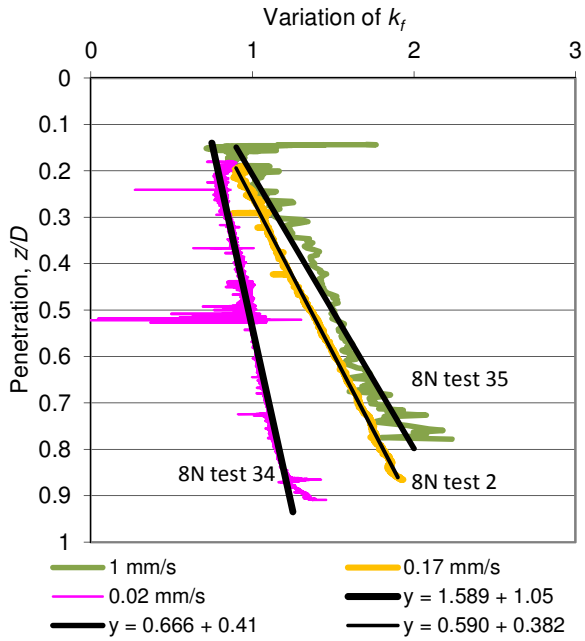

Figure 4.3.14. The interpolated permeability ratio (k_f) as a function with depth measured for different rates of skirt penetration.

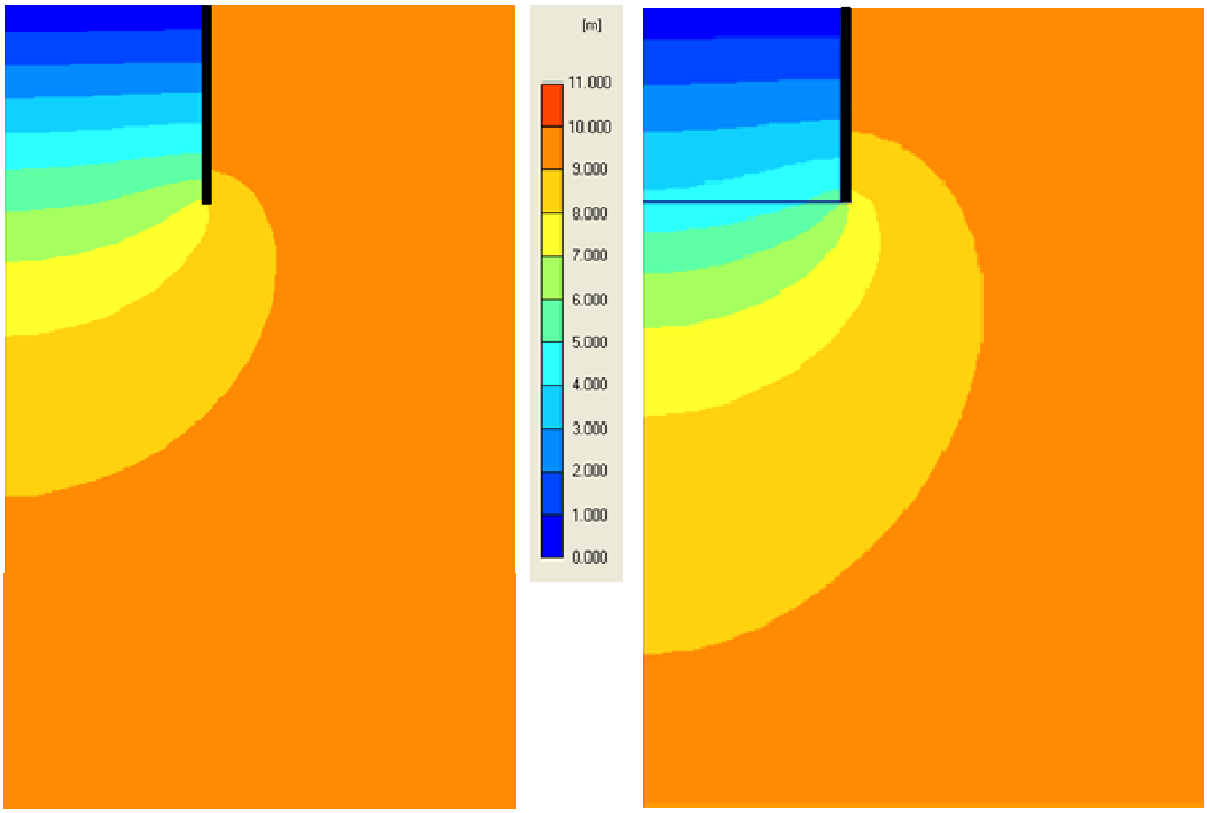

a b

Diagrams illustrating schematically the effect of soil permeability variation on the hydraulic gradient present during caisson installation in sand. In the first Figure, the sand has uniform permeability. In the second Figure, the soil inside the caisson has an assumed permeability which is three times larger than the surrounding material. The hydraulic gradient within the caisson for the second case is lower.

Figure 4.3.15

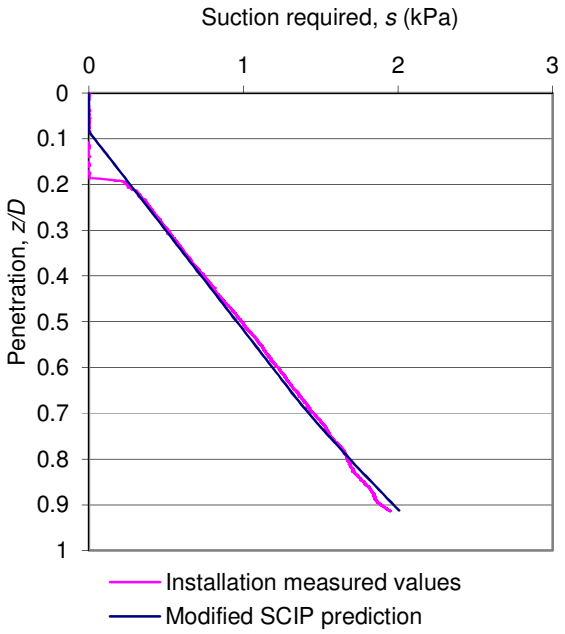

Figure 4.3.16. Suction required for installation in sand as a function of depth (8N test 2).

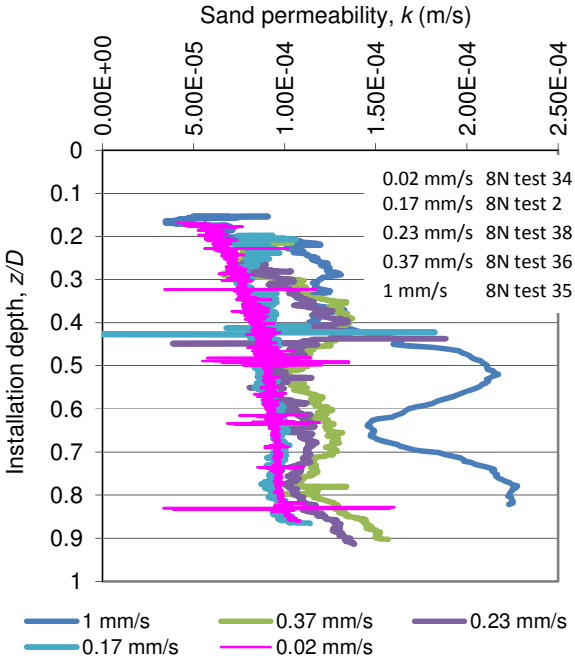

Figure 4.3.17. Plot of overall soil plug permeability measured during installation.

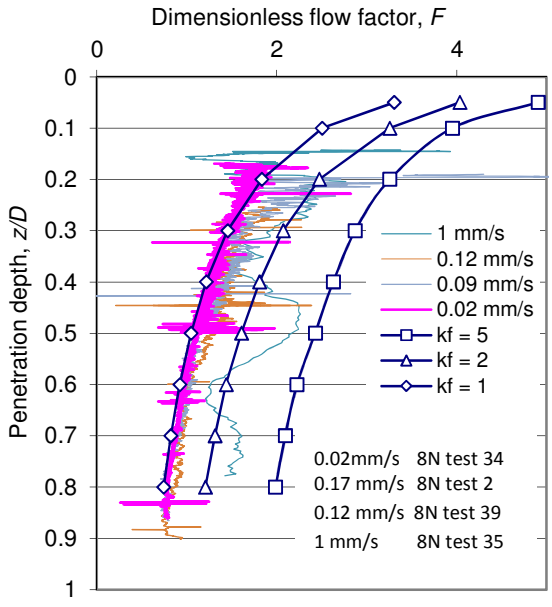

Figure 4.3.18. Chart of calculated *F* with respect to depth for different skirt tip penetration rates.

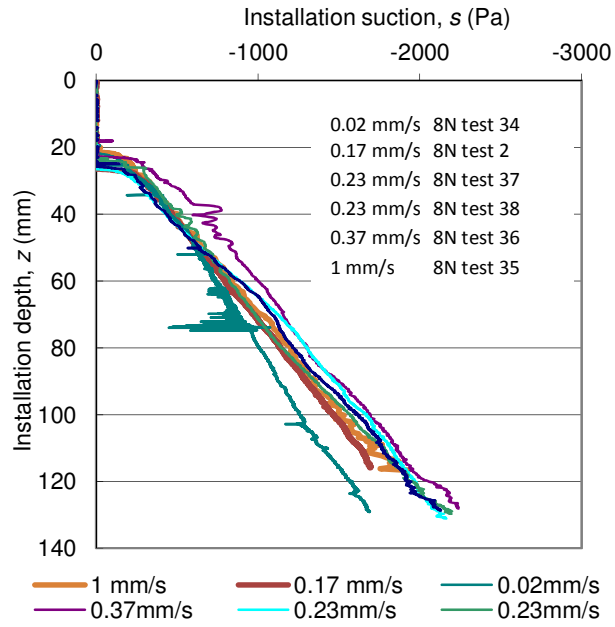

Figure 4.3.19. The influence of the rate of installation on the suction required for penetration.

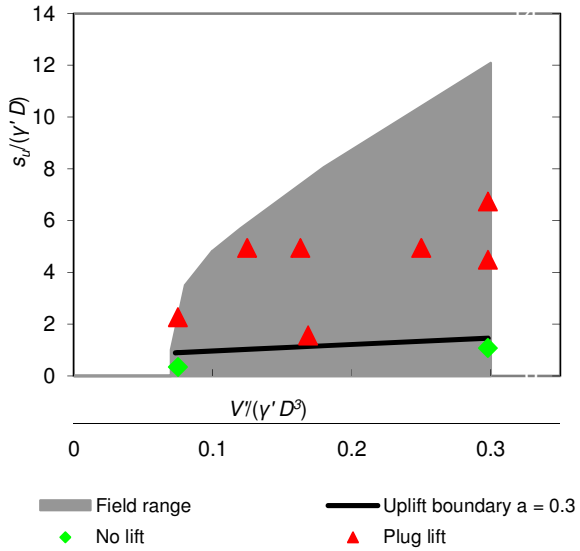

Figure 4.4.1. Plot of the uplift test results. Green diamonds show the results of tests which ended with installation. Red triangles show the tests which ended with plug lift being observed.

Figure 4.4.2. Photograph of Caisson 3 with lifted plug visible through the top of the lid.

Figure 4.4.3. Photograph of Caisson 5 with lifted plug visible through aperture created by bung removal.

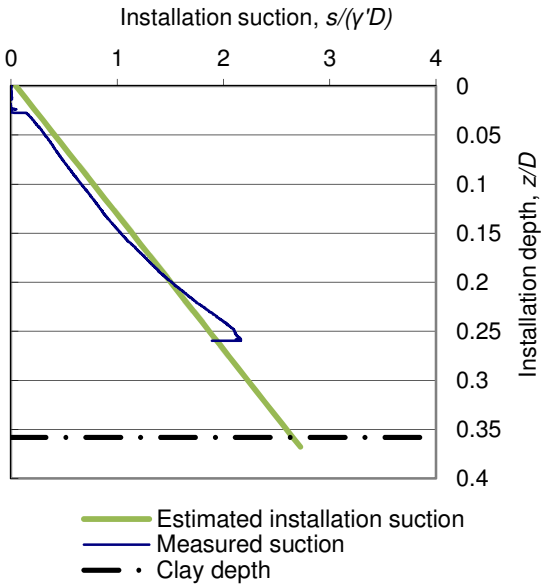

Figure 4.4.4. Installation suction plotted against displacement for Caisson 5 (Test: CS_5.1).

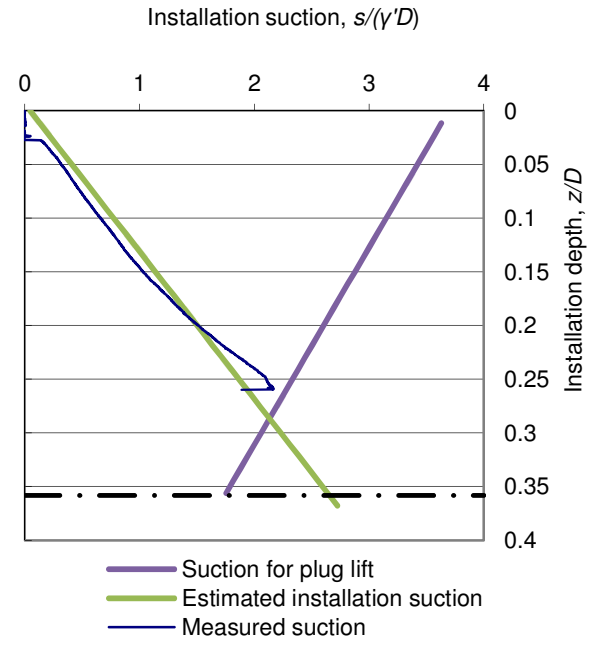

Figure 4.4.5. Plot of installation suction for Caisson 5 with an estimate of the suction required for plug lift included (Test: CS_5.1).

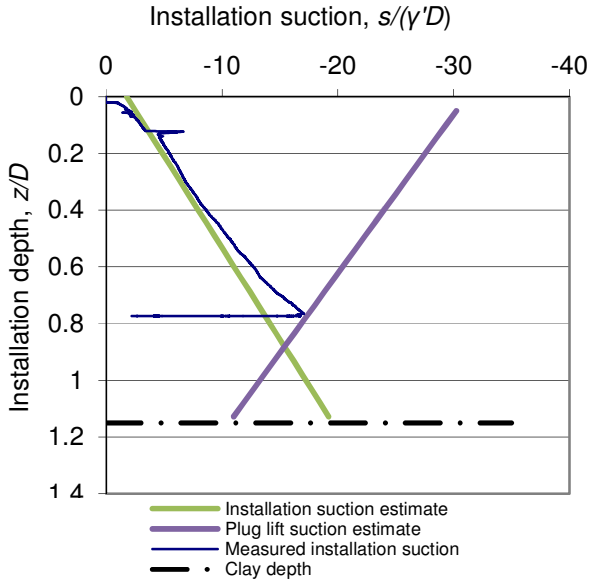

Figure 4.4.6. Installation suction plotted against displacement for Caisson 3 (Test: CS_3.3).

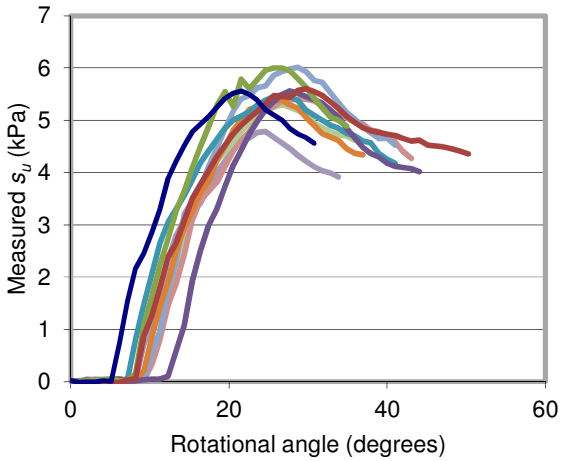

Figure 4.4.7. Plot of shear force measured using stepper motor controlled shear apparatus. The average peak shear force measured with a hand shear vane was 4.8 kPa which agrees well with the data recorded for the stepper motor controlled apparatus for which the average recorded strength was 5.5 kPa. The hand shear vane test could be undertaken more quickly than the motorized apparatus which enables more samples to be tested per unit time.

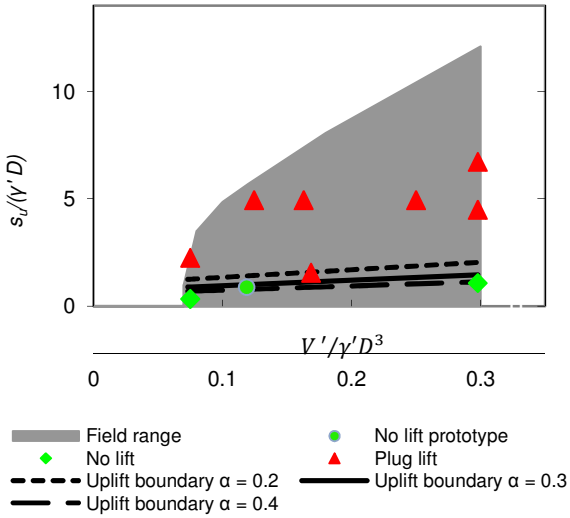

Figure 4.4.8. Plot of results for the uplift installations. The variation of the uplift boundary to changes in adhesion factor has been included.

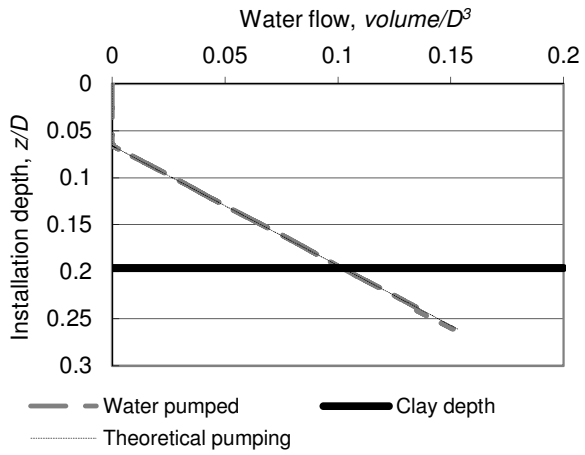

Figure 4.4.9. Pumped water volume plotted against installation depth (Test: CS_1.1). Also shown on the chart is the variation of water volume inside the caisson as the caisson is installed. It can be observed that the pumped water volume closely matches that necessary to be removed for caisson installation indicating that seepage volumes were low.

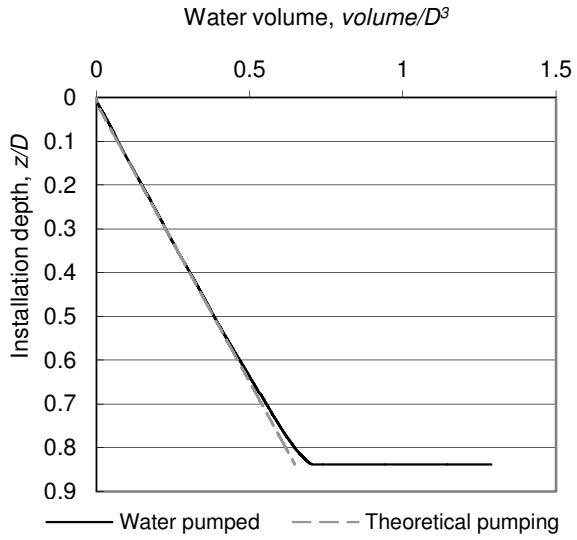

Figure 4.4.10. Plot of total pumped water volume. It can be observed that the pumped water volume closely matches that necessary to be removed due to the caisson volume up to the point where plug lift occurs. Where plug lift occurs, installation stops while water continues to be pumped from the interior (Test: CS_3.2).

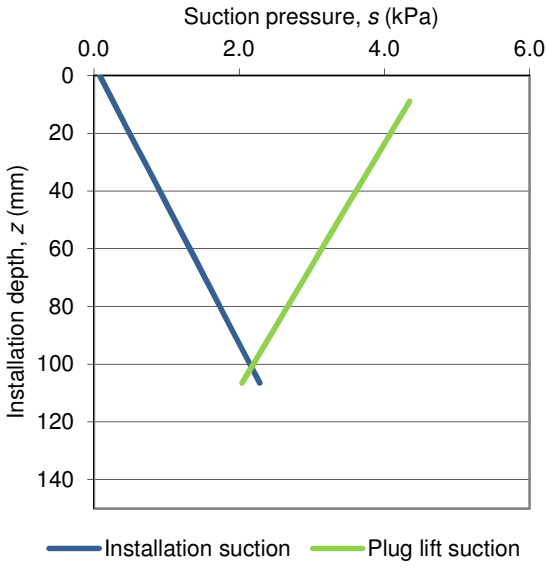

Figure 4.4.11. Estimates of suction required for plug lift and installation for Caisson 3.

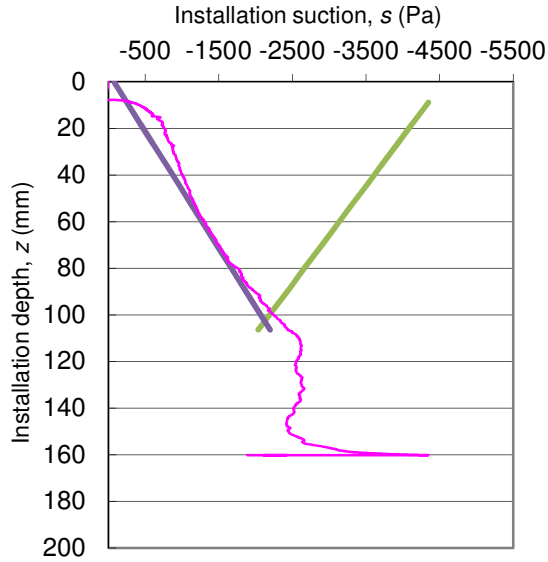

Figure 4.4.12. Comparison of recorded installation suction and the estimated suction required for caisson installation and plug lift (Test: CS_1.3).

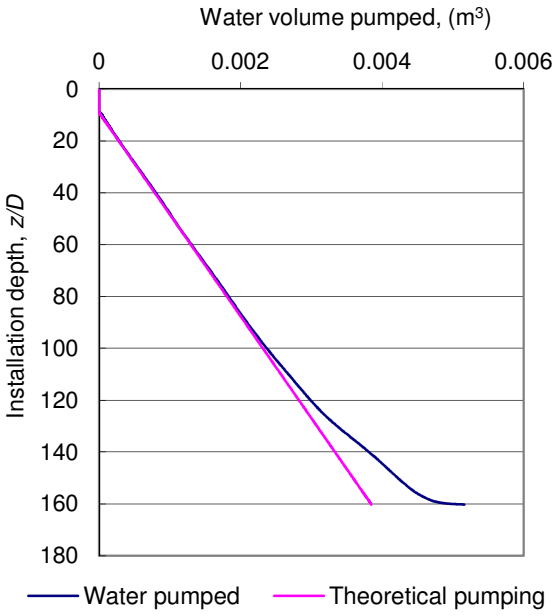

Figure 4.4.13. Plot of water pumped during installation experiment undertaken in clay over sand (Test: CS_1.3). The pumped water volume exceeds the installed caisson volume when the skirt tip approaches the clay/sand interface.

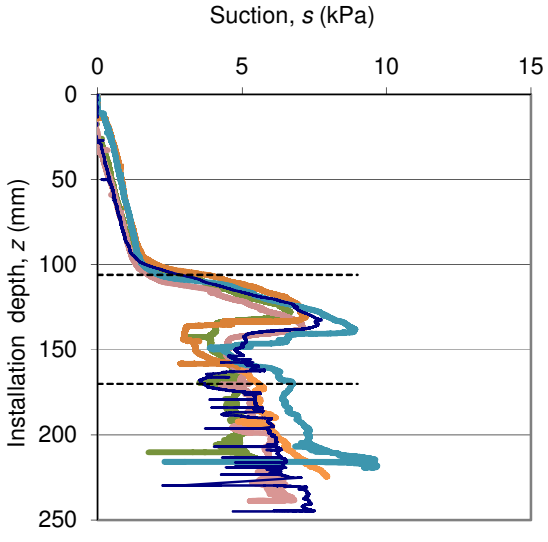

Figure 4.5.1. Plot of installation suction required to install the caisson into a soil sample consisting of homogeneous sand with a clay layer.

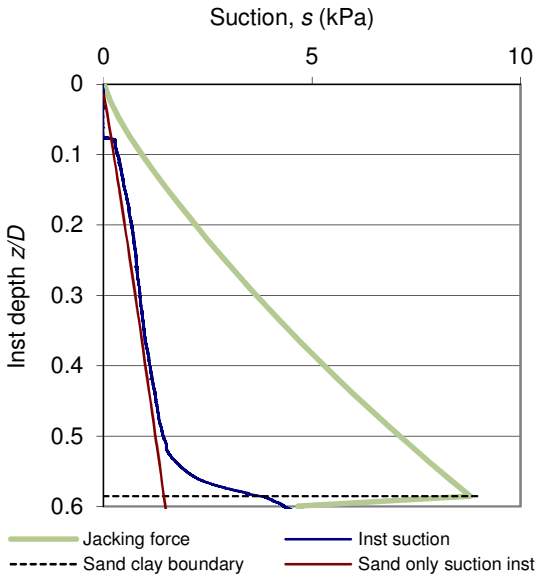

Figure 4.5.2. The suction measured during the installation of test SCS_3 compared with the suction estimated to be necessary for installation in homogeneous sand and the equivalent suction required to install the caisson by jacking.

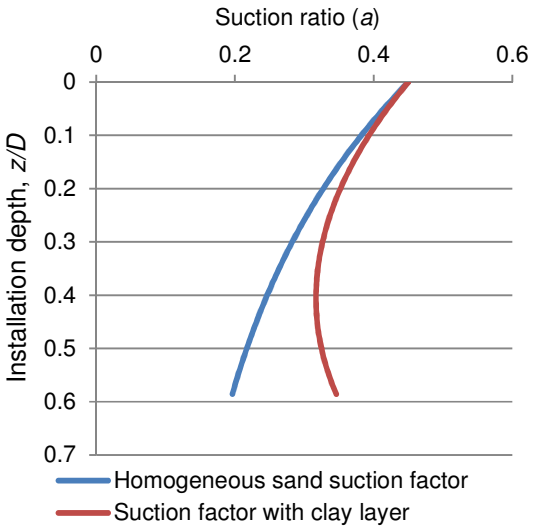

Figure 4.5.3. The proposed variation of suction factor (*a*) with non-dimensional depth for homogeneous sand and sand with a clay layer below.

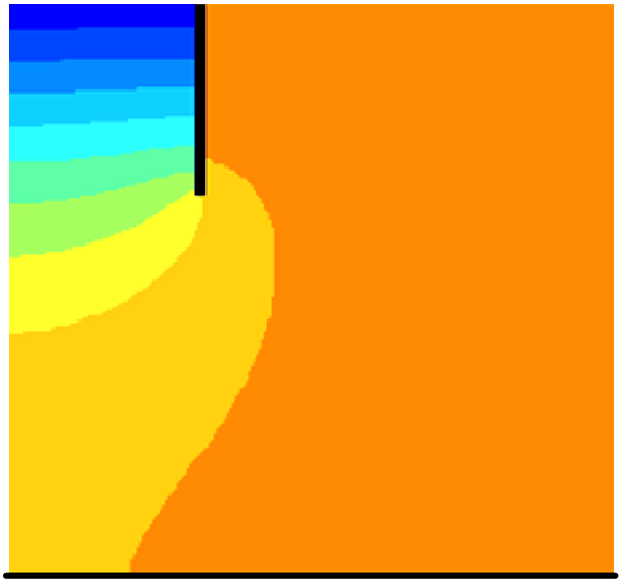

A

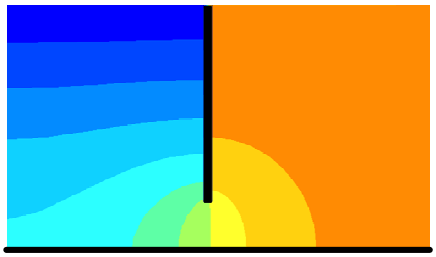

D

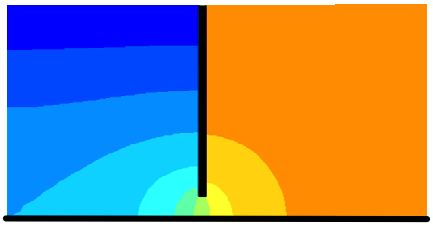

E

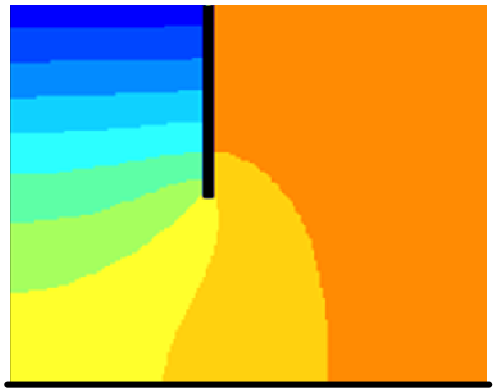

B

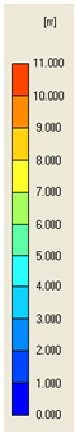

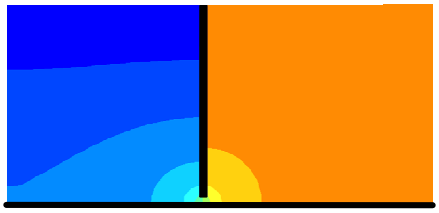

F

G

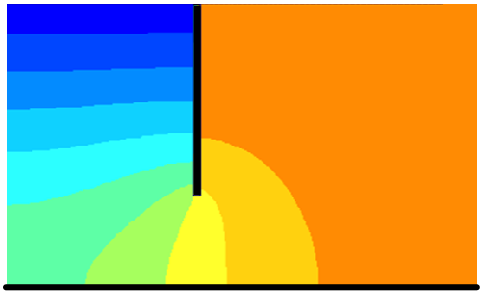

C

Installation of caisson into sand overlying impermeable clay. The skirt embedment depth is kept constant while the impermeable boundary is moved towards the skirt tip. This illustrates schematically the effect of the impermeable layer on caisson installation. The hydraulic gradient changes due to skirt penetration are not included in this sequence. As the skirt approaches the clay, the hydraulic gradient at the skirt tip becomes greater.

Figure 4.5.4.

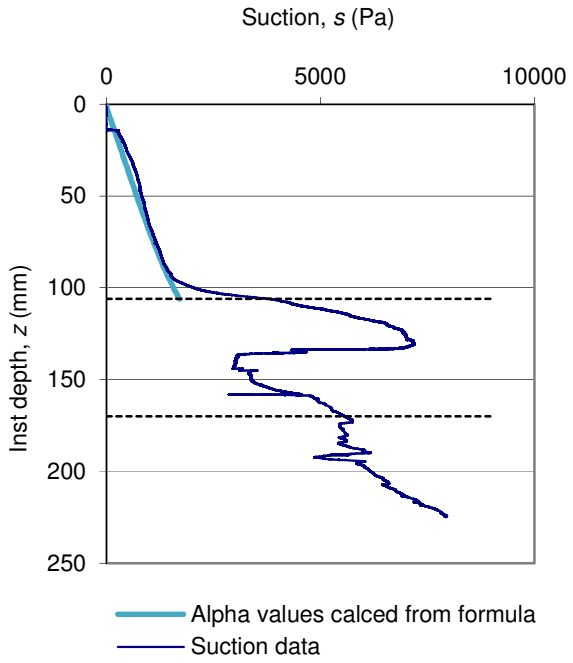

Figure 4.5.5. Suction estimate calculated for installation compared with the measured data recorded for test SCS_3.

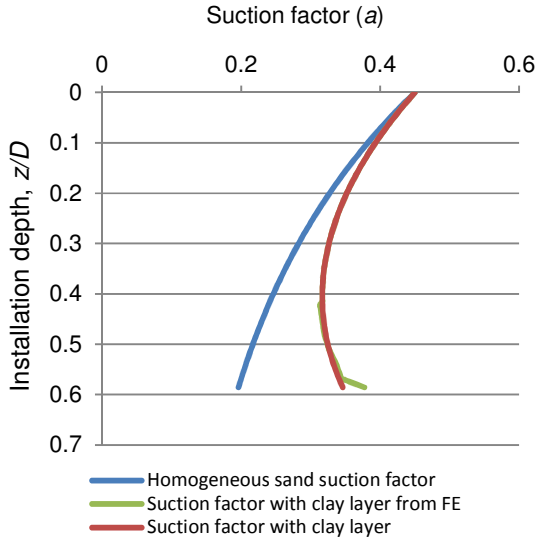

Figure 4.5.6. Values of alpha interpolated from FE results compared with the values proposed for a homogeneous sand installation.

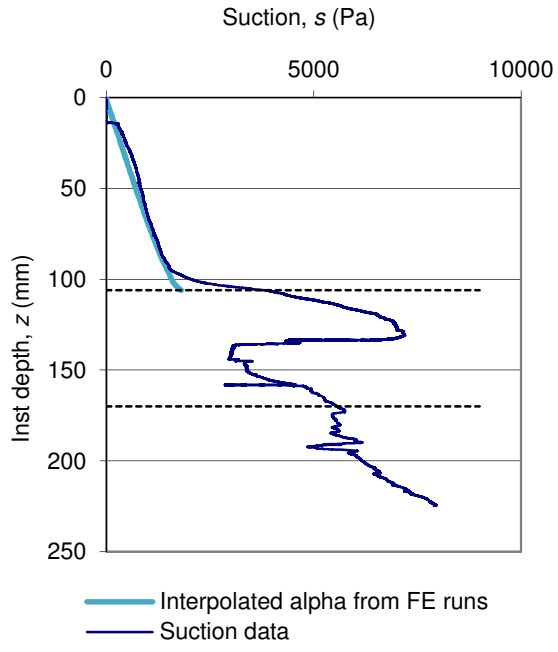

Figure 4.5.7. Suction recorded for test SCS_ 3 with the suction estimated to be necessary for installation using the interpolated values from FE analysis.

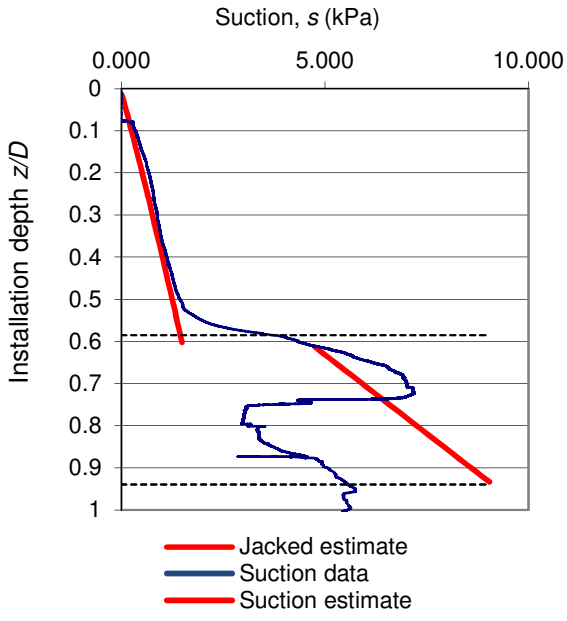

Figure 4.5.8. The suction recorded for the installation of test SCS_3 and the expected suction for installation in sand and clay.

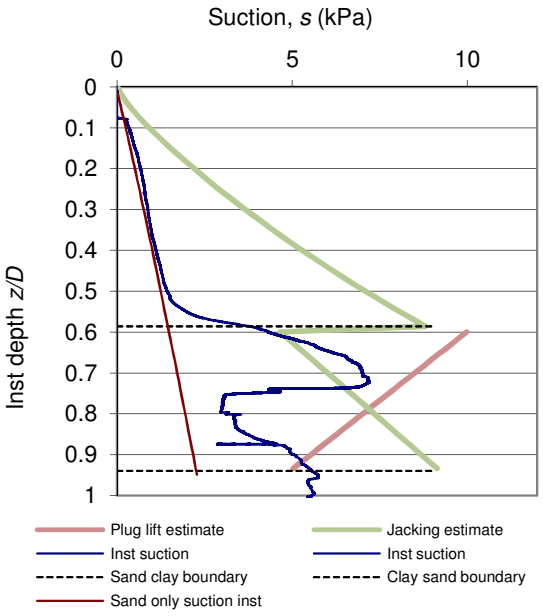

Figure 4.5.9. The suction recorded during installation of test SCS_3 compared with the estimated suction required for plug lift.

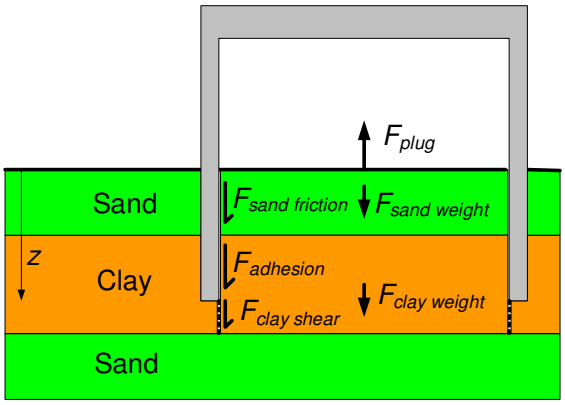

Figure 4.5.10. Diagram of forces assumed to act on plug during uplift in a sample of homogeneous sand with a clay layer.

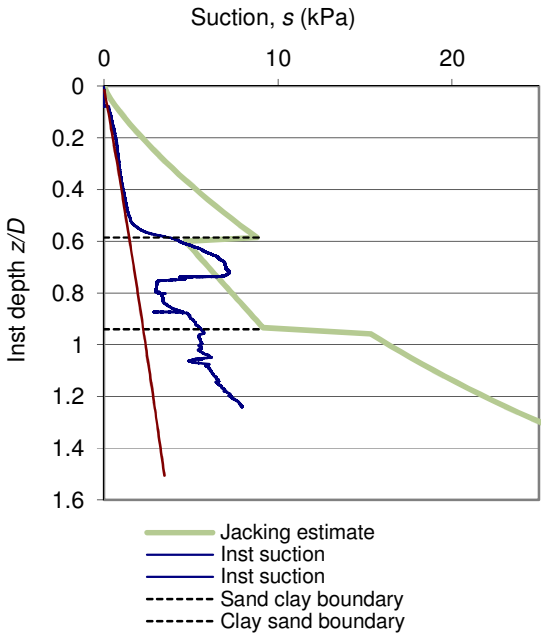

Figure 4.5.11. The suction required for installation in sand below a clay layer compared with the suction estimated to be required for installation in homogeneous sand and the estimated jacking force (SCS_3).

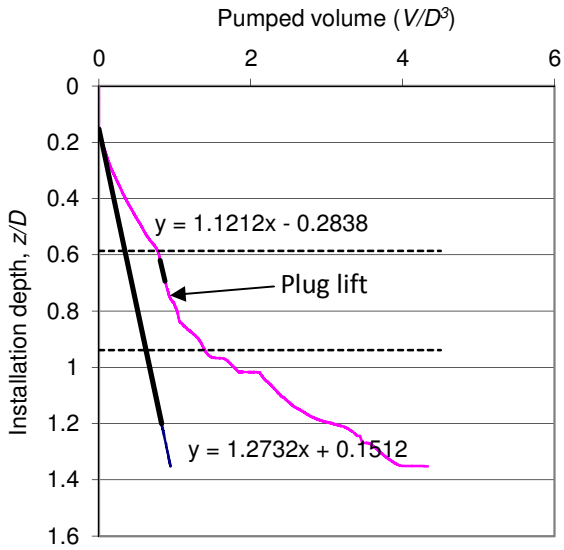

Figure 4.5.12. The pumped water volume for the installation of test SCS_1 and the water volume necessary to be pumped for installation of the caisson without seepage (black line). The gradients of the best fit lines are displayed on the graph adjacent to their respective lines.

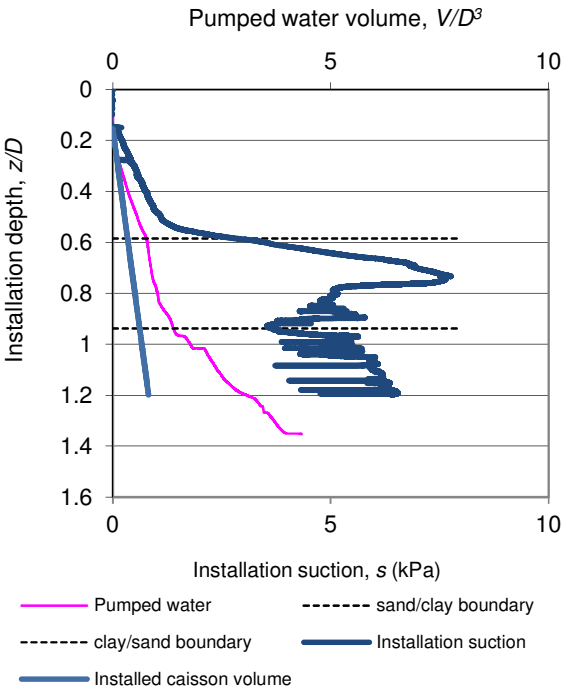

Figure 4.5.13. Plot of pumped water volume and installation suction for test SCS_1

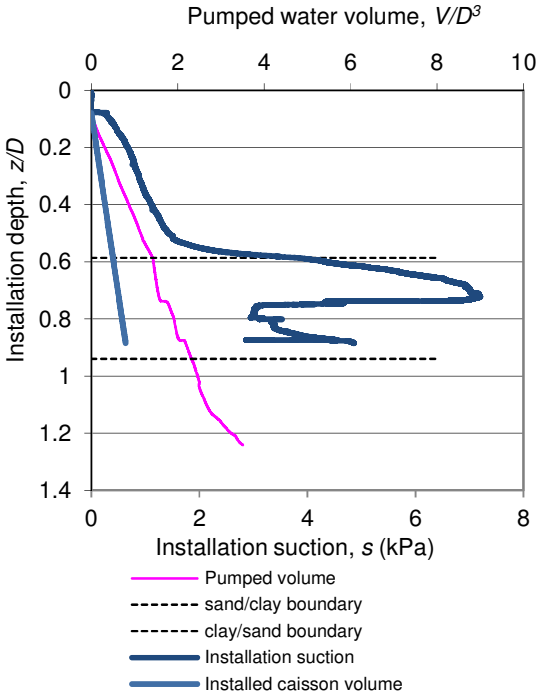

Figure 4.5.15. Plot of pumped water volume and installation suction for test SCS_3

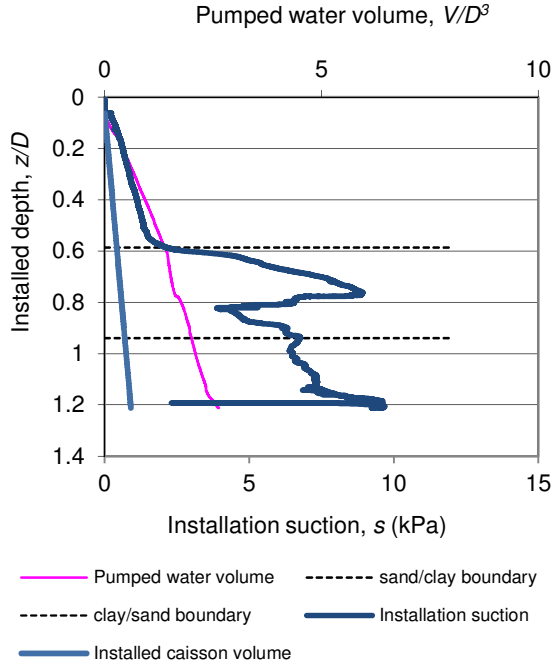

Figure 4.5.14. Plot of pumped water volume and installation suction for test SCS_2.

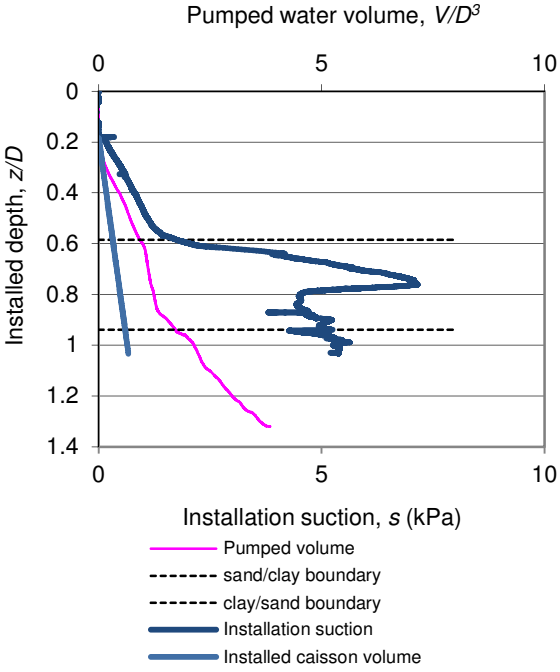

Figure 4.5.16. Plot of pumped water volume and installation suction for test SCS_4

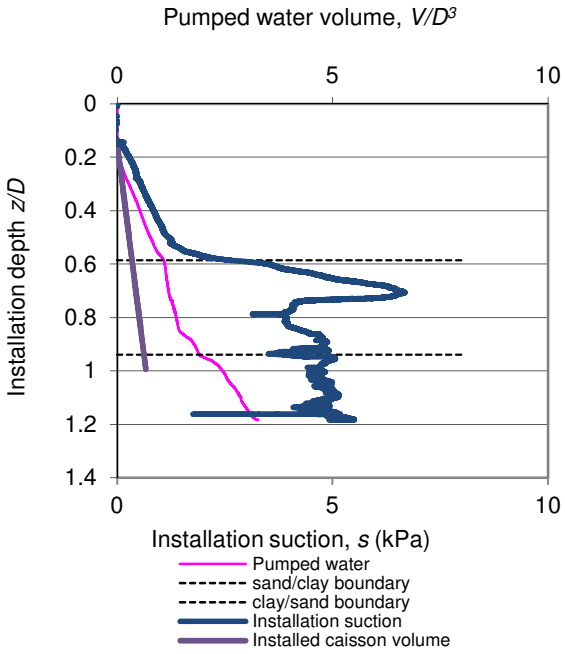

Figure 4.5.17. Plot of pumped water volume and installation suction for test SCS_5

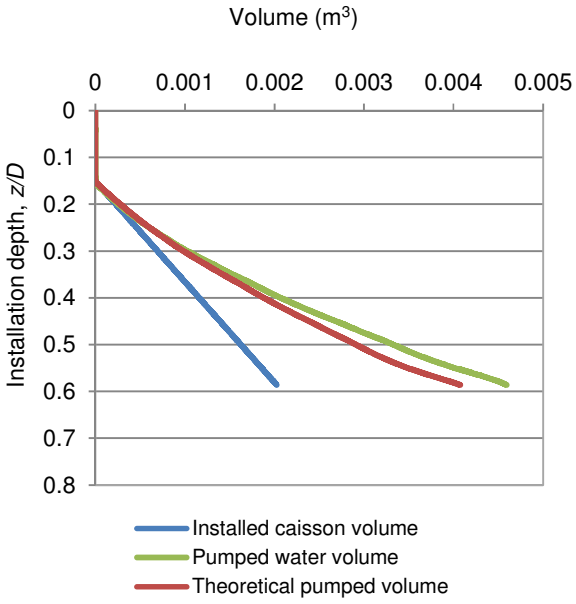

Figure 4.5.19. Pumped water volume plotted against estimated volume required during caisson installation for test SCS_1.

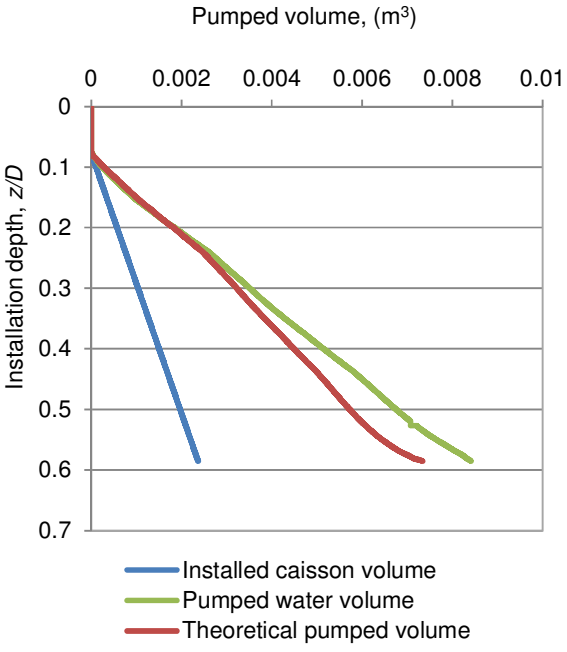

Figure 4.5.18. Pumped water volume plotted against estimated volume required during caisson installation for test SCS_3.

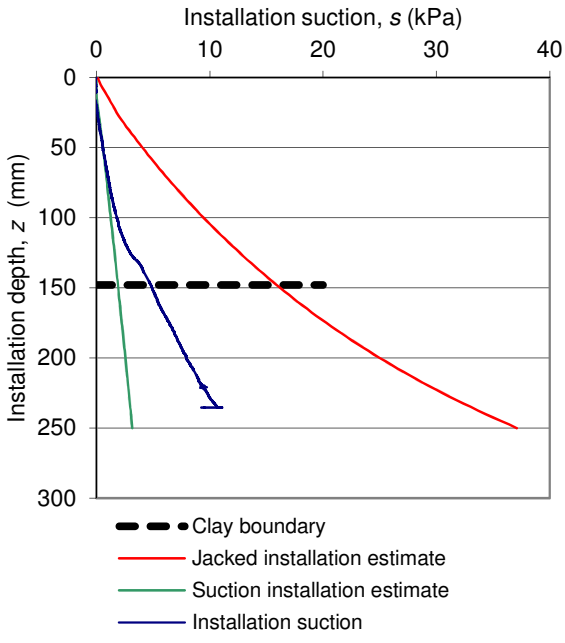

Figure 4.6.1. Test SIC_1. Installation into inclined clay layer at 150mm.

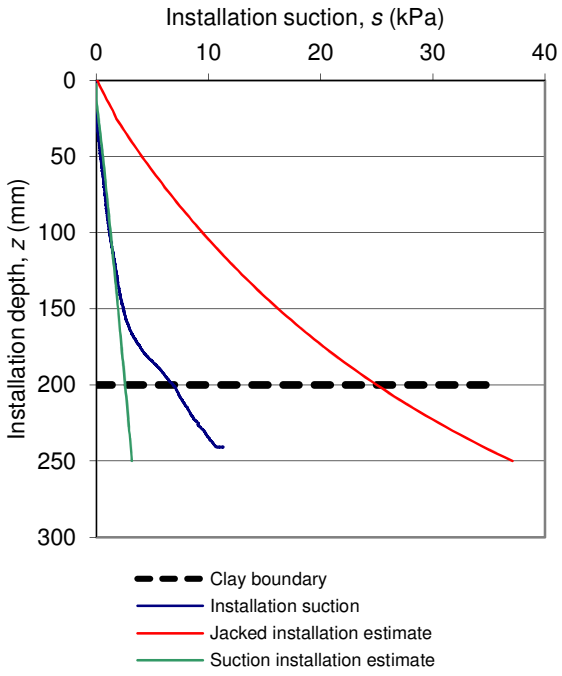

Figure 4.6.2. Test SIC_2. Installation into inclined clay at 200mm depth.

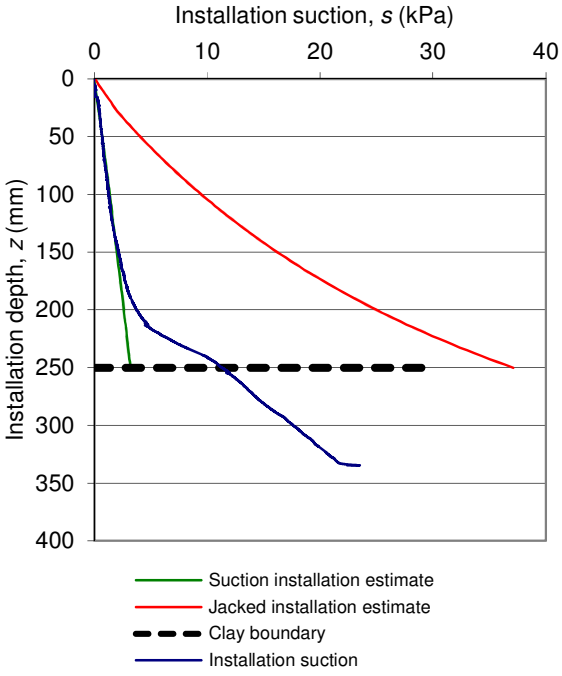

Figure 4.6.4. Test SIC_4. Installation into inclined clay at 250mm depth with low caisson self weight.

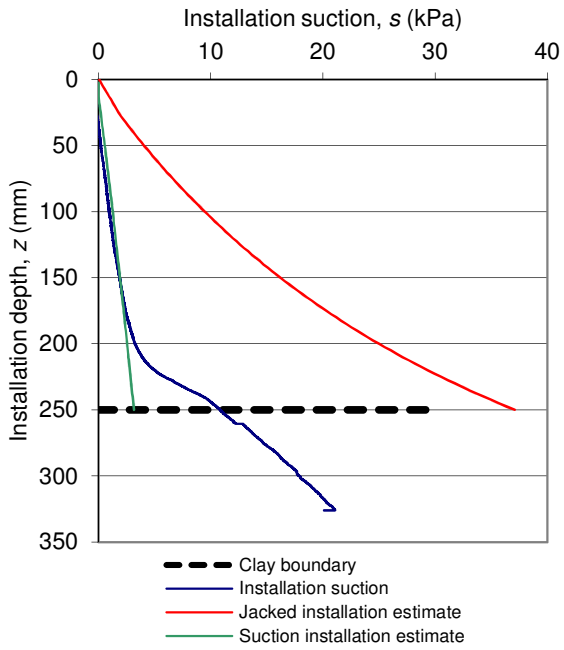

Figure 4.6.3. Test SIC_3. Installation into inclined clay at 250mm depth.

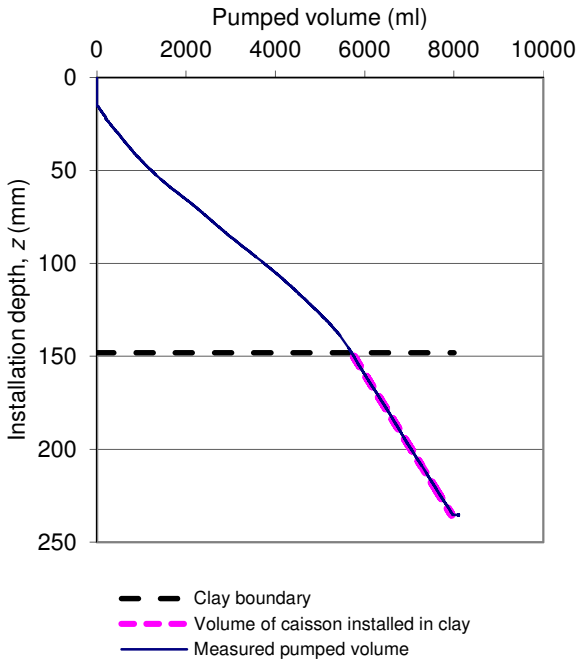

Figure 4.6.5. Pumped volume for test SIC_1.

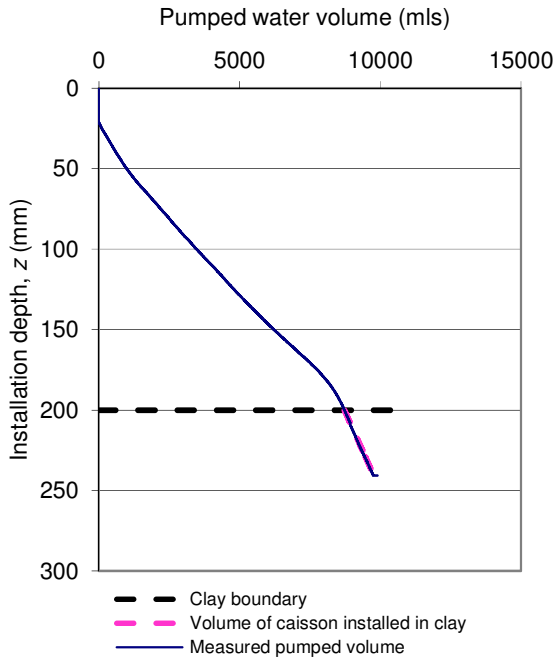

Figure 4.6.6. Pumped volume for test SIC_2.

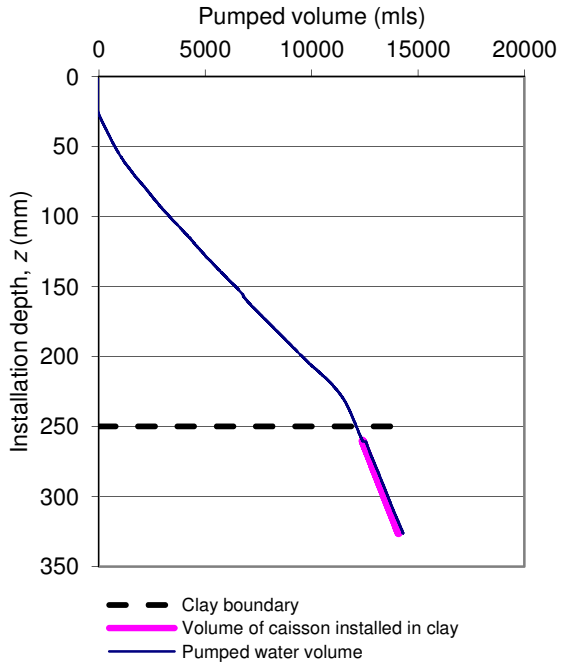

Figure 4.6.7. Pumped volume for test SIC_3.

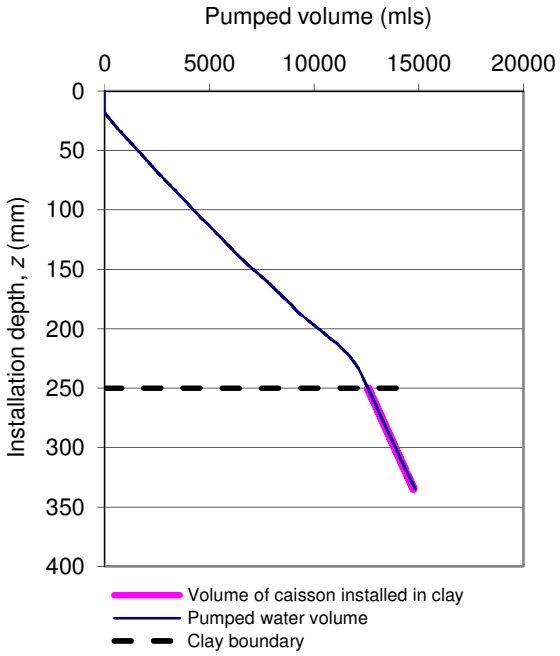

Figure 4.6.8. Pumped volume for test SIC_4.

Figure 4.6.9. Photograph showing sand disturbance caused by failure of the clay layer beneath. The disturbance caused to the sand can be observed at the left of the caisson where the depression extends to the skirt. A small depression can also be observed at the right hand side of the picture.

Chapter 5 Figures

Figure 5.1.1. Photograph of caisson capable of skirt tip injection. The tubes running down the side of the skirt supply high pressure water to the nozzles at the ends.

Figure 5.1.2. Photograph of inclinometer illustrating the small size packaging of the instrument.

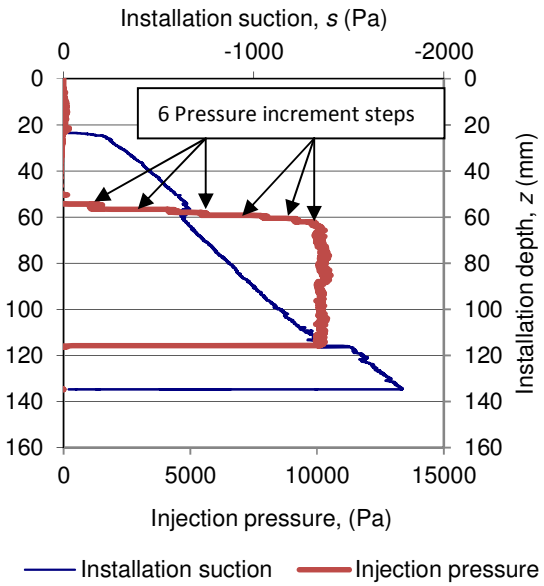

Figure 5.3.1. Plot of installation suction and injection pressure (8N test 23). The installation suction decreased when the injection pressure was applied and then increased immediately after injection was stopped.

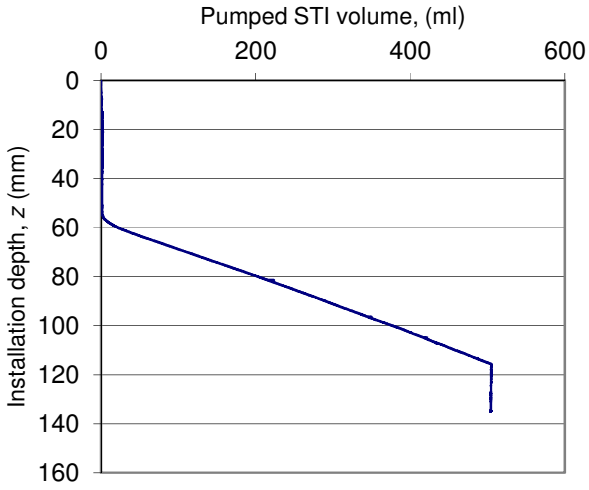

Figure 5.3.2. Plot of water pumped during the process of water injection at the skirt tip (8N test 23).

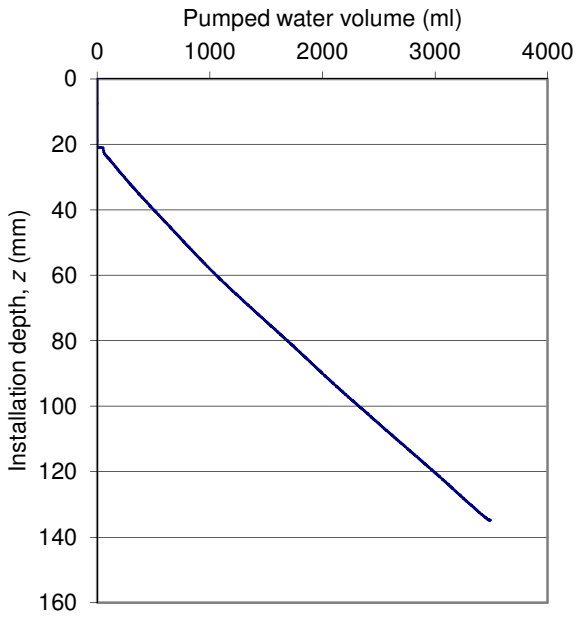

Figure 5.3.3. Plot of the water pumped out of the interior of the caisson during installation with STI (8N test 23).

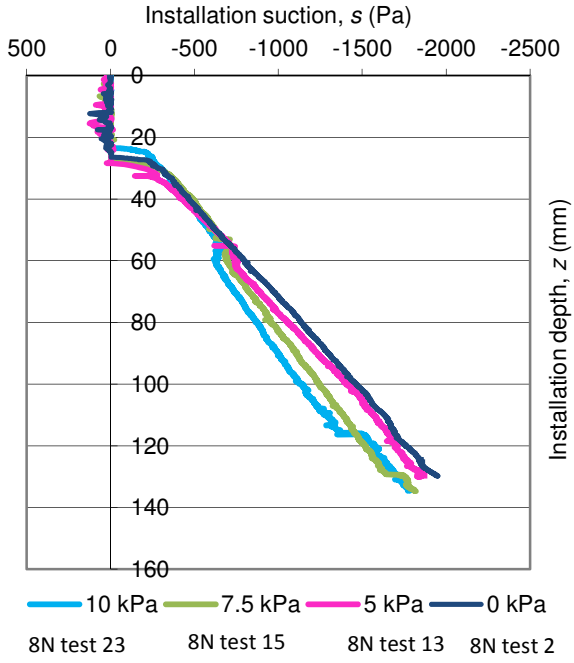

Figure 5.3.5. Plot of suction required to install Caisson 4 at a series of injection pressures.

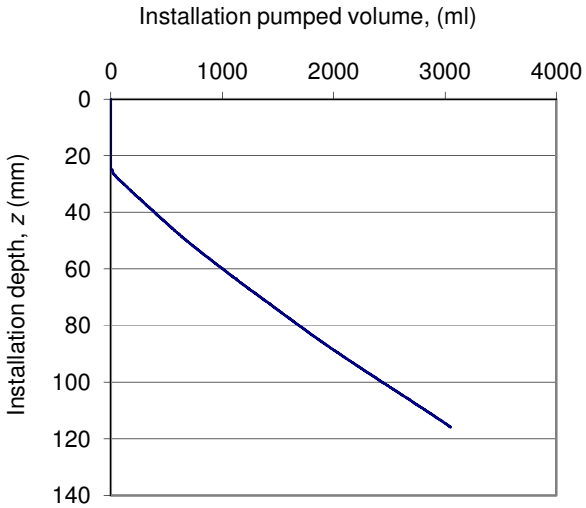

Figure 5.3.4. Plot of the water pumped out of the caisson during suction installation without STI (8N test 2).

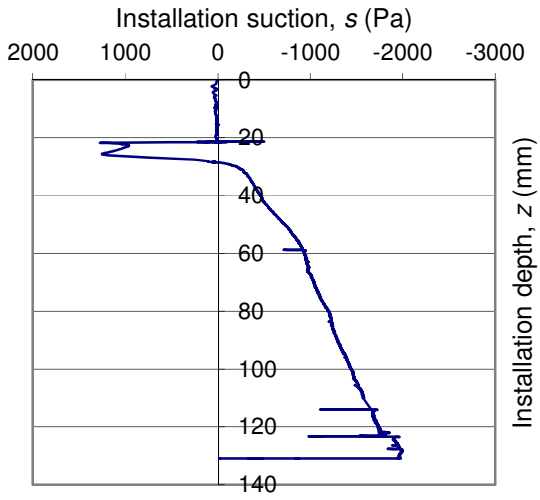

Figure 5.3.6. Suction required for installation of Caisson 4 with 5 kPa installation pressure (8N test 12).

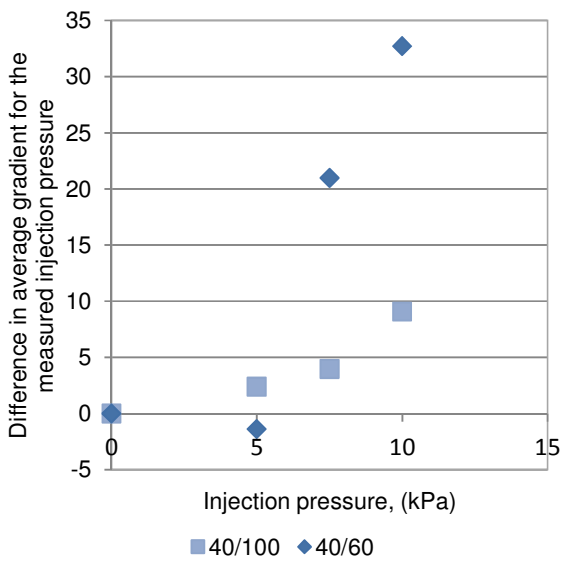

Figure 5.3.7. Change of average gradient as a function of injection pressure.

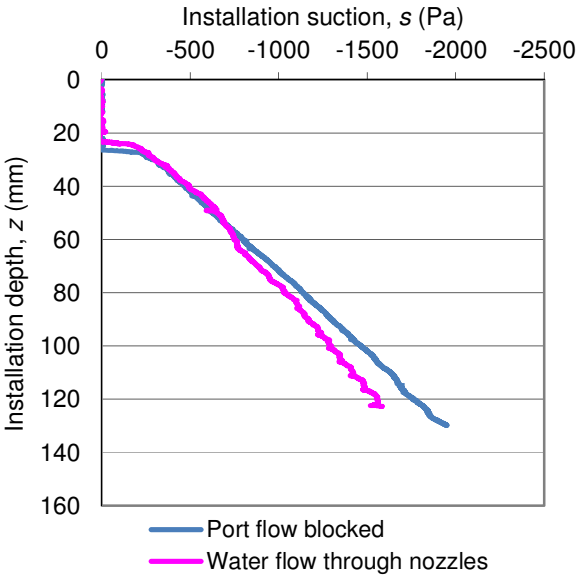

Figure 5.3.8. Plot of suction required for installation of a caisson with injection nozzles supplied by ambient water pressure. Suction for installation of a caisson with injection nozzle flow blocked (8N test 2) is shown for comparison.

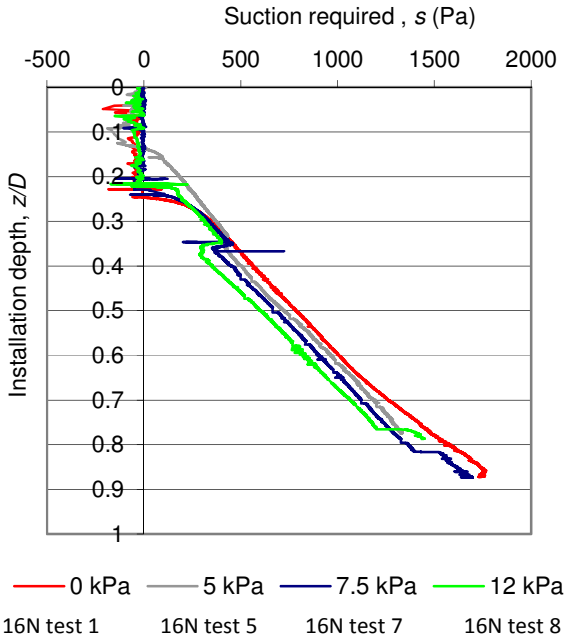

Figure 5.3.9. Suction required for caisson installation with 16 injection nozzles.

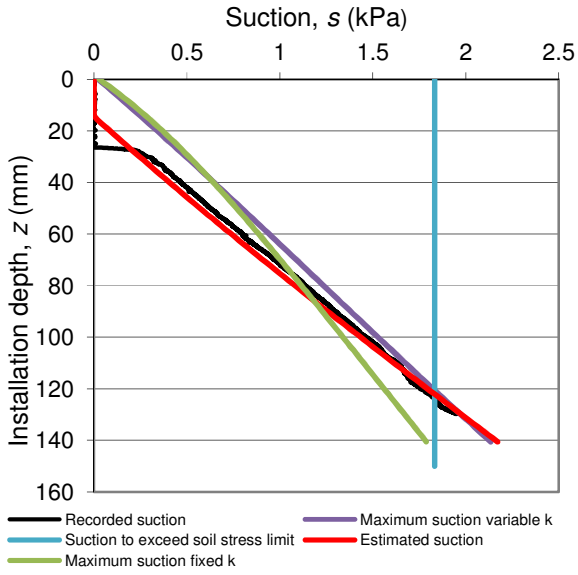

Figure 5.3.10. Plot of the measured suction pressure for installation of a caisson without STI and an estimate of the pressure required. Also shown are three estimates of the maximum penetration depth for these installation conditions.

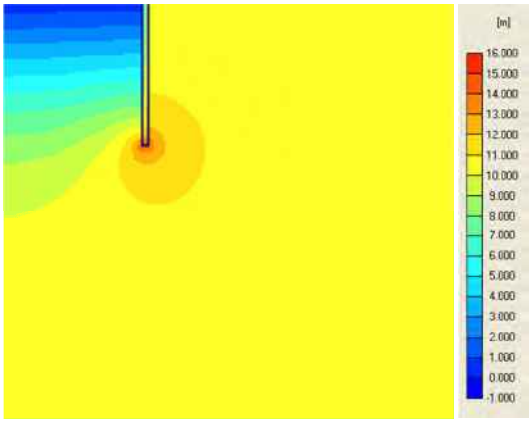

Figure 5.3.11. Diagram of the effect of STI. The hydraulic gradient inside the caisson is higher than that which would be present when suction installation is undertaken. This leads to piping failure at lower penetration depths.

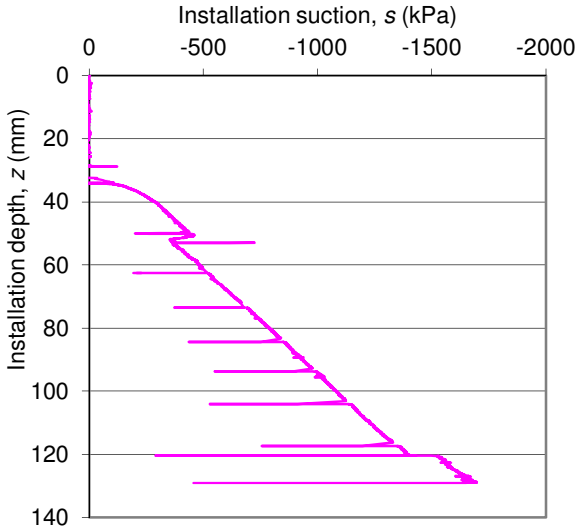

Figure 5.3.12. Installation suction for caisson installed with injection pressure of 7.5 kPa (16N test 7).

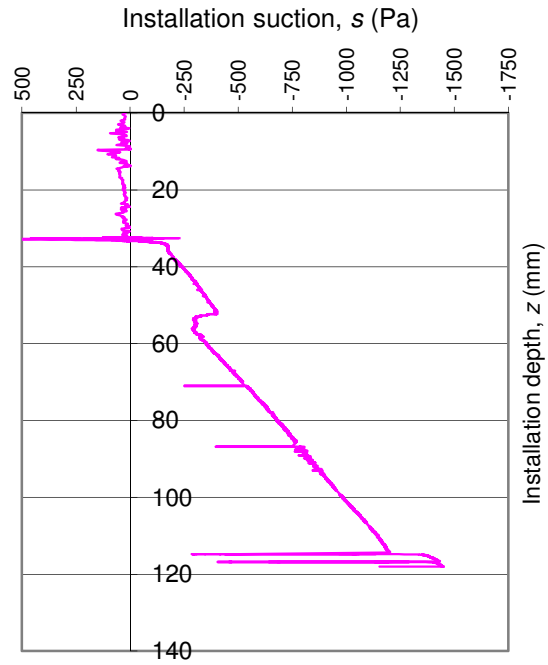

Figure 5.4.1. Installation suction and penetration depth for a test 16N_test 8 with injection pressure of 12.5 kPa.

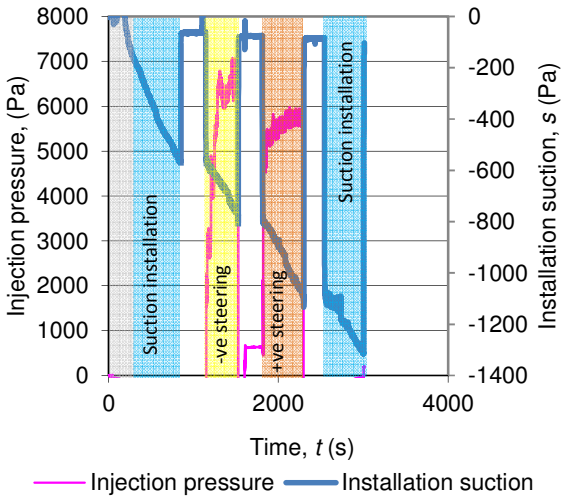

Figure 5.4.2. Plot of installation suction and injection pressure as a function of time (test: steered_31).

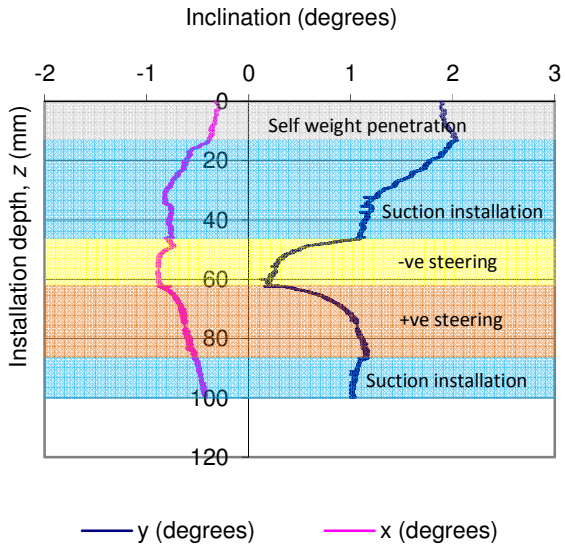

Figure 5.4.3. Plot of the variation of caisson inclination with depth of installation. Installation phases are shaded on the chart (test: steered_31).

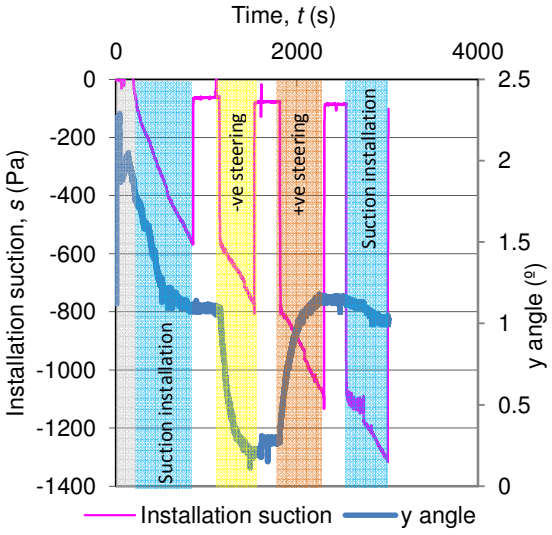

Figure 5.4.4. Plot of installation suction and θ_y with respect to time (test: steered_31).

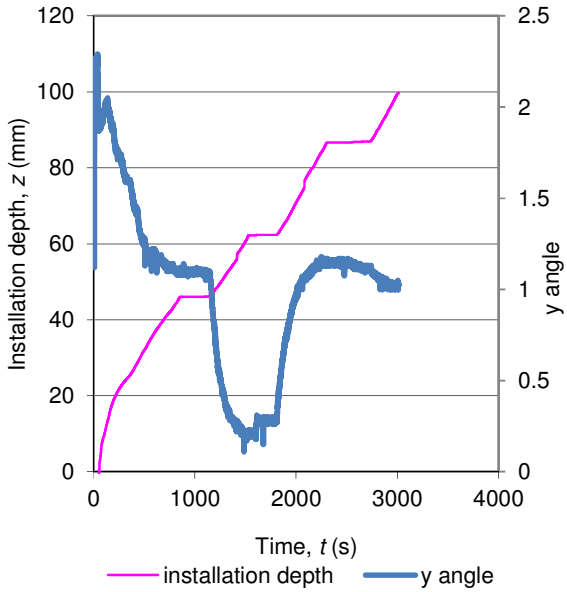

Figure 5.4.5. Plot of installation depth and θ_y against time. When installation was stopped, θ_y did not change. Significant changes only occurred during installation (test: steered_31).

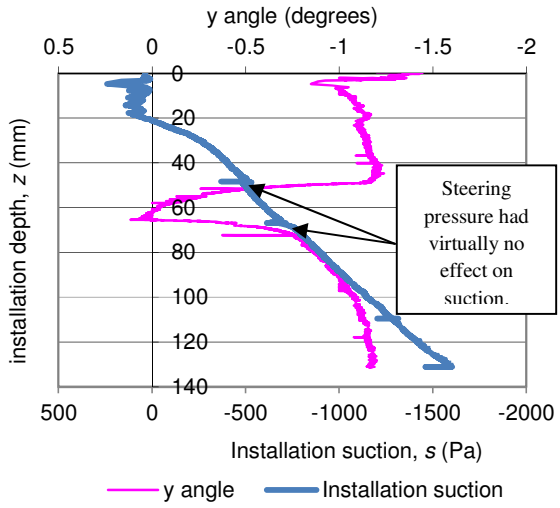

Figure 5.4.6. Plot of caisson inclination and installation pressure (test: steered_23).

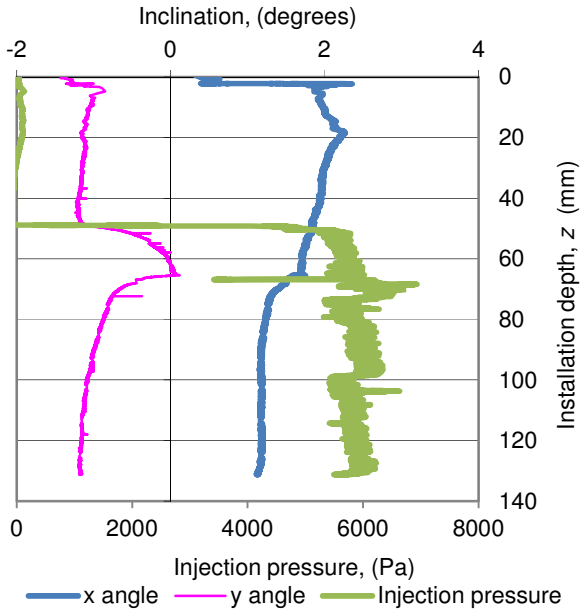

Figure 5.4.7. Plot of inclination and injection pressure for test Steered_23.

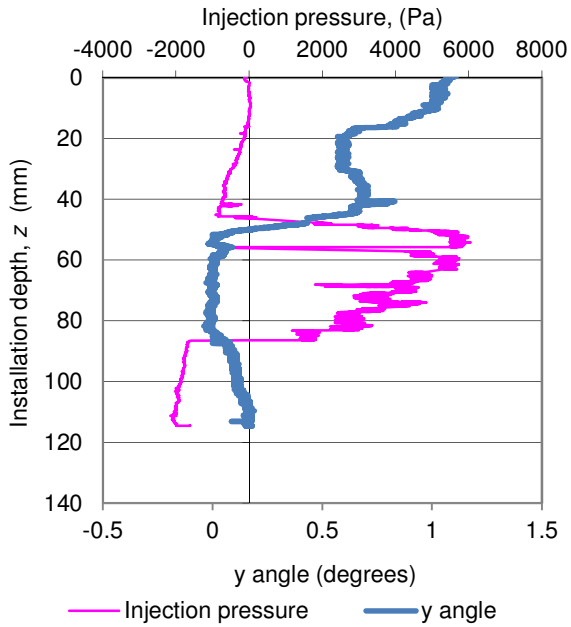

Figure 5.4.9. Results of angle control installation (Test: Steered_27). θ_y was maintained at an indicated angle of 0º.

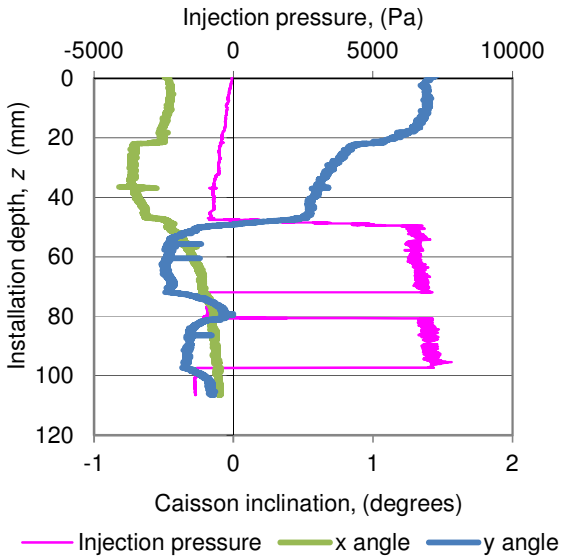

Figure 5.4.8. Plot of caisson inclination with single sided steering applied at shallow and deep installation depth (Test: Steered_28).

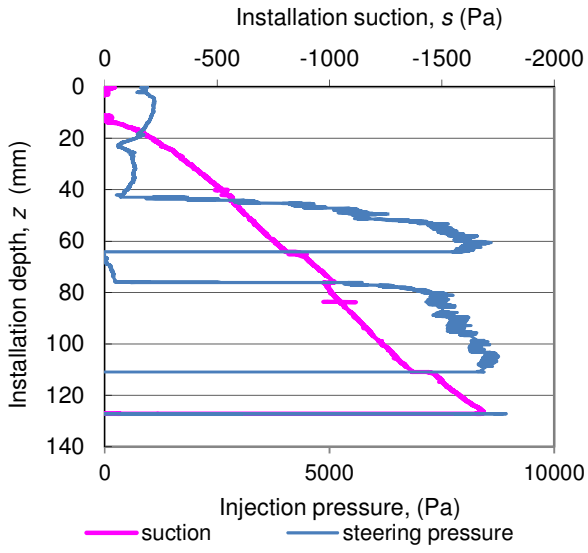

Figure 5.4.10. Plot of suction pressure variation as a function of installation depth. The change of suction pressure can be observed when steering is cut off then reapplied (test: steered_26).

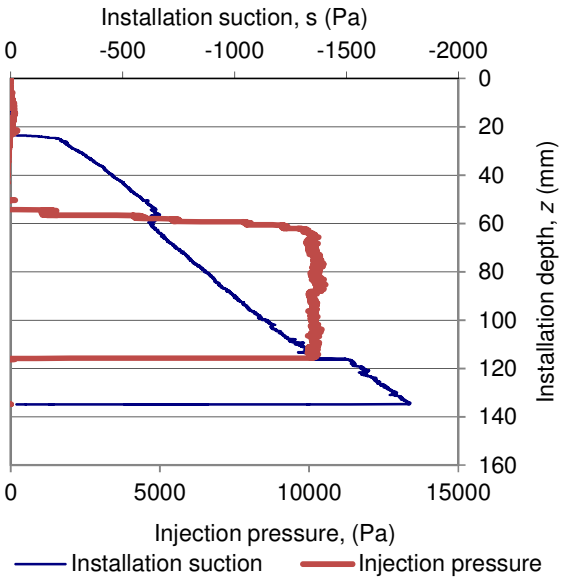

Figure 5.4.11. Plot of suction pressure variation as a function of installation depth for STI test 8N test 23. The change in suction pressure can be observed when injection is applied.

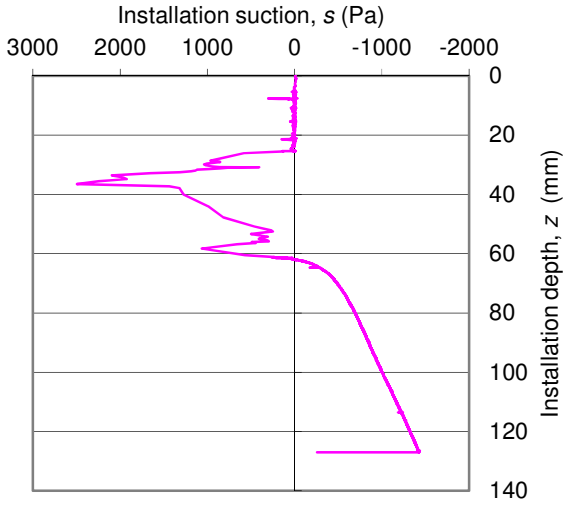

Figure 5.4.12. Plot of suction as a function of depth for installation where rate control was lost at the end of self weight penetration. Over pressure within the caisson reached levels of approximately 2.5 kPa. Self weight penetration reached a depth of over 60 mm (16N test 3).

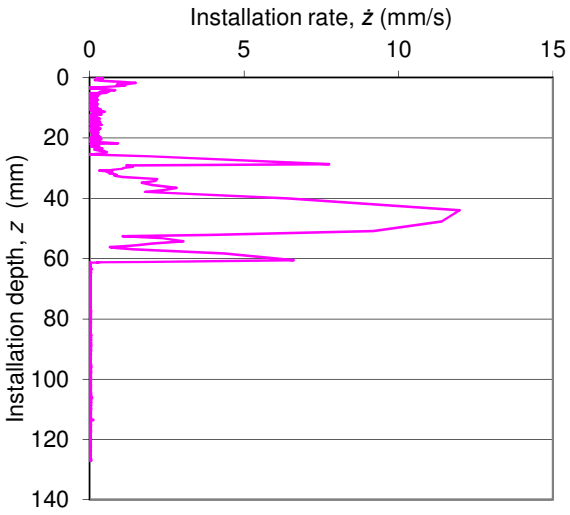

Figure 5.4.13. Plot of installation rate for installation where rate control was lost during self weight penetration. Maximum installation rate recorded was 12 mm/s. (16N test 3).

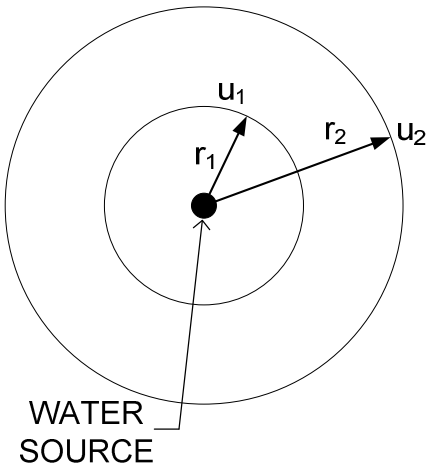

Figure 5.5.1. Diagram of water source and parameters used for the calculation of the dissipation of water pressure away from the source with distance.

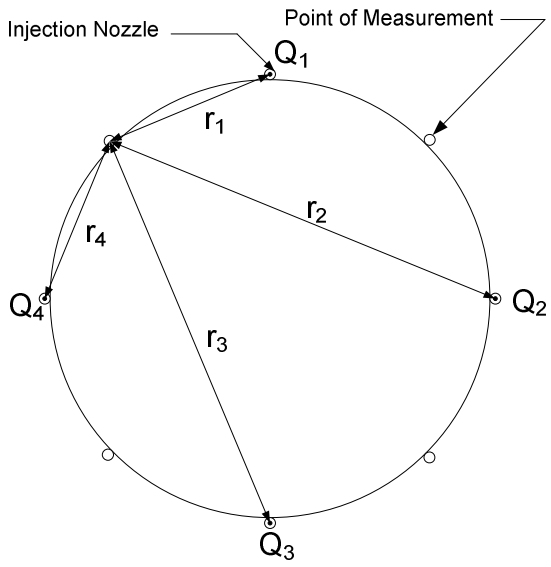

Figure 5.5.2. Geometry of the caisson used for the pore pressure dissipation test. Diagram shows points of injection and points of pressure measurement.

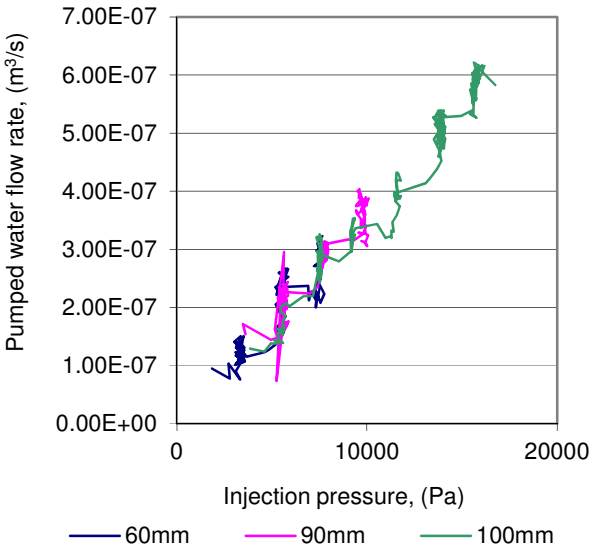

Figure 5.5.4. Plot of the variation of injected water flow rate against injection pressure. The lines correspond to the depths at which the flow rates were measured.

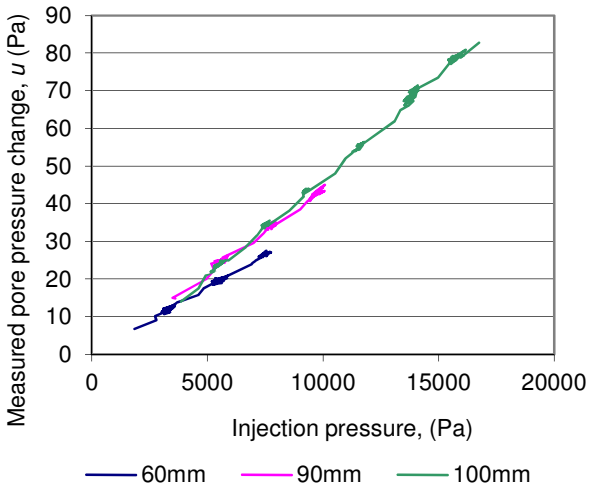

Figure 5.5.3. Graph of injection pressure and measured tip pressure. The depths correspond to the depths at which the tests were undertaken.

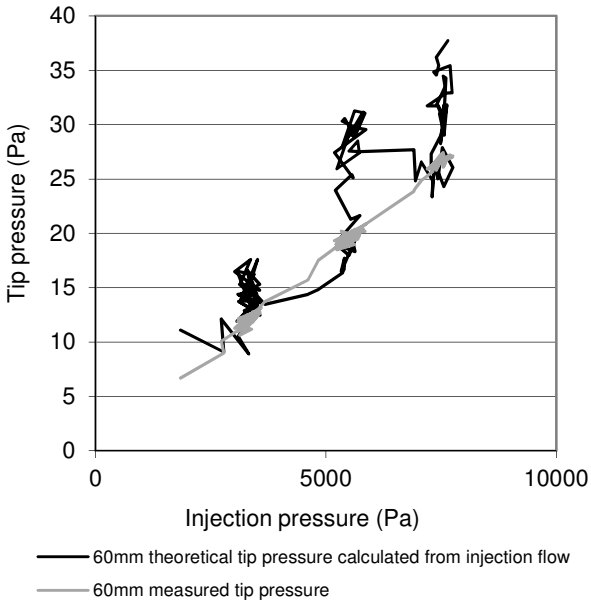

Figure 5.5.5. Measured pressure plotted against injection pressure. Results of calculations for estimation of water pressure change at the measurement points adjacent to the caisson skirt. Depth of test: 60 mm.

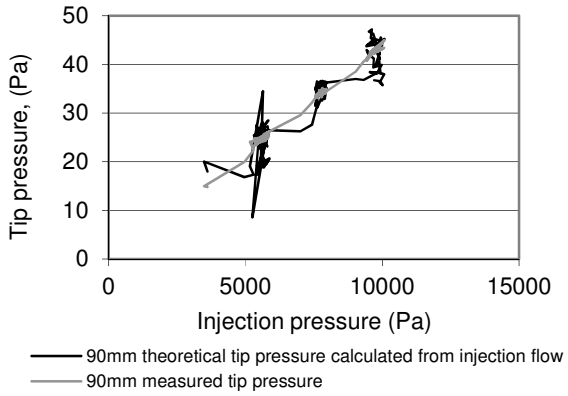

Figure 5.5.6. Measured and estimated water pressure changes at adjacent to the caisson skirt. Depth of test: 90 mm.

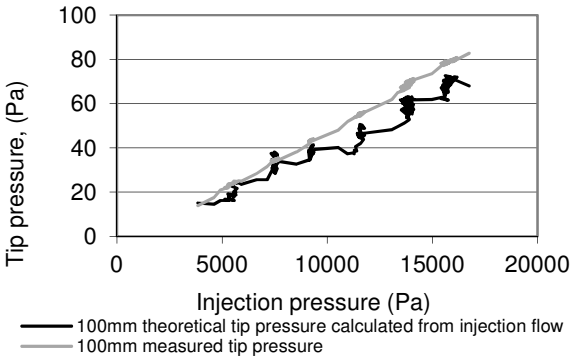

Figure 5.5.7. Measured and estimated water pressure changes at adjacent to the caisson skirt. Depth of test: 117 mm.

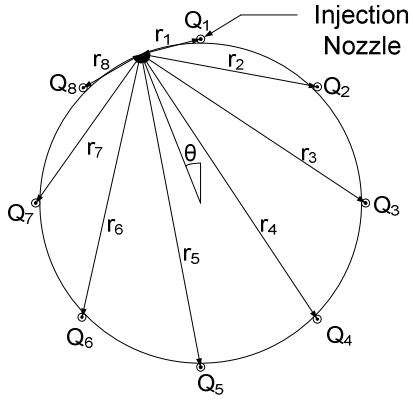

Figure 5.5.8. Diagram of geometry for the 8 nozzle caisson.

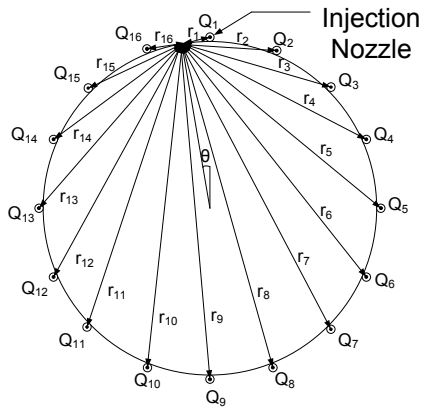

Figure 5.5.9. Diagram of geometry for the 16 nozzle caisson.

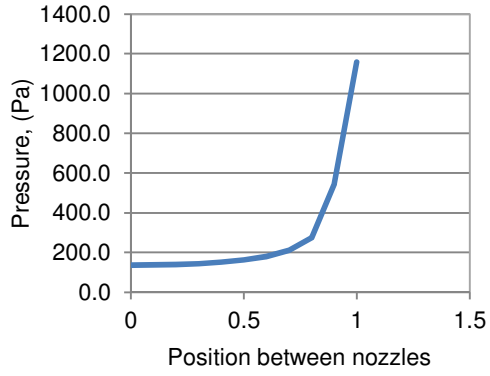

Figure 5.5.10. Calculated variation of water pressure for the 8 nozzle caisson using 5 kPa injection pressure.

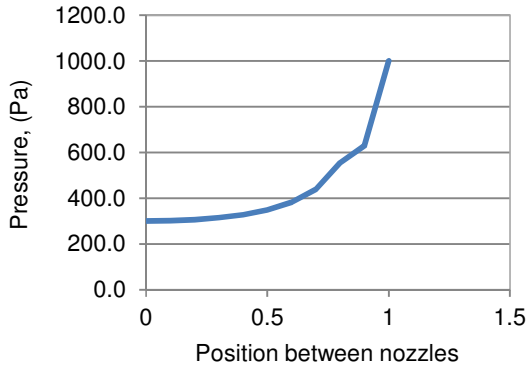

Figure 5.5.11. Calculated variation of water pressure for the 16 nozzle caisson using 5 kPa injection pressure.

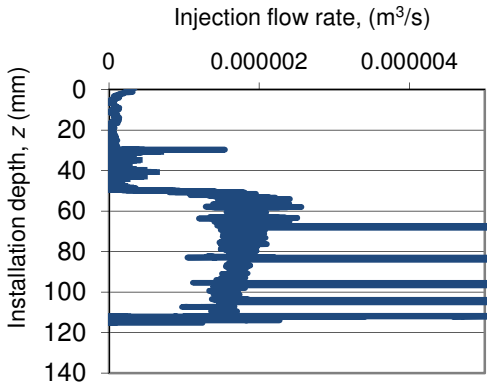

Figure 5.5.12. Flow rate measured during STI test at 12.5 kPa injection pressure for the 16 nozzle caisson (16N test 8).

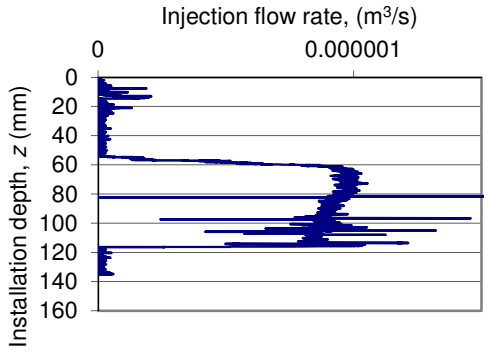

Figure 5.5.13. Flow rate measured during STI test at 10 kPa injection pressure for the 8 nozzle caisson (8N test 23).

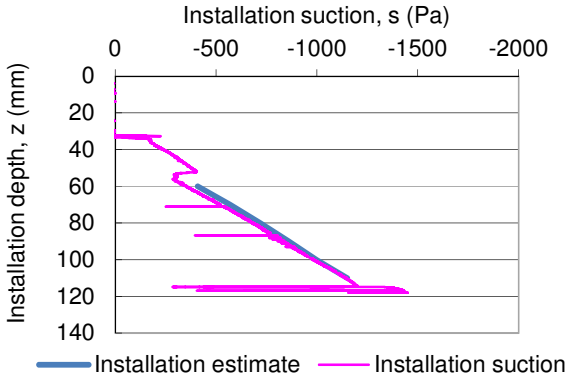

Figure 5.5.14. Installation suction estimate for the 16 port caisson and measured suction data from installation test using 12.5 kPa injection pressure (16N test 8).

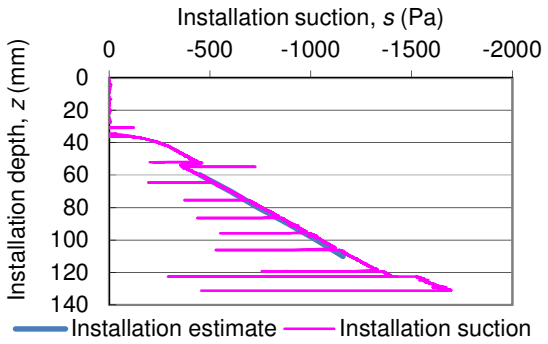

Figure 5.5.15. Installation suction estimate and measured suction data for the 16 port caisson using 7.5 kPa injection pressure (16N test 7).

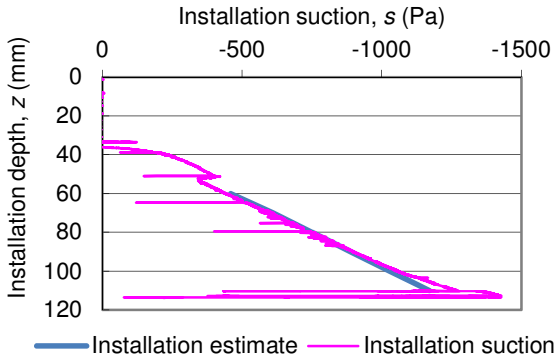

Figure 5.5.16. Installation suction estimate and measured suction data for the 16 port caisson test using 5 kPa injection pressure (16N test 4).

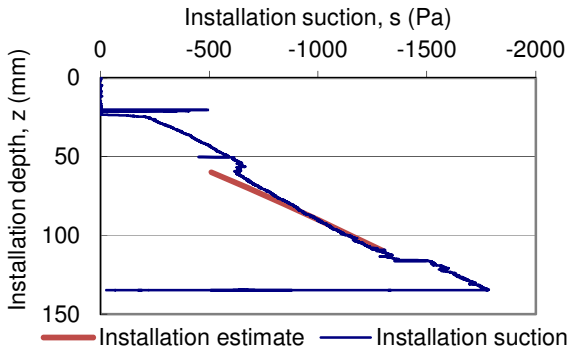

Figure 5.5.17. Installation suction estimate and measured suction data for the 8 port caisson using 10 kPa injection pressure (8N test 23).

Chapter 6 Figures

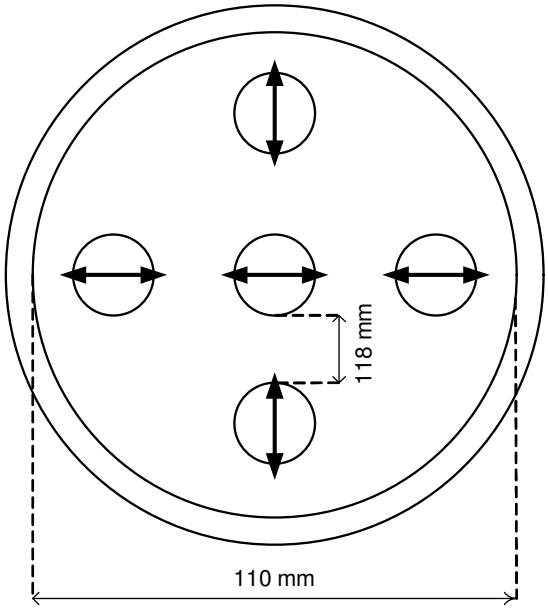

Figure 6.2.1. Locations of the experiments undertaken in the sample tank with directions of moment loading indicated.

Figure 6.2.3. Photograph showing the layout of the 3DOF rig and tank for the caisson grouting experiments. The caisson is shown in the picture placed on its lid to protect the skirt.

Figure 6.2.2. Photograph of Caisson 6 used for the grouting experiments.

Figure 6.2.4. Photograph of grout disc removed from caisson. The visible surface is the side in contact with the soil. The protruding grout bulb in the centre of the caisson arose from sand scour where suction had been applied to the interior of the caisson for installation.

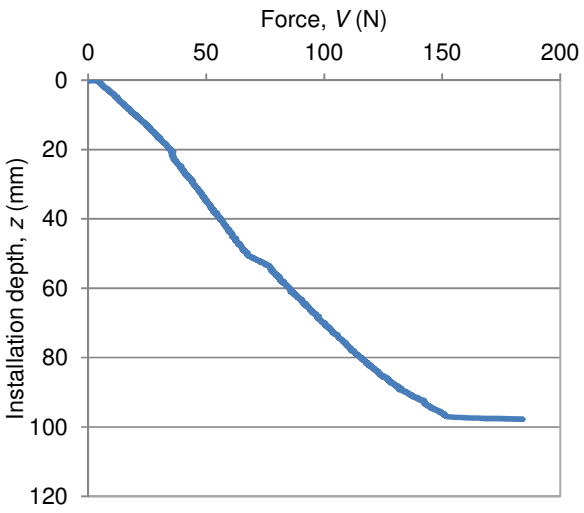

Figure 6.3.1. Force required to jack the caisson into sand (Test GC7.1).

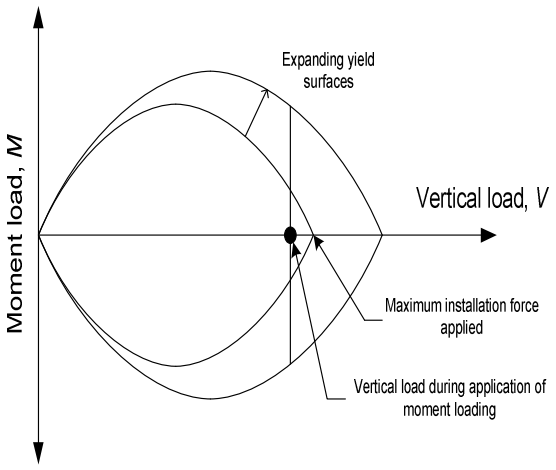

Figure 6.3.3. Diagram showing yield surface expansion during initial moment loading of a suction installed caisson.

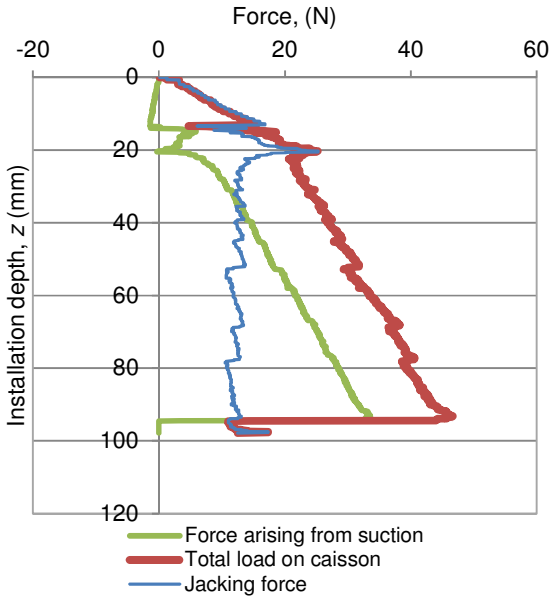

Figure 6.3.2. Plot of loads applied during suction installation before moment loading tests (Test GC7.5).

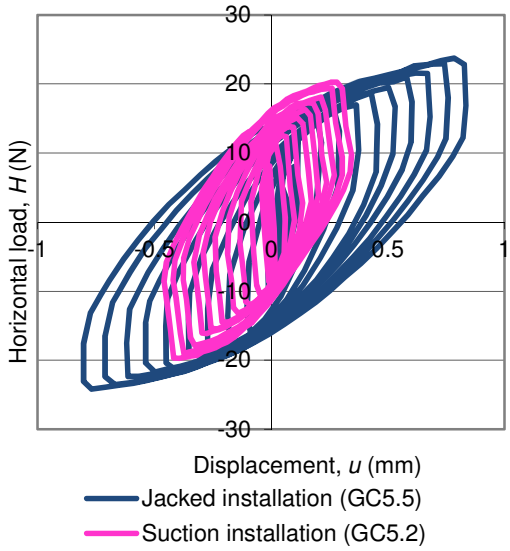

Figure 6.3.4. Plot of the variation of horizontal load with respect to displacement for moment loading.

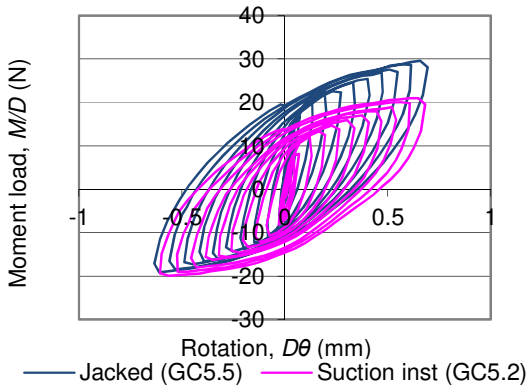

Figure 6.3.5. Plot of moment load and rotations recorded for cyclic loading.

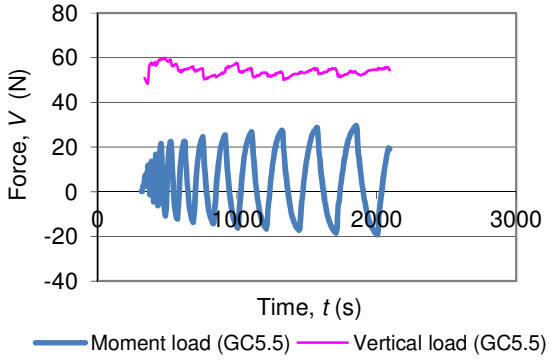

Figure 6.3.6. Plot of the variation of moment load and horizontal load with respect to time for the application of cyclic load (Test GC5.5).

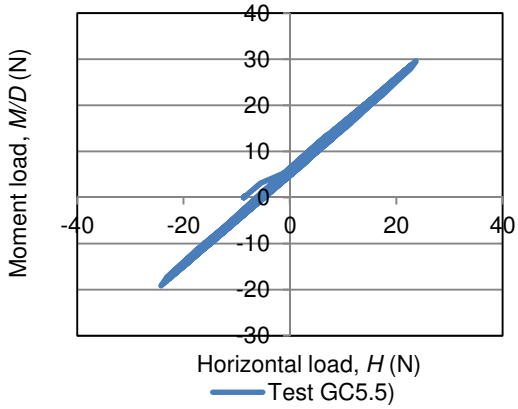

Figure 6.3.7. Plot of the variation of moment load against horizontal load for moment loading tests (GC5.5 shown). The ratio of moment load to horizontal load was maintained throughout cyclic testing.

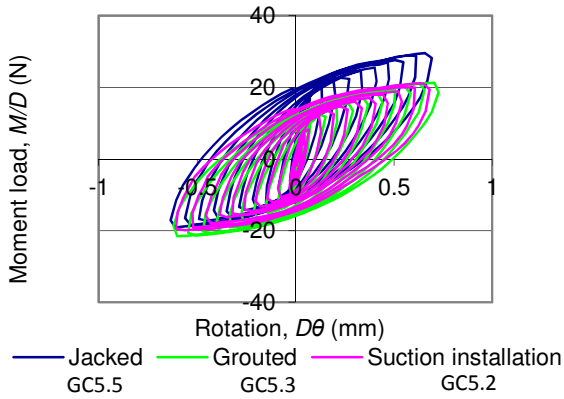

Figure 6.3.8. Plot of moment load response for caissons installed by jacking and suction with and without the use of grouting.

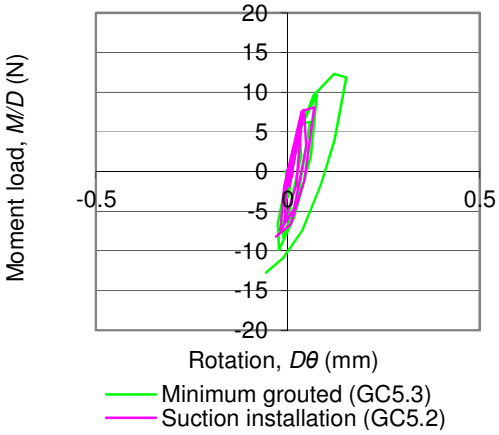

Figure 6.3.9. Moment load response for suction installed caissons at small rotations.

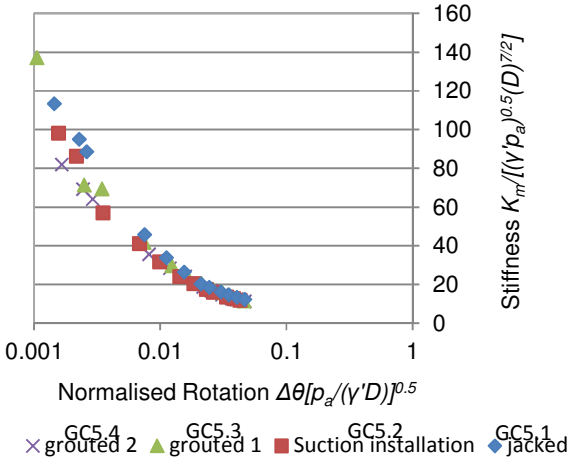

Figure 6.3.10. Normalised unloading stiffness of caissons installed into sand.

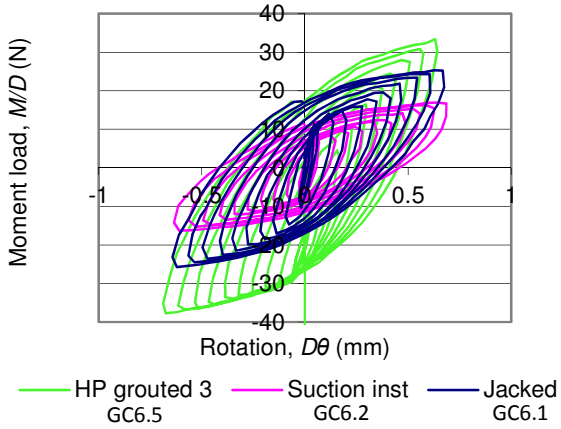

Figure 6.3.11. Moment load and rotation behavior for caisson grouted with high grout pressures.

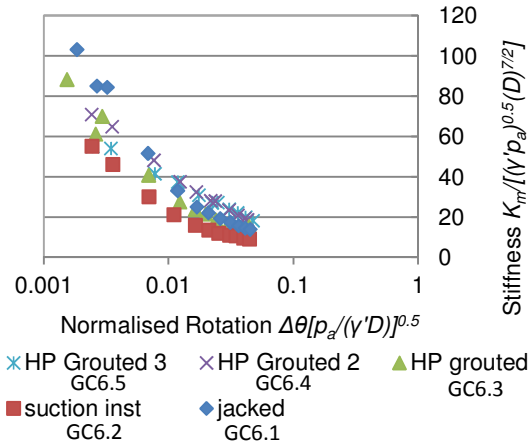

Figure 6.3.12. Plot of normalized unloading stiffness for caissons grouted with high injection pressures.

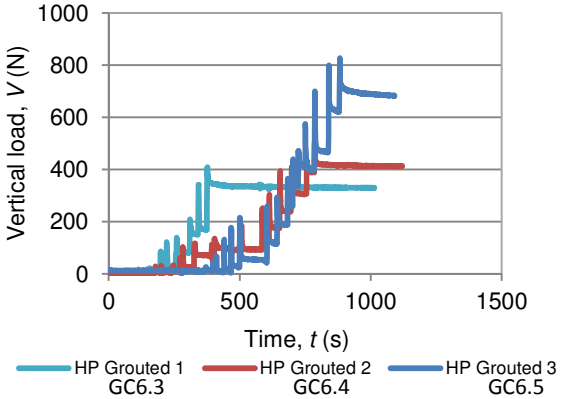

Figure 6.3.13. Plot of the forces measured by the load cell during grouting injection as a function of time.

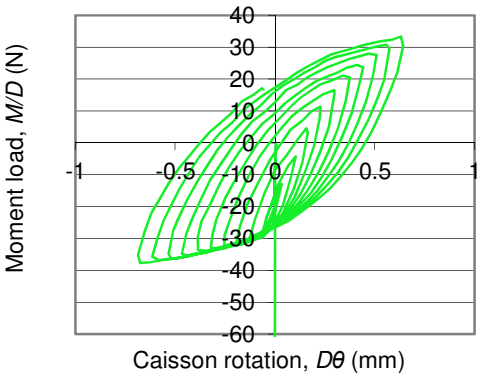

Figure 6.3.14. Moment load response for high pressure grouted caisson illustrating the non-symmetrical loading response (Test GC6.5).

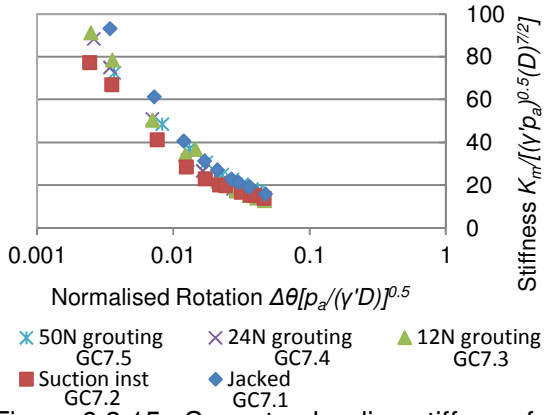

Figure 6.3.15. Secant unloading stiffness for caissons grouted at pressures relevant to those exerted by wind turbine structures.

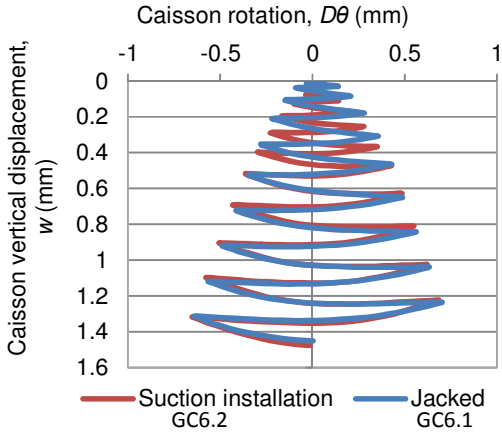

Figure 6.3.16. Comparison of the vertical displacement of caissons installed by jacking and by suction installation.

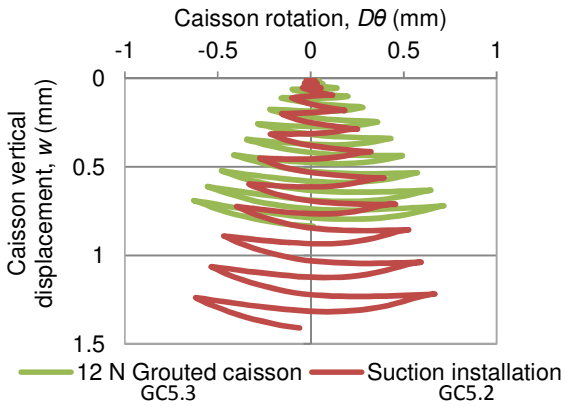

Figure 6.3.17. Plot of vertical displacement for grouted caissons installed by suction compared with ungrouted footings.

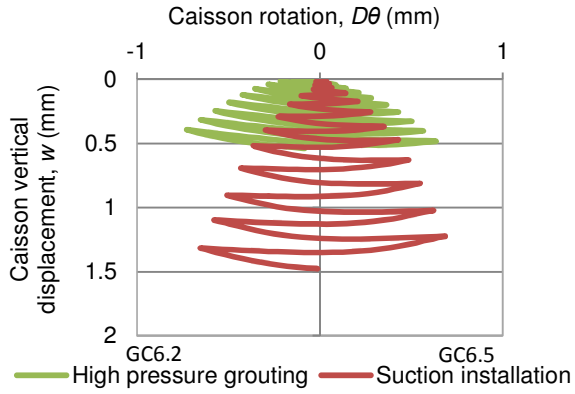

Figure 6.3.18. Plot of vertical displacement for very high pressure grouted caissons installed by suction compared with ungrouted footings.

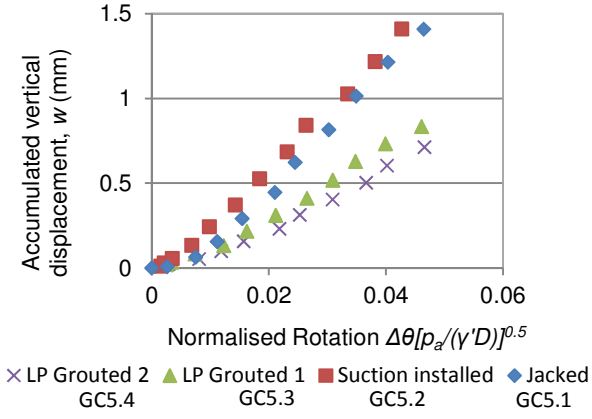

Figure 6.3.19. Plot of accumulated displacement against normalized cyclic rotation. Low grouting pressures used.

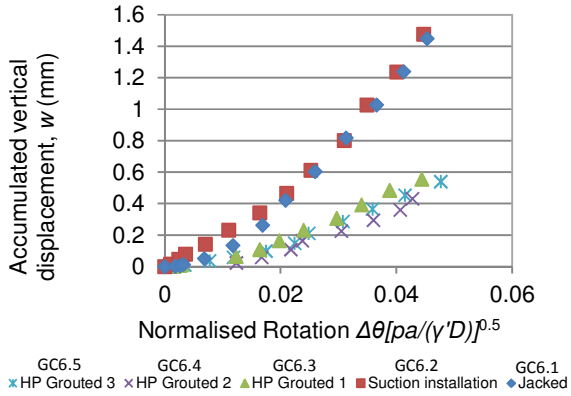

Figure 6.3.20. Figure of variation of accumulated displacements for high pressure grouted caissons as cyclic loading was applied.

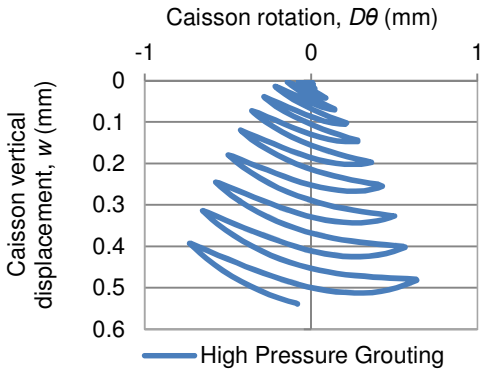

Figure 6.3.21. Settlement of suction installed, pressure grouted caisson (Test GC6.5). Upward displacement over the outward quarter cycle is large.

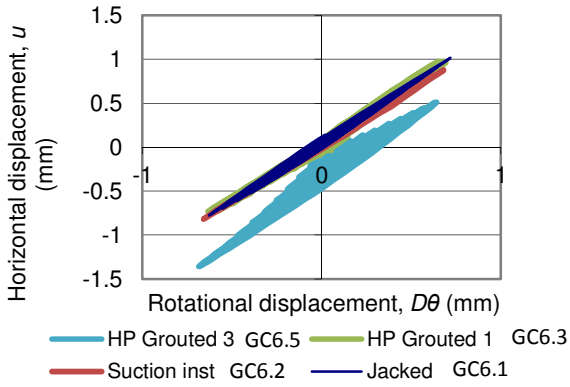

Figure 6.3.22. Plot of horizontal displacements recorded during caisson moment loading plotted against rotational displacement.

Chapter 7 Figures

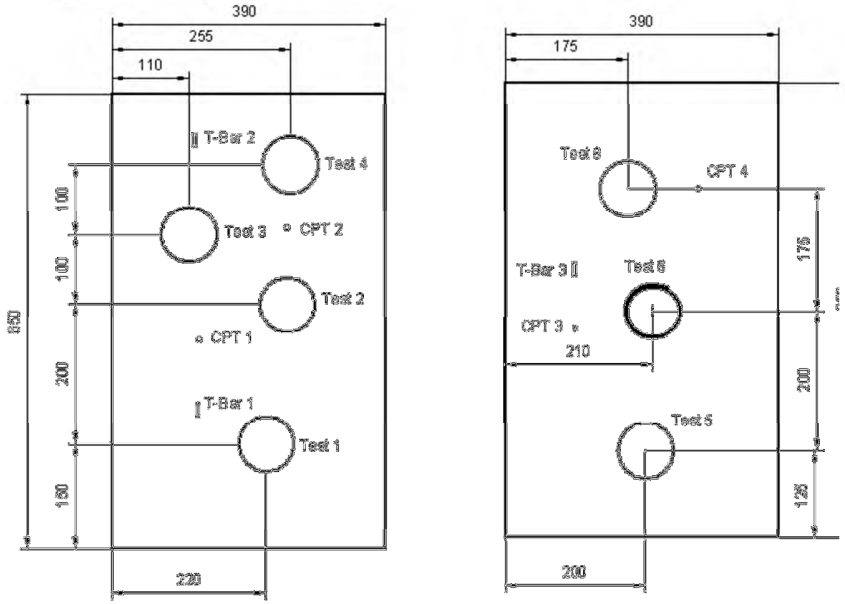

Figure 7.2.1. Locations of the tests undertaken in the UWA

Figure 7.2.2. Picture of the UWA beam centrifuge.

Figure 7.2.3. Close-up photograph of the actuator used in the UWA centrifuge.

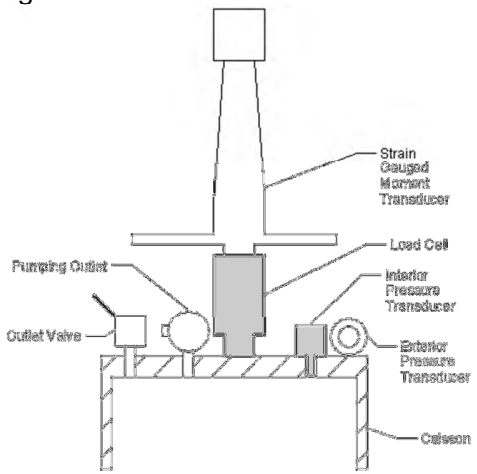

Figure 7.2.4. Diagram of loading arm used for installation experiments at UWA.

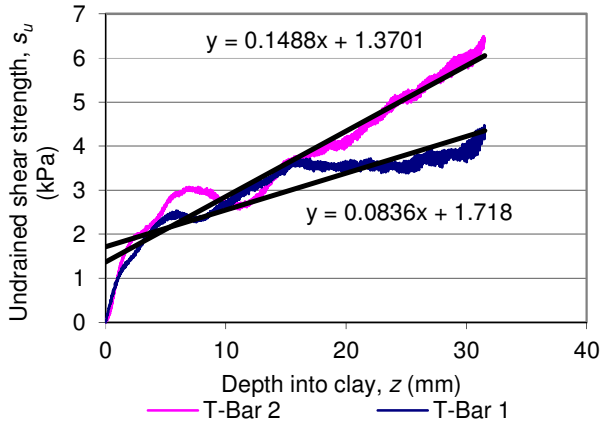

Figure 7.3.1. Plot of the T-bar results for 1g test sample.

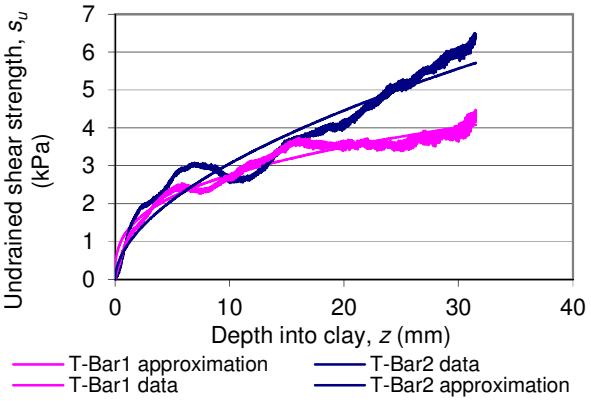

Figure 7.3.2. Figure showing the results of the least squares fit calculated using a programme written for this purpose in Matlab.

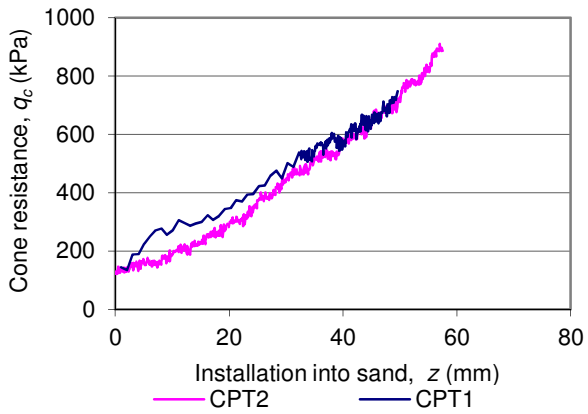

Figure 7.3.3. CPT results for 1g sample.

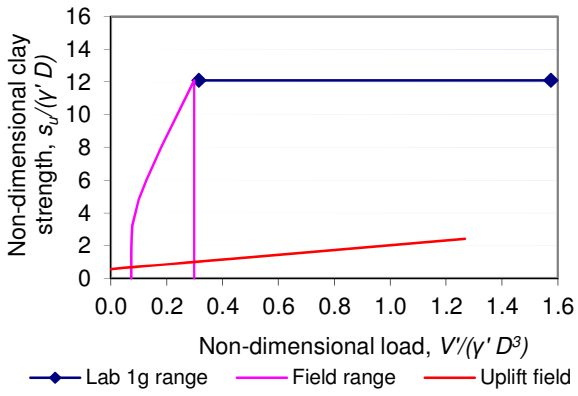

Figure 7.3.4. The installation conditions for the Perth 1g experiments plotted on the non-dimensional installation space presented in Chapter 2.

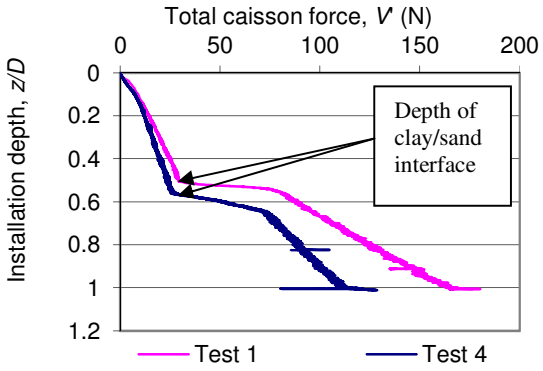

Figure 7.3.5. Plot of forces required for 1g jacked installation.

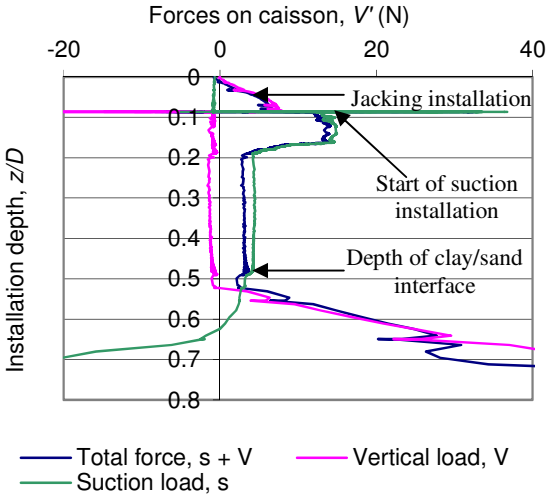

Figure 7.3.6. Plot of 1g suction and actuator forces for Test 2.

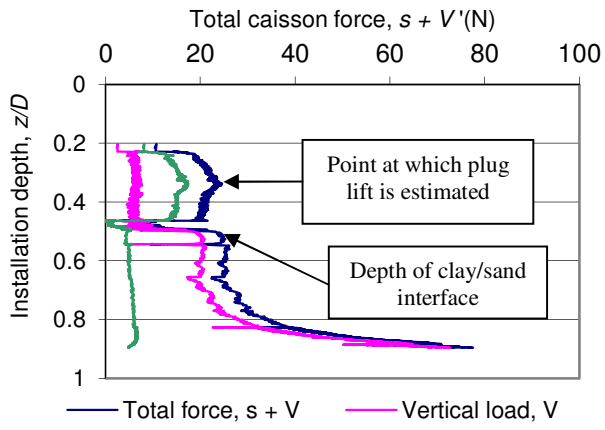

Figure 7.3.7. Plot of 1g suction and actuator forces for Test 3.

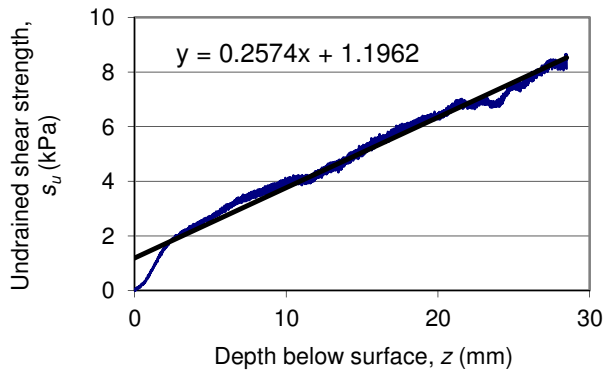

Figure 7.3.8. T-bar results for clay sample used in centrifuge.

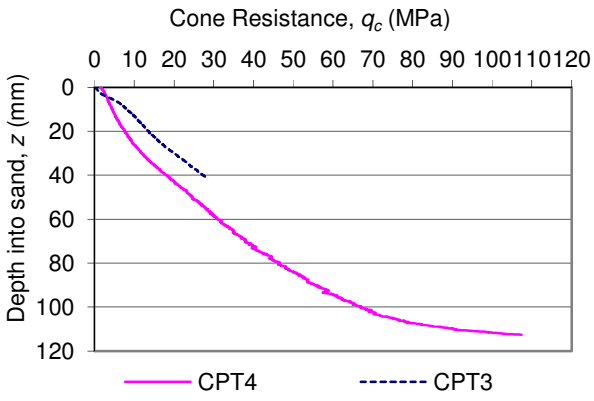

Figure 7.3.9. Plot of CPT results for 100g tests.

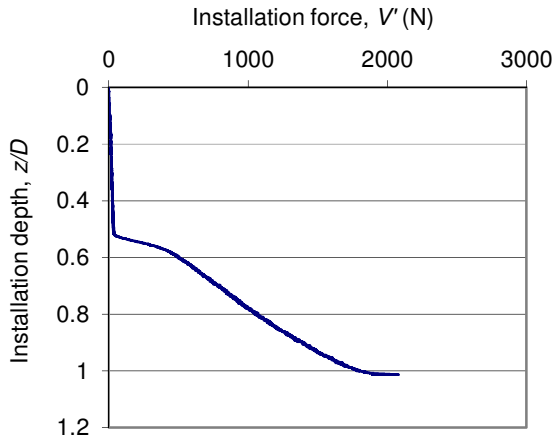

Figure 7.3.10. The forces recorded while jacking the caisson into the sample at 100g (Test 5).

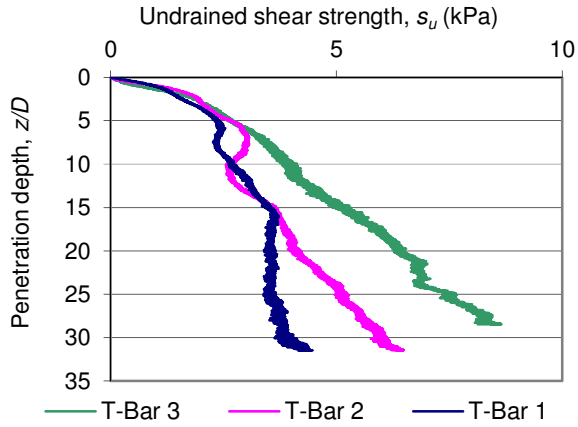

Figure 7.3.11. Comparison of T-bar tests undertaken at 1g and 100g.

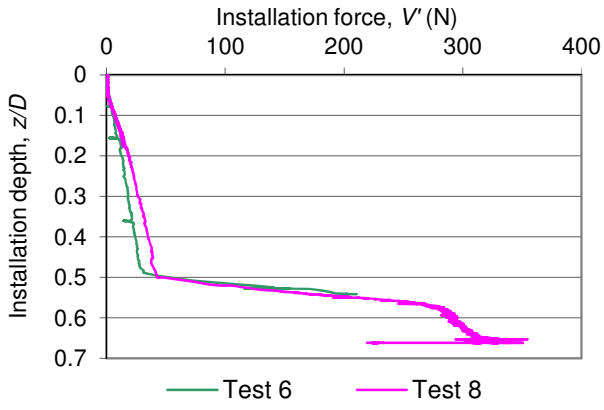

Figure 7.3.12. Total force plots for Tests 6 and 8 installed using a combination of suction and jacking.

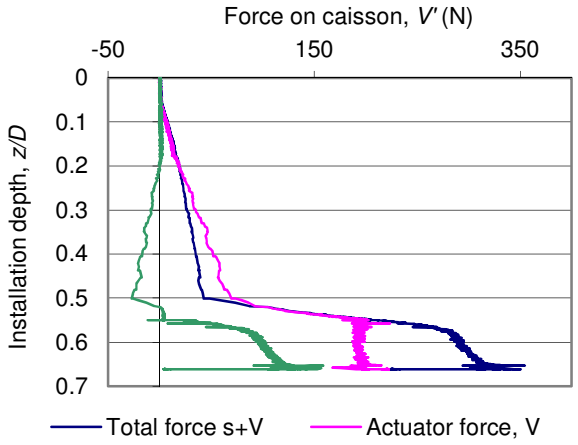

Figure 7.3.13. Actuator and suction forces recorded during the installation of Test 8 at 100g.

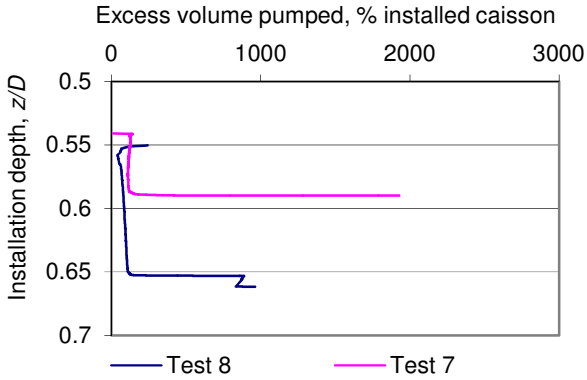

Figure 7.3.14. Excess water pumped during the installation of Tests 7 and 8.

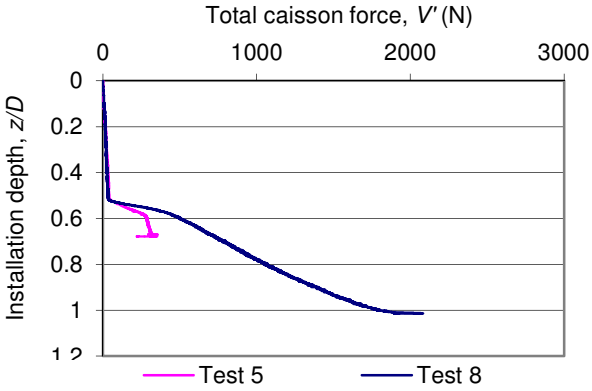

Figure 7.3.15. Comparison of the total force required for installation during Test 8 and that recorded during jacking in Test 5.

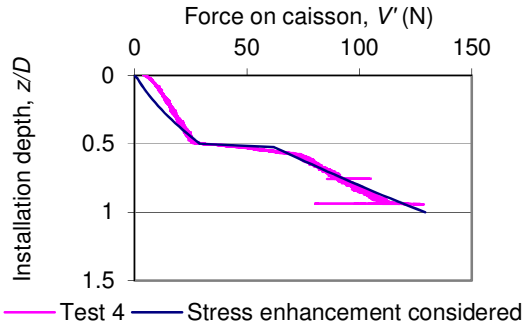

Figure 7.3.16. Installation force estimate for a jacked caisson compared with Test 4 measured data

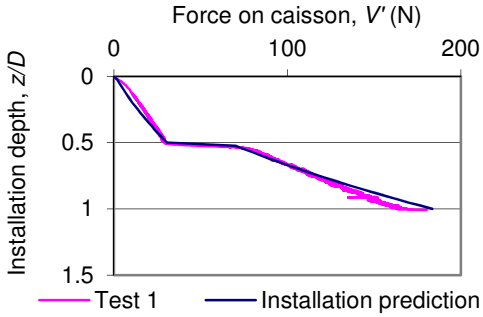

Figure 7.3.17. Installation force estimate for a jacked caisson compared with Test 1 measured data

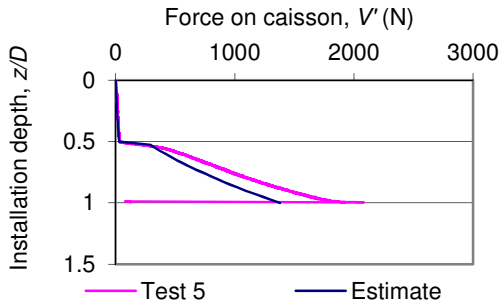

Figure 7.3.18. Estimation of 100g installation resistance using 1g test soil parameters

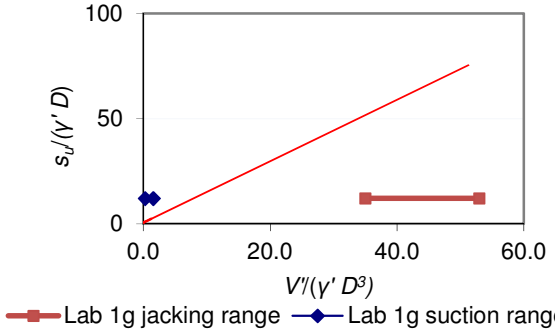

Figure 7.3.19. Plot of the 1g installations in non-dimensional space.

Appendix A

Data supplied to this project by Fugro Ltd. Description of soil conditions available for Round 2 wind farm development sites.

FUGRO LIMITED

Geotechnical Investigation for suction foundation installation of windfarms – UK

Thames Estuary Site

Geotechnical Unit	Geotechnical Description	Depth Ranges of Soil Units
Sea Bed Sediments	MEDIUM DENSE to VERY DENSE medium to coarse SAND	0-1 to 0-3
London Clay Formation (Weathered)	FIRM to STIFF CLAY	1-30 to 10-32
London Clay Formation	FIRM to HARD CLAY	20-32 to 20-40

Thames Estuary Site - First Possible Profile

Geotechnical Unit	Geotechnical Description	Depth Ranges of Soil Units
Sea Bed Sediments I	MEDIUM DENSE to VERY DENSE SAND	0-2 to 0-20
Sea Bed Sediments II (Sand Ridge Sediments)	DENSE to VERY DENSE medium SAND	0-20 to 10-22
Thames Estuary Channel Infill Sediments	VERY SOFT to SOFT becoming FIRM to STIFF with depth, CLAY with sand and gravel	10-30 to 10-40
London Clay Formation (Weathered)	FIRM to STIFF silty to sandy CLAY	10-40 to 20-50
London Clay Formation	FIRM to VERY HARD silty to sandy CLAY	20-50 to >50

Thames Estuary Site - Second Possible Profile

Written strength ranges (e.g. Medium Dense) are equivalent to the British Standard strengths

Liverpool Bay Site

Geotechnical Unit	Geotechnical Description	Depth Ranges of Soil Units
Sea Bed Sediments	MEDIUM DENSE to VERY DENSE medium to coarse SAND with pockets of gravel	0-2 to 0-15
Western Irish Sea Formation and Cardigan Bay Formation	VERY STIFF to HARD sandy CLAY with occasional gravel	2->50 to 15->50

Liverpool Bay Site - First Predicted Soil Profile

Geotechnical Unit	Geotechnical Description	Depth Ranges of Soil Units
Sea Bed Sediments	MEDIUM DENSE to VERY DENSE SAND with pockets of gravel	0-0 to 0-2
Sea Bed Sediments	MEDIUM DENSE to VERY DENSE sandy fine to coarse GRAVEL with cobbles and boulders	0-2 to 0-15
Western Irish Sea Formation and Cardigan Bay Formation	VERY STIFF to HARD sandy CLAY with occasional gravel	0->50 to 15>50

Liverpool Bay Site – Second Predicted Soil Profile

Geotechnical Unit	Geotechnical Description	Depth Ranges of Soil Units
Sea Bed Sediments	MEDIUM DENSE to VERY DENSE medium to coarse SAND with pockets of gravel	0-0 to 0-2
Coast Flat/ Estuarine Deposit	SOFT to VERY STIFF CLAY with sand and gravel	0-0 to 0-5
Western Irish Sea Formation A and B and Cardigan Bay Formation	VERY STIFF to HARD sandy CLAY with occasional gravel and DENSE to VERY DENSE SAND interbedded with HARD to VERY HARD CLAY	0-0 to 5-30
Mercia Mudstone	VERY WEAK to WEAK MUDSTONE	5->50 to 30>50
Sherwood Sandstone	Friable to well cemented SANDSTONE	5->50 to 30>50

Liverpool Bay Site - Third Predicted Soil Profile

Written strength ranges (e.g. Medium Dense) are equivalent to the British Standard strengths

FUGRO LIMITED

Spurn Site

Geotechnical Unit	Geotechnical Description	Depth Ranges of Soil Units
Sea Bed Sediments	MEDIUM DENSE to VERY DENSE sandy fine to coarse GRAVEL with occasional cobbles and boulders	0-1
Bolders Bank	STIFF to HARD very silty CLAY with fine to medium gravel, layers of sand and occasional gravel and cobbles	0-1 to 5-10
Chalk Group	STIFF to VERY HARD very silty carbonate CLAY with cobbles and boulders.	5-10 to >50

Spurn Site - First Possible Soil Profile

Geotechnical Unit	Geotechnical Description	Depth Ranges of Soil Units
Sea Bed Sediments	LOOSE to VERY LOOSE fine to medium SAND	0-2
	STIFF to VERY STIFF CLAY with fragments of chalk	0-2 to 0-12
	VERY STIFF to HARD slightly sandy CLAY	12-29
	HARD to VERY HARD slightly sandy CLAY with chalk fragments	29->50

Spurn Site - Second Possible Soil Profile

Geotechnical Unit	Geotechnical Description	Depth Ranges of Soil Units
Sea Bed Sediments	fine to coarse SAND with gravel and pockets of clay	0-1.5 to 0-2.0
	VERY STIFF to HARD sandy CLAY with occasional gravel and sand	2-15
	DENSE to VERY DENSE silty medium SAND with occasional layers and pockets of clay	15 to 14-42

Spurn Site - Third Possible Soil Profile

Geotechnical Unit	Geotechnical Description	Depth Ranges of Soil Units
Sea Bed Sediments	Slightly silty fine to medium SAND with shell fragments and flint	0-0.7
Chalk Group	VERY WEAK white CHALK (grade V to VI)	0.7 to 14-15

Spurn Site - Forth Possible Soil Profile

Written strength ranges (e.g. Medium Dense) are equivalent to the British Standard strengths